Università degli Studi di Messina

Dipartimento di Scienze Chimiche Biologiche Farmaceutiche ed Ambientali

Dottorato di Ricerca in "Biologia Applicata e Medicina Sperimentale" XXXI ciclo
Curriculum: Scienze del farmaco
SSD: CHIM/08

IDENTIFICATION OF NEW TYROSINASE INHIBITORS VIA COMPUTATIONAL STUDIES, SYNTHESIS AND STRUCTURAL CHARACTERIZATION

Ph.D. thesis of:
Laura IELO

Supervisor:
Prof. Laura DE LUCA

Coordinator of the Ph.D. course:
Prof. Maria Assunta LO GULLO

SEPTEMBER 2018

INDEX

Abbreviations

Abs	Absorbance
ADMET	Absorption, distribution, metabolism, excretion and toxicity
APT	Attached proton test
AUC	Area under the curve
CA	Caffeic acid
CicloDOPA	Indole leukodopachrome
COSY	Correlation spectroscopy
CPME	Cyclopentyl methyl ether
CyHex	Cyclohexane
DCE	Dichloroethane
DCM	Dichloromethane
DHI	5,6-Dihydroxyindole
DHICA	5,6-Dihydroxyindole-2-carboxilic acid
DMF	*N*,*N*-Dimethylformammide
DMSO	Dimethyl sulfoxide
DOPA	3,4-Dihydroxyphenylalanine
DTBB	4,4'-Di-*tert*-butylbiphenyl
EDG	Electron-donating group
EDIPA	*N*,*N*-Diisopropilethylamine
EF	Enrichment factor
EGF	Epidermal growth factor
ER	Endoplasmic reticulum
EtOAc	Ethyl acetate
EtOH	Ethanol
EWG	Electron-withdrawing group
FC	Flash chromatography

FF	Force fields
Gas	Genetic algorithms
GB/SA	Generalized-born/surface area
HBA	H-bond acceptor
HBD	H-bond donor
HBTU	*N*,*N*,*N*,*N*-Tetramethyl-O-(1*H*-benzotriazol-1-yl)uronium hexafluorophosphate
HEM	Human epidermal melanocytes
HEMn-MP	Human epidermal melanocytes neonatal moderately pigmented donor
HMBC	Heteronuclear multiple bond correlation
HMPA	Hexamethylphosporamide
HNB	4-(6-Hydroxy-2-naphthyl)1,3-benzendiol
HOPNO	2-Hydroxypyridine-*N*-oxide
HRMS	High resolution mass spectrometry
HSQC	Heteronuclear single quantum coherence
IL-1α	Interleukin 1 alpha
*i-Pr*MgCl	Isopropylmagnesium chloride
LBDD	Ligand-based drug design
LBVS	Ligand-based virtual screening
LDA	Lithium diisopropylamide
LiHMDS	Lithium bis(trimethylsilyl)amide
LNCy2	Lithium dicyclohexylamide
LTMP	Lithium 2,2,6,6-tetramethylpiperidide
MA	Matching algorithms
MC	Monte Carlo
MCSS	Multiple copy simultaneous search
MD	Molecular dynamics

MeCN	Acetonitrile
MeLi	Methyllithium
MeLi LiBr	Methyllithium lithium bromide
MeOH	Methanol
MITF	Microphthalmia-associated transcription factor
MPA	Methyl ester of p-coumaric acid
MW	Microwave
n-BuLi	*n*-Butyllithium
n-BuNH2	*n*-Butylamine
NI	Negatively ionizable areas
NMR	Nuclear magnetic resonance
NOESY	Nuclear overhauser effect spectroscopy
NP	Natural product
OCA	Oculocutaneous albinism
OPT	Optional
OTMS	Trimethoxyoctadecylsilane
PB/SA	Poisson Boltzman/surface area
PBA	Phenyl benzoic acid
PCA	*p*-Coumaric acid
PDB	Protein Data Bank
PI	Positively ionizable areas
PTU	Phenylthiourea
RMSD	Root-mean-square distance
ROC	Receiver operating characteristic
SARs	Structure-activity relationships
SBDD	Structure-based drug design
SBVS	Structure-based virtual screening

TAT	Twin-arginine traslocation
t-Boc	*tert*-Butyloxycarbonyl
TEA	Triethylamine
TFA	Trifluoroacetic acid
TGF-β1	Trasforming growth factor β1
THF	Tetrahydrofuran
TLC	Thin-layer-chromatography
TMBC	2,4,2',4'-Tetrahydroxy-3-(3-methyl-2-butenyl)chalcone
TMEDA	*N*,*N*,*N*',*N*'-Tetramethylethane-1,2-diamine
$TMSCH_2Li$	Trimethylsilylmethyllithium
TMSCl	Trimethylsilyl chloride
TNF-α	Necrosis factor α
TP	Positive hit
TyBm	Tyrosinase from *Bacillus megaterium*
TyH	Human tyrosinase
TyIs	Tyrosinase inhibitors
TyM	Tyrosinase from *Agaricus bisporus*
TyRPs	Tyrosinase related proteins
Tys	Tyrosinases
UV	Ultraviolet
VS	Virtual screening
WA	Weinreb amide
α-MSH	α-Melanocyte-stimulating hormone

PREFACE

The dissertation of this PhD thesis is divided in two parts: the first section and an appendix concerning my research works performed at University of Messina and University of Vienna respectively. The **first section** is focused on the development of new synthetic Tyrosinase inhibitors (TyIs) useful for the treatment of skin disorders. In particular, in the first three chapters I examined the target - in general - reporting its structure, function and catalytic mechanism (**Chapter 1**); an overview of the known inhibitors previously developed (**Chapter 2**); the disorders related to the dysfunction of Tyrosinases (Tys) activity and the applications of TyIs (**Chapter 3**).

For the design of new TyIs a rational approach was employed, thus in **Chapter 4** are illustrated all the computational methods used for this purpose. **Chapter 5** describes the results obtained concerning synthetic procedures, biological activity, structure-activity relationships (SARs).

In **Chapter 6** full experimental procedures employed for the synthesis are presented, as well as, docking studies, biochemical and pharmacological assays of the designed TyIs. The *in vitro* biochemical assays have been performed at University of Messina in collaboration with Prof. Maria Paola Germanò. The cytotoxicity effect in B16F10 melanoma cells has been evaluated in collaboration with Prof. Francesca Fais at the Department of Life Science and Environment, University of Cagliari. The crystal structures of the synthesized compounds in complex with the Tyrosinase extracted from *Bacillus megaterium* (TyBm) have been obtained in the laboratories of Prof. Fishman at the Department of Biotechnology and Food Engineering, Technion Israel Institute of Technology, Israel.

In the **Appendix** of this dissertation, the research work performed during the ten-months of external experience at University of Vienna - Department of Pharmaceutical Chemistry under the supervision of Prof. Vittorio Pace – is documented. It deals with the development of novel synthetic methods based on the use of homologating carbenoidic-like reagents. In particular, we established an unprecedented protocol enabling the telescoped *C1* or *C2* homologation of imine-type surrogates (*i.e.* chlorotrifluoroimidates) to the corresponding halo- or halomethylaziridines through a single synthetic operation. Such an Appendix is divided in 3 chapters structured as

follows: in **Chapter 1** the general features and reactivity of carbenoids and a brief overview on aziridines chemistry are provided; in **Chapter 2** I reported the results on the telescoped homologation of chlorotrifluoroimidates through lithium carbenoids and representative X ray conducted in collaboration with Dr. A. Roller, Insitute of Inorganic Chemistry, University of Vienna; in **Chapter 3** the experimental procedures employed, characterization data conducted in collaboration with Prof. W. Holzer (Department of Pharmaceutical Chemistry, University of Vienna), are provided.

Key words: Tyrosinase; arylpiperidine-piperazine; docking studies; organic synthesis; lithium halocarbenoids; aziridines.

SECTION I

AIM OF THE WORK

Tys (EC 1.14.18.1) are metalloenzymes, existing in all life domains, involved in the mammal biosynthesis of melanin. An excessive production of melanin can cause serious skin diseases. Thus, Tys inhibition is an established strategy to avoid these side effects and the development of TyIs gained high interest in the therapy of skin pathologies, as well as, in dermocosmetic treatments. Over the past 30 years several TyIs such as hydroquinone and kojic acid were developed, but unfortunately they showed relevant human toxicity. For this reason, there is still an urgent needing for new derivatives with better pharmacological characteristics. A web-research performed using the most popular database, PubMed, highlighted how the interest of this target, related to the treatment of skin diseases, is increased during the years considering the growing of the number of scientific publications from 1987 to date, as reported in graphic 1.

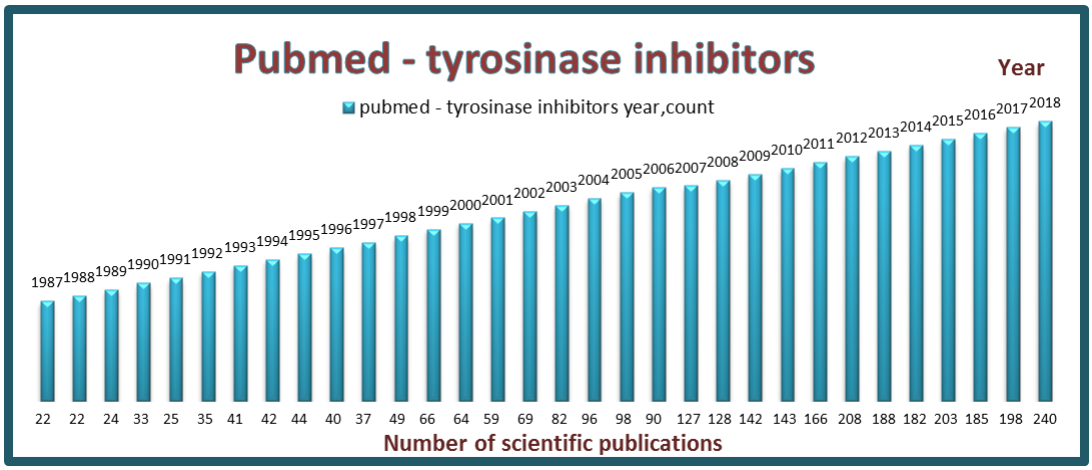

Graphic 1: Correlation between years and number of publications related to Ty inhibition through a PubMed research.

Thus, the purpose of my PhD project was the development of new synthetic TyIs with better pharmacological profile. Starting from a "lead compound" previously identified by my research group, a rational approach was employed to design new derivatives with various structural modifications clarifying the structure-activity relationships (SARs). In particular, a combination of crystallographic and docking studies were used and the so planned compounds were then synthetized and their biological activity was evaluated.

CHAPTER 1 TYROSINASE ENZYME

1.1 Enzymatic function

Tys are ubiquitous metalloenzymes exhibited across the most diversified life domains. They belong to the "type-3 copper" protein family as well as catechol oxidases, hemocyanins and laccases. In the active site of this protein family there is a conserved region characterized by six histidine residues coordinating two copper ions (CuA and CuB) located in a four helical bundle (figure 1).[1]

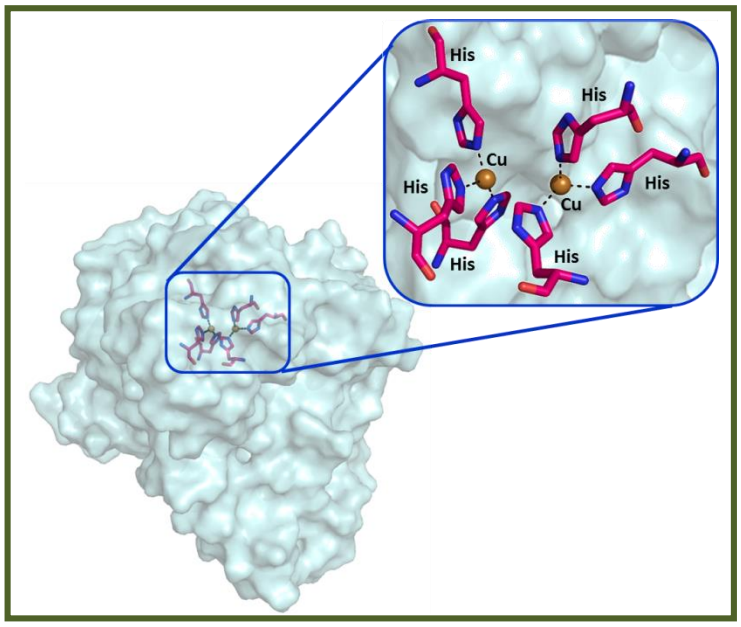

Figure 1: Tys active site. The six histidine residues are represented by pink stick and the two copper ions by brown spheres. The picture was generated using PyMol.[2]

Tys catalyze the first two steps of the Raper-Mason pathway, the hydroxylation of L-tyrosine to L-DOPA and the subsequent oxidation of L-DOPA to L-dopaquinone. The first activity is called tyrosine hydroxylase (monophenolase activity) and the second one *o*-diphenol oxidase, catechol oxidase or DOPA oxidase (diphenolase activity). Once dopaquinone is formed by the oxidative action of these enzymes, the pathway progresses through a series of spontaneous reactions leading to the final melanin pigments (figure 2). In animal melanocytes, all steps after *L*-dopaquinone formation were also thought to proceed spontaneously to form melanin pigment, but around 1980, a number of growing pieces of evidence indicated a lack of correlation among Tys activity, melanin formation in animal skin and hair and blood levels of melanocortin, the animal hormone that controls the melanogenic capacity of

melanocytes. Thus, it was highlighted the possibility that the hormonal control of melanogenesis acted on the other proteins involved in mammalian melanogenesis. Soon, data strongly suggested the existence of a post-Ty regulation in this process beyond *L*-dopaquinone or *L*-dopachrome formation.[3]

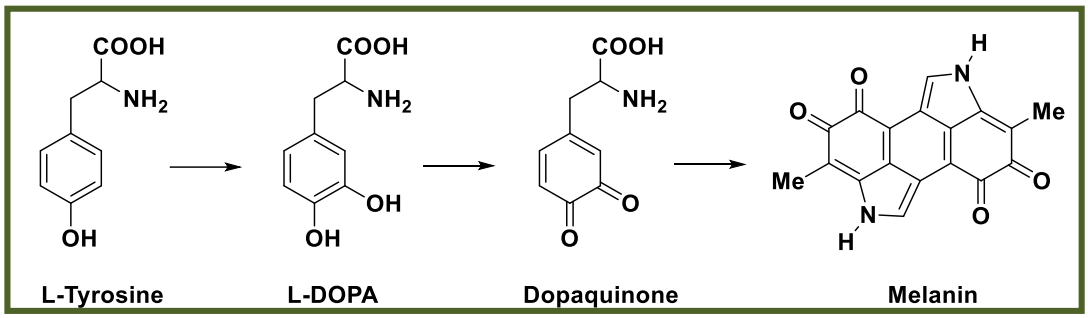

Figure 2: Raper-Mason pathway for the formation of melanin pigments.

1.2 Structure of the enzyme

The structure of the enzyme can be divided in three parts: *N*-terminal domain, central domain and *C*-terminal domain (figure 3).

- ***N*-terminal domain**. It is a transit peptide determining the final location of the enzyme. In plant, it directs the enzyme to the chloroplast; in human and mouse, it seems to be involved in melanosome transfer;[4] in mushrooms, since the Ty enzyme is cytoplasmatic, it does not contain a transit peptide although in some cases it is associated with the cell wall;[5] in bacteria the *N*-terminal domain is characterized by a TAT signal peptide responsible for proteins secretion.[1, 6]
- **Central domain**. It is characterized by six conserved histidine residues, coordinating by the CuA and CuB oxidizing ions.[1] This copper pair is the site of interaction of Ty with both molecular oxygen and its phenolic substrates. It is interesting also to note the presence of thioether bridge between one histidine residue of the active site and one cysteine residue observed in the central domain of Ty of *N. crassa*.[7] It seems that this bond can regulate the activity of the enzyme. In mushroom and *Aspergillus* Tys, it is also possible the formation of a thiother bridge. This is not the case of known prokaryotic, plants and mammalian Tys.[8]
- ***C*-terminal domain**. It is a transmembrane domain. In *Agaricus bisporus* and *Neurospora crassa*, Ty is a soluble cytosolic enzyme and does not contain a transmembrane region;[8] in plants no evidence was found for a *C*-terminal

transmembrane domain, however the presence of a transmembrane helix was suggested in this domain;[9, 10] mammalian Tys are melanosomal membrane proteins possessing a carboxyl tail oriented to the cytoplasm and a single membrane-spanning helix in the *C*-terminal portion of the proteins.[11]

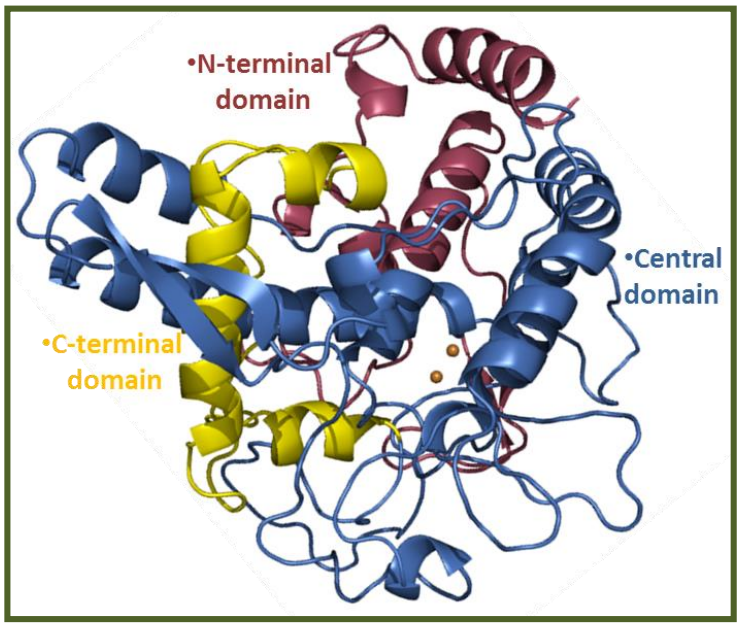

Figure 3: General structure of TyS. The picture was generated using PyMol.[2]

Tys active sites, as well as, most type-3 copper proteins, are provided by an additional protein domain defined as "placeholder".[8, 12] Usually, it is a bulky aromatic residue such as Phe or Tyr but, also a Leu residue can be present therein. It is located above the active site and is oriented parallel to the second coordinating CuB histidine residue. It was supposed that its role is to control the enzymatic activity and to prevent an undesirable oxidation of phenolic compounds, since in most cases the enzymatic activity is possible only after the removal of placeholder. An additional position which covers the active site is located above the CuA, according to literature, acting as blocker residue that participates in substrate orientation.[1, 13] However, while in some enzyme its role is extremely important, in others, it is neglectable.[1]

Tys from different sources possess both common and diverse features. The common features are related to the overall folding and the active site of the enzyme, in which the central copper-binding domain is conserved, containing strictly conserved amino acids residues.[14] The differences are relative to the signal sequence, carboxyl tail, *N*-glycosylation, copper incorporation mechanism and the number of cysteine residues

important for the formation of disulfide bridges.[15] Indeed, there are 17 cysteine residues in humans and mouse, 11 in plants, 0 or 1 in prokaryotes. They seem to have an important role in the correct folding of protein and in the acquisition process of copper ions.[8]

1.3 Ty catalytic mechanism

Ty is characterized by four discrete oxidation states (*deoxy*, *oxy*, *met* and *deact* form) relying on the oxidation state of the two copper ions in the active site (figure 4).

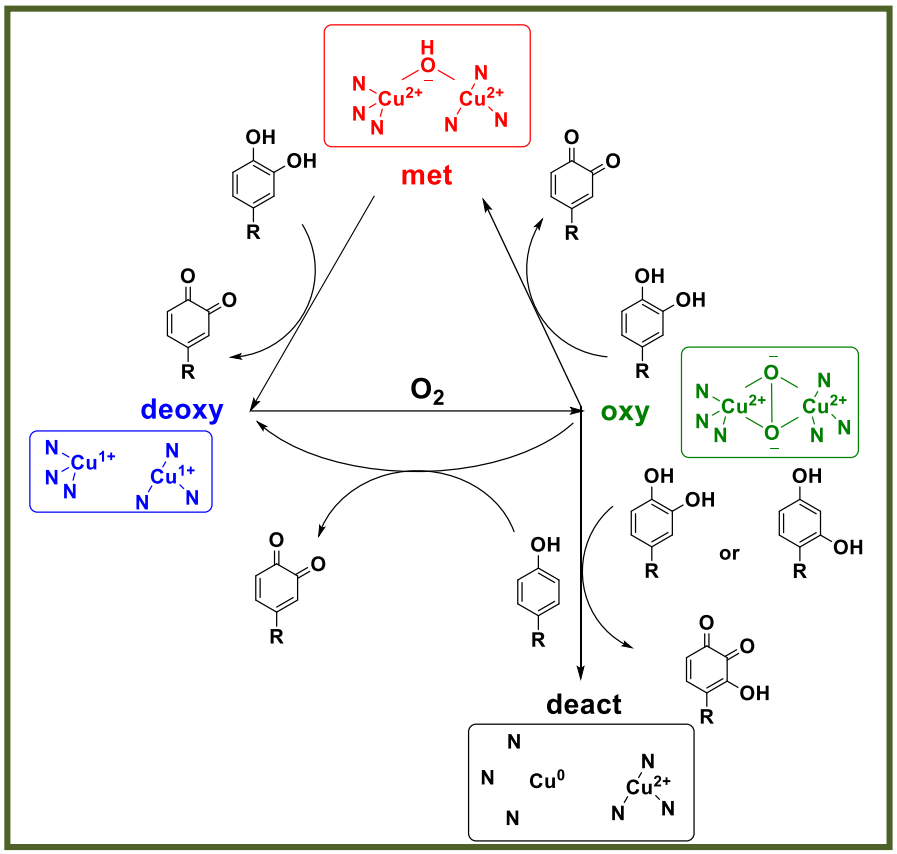

Figure 4: The four discrete oxidation states of Ty. Picture modified from reference [16].

Native Ty is present mainly as *met*-Ty, in which a hydroxyl ion is bound to the two copper ions [Cu(II)]. Phenols bind to *met*-Ty but are not oxidized by this form of the enzyme unlike catechols. In catechols oxidation process, *met*-Ty is reduced to *deoxy* state in which both coppers are now in the Cu(I) oxidation state. *Deoxy*-Ty rapidly binds dioxygen to give *oxy*-Ty in which the two oxygen atoms are held between the copper ions in the active site. The first oxidizing form of the enzyme is *oxy*-Ty which

oxidizes phenols and catechols by a monooxygenase and oxidase mechanism, respectively (figure 5).

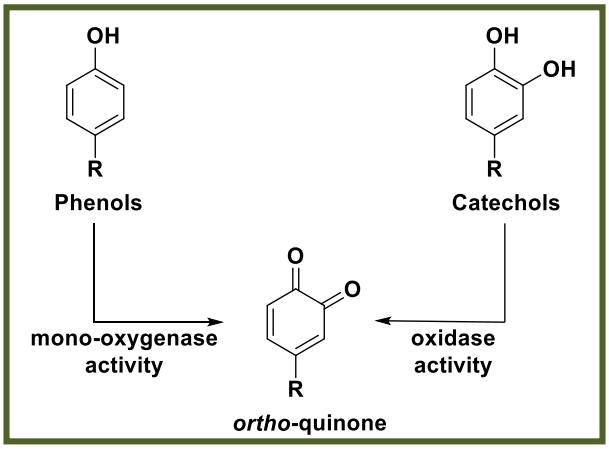

Figure 5: Oxidation process of phenols and catechols by a monooxygenase and oxidase mechanism respectively. Picture modified from reference [16].

Therefore, both phenols and catechols are oxidized by *oxy*-Ty to *ortho*-quinones in presence of dioxygen. During the catecholic cycle, a catechol is occasionally treated as a phenol and it is oxidized by *oxy*-Ty through a monooxygenase mechanism leading to the irreversible formation of *deact*-Ty in which one of the copper atoms has been reduced to the Cu(0) state and may diffuse out of the active center. This minor pathway eventually leads to total inactivation of the enzyme by catechols.[1, 16]

1.3.1 *Ortho*-quinones formation by oxidation of phenols: from *oxy*- to *deoxy*-Ty.

The phenol with its oxygen atom binds to CuA leading to a complex in which the substrate is bound to both copper ions by the electrophilic monoxygenation of the ring. This complex forms the *ortho*-quinone and *deoxy*-Ty by homolytic dissociation. The *deoxy*-Ty binding oxygen restores *oxy*-Ty and the phenol-oxidation cycle continues until the substrates (phenol and oxygen) are depleted (figure 6).[16]

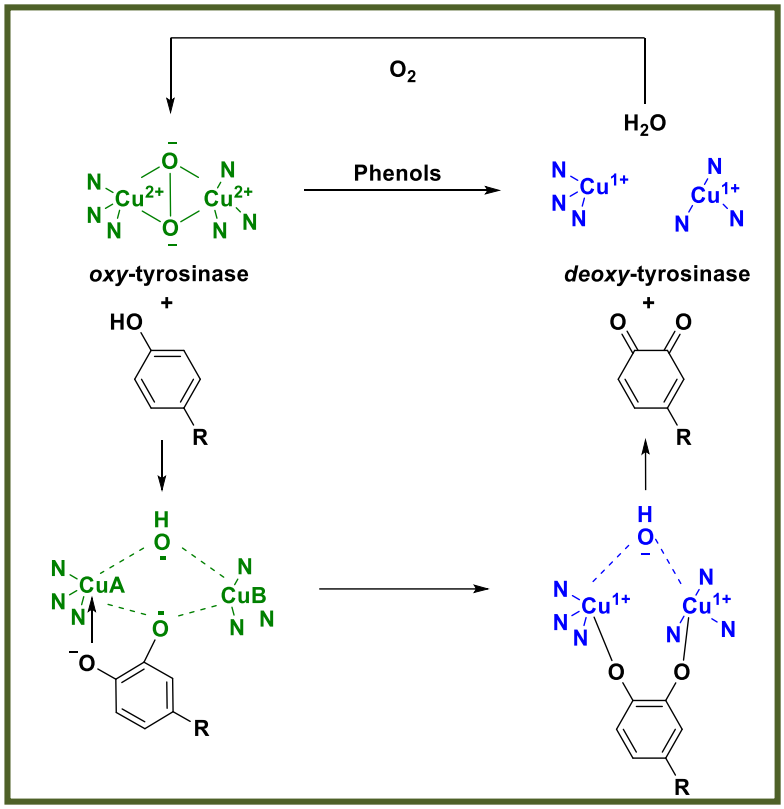

Figure 6: *Ortho*-quinones formation by oxidation of phenols: from *oxy*- to *deoxy*-Ty. Picture modified from reference [16].

1.3.2 *Ortho*-quinones formation by oxidation of catechols: from *oxy*- to *met*-Ty.

Catechols oxidation was proposed to proceed through CuB active site binding, unlike phenols that bind to CuA.[16] However, recent studies on Ty from *Bacillus megaterium* showed that both tyrosine and L-DOPA substrates were similarly oriented toward CuA trough π-π interactions with the second coordinating CuB histidine residue.[1] The oxidation cycle of catechols involves two steps characterized by deprotonation of the hydroxyl groups in which the oxygen atoms are coordinated with both copper atoms. In the first step, in which *oxy*-Ty is converted to *met*-Ty, the catechol/enzyme complex dissociates with the release of one of the oxygen atoms leading to the corresponding *ortho*-quinone and water. The resultant *met* form of the enzyme retains the oxidation state of the active site copper ions [Cu(II)] to which the remaining oxygen atom is coordinated, probably in a protonated form. In the second step of the process, another molecule of catechol reduces the active site copper ions to Cu(I) yielding *deoxy*-Ty and a second molecule of *ortho*-quinone. The oxidation states of the active site copper ions [Cu(II)] are then restored by binding dioxygen (figure 7).[16]

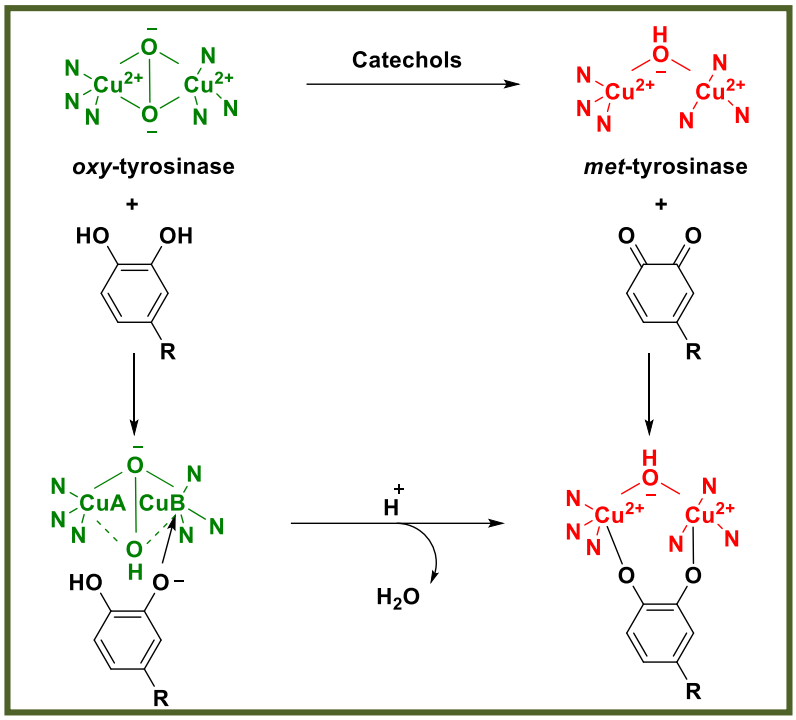

Figure 7: *Ortho*-quinones formation by oxidation of catechols: from *oxy*- to *met*-Ty. Picture modified from reference [16].

1.3.3 Auto-activation and the lag period: from *met*- to *deoxy*-Ty.

The initial *in vitro* monoxidation of phenolic substrate is extremely slow and oxidation slowly accelerates to its maximum velocity during an initial induction period defined as "lag period". In order to allow the binding of oxygen for monooxygenase activity, the copper atoms have to be in the Cu(I) state. The redox potential of copper favors a "resting state" of the active center atoms in the oxidized form $Cu(II)_2$. The activation of the monooxygenase function requires reduction of the active site copper atoms to $Cu(I)_2$. There are four ways which can be followed:

. direct reduction by hydrogen peroxide;

. reduction by a reducing agent such as ascorbate;

. redox exchange with other metals;

. reduction by a catecholic substrate.

The latter of these mechanisms is the most significant pathway (figure 8).[16]

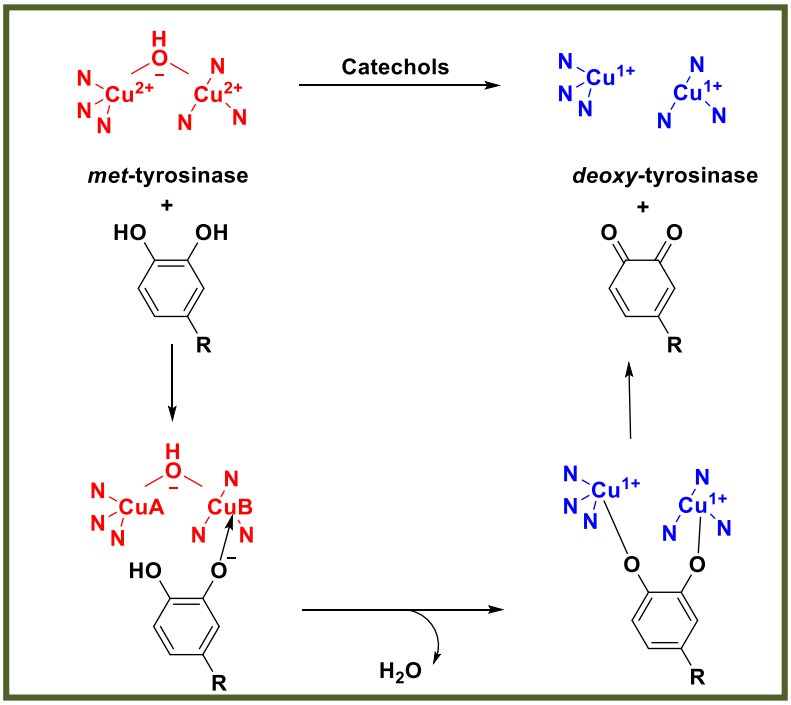

Figure 8: Auto-activation and the lag period: from *met*- to *deoxy*-Ty. Picture modified from reference [16].

The length of the "lag period" depends on several factors: the source of the enzyme; monophenol concentration (it is longer when the concentration of monophenol is growed); the concentration of the enzyme (it decreases with the growing of enzyme concentration but never totally disappearing) and after all, the presence of catalytic amount of *o*-diphenol or transition metal ions that completely abolish the lag period.[14]

1.3.4 Ty inactivation by catechols and resorcinols: from *oxy*- to *deact*-Ty.

Ty inactivation mechanism was proposed to proceed in different ways but not satisfactory explanation was available until 2007 when Land and coworkers proposed that catecholic substrates may sometimes be processed as phenols and oxidized by the monooxygenase pathway.[16, 17] Normally, the monooxygenation of a catechol conducts to the formation of an intermediate, which then gives 3-hydroxyquinone and *deoxy*-Ty. In the presence of an additional hydroxyl substituent, it supplies an alternative method of intermediate fragmentation. The reductive elimination of one of the copper atoms can lead to the deprotonation and quinone formation. This mechanism supports the idea that the inactivation process is related to the initial Ty concentration and, explains how the oxidative activity of Ty diminishes with the loss of half the active-site copper atoms, according to Dietler and Lerch.[18] (figure 9).

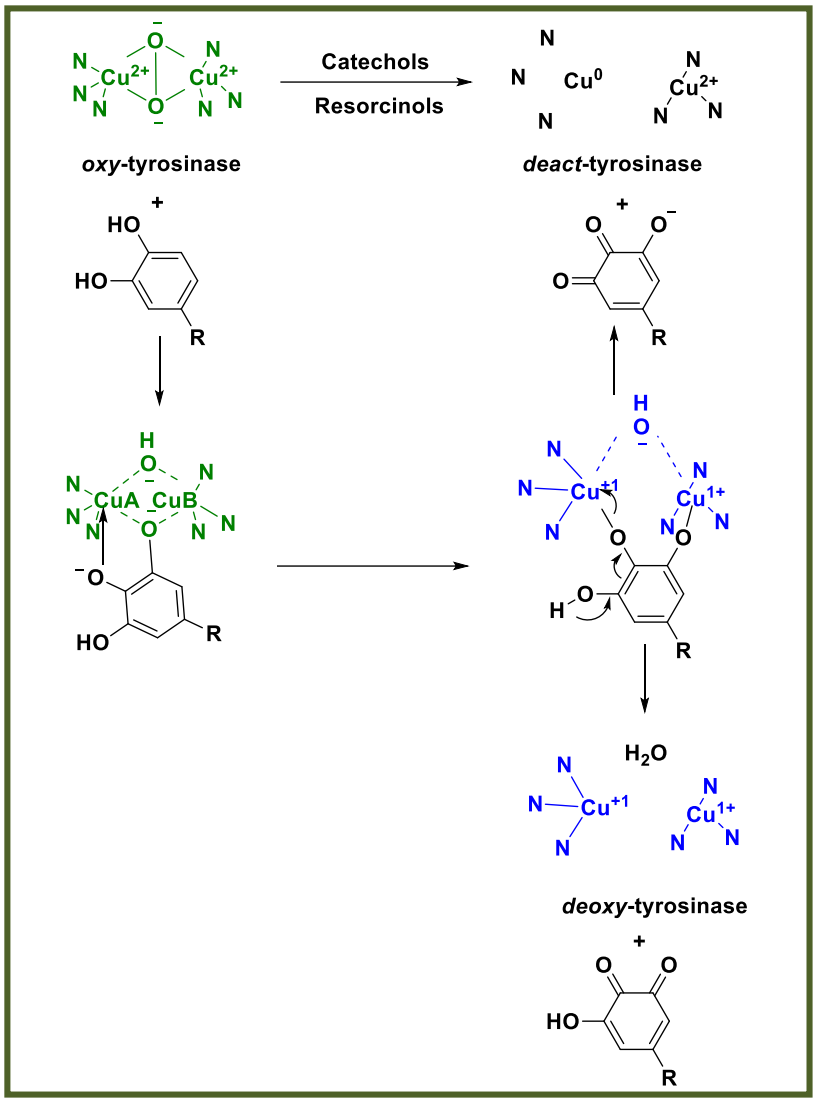

Figure 9: Ty inactivation by catechols and resorcinols: from *oxy*- to *deact*-Ty. Picture modified from reference [16].

1.4 Sources of Tys

As above mentioned, Tys are widespread in nature. They are present in various prokaryotes, as well as, in fungi, mammals, arthropods and plants: in mammals they are responsible for the melanin formation in skin and hair color; in fruits and vegetables for browning, following by cell damage; in plants, sponges and many invertebrates are important for wound healing and primary immune responses; in arthropods they play a crucial role in sclerotization; in bacteria they protect DNA from UV damage.[1]

1.4.1 Tys in Mushrooms

Tys were isolated from different fungus. In particular, from *Agaricus bisporus*,[19] *Neurospora crassa*,[20] *Amanita muscaria*,[21] *Lentinula edodes*,[22] *Aspergillus oryzae*,[23] Portabella mushrooms, *Pycnoporus sanguineus*[24] and *Lentinula boryana*.[25, 26]

1.4.1.1 Ty from *Agaricus bisporus*

Ty from *Agaricus bisporus* (TyM) is characterized by a H_2L_2 tetrameric structure with molecular weight of 120 kDa. In figure 10, the tetrameric structure of TyM co-crystalized with the natural inhibitor tropolone (PDB code 2Y9X) is reported.[27]

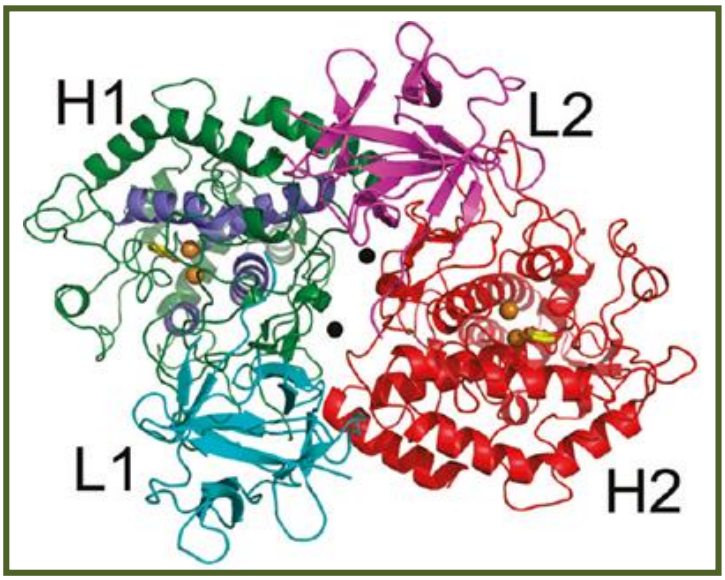

Figure 10: H_2L_2 tetrameric structure of TyM: H-1 (green), L-1 (cyan), H-2 (red) and L-2 (magenta). The holmium stabilizing ions and the copper ions are represented by black and brown spheres respectively; tropolone inhibitor is reported like yellow stick.
Picture modified from reference[27].

The L subunit (14 kDa) possesses a β-trefoil fold, consisting of 12 antiparallel β-strands assembled in a cylindrical barrel of six 2-stranded sheets. The biological role of this subunit is still unknown so, further research is needed. The H subunit (43 kDa) contains 13 α-helices, 8 mostly short β-strands and many loops. Its core structure is similar to the *Bacillus megaterium* Ty. It is larger if compared to the other type 3 copper proteins, possessing 100-120 more residues present in loops connecting the secondary structure elements of the core domain. The H subunit includes the Ty core region,[28] starting with the conserved Arg20 until Tyr365, containing the binuclear copper site, in which each copper ion is coordinated by three histidine residues. This site is located at the

heart of two pairs of antiparallel α-helices, which make an angle of nearly 90°, at the bottom of a spacious cavity in the surface of the H subunit. The first copper ion, CuA, is coordinated from His61, His85 and His94; the second one, CuB from His259, His263 and His296. Four of these His residues (61, 94, 259, 263) make hydrogen bonds with a carbonyl oxygen atom of a peptide, thus restricting their side chain rotational freedom and may contribute to the affinity for the metal. Whereas, His85 makes a thioether bond with Cys83 fixing its side chain orientation. His296 does not possess direct interactions with other protein residues but, its side chain is held in position by a hydrogen bond with an internal water molecule (figure 11).[27]

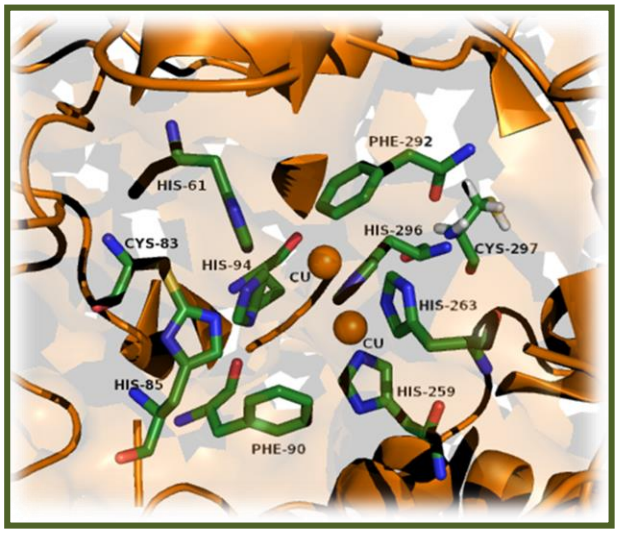

Figure 11: Active site of TyM (PDB code 2Y9X). CuA and CuB copper ions are represented by brown spheres and the main aminoacids of the pocket as green stick. The covalent thioether bond between Cys83 and His85 is shown as yellow stick.
The picture was generated using PyMol.[2]

Some Phe residues are important such as Phe90, which is positioned between His94, His259 and His296 while, Phe292 is placed between His61, His263 and His296, restricting the histidine side-chain conformations to maintain the integrity of the copper binding site.[29] The distance between CuA and CuB is 4.5 ± 0.2 Å, adopting a planar trigonal geometry. A water molecule or hydroxyl bridge binds the two copper ions, completing the four-coordinate trigonal pyramidal coordination sphere for both copper ions. Other important residues present in the active site are His244, Glu256, Asn260 and Ala 286.[27]

1.4.2 Tys in Bacteria

Tys have been reported in several species such as *Streptomyces*,[30] *Rhizobium, Symbiobacterium thermophilum, Pseudomonas maltophilia, Sinorhizobium meliloti, Marinomonas mediterranea, Thermomicrobium roseum, Bacillus thuringiensis*, *Pseudomonas putida*,[31] *Streptomyces castaneoglobisporus, Ralstonia solanacearum*, *Verrucomicrobium spinosum*[32] and *Bacillus megaterium*.[26, 33]

1.4.2.1 Ty from *Bacillus megaterium*

Ty from *Bacillus megaterium* (TyBm) is a homodimer consisting of two ellipsoid asymmetric monomers. The main secondary structure elements are α-helices, with the two copper ions placed at the core of a four-helical bundle. At the interface of the dimer are present some interaction between residues Trp41-Tyr267 and Arg37-Asn270. In particular, a hydrophobic center is formed by the interaction between Trp41-Tyr267 and Trp269-Phe48, including van der Waals and π-π interactions (figure 12).[33]

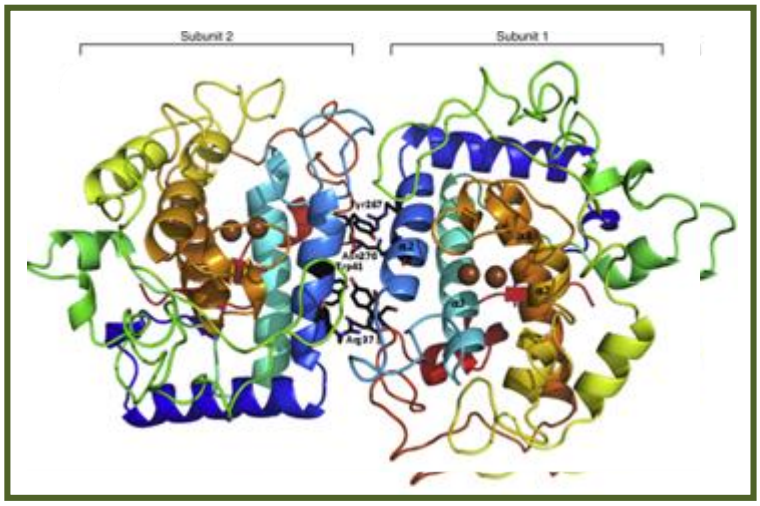

Figure 12: Homodimeric structure of TyBm. The stabilizing residues interactions are represented by black stick; copper ions like brown spheres and the 4 α-helices as a cartoon. Picture modified from reference [33].

The active site of TyBm is relatively exposed and no "placeholder" was identified. However, the Val208 residue, situated on a loop adjacent to CuA, was proposed as a modified gatekeeper controlling the entrance to the active site of TyBm. Movement of Val208 could direct the substrate correctly into the active site. Another important residue seems to be Arg209, positioning in proximity to the entrance of the active site, adjacent to His208. The movement in the position of Arg209 can cause pK_a changes in

the area, which could modulate the catalytic activity in the presence of a substrate. Each copper ion is coordinated by three histidine residues: CuA by His42, His69 and His60; CuB by His204, His208 and His231 (figure 13).[33]

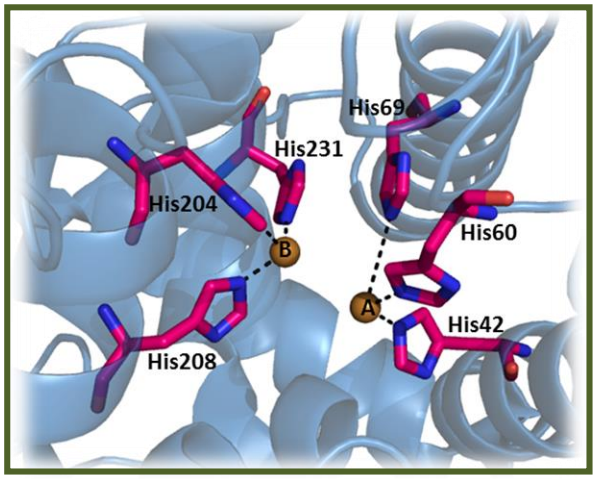

Figure 13: Active site of TyBm (PDB code 3NM8). The His residues are represented as pink stick and copper ions as brown spheres. The picture was generated using PyMol.[2]

1.4.3 Tys in Plants, Vegetables and Fruits

In fruits and vegetables Tys have been extracted from Monastrell grape, apple,[34] sunflower seed,[35] and *Solanum melongena*.[36] In plants, Tys are localized in the chloroplasts of healthy plant tissues, whereas its substrates are contained in the vacuole. *Portulaca grandiflora* (Portulacaceae) is a potent source of Tys.[37] It generally causes undesired enzymatic browning of farm products which subsequently leads to a significant decrease in the nutritional and market values. Since in plants the enzyme cannot catalyze the hydroxylation of monophenols, it only shows the diphenolase activity and, for this reason, it is called catechol oxidase (instead of Ty).[1]

1.4.4 Tys in Mammals

In mammals the Tys proteins family is composed of three members: the authentic Ty and two related proteins (TYRPs) named TYRP1 and TYRP2, respectively. All the three members of this family are metal-containing glycoproteins with a single transmembrane α-helix. They possess a common architecture of the tridimensional structure and are anchored to the melanosomal membrane through a *C*-terminal fragment sharing approximately 40% aminoacid identity and 70% similarity (figure 14).[38]

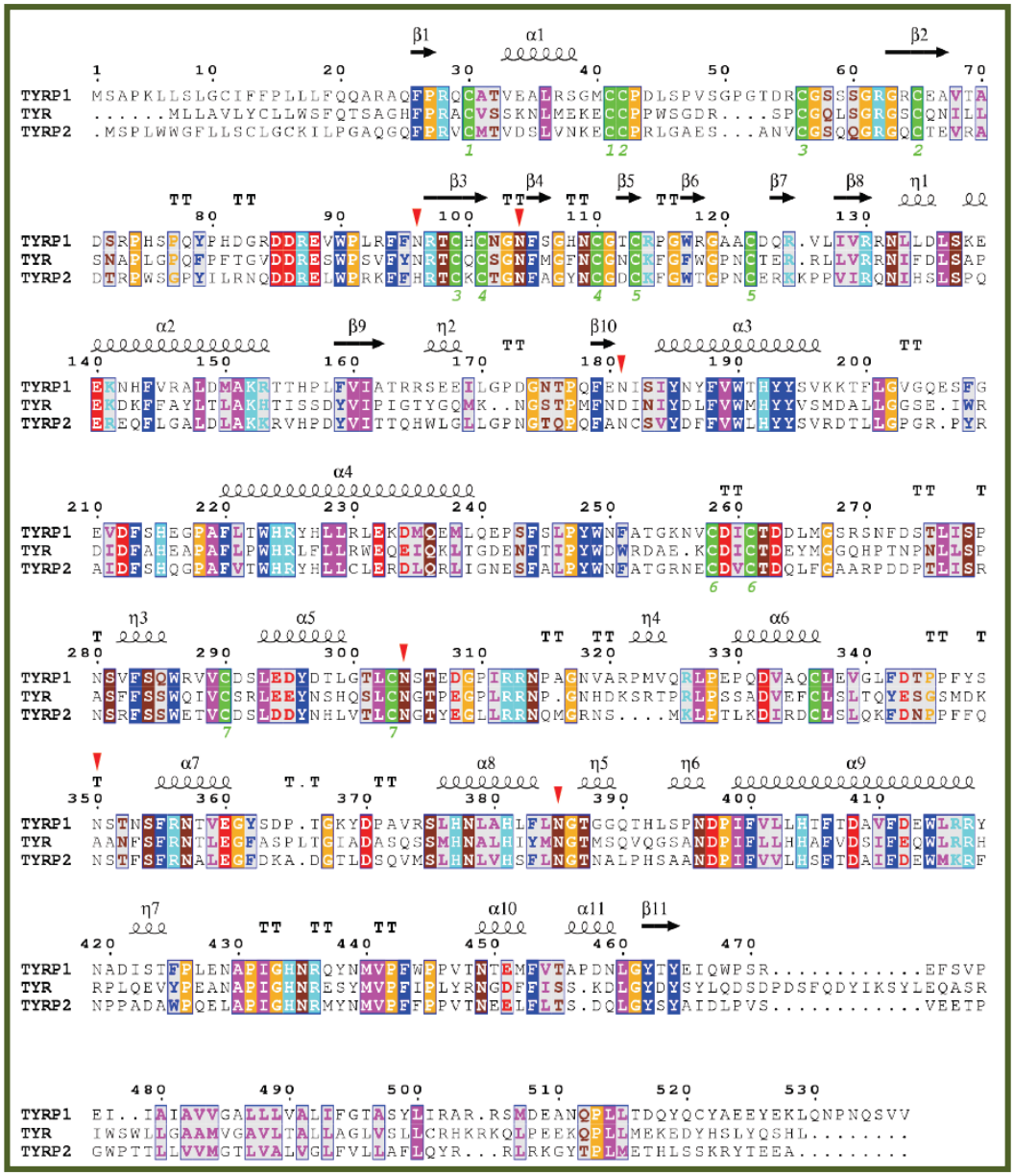

Figure 14: Alignment of human Ty and Ty-related proteins: amino acidic sequences. Picture modified from reference [38].

The Ty and TYRPs structures are composed by four conserved regions: *N*-terminal signal peptide, a large intra-melanosomal domain, a single transmembrane α-helix and a small, flexible *C*-terminal cytoplasmic domain. The intra-melanosomal domain contains a cysteine (Cys)-rich subdomain and a catalytic tyrosinase-like subdomain with two metal ion-binding sites. The Cys-rich domain is only found in mammalian Ty and TYRPs and is composed by an "EGF-like" region (epidermal growth factor) and another Cys-rich fragment at the central part of the sequence, between the two metal binding sites. Its core structure is formed by two pairs of short antiparallel β-strands from which a long loops emerge. It interacts with the tyrosinase-like subdomain *via* its

N-terminus and a long loop emerging from the EGF-like core and it is located far from the active site, at the opposite side of the molecule, suggesting that it unlikely affects the catalytic activity of TYRP1. The bulk of the protein is a globular intramelanosomal domain followed by a single transmembrane fragment and a small *C*-terminal tail oriented to the cytosol of melanocytes. The intramelanosomal domains of the three proteins are similar in length and contain a binuclear metal ion-binding motif with six conserved His residues. However, the *C*-terminal tails show very low homology and they were used to generate specific antibodies, PEP1, PEP7 and PEP8 for TYRP1, Ty and TYRP2, respectively. The specific reactivity of these antibodies against each *C*-tail allowed the differentiation, characterization and quantitation of the three proteins. The human melanogenic enzymes contain six or seven putative *N*-glycosylation sites, which are important for the proteins maturation. Ty contains seven N-glycosylation motifs (at Asn 86, 111, 161, 230, 290, 337, 371). TYRP1 has six sites (at Asn 96, 104, 181, 304, 350, 385), all glycosylated with various lengths of carbohydrate chains in the crystal structure. TYRP2 also contains six *N*-glycosylation motifs (at Asn 170, 178, 237, 300, 342, 377), four equivalent to the TYRP1 sites.[3, 38]

1.4.4.1 Human Ty

Unfortunately, no crystal structure of human Ty (TyH) is available and its precise catalytic mechanism is still under debate.[39] Nevertheless, a good model of TyH was generated on the basis of TYRP1 crystal structure co-crystallized with tyrosine substrate.[40] Assuming that tyrosine binds equally to TyH and TYRP1, the model suggests that the *p*-hydroxyl group interacts with the water molecule present between the two copper ions and with a serine residue (Ser394 in TYRP1 and Ser380 in TyH). Moreover, this serine residue seems to have an important role in substrate activation (figure 15).[38]

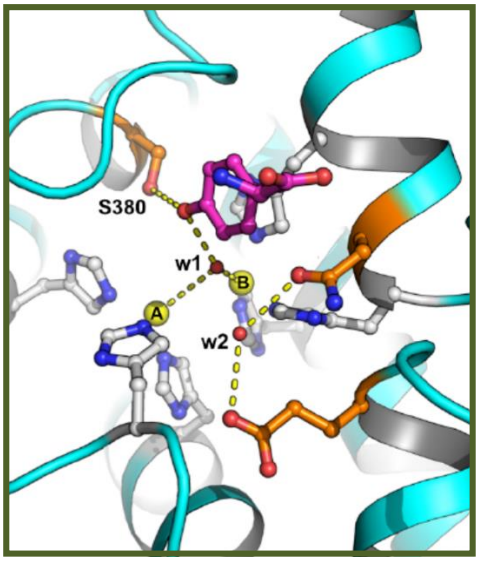

Figure 15: TyH model generated on the basis of TYRP1 crystal structure.
Picture modified from reference [38].

1.4.4.2 TYRP1

TYRP1 is a redox enzyme although it is unclear the reaction that it catalyzes. However, the most accepted function attributed to TYRP1 was the DHICA (5,6-dihydroxyindole-2-carboxylic acid) oxidase activity needed after TYRP2 action in the distal phase of melanogenesis.[41] It has a globular compact shape with strict interactions between the Cys-rich and Ty subdomains. The Ty-like subdomain possesses a four-helix bundle connected by long loops; it is similar to TyBm sharing 32% sequence identity. Two disulfide bonds stabilize the Ty subdomain. The core of Cys-rich subdomain has an epidermal growth factor (EGF)-like fold similar to the structure of the human epidermal growth factor, formed by two pairs of short antiparallel β-strands from which long loops emerge. They are stabilized by disulfide bonds. The subdomain associated with Ty-like subdomain is located far from the active site, at the opposite side of the molecule, making a direct effect on the activity of TYRP1. The active site contains two Zn ions instead of Cu (figure 16).[40]

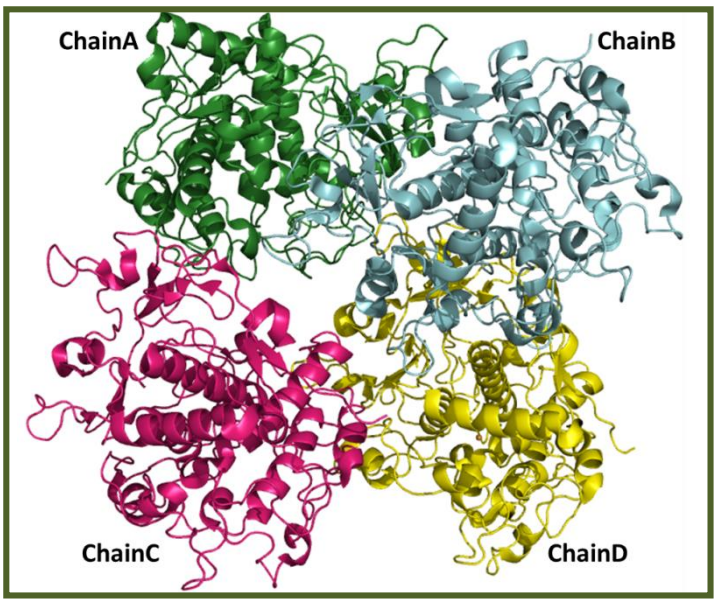

Figure 16: TYRP1 crystal structure (PDB code 5M8L). The four chains are represented as cartoon. The picture was generated using PyMol.[2]

Interestingly, TYRP1 binds typical Ty substrates and inhibitors (tyrosine, mimosine, kojic acid and tropolone). The binding of these compounds occurs via aromatic stacking interactions with His381, ligation of their keto- and hydroxyl groups to the zinc ions and hydrogen-bonding interactions with Ser394.[3, 38, 40]

1.4.4.3 TYRP2

TYRP2 contains two zinc ions in the active site. The TYRP2 gene was attributed to the enzyme dopachrome tautomerase which catalyzes the conversion of dopachrome to DHICA.[42-44] Tautomerization is a type of isomerization rearranging dopachrome to DHICA, rather than to DHI (5,6-dihydroxyindole) which is generated spontaneously by decarboxylation.[3] Dopachrome with its two hydroxyl groups was proposed to bind the zinc ions in a bidentate mode, each displacing a water molecule (figure 17).[40, 45] DHI is less stable and more toxic than DHICA:[46] in the eumelanin biosynthetic pathway it has an important role as regulatory control, preventing cytotoxicity and premature cell death.[47] The cytotoxicity of DHI has been exploited as a targeting concept in experimental melanoma therapy.[3]

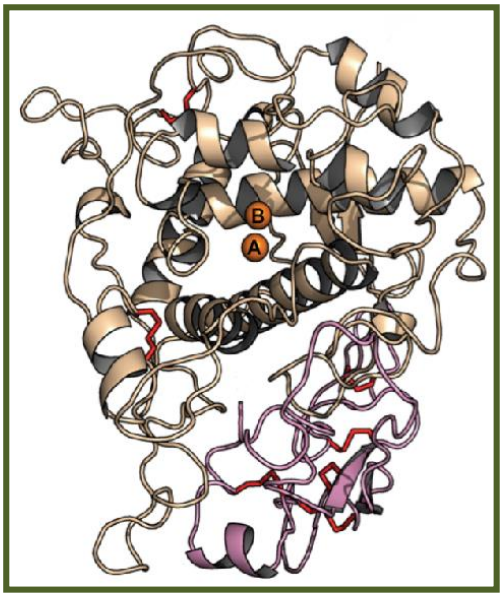

Figure 17: Homology model of intramelanosomal domain of TYRP2 based on crystal structure of TYRP1. Picture modified from reference [38].

1.5 Melanin

Ty is the key enzyme of melanin biosynthesis, performing a crucial role in skin, hair, eyes pigmentation and in skin protection from UV radiations.[48]

Melanogenesis can be regulated at three different levels:

1. Gene: Melanocytes migrate to the epidermis and hair follicles during embryo development.
2. Cellular: Melanosomes regulate melanogenesis according to their size, number and densities.
3. Subcellular: Gene expression defined by Ty, TYRP1, and TYRP2 enzymes controls melanogenesis at subcellular level.[49]

Despite the complexity of melanin biosynthetic pathway, the only limiting step is the conversion of *L*-tyrosine to *L*-DOPA since, in presence of oxygen, the subsequent reactions occur spontaneously at physiological pH value.[50] Melanocytes can produce different kind of melanin (figure 18):

- **Eumelanin**: It is a black or brown pigment and it is produced by the intramolecular cyclization of L-dopaquinone amine group, leading to the formation of the indole leukodopachrome (cicloDOPA). The redox reaction between leukodopachrome and *L*-dopaquinone leads to dopachrome and *L*-DOPA. Dopachrome decomposes gradually to give DHI or, can undergo enzymatic transformation by dopacromo-

tautomerase, thus forming DHICA. The dihydroxyindole DHI and DHICA are subsequently oxidized to eumelanin.[51]

- **Feomelanin**: It is a yellow or red pigment and it is produced from *L*-dopaquinone by addition of thiolic compound (generally cysteine or glutathione) producing 5-*S*-cysteinyl-dopa or glutationildopa. Subsequent oxidations give the benzothiazine intermediate 1,4-benzothiazinylalanine and then feomelanin (figure 18).[51]
- **Allomelanin**: It is a dark pigment and it is the less studied and most heterogeneous class of melanin pigments. It derives from phenolic monomers unlike tyrosine and does not contain dopaquinone-derived motifs in its structure based on other chinoid building blocks. Generally, it does not present nitrogen atoms and may have different characteristics depending on the organisms that we take into account. It can originate from catechols (especially in plants), 4-hydroxyphenylacetate (in some bacteria) or dihydroxynaphthalene (especially in microorganisms). In rare cases, allomelanin contains units of meta-diphenol unlike the usual *ortho* and *para* positions occupied in eumelanine.[14]

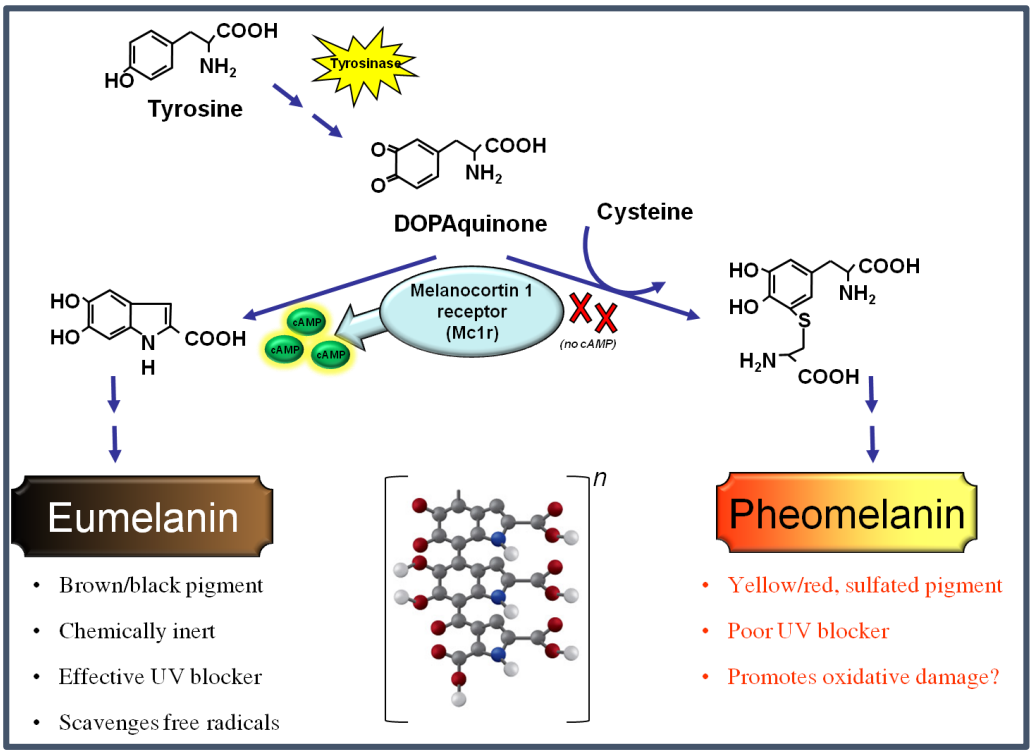

Figure 18: Biosynthetic pathway of melanin pigments.

In addition, another type of melanin is the neuromelanin, a dark pigment present in the brain in the substantia nigra-pars compacta, the locus ceruleus, the dorsal motor nucleus of the vagus nerve (cranial nerve X) and medial nuclei of the raphe. Ty constitutes also the key enzyme in the biosynthetic pathway of neuromelanin, thus it seems involved in Parkinson's diseases.[52-54]

CHAPTER 2 TYROSINASE INHIBITION

Introduction

Although a significant number of TyIs were identified so far, developing new agents featuring drug-like properties is an urgently demanded task. Unfortunately, only few of the known TyIs could reach clinical applications as skin-whitening agents, due to safety concerns and weak whitening effects.[49, 55]

2.1 Different approaches for hyperpigmentation treatment

Suppression of melanin production by melanocytes represents an approach for the hyperpigmentation treatment. Ty is the enzyme that directly modulates the amount of melanin production. Thus, an interesting approach to treat these disorders is regulating the Ty activity through: the transcription of its mRNA, its maturation via asparagine-linked oligosaccharide processing, the modulation of its catalytic activity and/or its degradation.[56]

2.1.1 Inhibition of Ty mRNA transcription

One of the possible approaches that can be used to decrease Ty activity is the regulation of the transcription of its encoding gene. Decreases of Ty mRNA levels in cultured melanoma cells can be induced by incubation with the thymidine analogs such as: 5-bromodeoxyuridine,[57] tumor promoter 12-*O*-tetradecanoylphorbol-13-acetate,[58-60] transforming growth factor β1 (TGF-β1)[61] necrosis factor α (TNF-α).[62] To reduce the production of melanin level it is possible also to use factors enabling the decrease of levels of mRNAs encoding Ty and/or microphthalmia associated transcription factor in cultured melanoma cells, melanocytes or melanoblasts.[63] Examples of these factors are: hydrogen peroxide,[64] ceramide,[65] and lysophosphatidic acid.[56, 66]

2.1.2 Aberrant Ty maturation

Human and murine Tys are glycoproteins with six highly conserved *N*-glycosylation sites. An abnormal glycosylation process in the endoplasmic reticulum (ER) or in the Golgi apparatus inhibits the correct protein folding and maturation, leading to hypopigmentation. Therefore, glycosylation inhibitors, such as glucosamine and

tunicamycin, inhibit the melanin synthesis in cultured melanoma cells with no apparent decrease in Ty levels.[67] Glutathione,[68] ferritin,[56] feldamycin[69] and calcium *D*-pantetheine-*S*-sulfonate[70] showed the same effect. *N*-Butyldeoxinojirimicin, acting as inhibitor of the ER-processing enzymes α-glucosidases I and II, blocks the Ty activity in B16 melanoma cells with little appreciable change in Ty level.[56, 71-73]

2.1.3 Increase of Ty degradation rate

The Ty synthesis and degradation are related processes influencing enzyme activity. When a TyI decreases the Ty level, acting also on its mRNA levels, it accelerates the degradation rate of Ty. Previously it was reported that the rate of enzymatic degradation increases as a consequence of the acidification of the melanoma cell culture medium, indicating that the degradation of the enzyme may depend on the environmental conditions surrounding the melanocytic cells.[74] Several intrinsic factors in the epidermis and other factors can regulate Ty degradation, such as[56]:

- **TGF-β1**: Keratinocytes synthesize and secrete numerous cytokines such as IL-1α, TNF-α[75] and TGF-β1.[76] Among them, TGF-β1 increases in a dose-dependent manner Ty inhibition and TYRP1 activity in B16 melanoma cells following treatment with cycloheximide.[56, 61]
- **TNF-α**: TNF-α is a cytokine present at the epidermal and dermal level, secreted during inflammatory processes or even in response to UV exposure. Although its role is not yet clear, recent studies suggested that this cytokine decreases the stability of Ty and TYRP1 reducing the levels of the corresponding mRNA.[56, 62]
- **Linoleic acid**: It is an unsaturated fatty acid (C18:2) representing the major component of biological cell membrane. Its topical application causes a decrease in UV-induced skin hyperpigmentation. Linoleic acid increases the degradation of Ty with little change in mRNA Ty levels.[56, 60]
- **2,2'-Dihydroxy-5-5'-dipropyl-biphenyl**: It is a phenolic compound decreasing melanin synthesis by degradation of Ty in cultured melanoma cells.[56, 77]
- **Tetradecanoylphorbol-13-acetate/phospholipase D2**: Tetradecanoylphorbol-13-acetate activates phospholipase D2 that is an enzyme which hydrolyzes phosphatidylcholine to generate phosphatidic acid. The over expression of phospholipase D2 decreases Ty levels in cultured melanoma cells.[56, 78]

- **25-Hydroxycholesterol**: It is an oxysterol regulating cholesterol homeostasis which decreases melanin synthesis in mouse melanocytes enhancing Ty degradation *via* a proteasome-independent mechanism.[56, 79]
- **Phenylthiourea (PTU)**: PTU is a potent Ty inhibitor decreasing the stability of the enzyme in a similar way of linoleic acid.[56, 80]

2.1.4 Indirect regulation of Ty activity

Skin pigmentation depends on environmental factors external to melanocytes, apart from the intracellular regulation of Ty activity. Thus, melanin synthesis can be also modulated by the indirect regulation of Ty activity. An example is given by the inhibition of cell-to-cell communication between keratinocytes and melanocytes. This process, that normally activates melanogenesis through paracrine cytokines, such as endothelin-1, can be inhibited with: chamomilla extract;[81] inflammation inhibitors such as glabridin;[82] *trans*-4-aminomethylcyclohexanecarboxylic acid, known as tranexamic acid.[56, 83]

2.1.5 Inhibition of Ty catalytic activity

In the last twenty years, numerous TyIs have been identified, from both natural and synthetic sources. Often the definition of "tyrosinase inhibitor" can be too general and non specific, since it is sometimes used in reference to inhibitors of melanogenesis, whose action mainly resides in some interference in melanin formation, independently of any direct inhibition of the enzyme. The inhibition of Ty activity, observed experimentally, may be the result of different mechanisms of action. Thus, it is possible to classify the inhibitors in six different categories[14]:

1. **Reducing agents**: They reduce dopaquinone to its *L*-dopa precursor avoiding the subsequent formation of dopachrome and therefore of melanin. An inhibitor acting with this mechanism is, for example, ascorbic acid.
2. ***o*-Dopaquinone scavengers**: They are for example thio-containing compounds, which react with *o*-dopaquinone forming colorless products. As a result, the melanogenic process is slowed until the inhibitors are completely consumed.
3. **Alternative enzyme substrates**: Among them there are some phenolic compounds, whose reaction products absorb in a different spectral range than dopachrome.

When these phenolic compounds show a good affinity towards the enzyme, the formation of the dopachrome is prevented and, for this reason, they are often erroneously classified as inhibitors.

4. **Non-specific enzymatic inactivators**: They non-specifically denature the enzyme inhibiting its activity. They are for examples bases or acids.
5. **Specific Ty inactivators**: *E.g.* suicidal inactivators (or mechanism-based inactivators). They act as substrates of Ty and form covalent bond with the enzyme causing an irreversible inhibition of activity.
6. **Specific Ty inhibitors**: They reversibly bind the enzyme reducing its catalytic activity.

Among these six different classes of compounds only the specific Ty inactivators (**5**) and the specific Ty inhibitors (**6**) are considered "true inhibitors", since they are able to bind the enzyme and inhibit its activity.[14]

2.2 Ty "true inhibitors"

The "true" TyIs are compounds able to bind the enzyme and inhibit its activity. Among them are reported derivatives from both natural and synthetic sources. Commonly, TyIs activity is assayed trough *in vitro* studies employing TyM commercially available and using kojic acid as reference compound (IC_{50} = 17.76 µM).[84] Kojic acid (5-hydroxy-2-(hydroxymethyl)-gamma-pyrone) is a fungal metabolite isolated from various species of *Aspergillus niger* and *penicillum*.[85] It acts as a good chelator for transition metal ions and a good "scavenger" of free radicals. It is employed as a whitening cosmetic agent for the skin and as a food additive to prevent enzymatic browning, although its usage in cosmetic is limited due to its instability and side effects.[86]

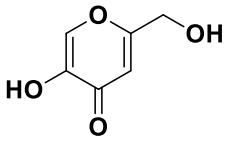

Kojic acid

Considering the mechanisms of action, TyIs can be classified into four classes (figure 19):

- **Competitive inhibitor**: It is a substance that binds the active site of the enzyme in a manner that prevent substrate engaging. It might be a copper chelator, non-metabolizable analog or derivative of the true substrate.
- **Uncompetitive inhibitor**: It is a compound that can bind only to the enzyme-substrate complex.
- **Non-competitive inhibitor**: It is a substance that binds the enzyme not in the catalytic site but in a different place compared to the substrates.
- **Mixed inhibitor (competitive and uncompetitive)**: It is a compound that can bind not only the free enzyme but also the enzyme-substrate complex. For most mixed-type inhibitors, the equilibrium binding constants for the free enzyme and the enzyme-substrate complex, respectively, are different.[14]

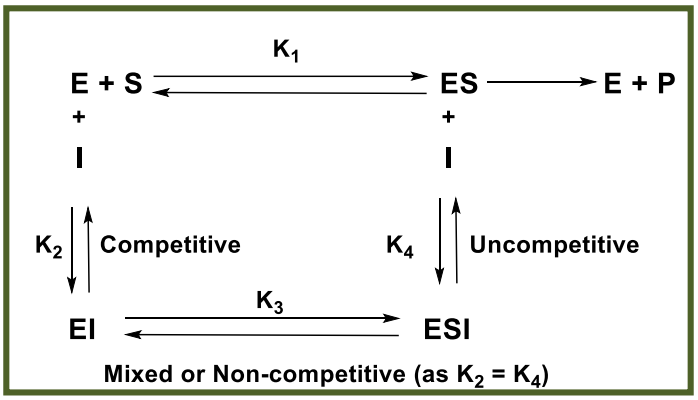

Figure 19: Mechanisms of action of reversible inhibitors. E, S, I and P represent the enzyme, substrate, inhibitor and product respectively; ES is the enzyme-substrate complex; EI e ESI are the inhibitor-enzyme complex and enzyme-substrate-inhibitor.
Picture modified from reference [14].

Another kind of inhibitors are the irreversible ones. They are also called specific inactivators, forming a reversible non-covalent complex with the enzyme (EI or ESI), that then reacts to produce the covalently modified "dead-end complex" E_i. The rate at which E_i is formed is called the inactivation rate or k_{inact} (figure 20). Irreversible inhibitors display time-dependent inhibition, and their potency cannot be characterized by an IC_{50} value. This is because the amount of active enzyme in a given concentration of irreversible inhibitor will be different depending on how long the inhibitor is pre-incubated with the enzyme. In contrast to the huge number of reversible inhibitors that have been identified, rarely irreversible inhibitors of Ty were found until now.[14]

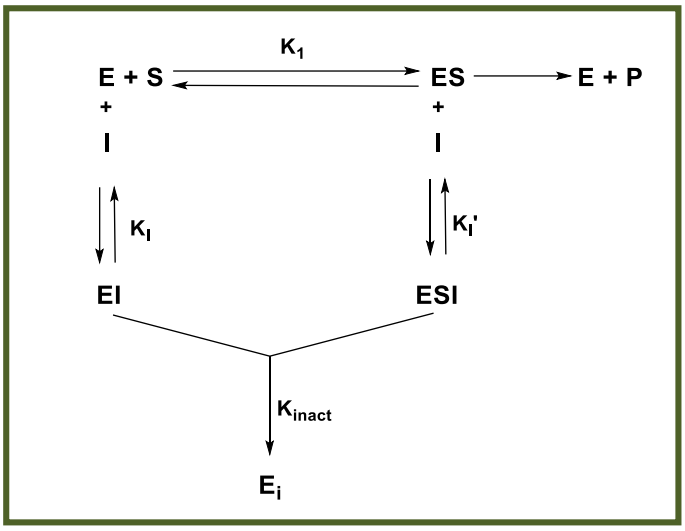

Figure 20: Mechanism of action of irreversible inhibitors. E and E_i represent the enzyme and the inactivate enzyme respectively; S, I and P are the substrate, inhibitor and product; ES, EI and ESI are the intermediates. Picture modified from reference [14].

Suicide substrates belong to the family of irreversible inhibitors. The mechanism of action of the suicide substrate has been extensively studied by Waley,[87] who proposed a simple branched reaction pathway as reported in figure 21, in which an intermediate Y may give either an active enzyme and product, or an inactive enzyme. The intermediate Y has a choice of reaction, governed by the partition ratio r, where r = (k+3)/(k+4). The r value is referred as the molar proportion for inactivation, *i.e.*, the number of molecules of inhibitors required to completely inactivate one molecule of the enzyme. It may be determined by plotting the fractional activity remaining against the ratio of the initial concentration of inhibitor to that of the enzyme. The intercept on the abscissa is 1 + r in the plot, when r > 1.[88] As in general irreversible inhibitors, the inhibitory strength of a suicide substrate is also not determined by an IC_{50} value but expressed by its r value, where a smaller r value of a suicide substrate means fewer inhibitor molecules are needed to inactivate all the enzyme activity and being more powerful inhibition.[14]

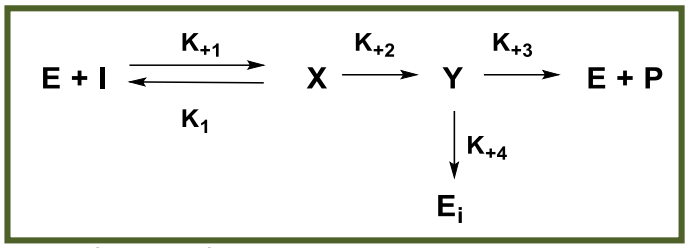

Figure 21: Mechanism of action of suicide substrates. E and E_i represent the enzyme and the inactivate enzyme respectively; P is the product; X is the first intermediate and Y is another intermediate. Picture modified from reference [14].

The primary canon to take into account to evaluate an inhibitor, in addition to the mechanism of action, is its inhibitory strength. It is usually expressed as the inhibitory IC_{50} value, which is the concentration of an inhibitor needed to inhibit half of the enzyme activity in the tested condition.[14] The K_i value represents the ligand-binding affinity to the enzyme. The lower K_i value means higher binding affinity, whereas higher K_i values means lower binding affinity. The K_i value for non-competitive inhibitors is essentially the same numerical value as the IC_{50} of the inhibitors, whereas for competitive inhibitors, the K_i is about one-half that of the numerical values of IC_{50}.[55]

2.2.1 Polyphenols

Polyphenols are a group of compounds containing multiple phenolic moieties. Flavonoids are the most numerous and best-studied polyphenols: they are present in the leaves, seeds, barks and flowers of plants and are responsible for the characteristic red and blue colors of berries, wines and certain vegetables. Flavonoids can be divided into seven groups: flavones, flavonols, flavanones, flavanols, isoflavonoids, chalcones and chatechin.[14] The general structure of flavonoids is reported in figure 22: they differ in the conjugation of A and B rings and in the arrangement of the substituents, such as hydroxyl, methoxy, glycosides *etc.*[86]

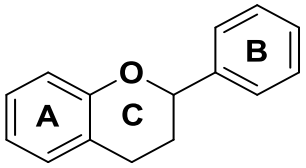

Figure 22: General structure of flavonoids.

Some flavonoids such as kaempferol,[89] quercetin[90] and morin[91] possess inhibitory activity against Ty, while other such as catechin and rhamnetin act as substrates suppressing Ty activity like a cofactor[92] or acting as a free radical scavenger such as rhamnetin.[86, 93]

2.2.1.1 Flavonols

Usually they are competitive inhibitors and their 3-hydroxy-4-keto moiety has a key role in copper chelation.[89, 94] Important flavonols are quercetin, myricetin, kaempferol.[91, 95] A synthetic derivative of kaempferol, 6-hydroxykaempferol resulted two times more active than kaempferol.[96] Although many flavonols have been identified as TyIs, the most active of these, quercetin, showed only 20% of the inhibitory strength of kojic acid. Thus, they have little potential in applications of skin whitening or food antibrowning.

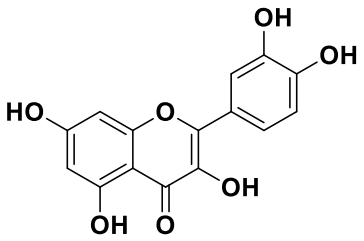

Quercetin

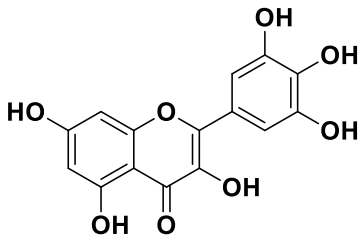

Myricetin

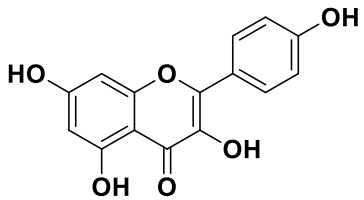

Kaempferol

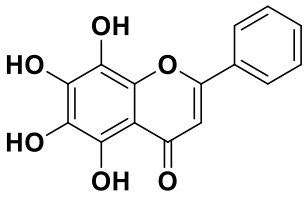

6-Hidroxy-kaempferol

2.2.1.2 Flavones, flavanones and flavanols

Citrus species extracts contain a huge number of flavonoids such as nobiletin (5,6,7,8,3',4'-hexamethoxyflavone), naringin (5,7,4'-trihydroxyflavone) and the neohesperidin (5,7,3'-trihydroxy-4'-methoxyflavone), but they possess low inhibitory activity compared to kojic acid.[97, 98]

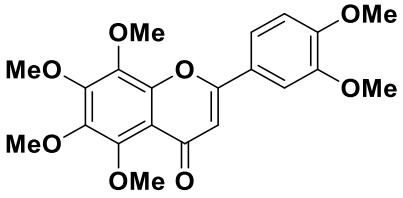

Nobiletin

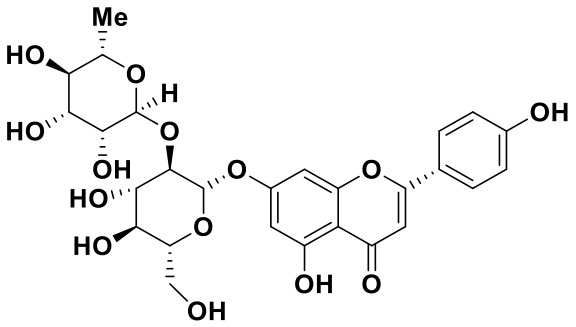

Naringin

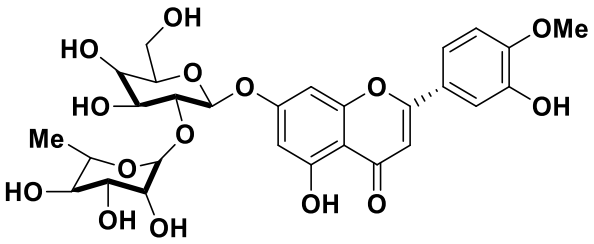

Neoesperidin

Also *Morus* species extracts contain flavonoids: norartocarpetin (5,7,2',4'-tetrahydroxyflavone), isolated from the steam barks, is 10.4-fold more active than kojic acid;[99] streppogenin (5,7,2',4'-tetrahydroxyflavanone) is a flavanone extracted from the roots of the plant possessing a very similar chemical structure than norartocarpetin (flavone) and thus similar activity against TyM.[100]

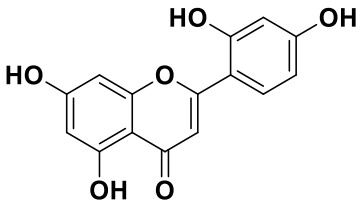

Norartocarpetin

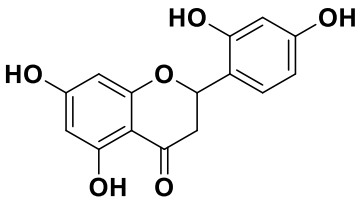

Streppogenin

Other two potent inhibitors are dihydromorin (5,7,2',4'-tetrahydroxyflavanol) and artocarpetin (5,2',4'-trihydroxy-7-methoxyflavone) isolated from *Artocarpus heterophyllus* wood.[101, 102]

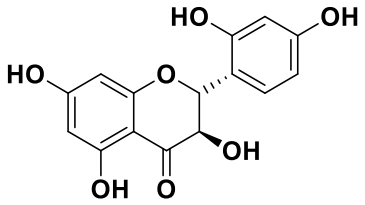

Dihydromorin

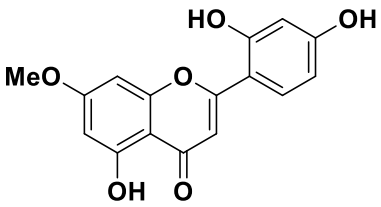

Artocarpetin

Taxifolin (5,7,3',4'-tetrahydroxyflavanol) instead, was isolated from the sprout of *Polygonum hydropiper* showing the same inhibitory activity of kojic acid.[103]

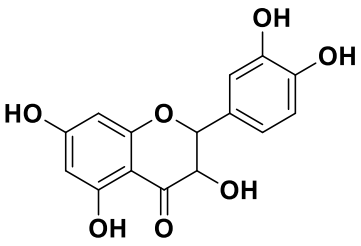

Taxifolin

In addition to the monomers, a flavone-flavanone dimer was isolated from marine plants *Garcinia subelliptica*, being 3.6-fold more active than kojic acid.[104]

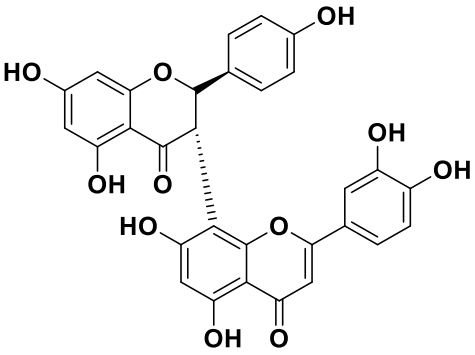

Flavone-flavone dimer

2.2.1.3 Isoflavonoids

A general structure of isoflavonoids is illustrated in figure 23. Chang *et al*.[14] reported that the number and position of hydroxyl groups in the A ring can affect both the mode and inhibitory strength of different compounds. An isoflavone presenting hydroxyl groups in both C6 and C7 of A ring increases more than ten times both the inhibitory activity and the affinity in comparison with isoflavones that have not

hydroxyl groups in A ring or only on the C7. Switching hydroxyl groups on C7 and C8 the mode of action completely changes, passing from a reversible competitive to an irreversible suicide form.

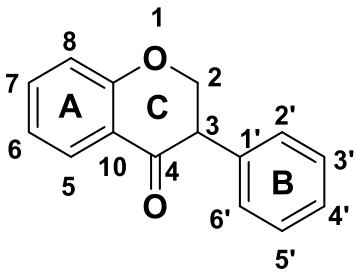

Figure 23: Isoflavonoids general structure.

From the roots of *Glycyrrhiza* species different isoflavonoids with Ty inhibitory activity were isolated. Among them, glabridine, a non-competitive inhibitor, resulted 15-fold more active than kojic acid.[82] Glyasperin C was isolated from the same part of the plant presenting an inhibitory activity 2-fold more than glabridine.[105]

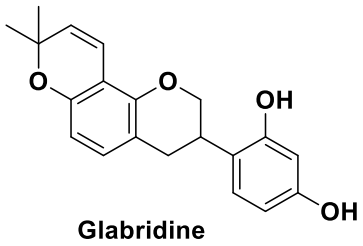

Glabridine

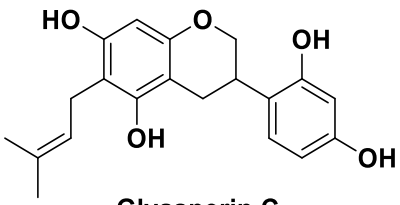

Glyasperin C

Lee *et al*. reported three TyIs extracted from *Lespedeza cyrtobotrya*: haginin A (2',3'-dimethoxy-7,4'-dihydroxyisoflav-3-ene) is a non-competitive inhibitor 10-fold more active than kojic acid; dalbergioidin (5,7,2',4'-tetrahyroxyisoflavan) is a non-competitive inhibitor; calycosin (4'-methoxy-7,4'-dihydroxyisoflavone) possesses inhibitory activity comparable to that of kojic acid showing two different mechanisms of action: inhibition of the enzyme activity and reduction of its expression.[106, 107]

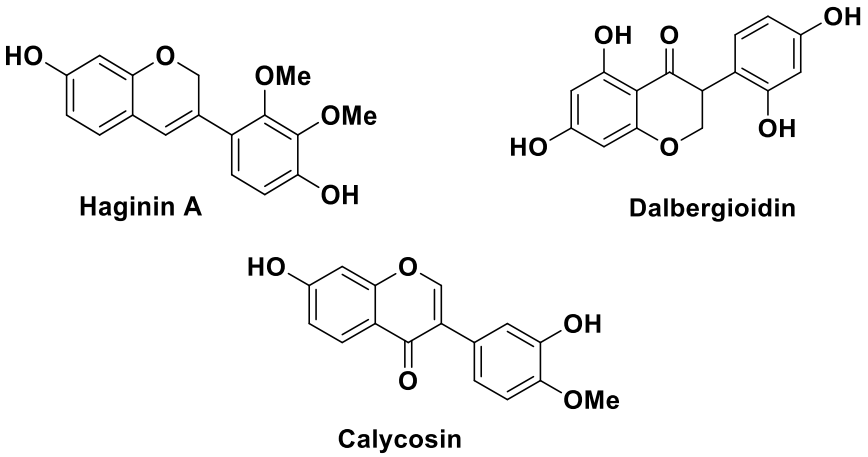

2.2.1.4 Chalcones

They are characterized by two aromatic rings in *trans* configuration separated by three carbon atoms, two of them linked through a double bond and the third is a carbonyl group (figure 24).

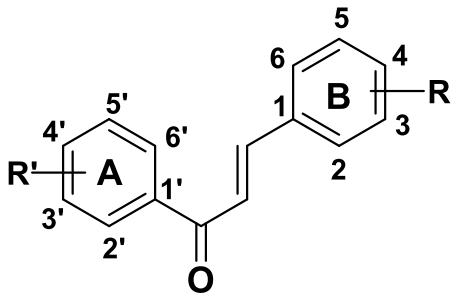

Figure 24: General structure of chalcones.

From the roots of various species of *Glycyrrhiza* were isolated three chalcones derivatives including: licuraside, isoliquiritin and licochalcone A, the last one resulted 5.4-fold more active than kojic acid.[108]

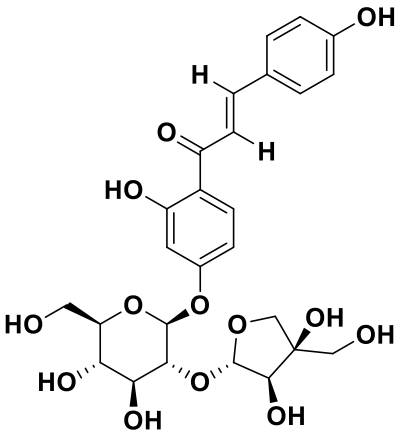

Licuraside

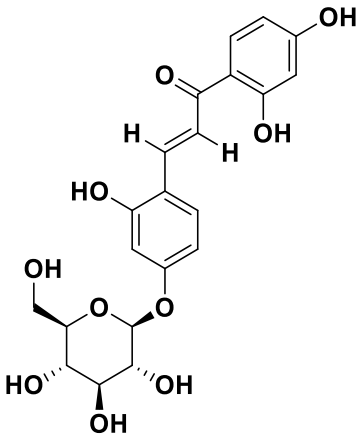

Isoliquiritin

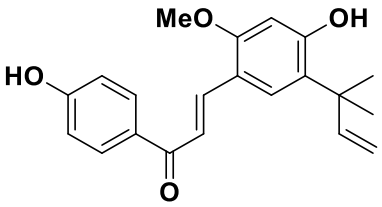

Licochalcone A

Another potent inhibitor isolated from *Sophora flavescens* is kuraridin, which is 34-fold more active than kojic acid.[108]

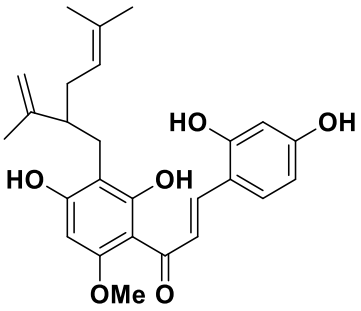

Kuraridin

Recently, 2,4,2',4'-tetrahydroxy-3-(3-methyl-2-butenyl)-chalcone (TMBC) extracted from the stems of *Morus nigra*, has proved to be a potent inhibitor being 26-fold more potent than kojic acid.[109] The 4-resorcinol moiety (2,4-dihydroxyl group) in the aromatic ring detains a crucial role in chalcones inhibitory activity.[110, 111] Moreover, the simultaneous presence of a lipophilic moiety can contribute to increase the activity.[14]

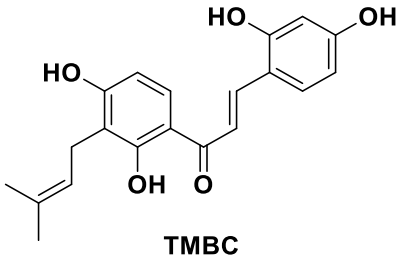

TMBC

Some natural chalcones isolated from *Morus australis* resulted good TyIs. In particular, compound **1** resulted more potent than arbutin (IC_{50}= 164 µM) with an IC_{50} value of 0.21 µM.[49, 112]

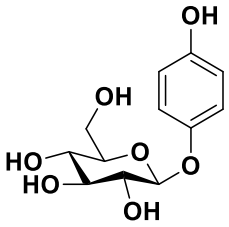

Arbutin

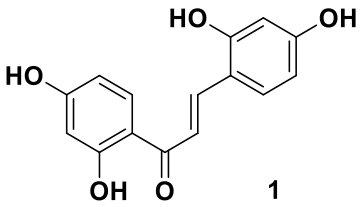

1

Radhakrishnan *et al*. reported some azachalcones as TyIs. Compounds **2** and **3** resulted more potent than kojic acid with an IC_{50} value of 1.70 and 2.30 µM respectively, revealing that the presence of pyridine ring was important for the activity.[113] They also identified some chalcones with oxime functionality such as compounds **4** and **5** with an IC_{50} value of 4.77 and 7.89 µM, respectively.[49, 114]

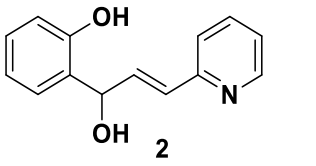

2

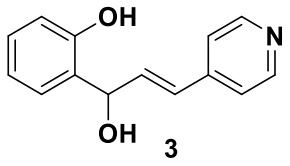

3

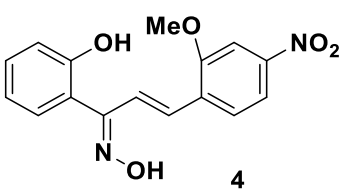

4

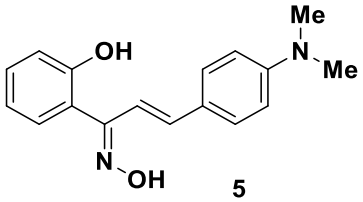

5

2.2.1.5 Stilbene

They consist of an ethene double bond substituted with a benzyl ring on both carbon atoms. Resveratrol (*trans*-3,4',5-trihydroxystilbene) is a natural stilbenoid present in grape and wine showing an IC_{50} value of 250 µM on TyM.[115] Resveratrol analogs represent a good challenge for Ty inhibition. Among the compounds extracted from *Morus alba* promising TyIs were found. In particular, oxyresveratrol (2,4,3',5'-tetrahydroxy-*trans*-stilbene) with an IC_{50} value of 1.7 µM, 2,4,3'-trihydroxydihydrostilbene with an IC_{50} value of 0.8 µM and dihydrooxyresveratrol with an IC_{50} value of 0.3 µM.[49, 116]

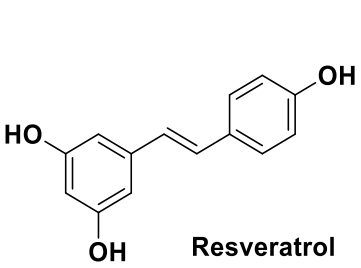

Resveratrol

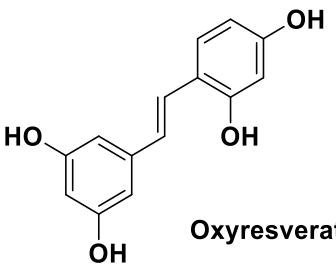

Oxyresveratrol

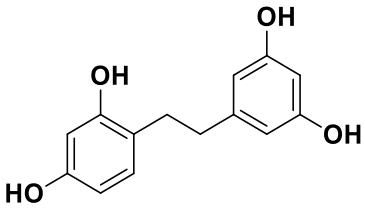

2,4,3'-Trihydroxydihydrostilbene

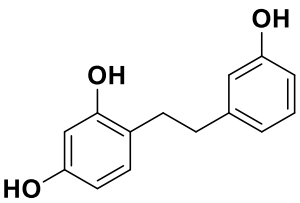

Dihydroxyresveratrol

Fenco *et al*. reported resveratrol derivatives in which the –CH group was substituted with nitrogen to produce a Schiff base, observing an increase of inhibitory activities compared to resveratrol.[117] Among this class of compounds the *para*-hydroxyl substituted one (**6**) showed the higher inhibitory activity with an IC_{50} value of 145 µM.[49]

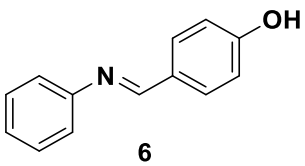

6

Bae *et al*. presented a series of aza-resveratrol, in particular the (*E*)-4-((4-hydroxyphenylimino)methyl)benzene-1,2-diol derivative showed an IC_{50} value of 17.22 µM.[118] Considering diazenyl compounds, the (*E*)-2-((2,4-dihydroxyphenyl)diazenyl) phenyl-4-methylbenzensulfonate was identified with an IC_{50} value of 17.85 µM.[49]

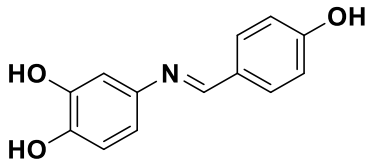

(*E*)-4-((4-Hydroxyphenylimino)-methyl)benzene-1,2-diol

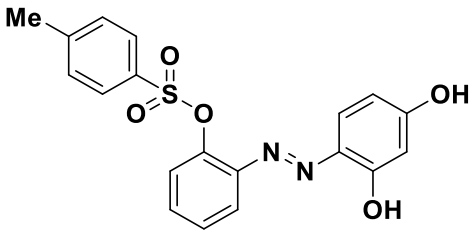

(*E*)-2-((2,4-Dihydroxyphenyl)diazenyl)-phenyl-4-methylbenzensulfonate

Other stilbenes inhibiting Ty activity are: chloroporin (4-geranyl-3,5,2',4'-tetrahydroxy-*trans*-stilbene) extracted from the heartwood of *Chlorophora excelsa*, is 14.8-fold more active than kojic acid;[119] gnetol (2,6,3',5'-tetrahydroxy-*trans*-stilbene) isolated from the roots of *Gnetum gnemon*, is 30-fold more active than kojic acid;[120] piceatannol (3,5,3'4'-tetrahydroxy-*trans*-stilbene) isolated from grapes and red wine is 32.7-fold more active than kojic acid.[121]

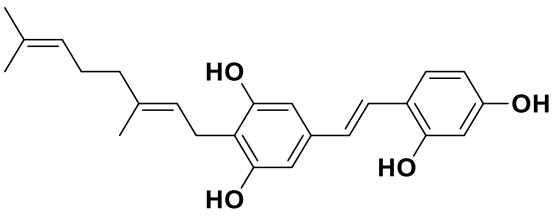

Chloroporin

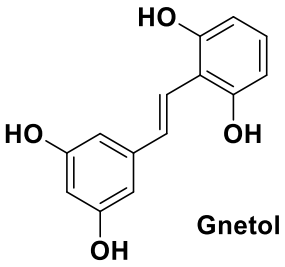

Gnetol

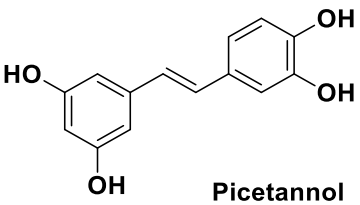

Picetannol

A potent synthetic derivative of oxyresveratrol was reported by Chung and Suh. It is the HNB [4-(6-hydroxy-2-naphthyl)-1,3-benzendiol] which exhibited 546-fold more inhibitory activity than kojic acid representing one of the strongest Ty inhibitor.[122]

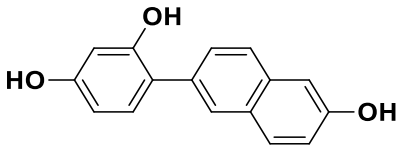

HNB

2.2.1.6 Coumarines

They are lactones of phenylpropanoid acid with a *H*-benzopyranone nucleus. One of the most famous coumarines is aloesin, isolated from *Aloe vera*. It does not show any cytotoxicity in cellular assays or skin irritation in human studies, thus it is employed in topically applied cosmetics.[123, 124] Other active coumarines are: aesculetin isolated from the seeds of *Euphorbia lathyris*, less active than kojic acid;[125] 9-hydroxy-4-methoxypsoralen extracted from *Angelica dahurica*, 6-fold more active than kojic acid;[126] 8'-epicleomiscosin A isolated from the aerial parts of *Rhododendron collettianum*, 12.8-fold more active than kojic acid.[127]

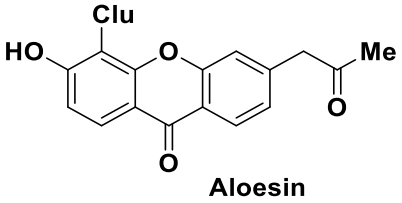

Aloesin

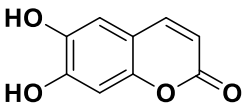

Aesculetin

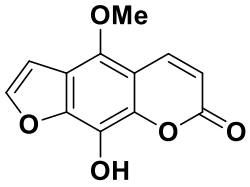

9-Hydroxy-4-methoxypsoralen

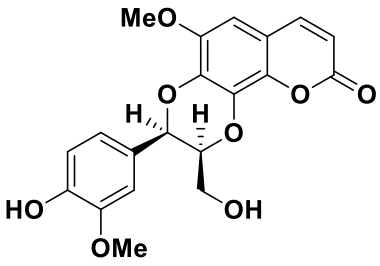

8'-Epi-cleomiscosin

2.2.2 Peptides and Peptidomimetics

Recently peptides such as dipeptides,[128] cyclic peptides,[129] oligopeptides[130] and kojic acid peptides[131] represented a good challenge as cosmetic agents. In particular, an octapeptide P3 (Arg-Ala-Asp-Ser-Arg-Ala-Asp-Cys) and a decapeptide P4 (Tyr-Arg-Ser-Arg-Lys-Tyr-Ser-Ser-Trp-Tyr) resulted potent TyM and TyH inhibitors without inducing melanocyte cytotoxicity.[132]

Li *et al*.[133] reported a series of kojic acid derivatives, hydroxypyridinone-*L*-phenylalanine conjugates, revealing that the length of alkyl chain influence the inhibitory activity. In particular, compound **7** (IC_{50}= 42.8 µM) presenting a hexyl chain, is less potent than **8** (IC_{50}= 12.6 µM) with octyl chain.[49]

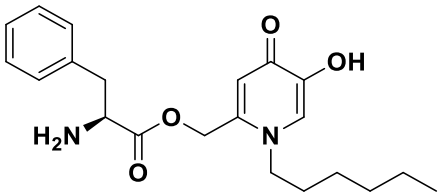

7

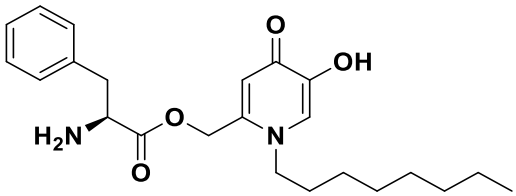

8

Zhao *et al*.[134] indicated hydroxypyridinone-*L*-amino acid conjugates as TyM inhibitors, reaching the best results with compounds **9** (IC_{50}= 2.79 µM) and **10** (IC_{50}= 26.20 µM).[49]

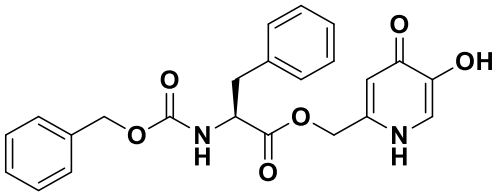

9

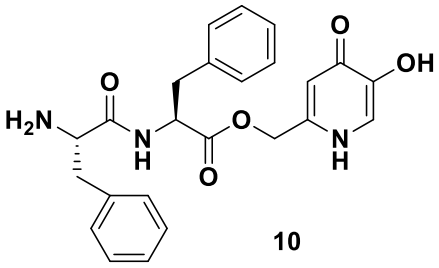

10

2.2.3 Biphenyl derivatives

Phenolic compounds demonstrated to be good TyIs, including some biphenolic derivatives like 4,4'-dihydroxybiphenyl (IC_{50}= 1.91 µM), fortuneanoside E (IC_{50}= 140 µM), honokiol (IC_{50}= 67.9 µM).[135, 136]

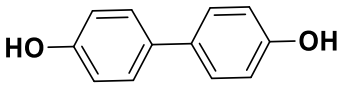

4,4'-Dihydroxybiphenyl

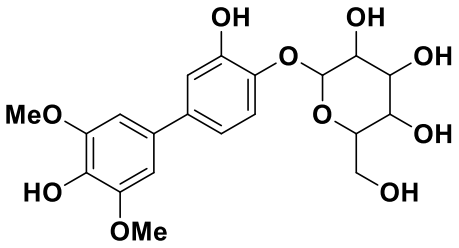

Fortuneanoside E

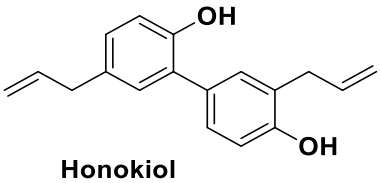

Honokiol

Considering these results, a new series of byphenolic compounds was reported. Derivatives with electron-donating substituents (methoxy and amino groups, **11** and **12** respectively) and pyridine moiety inhibited TyM at 250 μg/mL concentration likewise kojic acid.[137]

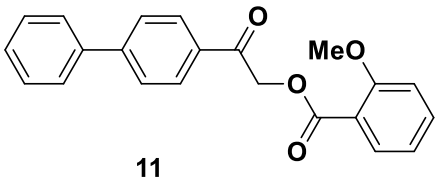

11

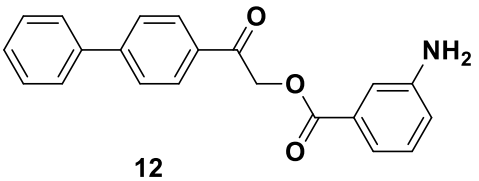

12

Among this class of compounds thiazoline-substituted biphenyls derivatives demonstrated to be potent TyIs. The most promising inhibitor resulted the derivative with a hydroxyl group and a thiazolidine ring (**13**) showing an IC_{50} value of 0.61 μM.[138]

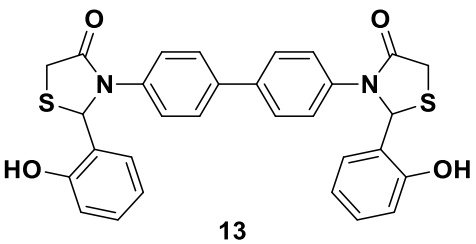

13

Oyama *et al*. detected phenyl benzoic acid (PBA) as a hopeful scaffold for Ty inhibition and thus PBA-derivatives were reported. In particular, 3-phenyl benzoic acid (3-PBA, IC_{50}= 36.32 μM) resulted a stronger inhibitor than the isomers 4-PBA (IC_{50}= 216.05 μM)

and 2-PBA (IC_{50}> 1000 µM) suggesting that the *meta*-substitution is favorited.[139] Furthermore, they highlighted that the introduction of a hydroxyl group in *para* position of PBA-isomers was always good especially for 4-PBA derivative (**14**) showing an IC_{50} value of 14.70 µM.[49, 140]

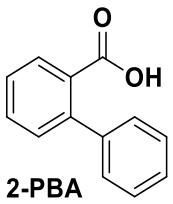

2-PBA

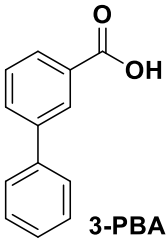

3-PBA

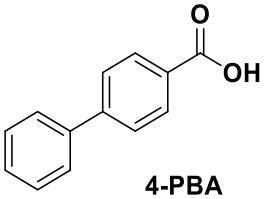

4-PBA

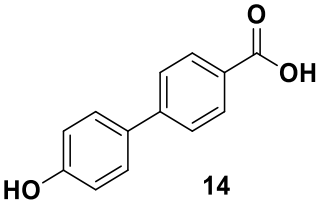

14

2.2.4 Indole derivatives

Ferro *et al*. identified indole derivatives (**15**, IC_{50}= 312 µM; **16**, IC_{50}= 224 µM; **17**, IC_{50}= 372 µM) as TyIs. In particular, the substitution at the indole *N*1-position with the 4-fluorobenzyl moiety influenced positively the activity unlike diketo group.[84] A promising candidate, compound **18** presenting an IC_{50} value of 7.56 µM, was reported.[49, 141]

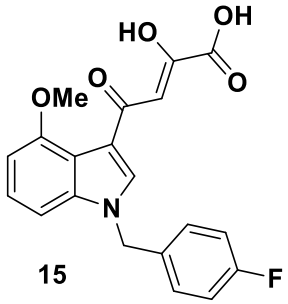

15

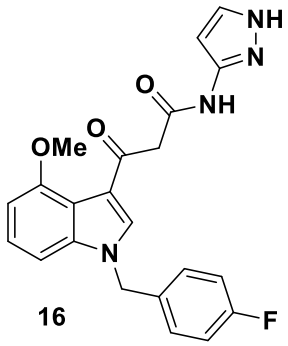

16

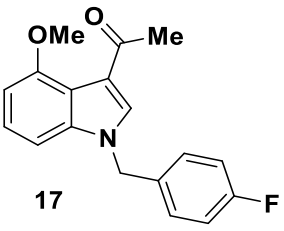

17

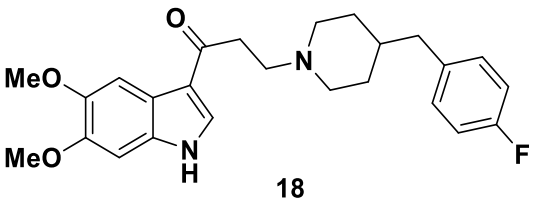

18

2.2.5 Thiourea and Thiosemicarbazone derivatives

Phenylthiourea (PTU) derivatives demonstrated an interesting activity as TyI, as a consequence of the chelation of the active site copper ions with their sulfur atom. Jung *et al*. described some compounds highlighting that sulfur atom was necessary for the chelating ability; direct linking of π-planar to thiourea unit was necessary; hydrophobic substituent at *para*- or *meta*- position (compound **19** (IC_{50}= 1.4 μM) and **20** (IC_{50}= 0.6 μM) respectively) on the aryl ring was tolerated while *ortho* substitution (**21**, IC_{50}> 100 μM) cancelled the activity.[142, 143]

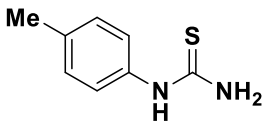

19

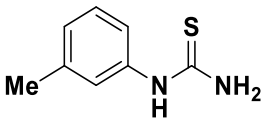

20

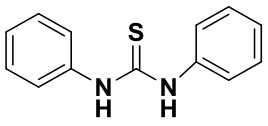

21

Choi *et al*. discovered ethionamide (IC_{50}= 4.0 μM) and its analogs, including prothionamide (IC_{50}= 4.5 μM), as TyIs showing that the thiocarbamide unit was fundamental for the activity. Pyridine-2-carbothioamide (IC_{50}> 1.0 μM) and thiobenzamide (IC_{50}= 2.8 μM) decreased melanin production in B16 cells.[144] Further studies indicated some antithyroid drugs as TyIs such as carbimazole (IC_{50}= 186 μM) and thiouracil (IC_{50}= 128 μM).[145]

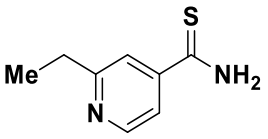

Ethionamide

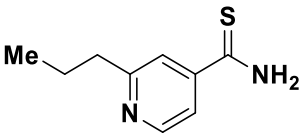

Prothionamide

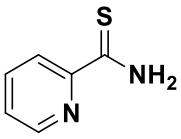

Pyridine-2-carbothioamide

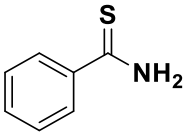

Thiobenzamide

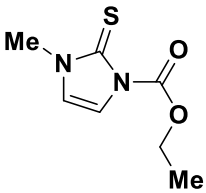

Carbimazole

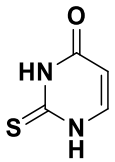

Thiouracil

You *et al*. reported 4- and 3-aminoacetophenones derived thiosemicarbazones as TyIs. In particular, acylamino compounds **22** (IC_{50}= 0.508 μM), **23** (IC_{50}= 0.372 μM) and **24** (IC_{50}= 0.291 μM) possess promising inhibitory activity.[146]

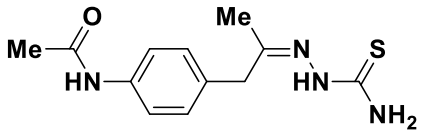

22

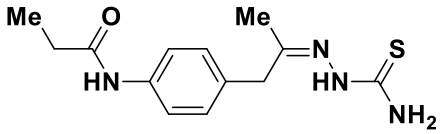

23

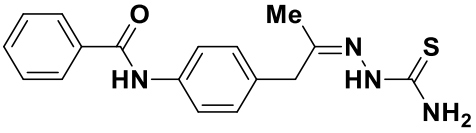

24

In another study, 4-alkoxy and 4-acyloxy-phenylethylenethiosemicarbazone analogs were identified to be good TyIs such as compounds **25** (IC_{50}= 0.42 µM), **26** (IC_{50}= 0.188 µM) and **27** (IC_{50}= 0.072 µM).[147]

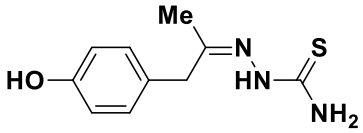

25

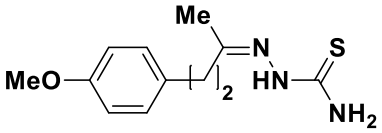

26

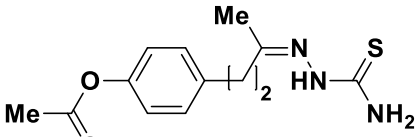

27

2.2.6 Hydroxycinnamic acid derivatives

Caffeic acid (CA) is a phenolic compound present in vegetables, fruits, grains and seeds possessing anti-oxidant, anti-tumor, anti-inflammatory, anti-microbial and anti-diabetic properties. Kwak *et al*. reported CA derivatives, caffeoyl-amino acydil-hydroxamic acids, as TyIs. In particular, caffeoyl-phenylalanyl-hydroxamic acid possesses an IC_{50} value of 4.9 µM.[148]

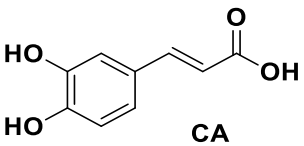

CA

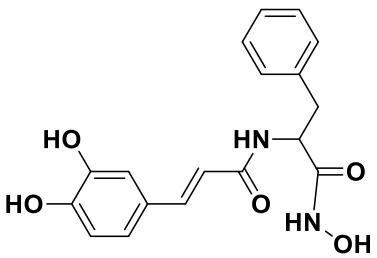

Caffeoyl-phenylalanyl-hydroxamic acid

Chlorogenic acid is a natural hydroxycinnamic acid derivative present in coffee, pears and apples possessing anti-inflammatory, anti-diabetic, anti-viral and anti-oxidant properties. It was reported as TyI, suppressing the melanin content in B16 cells at 500 μM concentration.[49, 149]

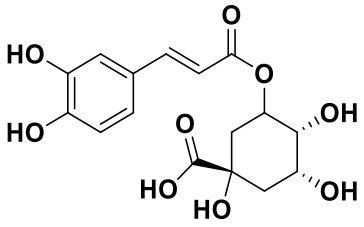

Chlorogenic acid

2.2.7 Kojic acid derivatives

In order to try to avoid the side effects related to the use of kojic acid in cosmetic products, some researchers developed kojic acid synthetic derivatives. Saghaie *et al*. identified a series of 3-hydroxy-4-pyridone analogs, highlighting that the compounds with two free hydroxyl groups were more potent than those with a single hydroxyl group. Compound **28** presented the best result with inhibitory activity comparable to that of kojic acid.[150]

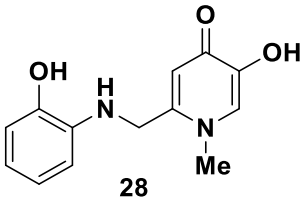

28

Rho *et al*. reported some kojic acid dimeric analogs. Compound **29** possessing propane 1,3-dithioether group, showed the best activity being 25-fold more than kojic acid.[151]

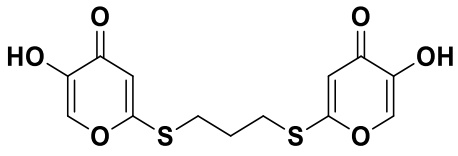

29

Noh *et al*. identified mono and dipeptide conjugated kojic acid, in which amino acid moieties were connected to kojic acid *via* a carbamate linkage. The best result was obtained for compound **30**, which resulted 6-fold more potent than kojic acid.[152]

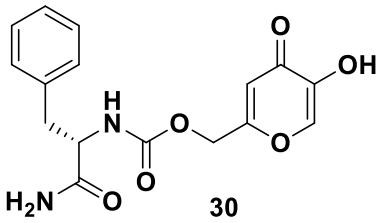

30

Li *et al*. prepared a series of 4-pyridone-phenylalanine derivatives, showing that compound **31** was 2-fold more potent than kojic acid.[133]

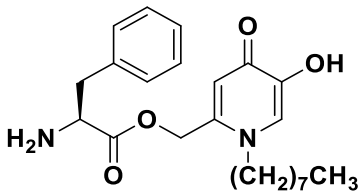

31

2.2.8 Human Ty inhibitors

The inhibitory activity of kojic acid against TyH (IC_{50}= 571.17 μM) demonstrated to be 10-fold less potent in comparison to TyM (IC_{50}= 53.70 μM). Other TyM inhibitors like phenylthiourea, L-mimosine, cinnamic acid, benzoic acid and aesculetin resulted more active for TyM inhibition than TyH.[153] 4-Butylresorcinol, a resorcinol derivative, is a potent melanogenesis inhibitor showing inhibition against TyH, TYRP1 *in vitro* as well as in B16 melanoma cells.[154] In melanoDerm skin model, 4-butylresorcinol proved to be a good TyI with an IC_{50} value of 13.5 μM, thus reducing the appearance of age spots within eight weeks. As a consequence, it resulted a promising inhibitor in pigmentation disorders treatment, indeed topical cream containing 0.1-0.3% of 4-butylresorcinol are employed in melasma treatment.[155, 156]

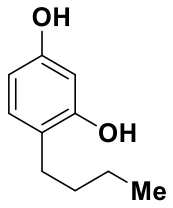

4-Butylresorcinol

Linderanolide B and subamolide A are two natural compounds which at a dosage of 1 µM concentration reduce TyH activities and melanin formation in human epidermal melanocytes (HEM), neonatal, moderately pigmented donor (HEMn-MP). In zebrafish, they showed notable reduction in pigmentation level with no toxicity.[157, 158]

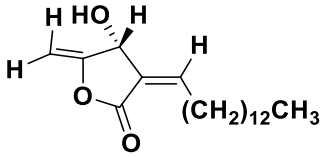

Linderanolide B

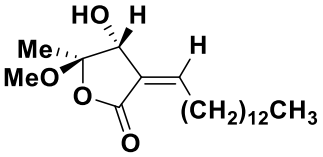

Subamolide A

Erdtman *et al*. identified three regioisomers of thujaplicins (isopropyl cycloheptatrienolones) isolated from *Thuja plicata* as TyH inhibitors. In particular, β- and γ-thujaplicins inhibited TyH with an IC_{50} value of 8.98 and 1.15 µM respectively.[159] These compounds possess the general structure of tropolone, a TyI employed sometimes as reference compound to compare the inhibitory activity of new derivatives.

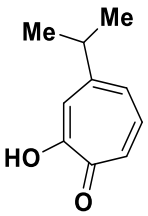

β-Thujaplicin

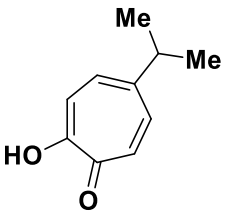

γ-Thujaplicin

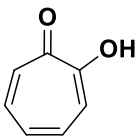

Tropolone

Okombi *et al*. investigated natural aurones [*Z*-benzylidenebenzofuran-3(2*H*)-ones], reveling that 4,6,4'-trihydroxyaurone induces 75% inhibition at 0.1 mM, more than kojic acid.[49]

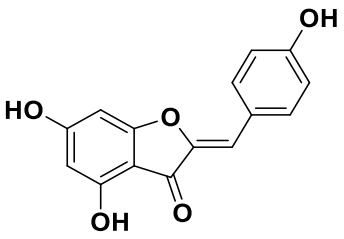

4,6,4'-Trihydroxyaurone

Haudecoeur *et al*. reported some TyH inhibitors possessing a 2-hydroxypyridine-*N*-oxide (HOPNO) moiety in aurone backbone. Compound **32** was found to be the most active derivative with an IC_{50} value of 16.6 µM.[160]

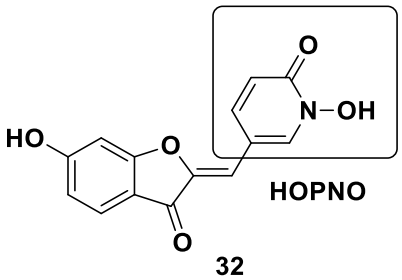

32

An *et al*. identified *p*-coumaric acid (PCA) as a stronger inhibitor of melanogenesis in murine melanoma cells stimulated with α-MSH than similar compounds such as 3-(4-hydroxyphenyl)propionic acid, cinnamic acid and caffeic acid.[161] Song *et al*. evaluated the inhibitory activity on TyH of PCA and its methyl ester (MPA) in human epidermal melanocytes highlighting that PCA and MPA inhibit TyH with an IC_{50} value of 3.0 and 30 µM respectively.[162] Seo *et al*. conducted *in vivo* studies for the use of PCA as hypopigmenting agent in human reveling that cream which contains 1.5% of PCA decreases UV-induced erythema formation and pigmentation in human skin.[49, 163]

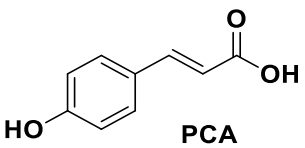

PCA

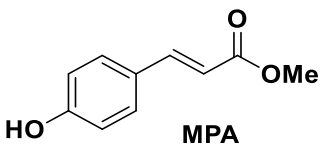

MPA

CHAPTER 3 PHARMACEUTICAL INTEREST OF Ty

3.1 Ty related disorders

An irregular Ty activity determines an abnormal production of melanin pigments. The reduced enzymatic activity leads to lower production of melanin associated to diseases such as vitiligo and oculocutaneous albinism type 1. While an increased activity of the enzyme leads to an excessive production of melanin resulting in skin hyperpigmentation, such as melasma, and melanoma.

3.1.1 Vitiligo

Vitiligo is an autoimmune and the most common depigmenting disorder. It is characterized by a hypopigmentation of the skin due to a selective destruction of melanocytes. Typical vitiligo lesions are defined as milky white, non-scaly macules with distinct margins classified into two major forms:

- Non-segmental vitiligo: It is the commonest form also known as vitiligo, characterized by symmetrical and bilateral white patches.
- Segmental vitiligo: It usually has a unilateral distribution.

Overall, a progressive and irregular loss of pigmentation from skin, hair and sometimes mucosa, remains the basis of diagnosis of vitiligo.[164]

3.1.2 Oculocutaneous albinism type 1 (OCA1)

It is determined by a mutation of the gene that codes for Ty, generally characterized by the total absence of melanin in the skin, hair and eyes at birth. In general, different phenotypes of OCA1 are observed that depend on the amount and residual activity of the enzyme produced by mutant alleles. On the basis of this residual enzymatic activity, OCA1 is classified into two different subtypes:

OCA1A: It is the most severe form of OCA, in which the mutations of the Ty gene completely abolish the activity of the enzyme. It determines white hair, brows and lashes, and white skin at birth. Skin lesions such as nevi are pink and unpigmented. The irides are blue and fully translucent at birth and remain so throughout life. In addition, nystagmus, photophobia and strabismus are problematic.

OCA1B: In this case Ty gene mutations allow a 5-10% residual activity. Even if at birth there is a minimal presence or total absence of melanin, with time a progressive melanization can occur. The level of pigmentation varies from a very low amount of skin pigment to almost normal skin pigmentation. Affected individuals typically have white or very light hair at birth and develop observable light yellow hair color by age one to three years. The development of pigment in scalp hair is progressive.[165]

3.1.3 Melasma

Melasma is a hypermelanosis of the face affecting more frequently women with dark skin due to high melanin content. It is characterized by light-to-dark brown symmetrical, homogeneous, irregular patches or macules. Although its etiology is not clearly understood, sun exposure, hormones, pregnancy, use of phototoxic drugs, genetic influences, use of cosmetics, and anticonvulsant drugs are among the predisposing factors. Tremendous emotional stress and psychological distress are chronic emotions brought about by melasma. Considering the clinical pattern, it is possible to classified melasma in: centrofacial, the most common, involving the cheeks, forehead, upper lip, nose and chin; malar, implying the cheeks and nose; mandibular, implicating lesions that occur over the ramus of the mandible.

It is possible also to classify melasma according to the time of its treatment as transient (when it retracts within a year of termination of stimulus, *e.g.*, post-pregnancy) or persistent (when it persists more than a year after the stimulus has been removed). Finally, it is classified into four different histological types according to its depth in the skin in epidermal, dermal, mixed type and intermediate melasma.[166]

3.1.4 Melanoma

Cutaneous melanoma is a tumor deriving from the transformation of the melanocytes. It is quite rare in children and affects mostly people around 45-50 years. It represents only a small percentage (about 5%) of all skin-affecting tumors. It is related to an excessive exposure to ultraviolet light, disorders of the immune system (due for example to previous chemotherapies or transplants), inherited diseases (for example the xeroderma pigmentoso, in which DNA is not able to repair damage caused by radiation). The risk increases in people with freckles, moles or with light eyes, hair and

skin and in people with a close relative affected by this tumor. The cutaneous melanomas can originate or from intact skin or from pre-existing moles. From the clinical point of view, we distinguish four kind of tumor: superficial diffusion melanoma (the most common, represents about 70% of all cutaneous melanomas), lentigo maligna melanoma, acral lentiginous melanoma and nodular melanoma (the most aggressive, represents approximately 10-15% of cutaneous melanomas). Unlike the first three types, which initially have a superficial growth, nodular melanoma is more aggressive and invades the tissue in depth since its early stages. The main symptom of cutaneous melanoma is changing in the characteristics of a mole or the appearance of a new one. The characteristics of a mole indicating the presence of a melanoma are summarized thanks to the abbreviation **ABCDE**:

• **A**: **A**symmetry in the form (a benign mole is generally circular or otherwise roundish, a melanoma is more irregular);

• **B**: Irregular and indistinct **B**orders;

• **C**: Variable **C**olor;

• **D**: Increasing **D**imensions;

• **E**: The **E**volution of the mole that, in short time, shows changes in appearance.[167]

3.2 Applications of TyIs

3.2.1 Agriculture and Food Industry

TyIs can be used in the browning process of fruit and vegetables, altering the organoleptic characteristics and properties of the products. The enzymatic browning rate depends on the concentration of active Ty and phenolic compounds, on the oxygen availability, on pH and temperature. To address this problem, various methods have been identified, including the use of autoclaves and bleaching methods but these processes cause significant weight and nutrient losses in the products. An alternative approach is the use of microwave energy, which however has the main disadvantage of generating a temperature gradient. Several compounds are reported to inhibit Ty but their employing is controversial such as ascorbic acid, sodium bisulfate and other reducing agents. The use of sulfites is restricted due to their potential health effects while 4-hexylresorcinol is considered safe in food industry.[168]

3.2.2 Cosmetic Industry

Ty is the most prominent target for the inhibition of melanogenesis since it is responsible of melanin synthesis. Thus, most of cosmetics or skin lightening agents commercially available are TyIs such as hydroquinone, arbutin, kojic acid, *L*-ascorbic acid, ellagic acid but only some of them are used as skin clearing agents, mainly due to various safety issues.[55]

Hydroquinone is a natural compound that inhibits Ty in different ways: interacting with the copper ions in the active site; altering the functioning of the melanosomes; causing oxidative damage to the lipid membrane and to the proteins of the melanocytes. It is a very effective compound but it causes various side effects because it is mutagenic to mammalian cells and induces contact dermatitis, irritation, transient erythema, burning, prickling sensation, leukoderma, chestnut spots on the nails, hypochromia and ochronosis.[169-172]

Arbutin is a prodrug of hydroquinone which catabolizing to benzene metabolites can be toxic for bone marrow.[173]

Kojic acid is carcinogenic, instable during storage and can causes sensitization problems, contact allergies and dermatitis.[174]

L-Ascorbic acid (Vitamin C) is sensitive to heat and degrades easily.[175]

Ellagic acid is insoluble and thus poorly bioavailable.[176]

The EU Cosmetic Regulation bans the use of corticosteroids, hydroquinone, monobenzyl hydroquinone, tretinoin and mercury salts as whitening agents.[49, 55]

Lightening properties are also attributed to polyphenols. They possess lower side effects compared to arbutin and kojic acid, so they are more suitable for cosmetic use, even if the results and efficacy are often based on studies carried out only *in vitro* or on laboratory rats.

Green tea derivatives are polyphenols with antioxidant, anti-inflammatory and anti-carcinogenic action.[177] Numerous studies have shown their ability to suppress the carcinogenic activity of UV rays by virtue of the marked skin photoprotective action. This is why they represent valid ingredients to be associated with common sunscreens.[178]

Among the polyphenols there are also **oxyresveratrol** and **resveratrol**, the last possesses lower inhibitory activity but it is a safe molecule, free of irritating effects.

The antioxidant molecules, for which a lightening/depigmenting activity has been assessed, are:

Alpha Lipoic Acid, thanks to the ability to chelate copper ions, it is able to inhibit Ty and thus suppress the formation of DOPA-quinone derivatives.[179] One of its derivatives, **Dihydrolipoic Acid**, has been shown to have a greater antioxidant activity since it reacts with both the superoxide radicals and the hydroxyl radicals. Moreover, it is able to increase the intracellular levels of glutathione (tripeptide with antioxidant properties) favoring its synthesis ex novo and this determines a further reduction of the sensitivity to UV rays. Both acids have been shown to block the expression of the factor regulating the development and life of keratinocytes (MITF), with inhibition of Ty and enhancement of the lightening effect.[180] Lipoic acid has long been used in many cosmetic preparations but some cases of contact dermatitis have been reported.

Vitamin E, or alpha-tocopherol, is a fat-soluble vitamin present in vegetables rich in lipids and in the oils extracted from them (wheat germ oil, coconut oil, etc.). Its primary function is to inhibit the oxidation of cutaneous lipids and their rancidity. In cosmetics it is used in esters form, more stable and easy to formulate, releasing *in vivo* vitamin E by the action of skin esterase. The association with vitamin C, which enhances its antioxidant efficacy, has given positive results in the treatment of facial hyperpigmentation. Furthermore, preliminary studies suggest that the α-tocopheryl ferulate (compound given by the association between ferulic acid and vitamin E) seems to indirectly inhibit tyrosine-hydroxylase, in cultures of human melanoma cells, with superior efficacy to that demonstrated by arbutin and kojic acid.[181]

CHAPTER 4 MOLECULAR MODELING

Introduction

In drug discovery process, apart from traditional approaches based on step-wise synthesis and screening of large number of compounds, the use of computational techniques for the discovery of potential drugs can be taken into account, saving time and reducing costs process.[182, 183]

Molecular modeling includes all the theoretical and computational techniques used to visualize three-dimensional molecular structures and simulate their dynamic behavior *in vacuum*, in a solvent or inside a receptor. To date it is possible in a short time to determine the geometry of a molecule, to analyze its possible conformations evaluating which of these is the most probable, to calculate properties such as energy, molecular orbitals, electronic density, lipophilia and the surface accessibility to solvent. All this information can be used for the design and optimization of biological active molecules (drug design).

In particular, two different approaches can be used:

- **Structure based drug design (SBDD)**: In this kind of approach, it is fundamental the structural information of drug target, usually determined by x-ray crystallography or NMR experiments.[183] The crystal structure of the single protein (apo-protein) or of the protein-ligand complex is available in the *Protein Data Bank* (PDB).
- **Ligand-based drug design (LBDD)**: This method is used when there is not information about the 3D structure of target. Thus, it is important to know active molecules that bind the target of interest.[183]

4.1 Molecular docking

One of the computational tools widely employed in drug discovery projects is the docking methodology. It was developed during the early 1980s by Kuntz and coworkers,[184] representing a crucial component from hit identification to lead optimization in medicinal chemistry due to its low cost and short time.

There are different kind of interactions playing an important role in biological pathways such as: enzyme-substrate, drug-protein, drug-nucleic acid and protein-nucleic acid. Among them, *protein-ligand docking* is a particularly interesting research

area due to its importance in structure-based drug design[185-187] and it will be the subject of the present thesis. Molecular docking is a "structure-based" type technique and it can be defined as an optimization method that identifies the best orientation of a ligand that interacts with a protein.[188, 189] Several are the variables involved in this procedure such as: the ligand active conformation and its orientation within the binding site, the binding site conformation. In physiological conditions, both ligand and protein modify their conformation to obtain the best interaction (induced adaptation). The aim of this process is to identify an optimized conformation for both the protein and the ligand, reducing to a minimum the free energy of the system (**ΔG**), that is important because it represents the affinity of the molecule for its receptor, expressed as follows:

$$\Delta G° = \Delta H° - T\Delta S° = -RT\ln K_a$$

Where **ΔH** and **ΔS** are the enthalpy and entropy variation respectively; **R** is the gas constant 8,314 $JK^{-1}mol^{-1}$; **T** is the temperature in Kelvin; $\mathbf{K_a}$ is the dissociation rate.[190]

The docking procedure employs two major steps. The process starts with the application of an algorithm that examines the several degrees of conformational freedom of small molecules, “posing” them in the binding site. Thus, the generated poses are evaluated by scoring functions which allow the evaluation of the interactions between the ligand and the potential target as well as the entropic cost of the ligand conformation. Then, the poses will be ranked. Some of the scoring functions adopted for molecular docking try to estimate the binding free energy of the ligand-target complex. Unfortunately, this estimation is not always reliable because of the high error associated to it.

A docking program can be considered good if:

- It is able to reproduce the experimental binding modes of ligands. To probe this ability, a ligand is taken out of the 3D X-ray structure of its protein–ligand complex and docked back into its binding site to compare the two poses. A root-mean-square distance (RMSD) between the two is calculated, considering successful a predicted binding mode if the RMSD is below a certain value.
- Its scoring function is able to score and rank ligands according to their experimental binding affinities. To evaluate this, the predicted binding affinities

and scores are compared with the experimental binding affinities. The standard deviation is the key indicator for the quality of the predicted affinities.

In order to have a good docking accuracy, the choice of some parameters is very important.[191] Many different softwares can be used for molecular docking, in particular in this work GOLD (**G**enetic **O**ptimization for **L**igand **D**ocking) program was used. [192]

4.1.1 Algorithms in molecular docking

Docking programs employ different algorithms to find the correct pose of ligand in the interaction with the protein.

Considering the algorithms involved in the ligand flexibility, they can be divided in three categories: systematic, stochastic and deterministic searches algorithms.[186]

4.1.1.1 Systematic algorithms

These algorithms consider a grid of values for each degree of freedom in a combinatorial way. The number of evaluations increases rapidly with the growing of freedom degrees and to prevent the algorithm from space which is known to lead to the wrong solution, it is necessary to insert the termination criteria.[185]

There are several examples of those algorithms such as:

- **Matching algorithms** (**MA**): They are very fast and map a ligand into an active site of a protein, representing them as pharmacophores.[193]
- **Simultaneous Search** (**MCSS**): They are fragment-based methods for designing or modifying ligands to increase the affinity in the binding with a target protein.[194, 195]

4.1.1.2 Stochastic algorithms

They perform random changes on the freedom degrees of the system (to a single or a population of ligands). Examples of this class of algorithms are:

- **Monte Carlo (MC)**: They are based on the Maxwell-Boltzmann probability and generate poses of the ligand through bond rotation, rigid-body translation or rotation. The conformation obtained by this transformation is tested with an energy-based selection criterion. If it passes the criterion, it will be saved and

further modified to generate the next conformation. The iterations will proceed until the predefined quantity of conformations is collected.[196]

- **Genetic algorithms (GAs)**: They use concepts based on the language of natural genetics and biological evolution. In molecular docking, the disposition of a ligand and a protein is defined by a set of values describing the translation, orientation and conformation of the ligand respect to the protein: these are the ligand's *state variables* and, in the GA, each state variable corresponds to a gene. The ligand's state corresponds to the genotype, whereas its atomic coordinates correspond to the phenotype. In molecular docking, the *fitness* is the total interaction energy of the ligand with the protein, and it is evaluated using the energy function. Molecular recognition of receptor sites uses a genetic algorithm with a description of desolvation.[197] Genetic algorithms is employed in GOLD program.[192]
- **Tabu algorithm**: It considers conformational space areas already explored.[198, 199]

4.1.1.3 Deterministic algorithms

They can establish the movement made to generate the next state, which generally has the same or a lower energy than the initial state.

The two major simulation methods are:

- **Molecular dynamics (MD)**: It represents the flexibility of both ligand and protein. MD simulations are efficient at local optimization but they progress in very small steps and thus have difficulties in stepping over high energy conformational barriers, which may lead to inadequate sampling.[200-202]
- **Energy minimization**: It is only able to reach local minima, so it is used associated with other methods.

4.1.2 Scoring functions

The two important aspects of a scoring function are speed and accuracy. An ideal scoring function has to be efficient and reliable. Basically there are three kind of scoring functions: empirical, knowledge-based and force-field-based.[203]

4.1.2.1 Empirical scoring functions

In this kind of score, a complex binding energy can be considered as a sum of empirical energy terms such as Van der Waals, electrostatic, hydrogen bond energies and desolvation, entropy, hydrophobicity terms reproducing experimental data, such as binding energies and/or conformations.

Examples of empirical scoring functions are: GlideScore,[204] SYBYL/F-Score,[205] LigScore,[206] LUDI,[207] and ChemScore.[208]

4.1.2.2 Knowledge-based scoring functions

They derive directly from the structural information in experimentally determined protein-ligand complexes. The principle behind knowledge-based scoring function is the potential of mean force,[209] which is defined by the inverse Boltzmann relation:[210, 211]

$$w(r) = -k_B T \ln[\rho(r)/\rho^*(r)]$$

where k_B is the Boltzmann constant; **T** is the absolute temperature of the system; **ρ(r)** is the number density of the protein-ligand atom pair at distance **r** in the training set; **ρ*(r)** is the pair density in a reference state where the interatomic interactions are zero.

Examples of knowledge-based scoring function include DrugScore,[212] GOLD/ASP[213] and potential of mean force (PMF).[185, 214]

4.1.2.3 Molecular mechanics force fields (FF)

They are based on decomposition of the ligand binding energy within van der Waals, electrostatic and bond stretching/bending/torsional energies, using a set of derived force-field parameters such as AMBER[215] or CHARMM.[202, 216] One of the major challenges in FF scoring functions is how to account for the solvent effect. The most rigorous FF methods are to treat water molecules explicitly. However, these methods are computationally expensive.[217] To reduce the computational expense, accelerated methods have been developed while preserving the reasonable accuracy by treating water as a continuum dielectric medium. The Poisson-Boltzmann/surface area (PB/SA)

models[218] and the Generalized-Born/surface area (GB/SA) models[219] are typical examples of such implicit solvent models.[220]

4.1.3 GOLD software

It is an automatic docking program that uses a genetic algorithm to generate the single poses for the orientation of flexible ligands within the protein binding site. This algorithm allows the exploration of large conformational spaces, representing each spatial arrangement of the protein and the ligand as a "gene" with its score calculated by the scoring function. The solution with the highest score should represent the correct position of the ligand in the receptor. Usually docking simulation is achieved using a flexible ligand and a rigid receptor, but in the last few years, the use of a flexible receptor, especially in the backbone, represents a good challenge.

4.1.3.1 Genetic algorithm in GOLD program

The Genetic algorithms (GAs) belong to the class of stochastic algorithms. GOLD program employs a so-called island-based genetic algorithm. This means that not only one large population of chromosomes is manipulated, but also several sub-populations (*i.e.* islands) are considered and individual chromosomes can migrate among them. This feature improves the efficiency of the algorithm.

Ligand degrees of freedom are codified as binary strings called genes. These genes generate the “chromosome”, that represents the ligand pose. Starting from an initial population of “chromosomes”, randomly generated, the genetic algorithm applies two genetic operators, crossover and mutation. The crossover operator requires two “parents” and produces two “children”, by appropriate recombination of the two parents’ characteristics, while the mutation operator requires a “parent” and produces a “child”, through random changes on a single parent. The parent chromosomes are randomly selected from an existing population. The survival of the best individuals ensures that the population should move towards an optimal solution, thus the most correct docking pose.[191, 221, 222] The quality of results depends on: the starting genes, the number of evolutionary events and the scoring function adopted to select the most favorable conformers. Thus, in contrast with the only reproduction operator, crossover and mutation allow the exploration of the conformational space through the

introduction of children chromosomes to be submitted to a new cycle of genetic operations. The whole cycle is repeated until some generations are defined and/or until some conditions (*i. e.* RMSD, ΔG) are satisfied. GOLD software uses an island-based genetic algorithm search strategy[223] and includes rotational flexibility for selected receptor hydrogen along with full ligand flexibility. The ligand is flexible, while the receptor is rigid.

4.1.3.2 Scoring function in GOLD program

The scoring functions are mathematical methods used to predict the non-covalent force of interaction between two molecules that form a complex. The original GOLD scoring function is the GoldScore fitness function. It has been optimized for the prediction of ligand binding positions and it is defined as the sum of the following components: the energy of the H-bonds between the protein and the ligand, the internal energy of the ligand in the binding pose and the van der Waals interaction energy of the bound complex.[191, 202]

4.2 Pharmacophore modeling

A pharmacophore can be defined as the smallest structural unit of a molecule responsible of its biological activity.

It is based on different kind of interactions that a drug can made with its receptor such as: hydrogen bonding, charge transfer, electrostatic and hydrophobic interactions. A pharmacophore model is a group of chemical features aligned in three dimensional space, representing the interactions of small organic ligands with a macromolecular receptor.[224]

Several software can be employed for that kind of approach, in particular in this work we used **Ligand Scout** program.[224]

4.2.1 Ligand Scout

Ligand Scout is a software able to develop pharmacophore models using two different kind of approaches: structure-based and ligand-based drug design.

LigandScout employs algorithms that allow to interpret the characteristics of the ligand, fundamental prerogative to obtain a pharmacophore that identifies the active

conformation of the molecule. The group of chemical features characterizing a pharmacophore model can be categorized into: hydrogen bond interactions, hydrophobic area and charge-transfer interactions.

- **Hydrogen bond interactions**: A hydrogen bond is established when a covalently bound hydrogen with a positive partial charge interacts with another atom with a negative partial charge.[225] In particular, we have a H-bond donor (**HBD**) and a H-bond acceptor (**HBA**). The bond is directional and the optimum orientation occurs when the model assumes an angle of 180°.

  HBD atoms are considered: nonacidic hydroxyls (all OHs except sulfonic, sulfinic, carboxylic, phosphonic or phosphinic acids), thiols, acetylenic hydrogens, and NHs (except tetrazoles and trifluoromethyl sulfonamide hydrogens). If the heavy atom of a hydrogen bond acceptor within the surrounding macromolecule is found in the distance range of 2.5 to 3.8 Å of the marked atom, a hydrogen bond donor feature is created. It consists of a “green poinert”.[224]

  HBA atoms are considered: hydroxyl oxygen, thiol sulfur, acetylene carbon, or nitrogen. The heavy atom on the acceptor can be replaced by a fluorine atom. Although this kind of interaction is different from a chemical point of view, it is similar for the complementary group on the macromolecular side and it was integrated into the group of hydrogen bond acceptors. The macromolecule is searched for a hydrogen bond acceptor atom within the distance range of 2.5 to 3.8 Å. If a suitable acceptor atom is found, a hydrogen bond donor feature is created. It consists of a “red pointer”.[224]

- **Hydrophobic areas**: The hydrophobic areas are represented by yellow or blue (in the specific case of aromatic rings) spheres indicating the presence of carbon chains or aromatic rings. They are identified on the basis of a scoring function. If there is a complementary hydrophobic function on the target at a distance between 1 Å and 5 Å, the pharmacophore will be characterized by the presence of a hydrophobic feature.

  To reflect the steric constraints coupled with hydrophobic interactions, exclusion volume spheres are added at the coordinates of the lipophilic center on the macromolecule side. They are areas occupied by portions of the target

macromolecule and therefore inaccessible to the ligand, represented in the pharmacophore model by gray spheres.[224]

- **Charge-transfer interactions:** They are based on the physical law of Coulomb, which describes the behavior of entities that possess a charge considering that "opposite charges attract each other" and that "the strength of the interaction is inversely proportional to the distance". Positively ionizable areas (**PI**) are represented by atoms or groups of atoms that can be protonated at a physiological pH such as: basic amines, basic secondary amidines, basic primary amidines, basic guanidines and positive charges not adjacent to a negative charge. Negatively ionizable areas (**NI**) are atoms or groups of atoms that can be deprotonated at physiological pH such as: trifluoromethyl sulfonamide hydrogens, sulfonic acids, phosphonic acids, sulfinic, carboxylic or phosphinic acids, tetrazoles and negative charges which are not neutralized by an adjacency to a positive charge. If an area with these ionizable complementary groups is found in the target macromolecule in a distance between 1.5 Å and 5.6 Å, the corresponding feature is added to the pharmacophoric model. It is represented by a blue sphere in the case of positive ionizable area or by bordeaux sphere in the case of a negative ionizable area.

4.3 Virtual screening database

Virtual Screening (**VS**) is a computational method employed in drug discovery with the aim to find new pharmacologically active compounds, screening small molecules libraries in order to identify which are most likely to bind to a drug target, typically a protein receptor or enzyme.[226] The experimental protocol can be described as follows:

- **Protein Preparation**: Generally, a PDB structure file consists only of heavy atoms and may contain water molecules, cofactors, ligands, metal ions and there is not information on bond orders, topologies or formal atomic charges. Ionization and tautomeric states are also unassigned in most cases, residue side chains or larger loops may be missing because of low resolution of a particular protein area, and steric clashes may exist.[226]

- **Binding Site Identification**: It is a pocket typically a concave, having a variety of probable hydrogen bond donors and acceptors and hydrophobic characteristics.[226]
- **Database Preparation**: Usually, databases of natural or synthetic compounds can be used. These databases often contain a vast amount of small-molecule compounds varying from several tens of thousands to several millions.[226]
- **Screening**: Two kind of approaches ca be used: ligand-based virtual screening (LBVS) and structure-based virtual screening (SBVS). In the case of LBVS we have not information about the 3D structure of the protein. In this work we used a SBVS approach.[226]
- **Selection of candidates**: The selection of the best candidates can be made using different approaches such as: pharmacophore modeling techniques, docking studies and filters based on molecular descriptors of chemical-physical characteristics, such as absorption and bioavailability. An example of a filter consists in the application of the so-called “Lipinski Rule of Five",[227] which asserts that drug-like compounds should have molecular weight lower than 500, lipophilicity (logP) lower than 5, less than five hydrogen bond donors, and less than 10 hydrogen bond acceptors.[226]
- **Synthesis and biological assays of selected compounds**: The so selected compounds can be synthetized, extracted or purchased to test the biological activity.[226]

The advantage of Virtual Screening consists in the possibility to exploit speed and economy of this approach, especially in the data collection phase, since the number of molecules to be investigated can extend from tens to thousands of homologues. Thus, it is not necessary to summarize all them in the laboratory for then test the pharmacological activity. In this way, we can focus in molecules possessing best features, with significant benefits in terms of cost and time.

CHAPTER 5 RESULTS AND DISCUSSION

5.1 Starting point: Discovery of a promising Ty inhibitor and structural modifications

The aim of this PhD project was the development of new compounds able to inhibit Ty enzyme. Previous studies carried out at the medicinal chemistry laboratory of the University of Messina, where I performed my research work, allowed the identification of a new class of TyM inhibitors bearing indolic scaffold and benzylpiperidine portion. In particular, our CHIME 1.5 database (a collection of small molecules synthesized in our laboratory in the last decade) was screened employing mushroom Ty (TyM) to evaluate the inhibitory activity. The most active compound resulted 3-(4-benzylpiperidin-1-yl)-1-(1*H*-indol-3-yl)propan-1-one (**33**, figure 25) with an IC_{50} value of 255 µM on diphenolase TyM activity. Afterwards, different structural modification regarding indolic nucleus (presence of methoxy substituents at 5 and/or 6 position) and benzylpiperidine portion (presence or absence of fluorine atom in para position of the aromating ring), led to the most active compound 1-(5,6-dimethoxy-1*H*-indol-3-yl)-2-(4-(4-fluorobenzyl) piperidin-1-yl)propan-1-one (**18**, figure 25).[141]

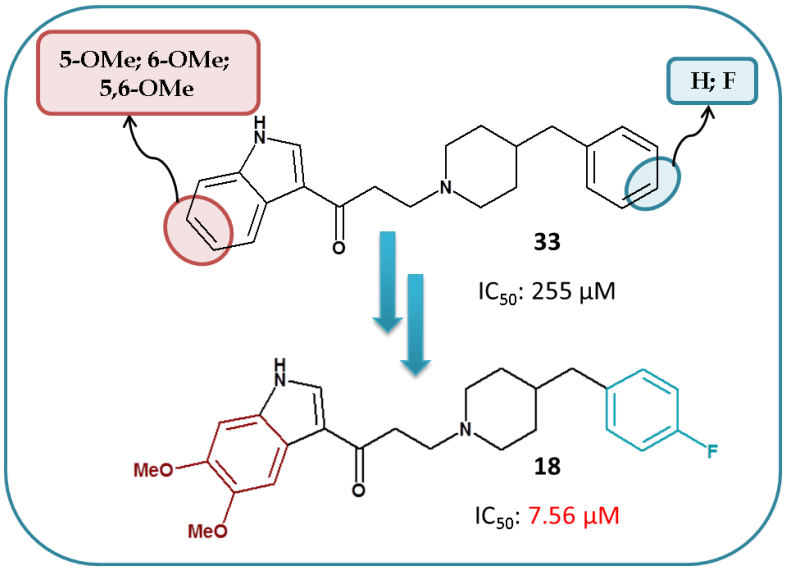

Figure 25: Structural modification of compound **33** leading to the most active derivative 1-(5,6-dimethoxy-1 -indol-3-yl)-2-(4-(4-fluorobenzyl)piperidin-1-yl)propan-1-one (**18**).[141]

In compound **18** the 5,6-dimethoxy substitution is associated with the introduction of a fluorine atom affecting TyM diphenolase activity as a mixed-type inhibitor (figure 26)

with an IC_{50} value of 7.56 µM, 35-fold more potent than derivative **33** and 3-fold more active than kojic acid of reference (IC_{50}= 17.76 µM).[141]

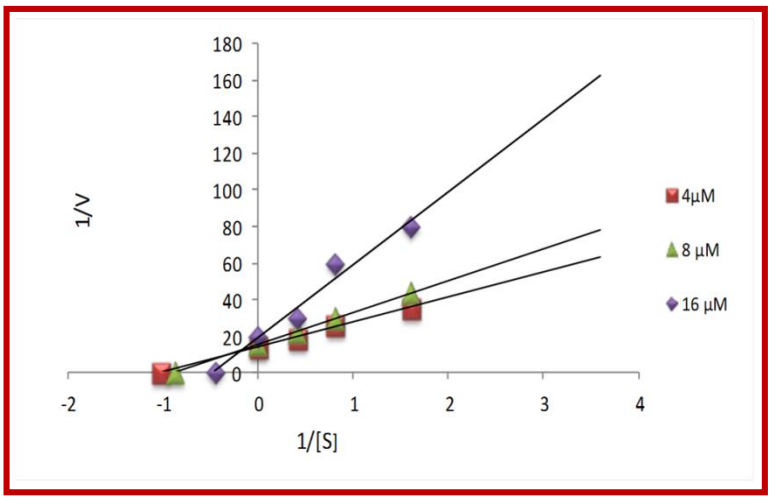

Figure 26: Lineweaver-Burk double reciprocal plots of compound **18**. The diphenolase activity of TyM was measured as a function of increasing concentration of L-DOPA. It gave straight lines with different slopes intersecting one another in the second quadrant. The reduced values of both V_m and K_m indicated that compound **18** is a mixed-type inhibitor.[141]

These data encouraged us to design and synthesize a new series of derivatives with different structural modification considering inhibitor **18** as "lead compound".[141]

5.1.1 Structural modifications of derivative 18 indolic scaffold

In order to understand the impact of indolic nucleus on TyM inhibitory effects, a new series of compounds was designed maintaining the 3-(4-(4-fluorobenzyl)piperidin-1-yl)propan-1-one tail of derivative **18** and changing the indolic scaffold with other aromatic or hetero-aromatic fragments. Therefore, the *N*-substituted 3-(4-(4-fluorobenzyl)piperidin-1-yl)propanamides (**36**, **39a-c**) were synthesized and their synthetic pathways are reported in scheme 1.[141]

Scheme 1:

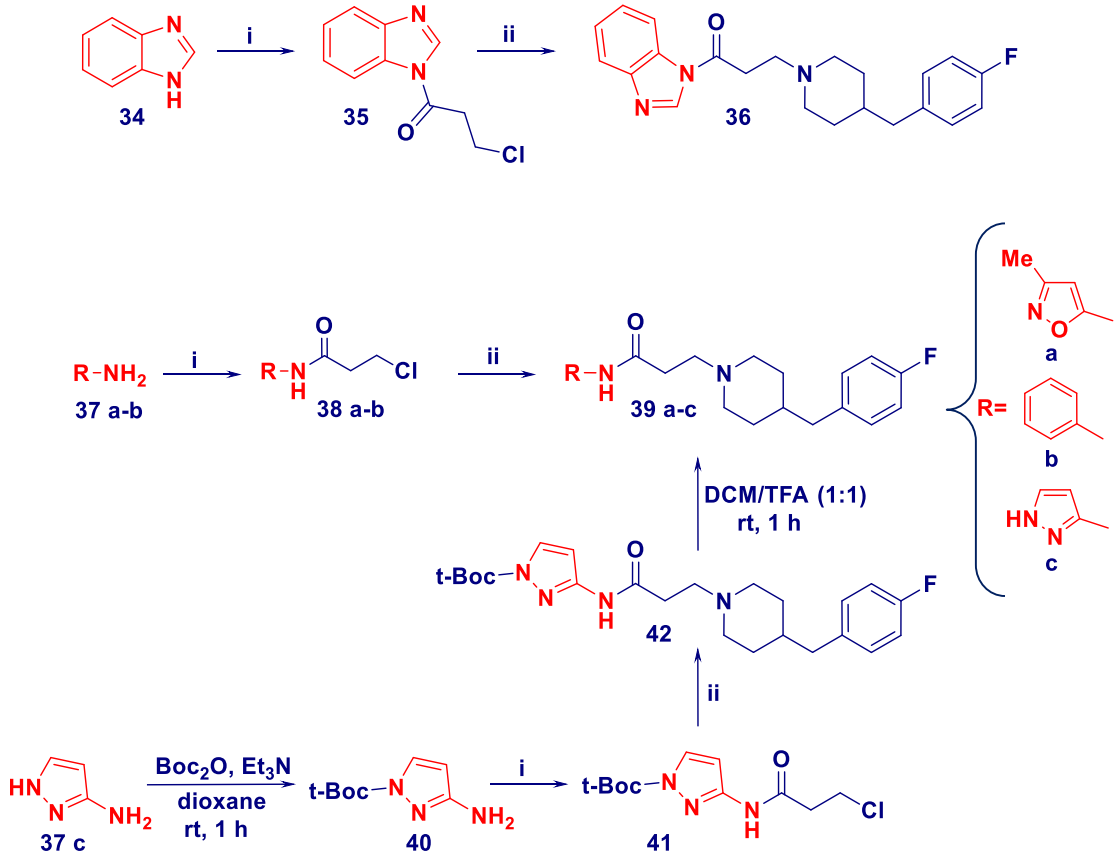

Reagents and conditions: i) 3-chloro-propionyl chloride, THF, rt, 2 h or 3-chloro-propionyl chloride, THF, K_2CO_3, rt, 16 h; ii) 4-(4-fluorobenzyl)piperidine, K_2CO_3, DMF, reflux, 2 h.

The derivatives **36**, **39a-c** were synthesized in two steps starting from the suitable amines. The reaction was carried out with 3-chloropropionyl chloride to obtain the intermediates **35**, **38a-b**, **41** which then were coupled with 4-(4-fluorobenzyl)piperidine (**43**) to give the desired compounds (**36**, **39a-c**). For the aminopirazole derivative (**39c**), firstly the amino group of starting material (**37c**) was opportunely protected (**40**) and finally, the desired compound (**39c**) was obtained by deprotection of derivative **42** with a mixture of DCM and TFA. Next, we designed and synthesized the ketone **45** as isostere of compound **39b** to probe the role of the NH interaction. The synthetic pathway of compound **45** is reported in scheme 2.[141]

Scheme 2:

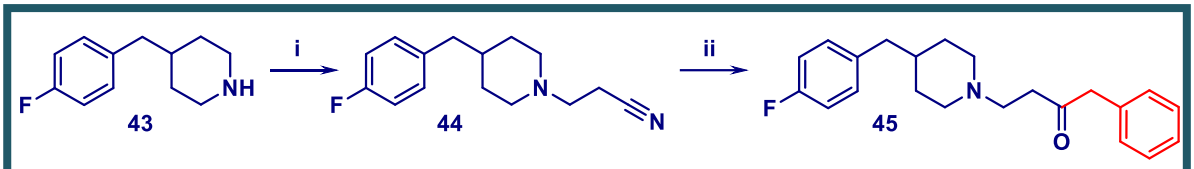

Reagents and conditions: i) 3-bromopropane-nitrile, DCM, TEA, rt, 6 h; ii) benzylmagnesium chloride, Et_2O, reflux, 5 h.

The intermediate **44** was prepared, in good yields, using 3-bromopropane nitrile and 4-(4-fluorobenzyl)piperidine (**43**) in alkaline medium by TEA. Afterwards, the intermediate **44** was converted in the final compound (**45**) under Grignard conditions using benzylmagnesium chloride.[141]

5.1.2 Inhibitory activity of derivatives 36, 39a-c, 45 on TyM

For all compounds thus obtained, the inhibitory activity using mushroom Ty enzyme extracted from *Agaricus bisporus* was evaluated, considering the inhibition of the oxidation of L-DOPA in dopaquinone (diphenolase activity). Results of biological assays are reported in table 1 in which kojic acid was used as reference standard.[141]

Table 1: Inhibitory activity of compounds **36**, **39a-c**, **45** compared to inhibitor **18** and kojic acid of reference.

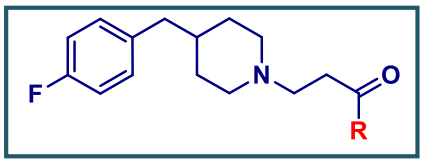

COMPOUND	R	Diphenolase activity IC_{50} (μM)[a]
36	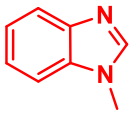	159.24 ± 18.65
39a	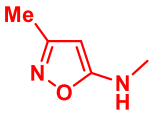	110.95 ± 18.55
39b	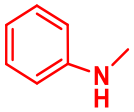	27.90 ± 0.99
39c	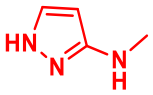	39.58 ± 9.61
45	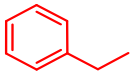	83.00 ± 6.54
18	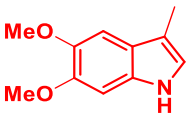	7.56 ± 1.90
Kojic acid		17.76 ± 0.18

[a] All compounds were examined in a set of experiments repeated three times;
IC_{50} values of compounds represent the concentration that caused 50% enzyme activity loss.

All compounds resulted less active than derivative **18** and kojic acid of reference. The substitution of indole nucleus with phenylamine moiety (**39b**) or pyrazole ring (**39c**) led to a moderate loss of activity, while the introduction of benzimidazole (**36**) or 3-methylisoxazole (**39a**) moieties produced a sharp decrease of inhibitory activity. Overall, the most active inhibitor **39b** displayed inhibitory potency comparable to that of kojic acid.[141]

5.1.3 Docking pose of derivative 18 in the active site of TyM

In order to obtain a plausible binding mode of inhibitor **18** in the active site of the enzyme, we performed docking studies employing the structural coordinates (PDB code 2Y9X) of TyM from *Agaricus bisporus*[27] in complex with the potent inhibitor

tropolone (IC_{50}= 0.4 μM)[228, 229] using GOLD as software.[192] The 4-(4-fluorobenzyl) piperidine moiety of compound **18** was projected in a cavity forming π-π interaction with His263, cation-π interaction with His244, Van der Waals interaction with Val283 and overlap the crystal structure orientation of inhibitor tropolone (yellow stick) sharing some keys features. The indole nucleus, occupying the binding area adjacent to the entrance of catalytic pocket cavity, was characterized by several specific contact: hydrogen bonds between the two oxygen atoms of methoxy groups and Asn81; hydrogen bond between NH and carbonyl oxygen of His85. Finally, it was possible to highlight the formation of a liphophilic "sandwich" between derivative **18** piperidine ring and Val248, Val283 residues (figure 27).[141]

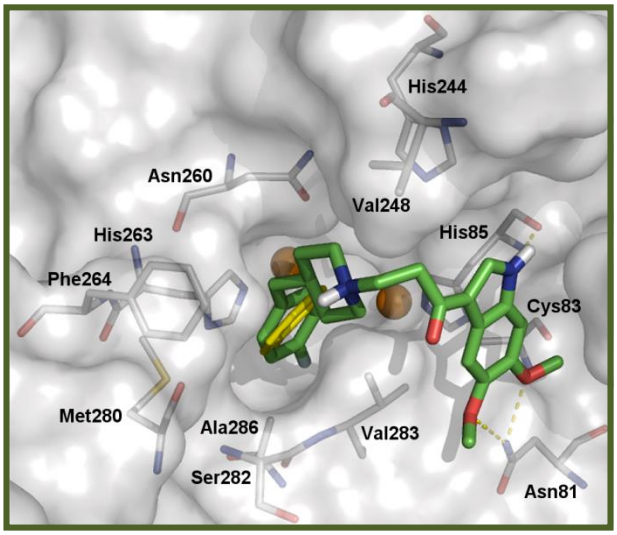

Figure 27: Docking pose of compound **18** (green stick) and tropolone (yellow stick). The copper ions are represented by brown spheres and the hydrogen bonds are drawn as yellow dashed lines.[141] The figure was generated using PyMol.[2]

5.1.4 Evaluation of the activity of the main molecular fragments of compound 18

In order to have more information about the interactions formed by the inhibitor **18** in the active site of TyM, we decided to evaluate the inhibitory activity of its main molecular fragments that seem to occupy two different cavities in the catalytic site of TyM: 4-(4-fluorobenzyl)piperidine (**43**), 1-(5,6-dimethoxy-1*H*-indol-3-yl)ethanone (**46**), 1-ethyl-4-[(4-fluorophenyl)methyl]piperidine (**47**), 4-[(4-fluorophenyl)methyl]-1-methyl piperidine (**48**) (figure 28).[141]

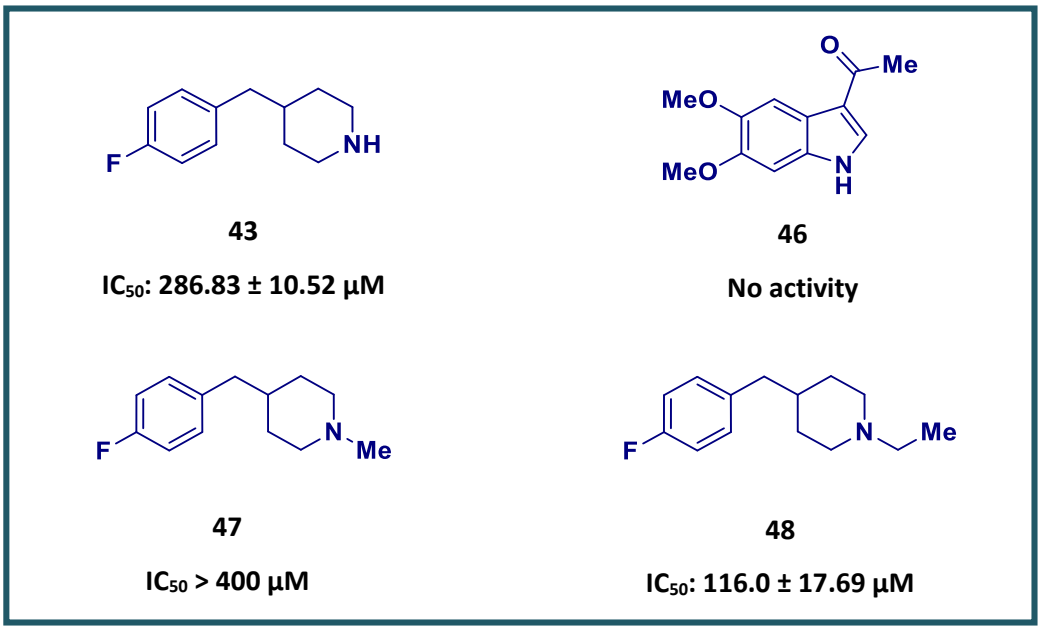

Figure 28: Chemical structures and inhibitory activities (IC_{50} value) of the main molecular fragments of compound **18**.[141]

Figure 28 displays the structures of chosen fragments and their IC_{50} values. It is interesting to note that the 4-(4-fluorobenzyl)piperidine portion (**43**) and its *N*-ethyl derivative (**48**) inhibited TyM activity, unlike the *N*-methyl analog (**47**) and compound **46**. Thus suggesting that the indole derivative (**46**), small heterocyclic moiety, occupies a binding region which is not sufficient to address inhibitory effects or that it is not able to occupy it.[141] Therefore, we supposed that the 4-(4-fluorobenzyl)piperidine portion of compound **18** is fundamental for inhibitory activity considering both biological assay and docking studies, the last suggesting that this moiety is inserted in the catalytic site.[141]

5.1.5 Synthesis of derivatives 46-48

As depicted in scheme 3, derivative **47** was obtain by reaction of 4-(4-fluorobenzyl)piperidine, paraformaldehyde and formic acid[230] while for compound **48** the reaction was carried out in presence of 4-(4-fluorobenzyl)piperidine and iodoethane in alkaline medium for K_2CO_3.[230]

Scheme 3

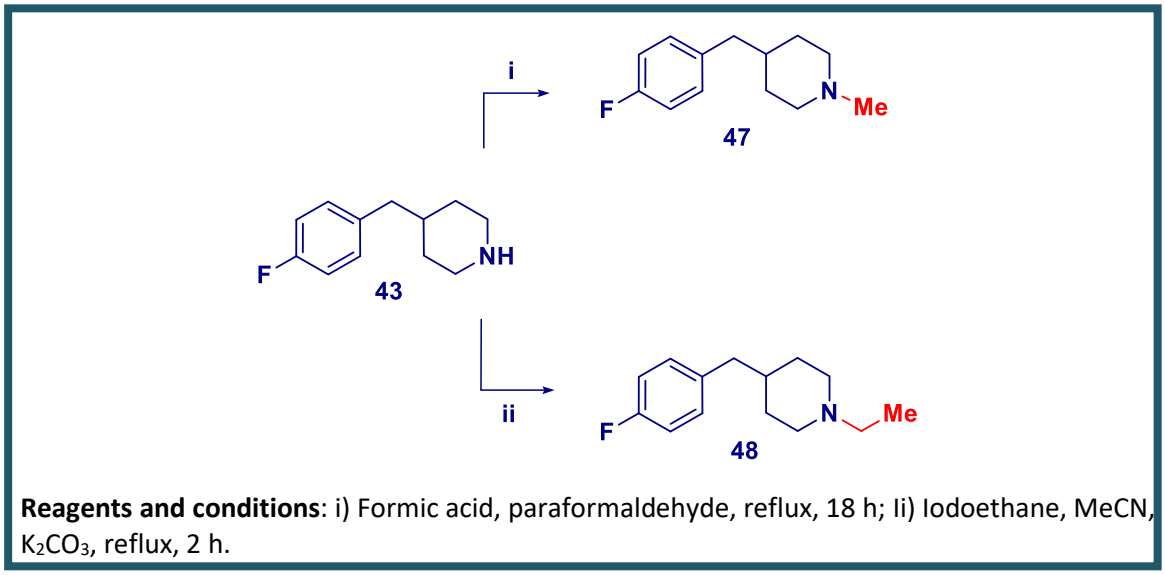

Reagents and conditions: i) Formic acid, paraformaldehyde, reflux, 18 h; Ii) Iodoethane, MeCN, K_2CO_3, reflux, 2 h.

In scheme 4 is reported the synthesis of the indole derivative (**46**), obtained under Vilsmeier-Haack conditions using phosphoryl chloride and an excess of *N*,*N*-dimethylacetamide.[141]

Scheme 4

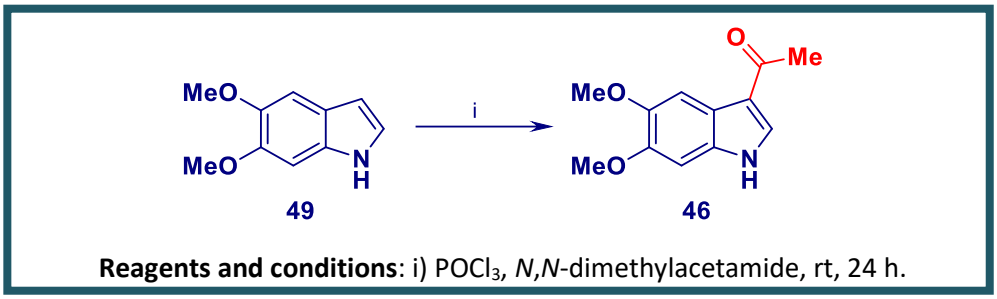

Reagents and conditions: i) $POCl_3$, *N*,*N*-dimethylacetamide, rt, 24 h.

5.1.6 X-ray studies of derivative 18 in complex with TyBm

To further validate the predicted docking pose of compound **18**, preliminary X-ray studies of inhibitor **18** co-crystal structure in complex with Ty from *Bacillus magaterium* (TyBm) were carried out at 2 Å resolution. How is shown in figure 29, the 4'-fluorophenyl moiety of compound **18** is situated between the two copper ions, with the aromatic ring stabilized through π-π interactions with residue His208. These results confirm our assumption regarding the importance of 4-(4-fluorobenzyl)piperidine portion in inhibitory activity.[141]

The crystal structures of all our derivatives have been obtained in the laboratories of Prof. Fishman at the Department of Biotechnology and Food Engineering, Technion Israel Institute of Technology, Israel.

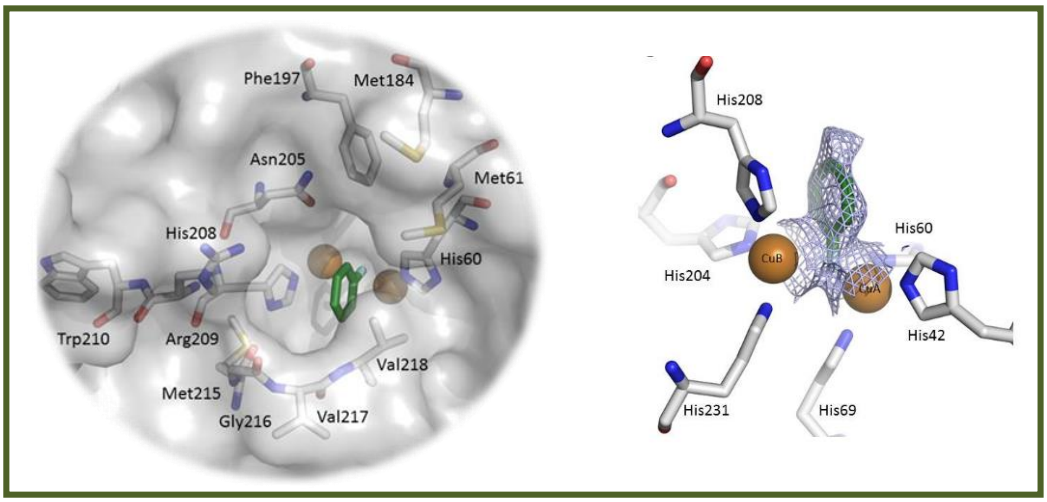

Figure 29: Co-crystal structure of the 4'-fluorophenyl portion of inhibitor **18** and TyBm.[141] The picture was generated using PyMol.[2]

As the substrate was not fully visualized, this structure was not deposited in the protein data bank but it represents for us a good starting point for the development of a further series of compounds.[141]

5.2 Design and synthesis of a series of 4-(4-Fluorobenzyl)piperidine and 1-(4-Fluorobenzyl)piperazine derivatives

Considering derivative **18** as promising TyI and on the basis of the structure–activity relationship (SAR) studies highlighting the importance of the 4'-fluorobenzyl moiety embedded in the 4-position of the piperidine fragment for the TyM inhibitory effects, we decided to design new inhibitors bearing 4'-fluorobenzyl moieties as the crucial structural requirement for the recognition of the TyIs in the catalytic site.

5.2.1 Docking studies of derivative 48

Our starting point was the fragment 1-ethyl-4-[(4-fluorophenyl)methyl]piperidine (**48**, IC_{50} = 116.0 µM) (figure 28). Docking studies were performed using the structural coordinates (PDB code 2Y9X) of the potent inhibitor tropolone in complex with TyM by GOLD software (figure 30). Assessing the high flexibility of compound **48**, we have applied the "scaffold match constraint approach" for the 4'-fluorophenyl moiety

considering the co-crystal structure of compound **18** in which this portion is situated between the two copper ions (see figure 29).[231]

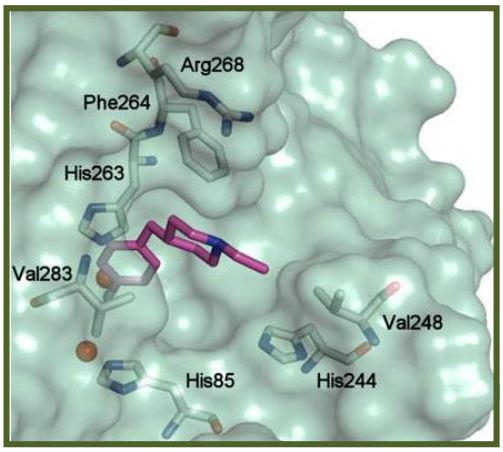

Figure 30: Docking pose of compound **48** in the active site of TyM (PDB code 2Y9X).[231] The picture was generated using PyMol.[2]

Figure 30 shows the docking pose of derivative **48**: apart from the expected key π-π interactions between His263 (His 208 in TyBm, figure 29) and the 4'-fluorophenyl ring, the *N*-ethylpiperidine portion of compound **48** seems to engage profitable contacts with the hydrophobic area fixed by residues Val248, Phe264 and Val283. Moreover, close to the *N*-ethyl substituent there is a wide pocket which might be an amenable area to further investigate SARs for this class of compounds.

On the basis of this binding mode, we designed a small series of **48** analogs bearing *N*-acyl moieties.[231]

5.2.2 Synthesis of 4-(4-Fluorobenzyl)piperidine and 1-(4-Fluorobenzyl)piperazine analogs

The first synthesized compound was 1-(4-(4'-fluorobenzyl)piperidin-1-yl)ethanone (**51**), obtained by acetylation of commercially available 4-(4'-fluorobenzyl)piperidine (**43**) (scheme 5). Then we replaced the acetyl group with other bulky substituents able to make favorable hydrophobic interactions to obtain derivatives **52-54** as reported in scheme 5.[231]

Scheme 5

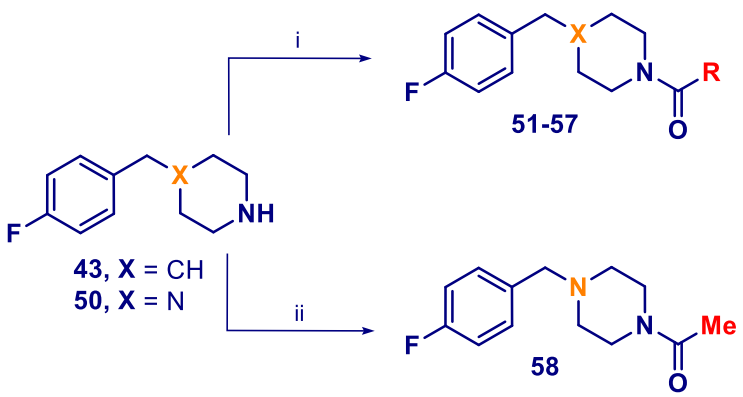

	R	X
51	CH_3	CH
52	C_2H_5	CH
53	*iso*-C_3H_7	CH
54	C_6H_5	CH
55	C_2H_5	N
56	*iso*-C_3H_7	N
57	C_6H_5	N

Reagents and conditions: i) Appropriate acyl chloride, DMF, K_2CO_3, MW, 5 min, 100 °C,200 W; ii) acetyl chloride, TEA, THF, 0 °C, rt, 10 min.

In the second round of our structural modifications we decided to change the central piperidine core with piperazine one. In particular, we selected the piperazine linker on the basis of the measured inhibitory properties of 1-(4-fluorobenzyl)piperazine (**50**) fragment, wich resulted in about 3-fold higher inhibition than 4-(4-fluorobenzyl)piperidine (**43**) against diphenolase activity of TyM (IC_{50} = 85.5 µM *versus* 286.83 µM). As shown in scheme 5 we have synthesized the designed amide derivatives **55-58** as piperazine analogs of amide **51-54.** For compound **58** the reaction was carried out at room temperature in the presence of TEA. Whereas, the amides **51-57** were obtained by applying microwave irradiations in alkaline medium for K_2CO_3 but this pathway does not allow us to achieve the desired compounds in good yields.[231]

5.2.3 Biological activity of derivatives 51-58

All of the new synthesized derivatives (**51-58**) were tested as inhibitors of TyM against diphenolase activity and the results are summarized in table 2.[231]

Table 2: Inhibitory activity of compounds **43**, **50**, **51-58** compared to amine **48** and kojic acid of reference.

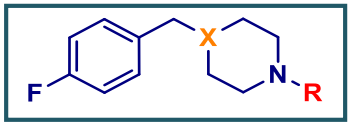

COMPOUND	R	X	Diphenolase activity IC_{50} (μM)[a]
43	**H**	**CH**	286.83 ± 1.05
50	**H**	**N**	85.50 ± 0.67
51	**CH_3CO**	**CH**	25.11 ± 0.98
52	**C_2H_5CO**	**CH**	24.10 ± 0.62
53	***iso*-C_3H_7CO**	**CH**	35.26 ± 0.97
54	**C_6H_5CO**	**CH**	19.50 ± 0.44
55	**C_2H_5CO**	**N**	51.08 ± 4.88
56	***iso*-C_3H_7CO**	**N**	30.90 ± 1.90
57	**C_6H_5CO**	**N**	13.34 ± 0.73
58	**CH_3CO**	**N**	45.85 ± 1.31
48	**CH_2CH_3**	**CH**	116.0 ± 17.69
Kojic acid			17.76 ± 0.18

[a] All compounds were examined in a set of experiments repeated three times;
IC_{50} values of compounds represent the concentration that caused 50% enzyme activity loss.

The amide **51** (IC_{50}= 25.11 μM) possesses an inhibitory activity 5-fold higher than the previously reported amine **48** (IC_{50}= 116.0 μM). Amides **52** and **54** demonstrated similar potencies to that of the parent compound **51**. Among the series of piperazine-based amides, the most active inhibitor was the [4-(4-fluorobenzyl)piperazin-1-yl](phenyl)methanone (**57**), suggesting that the combination of the *N*-benzoyl substituent with the piperazine core induced an improvement in the inhibitory effects.[231]

5.2.4 X ray studies of derivative 51 in complex with TyBm

In order to understand the intricate binding mode of this first series of amides (**51-58**) we attempted to gain crystal structures of them in complex with TyBm, obtaining it only for amide **51** at 2.7Å resolution (figure 31): the 4'-fluorobenzyl portion is oriented to CuA at a distance of 1.9 Å and it is stabilized by hydrophobic π-π interactions with His208; a hydrogen bond is keep between Arg209 and the oxygen atom of the amide carbonyl group (figure 31B), likewise as reported by Goldfeder *et al*. for tyrosine and L-DOPA.[232] The binding pocket of TyBm and TyM are quite similar[1] and the orientation

of amide **51** in the active site of TyBm is analogous to the recently determined structures with kojic acid and hydroquinone,[233] as well as docking studies with novel biphenyl ester derivatives,[137] supporting the role of this compound as a Ty inhibitor. Comparing the binding poses of amide **51** and kojic acid (PDB 5I38) was highlighted the movement of Arg209 (figure 31C). The flexibility of this residue was referred for TyBm,[234] promoting the stabilization of ligands in the active site.

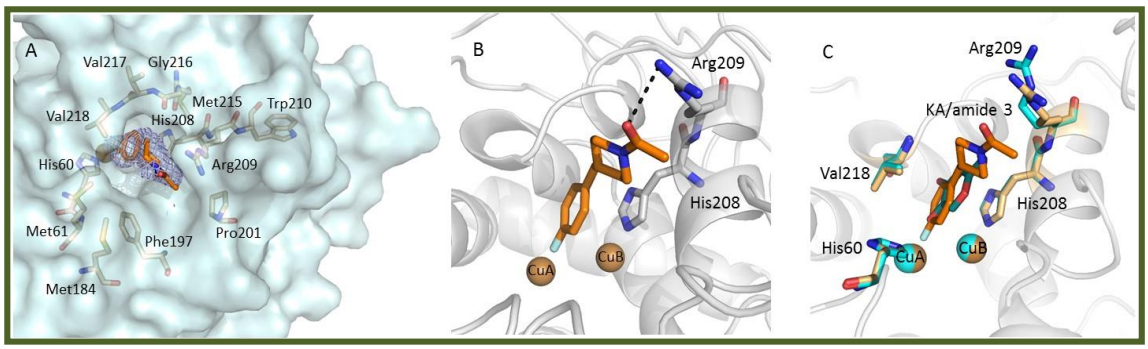

Figure 31: A) Compound **51** (orange stick) in the active site of TyBm (cyan surface) with its mFO-DFC electron density polder map (blue wire) contoured at 3σ. Copper ions are represented as brown spheres and amino acid residues as light blue sticks. B) Compound **51** (orange stick) in the active site of TyBm with the oxygen atom of the carbonyl group forming a hydrogen bond with Arg209. C) Superposition of kojic acid (cyan, PDB 5I38) and compound **51** (orange stick) in the catalytic site of TyBm. They are oriented through hydrophobic interactions with His208; copper ions, residues Val218 and His60 are equal, whereas Arg209 moves.[231] All the structures presented were generated using PyMol.[2]

Furthermore, to correlate the structural information with biochemical results, we attempted to assess the IC_{50} values of derivative **51** with TyBm, but it was not possible due to the poor solubility of derivative in buffer, necessitating the use of DMSO as a co-solvent in biochemical experiments.[231]

5.2.5 Docking studies of compound 51

To gain further insights into the binding mode of inhibitor **51** in the catalytic site of TyM, docking analysis were performed (figure 32A) applying the appropriate flexibility to the side chains of the protein: the 1-(4-fluorobenzyl) fragment establishes π-π interactions with His263, the oxygen atom of carbonyl group of derivative **51** keep a hydrogen bond with Arg268 similar to that found for Arg209 in the adduct TyBm/**51** (see figure 31B). The results thus obtained, support the reliability of our docking

simulations since the docking pose of amide **51** (figure 32A) is in agreenment with the crystal structure reported in figure 31B.

Overall, we analyzed the interactions with TyM of all tested compounds as reported for the best active inhibitor **57** (IC_{50} 13.34 µM) displayed in figure 32B.

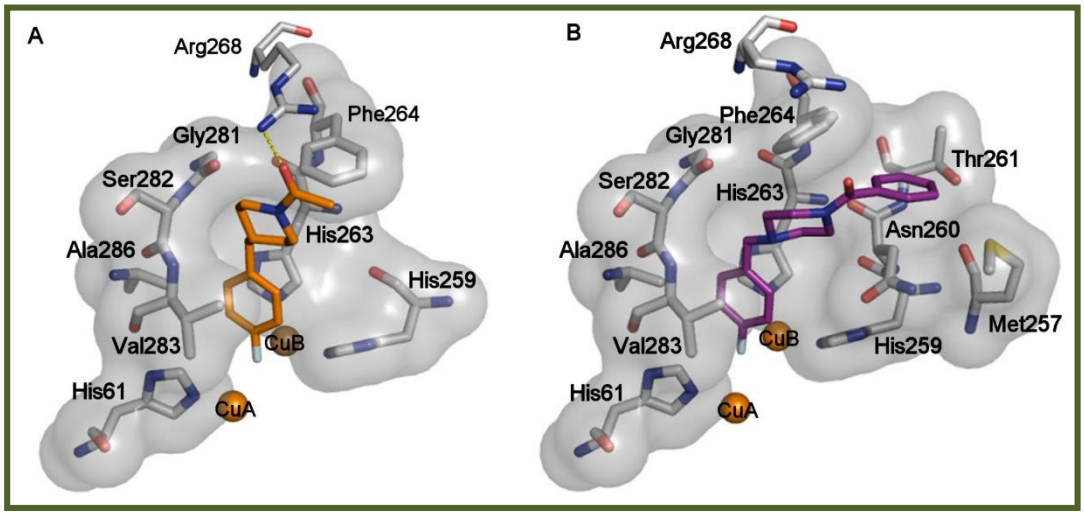

Figure 32: Plausible binding mode of compounds **51** (A) (orange stick) and **57** (B) (purple stick) in the active site of TyM (PDB code 2Y9X). Key residues of the pocket are presented as grey sticks and hydrogen bond interactions by dotted lines.[231] The interactions between TyM and inhibitors **51** and **57** were examined using PyMol[2] and LIGPLUS.[235]
The picture was generated using PyMol.[2]

The 1-(4-fluorobenzyl) fragment of derivative **57** maintains a very similar binding mode respect to **51**. The benzoyl moiety instead fits in a region located at the entrance of the catalytic area characterized by aminoacid residues Met257, Asn260, Thr261 and Phe264 keeping the inhibitor **57** in a good orientation in the catalytic pocket. The hydrogen bond of carboxylic oxygen with Arg268 that we have seen for acetamide **51** was replaced by hydrophobic interactions between the phenyl ring and the two residues Met257 and Phe264.[231]

5.2.6 Design of derivatives 59-70

Considering the interesting activity of benzamide **57** and its binding mode informations, we designed a new series of derivatives (**59-70**) possessing both hydrophobic/hydrophilic substituents in *ortho*, *meta* and *para* position of the benzoyl ring in order to explore further possible interactions in TyM active site.[231]

5.2.7 Synthesis of derivatives 59-70

Primarily, we chose the following substituents: fluorine atom and methyl, methoxy, hydroxyl groups. In order to improve the yields of the reactions respect to the first series of obtained amides **51-58**, we tried to change the reaction conditions. In particular, in the coupling of 1-(4-fluorobenzyl)piperazine (**50**) with the proper benzoylchlorides, we employed EDIPA as base conversely of K_2CO_3 and DCM as solvent instead of DMF. For derivatives **59-61** the reaction was carried out at room temperature for 5 h, reaching very good results with a growing of reactions yields from 10-20% to 50-60%. Particularly interesting was the employment of microwave irradiation for compounds **62-67** leading to 70-90% yields. The methoxy derivatives **59-61** were then converted to the corresponding hydroxyl ones **68-70** by treatment with boron tribromide (scheme 6).[231]

Scheme 6

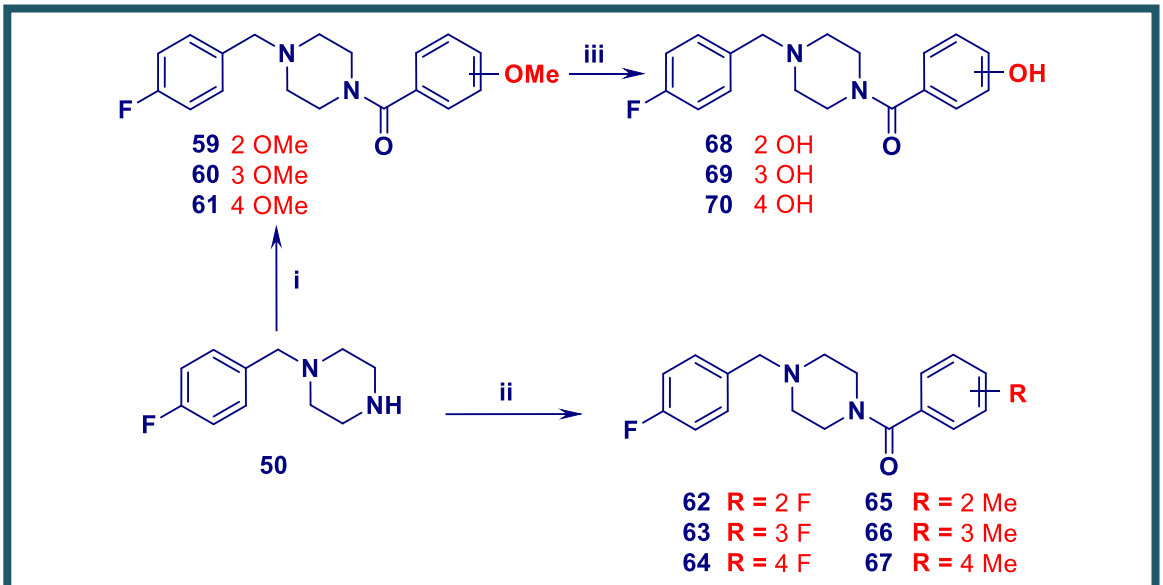

Reagents and conditions: i) Suitable benzoyl chloride, DCM, EDIPA, rt, 5 h; ii) suitable benzoyl chloride, DCM, EDIPA, MW: 10 min, 50 °C, 200 W; iii) BBr_3, DCM, 0 °C, rt, 24 h.

5.2.8 Biological activity of derivatives 59-70

In table 3 are reported the IC_{50} values of this new series of benzamides **59-70**. In general, a prominent increase of TyM inhibition, compared to the first series of tested derivatives was achieved. The amide **59** resulted the most active inhibitor, being 6-fold more potent than the unsubstituted one **57** and more potent than kojic acid of

reference. By modifing the 2-methoxysubstituent with other electron-donating groups (EDG), such as methyl or hydroxyl groups, we found that both the obtained compounds **65** and **68** presented high inhibitory activity.[231]

Table 3: Inhibitory activity of compounds **59-70** compared to unsubstituted analog **57** and kojic acid of reference.

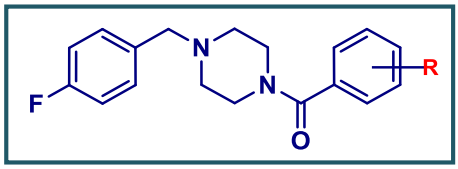

COMPOUND	R	Diphenolase activity IC_{50} (µM)[a]
59	**2 OMe**	2.03 ± 0.89
60	**3 OMe**	27.04 ± 0.05
61	**4 OMe**	9.14 ± 2.16
62	**2 F**	3.75 ± 0.37
63	**3 F**	54.68 ± 6.03
64	**4 F**	7.77 ± 2.89
65	**2 Me**	5.25 ± 1.60
66	**3 Me**	173.82 ± 1.5
67	**4 Me**	33.13 ± 4.50
68	**2 OH**	7.06 ± 0.62
69	**3 OH**	12.64 ± 1.41
70	**4 OH**	27.41 ± 0.16
57	**H**	13.34 ± 0.73
Kojic acid		17.76 ± 0.18

[a] All compounds were examined in a set of experiments repeated three times;
IC_{50} values of compounds represent the concentration that caused 50% enzyme activity loss.

It was interesting to note that the substitution in *meta* or *para* position of benzoylic ring, generally led to less active compounds, in particular for the 3methyl-substituted derivative (**66**) resulting 35-fold low active than the *ortho*-substituted analog (**65**). The presence of a fluorine atom as a small electron withdrawing group (EWG) resulted in improvement of affinity when compared with the unsubstituted analog (**57**).

Moreover, the kinetic mechanism of action of the most promising inhibitor **59** on the TyM diphenolase activity was evaluated using Lineweaver-Burk double reciprocal plots (figure 33). The plots of 1/V versus 1/[S] gave straight lines with different slopes intersecting the horizontal axis. These data suggest that compound **59** acts as a non-competitive inhibitor since it is able to bind with equal affinity to the free enzyme as

well as to the enzyme-substrate complex. The increase in concentrations of **59** corresponds to the decrease of V_{max} values, while K_m values remain unchanged. Therefore, it is assumed that the inhibitor might occupy the active site as well as hinder the access of substrate L-DOPA.[27, 236]

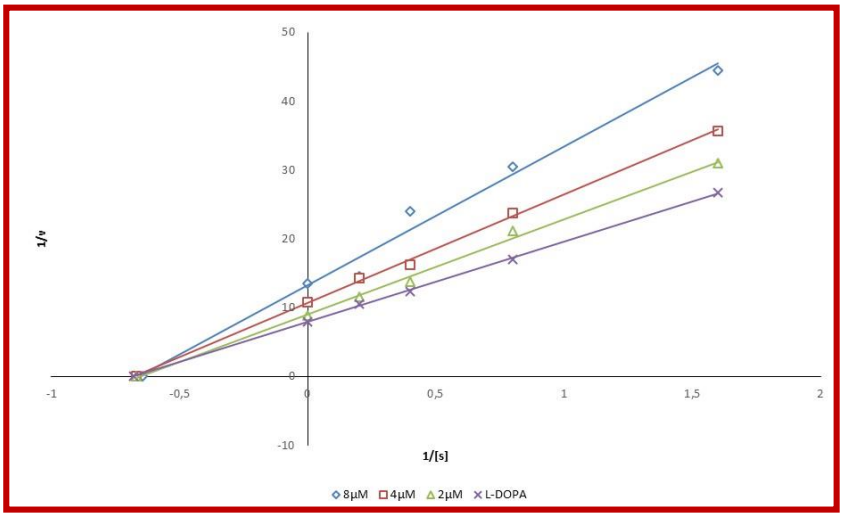

Figure 33: Lineweaver-Burk plots for the inhibition of TyM on diphenolase activity in presence of the inhibitor **59**.[231]

5.2.9 Docking studies of derivative 59

We also analysed the binding mode of the inhibitor **59** within TyM pocket. It is almost superimposable to the binding pose of unsubstitued analog **57** (figure 34), since they share very similar molecular interactions. Notably, the 2-methoxy-substituent of **59** is projected towards residue Val248 thus making an additional hydrophobic interaction. Overall, the proposed binding mode for the best active ligand **59** was in good agreement with our biochemical assays for which **59** displayed non-competitive inhibition of TyM.

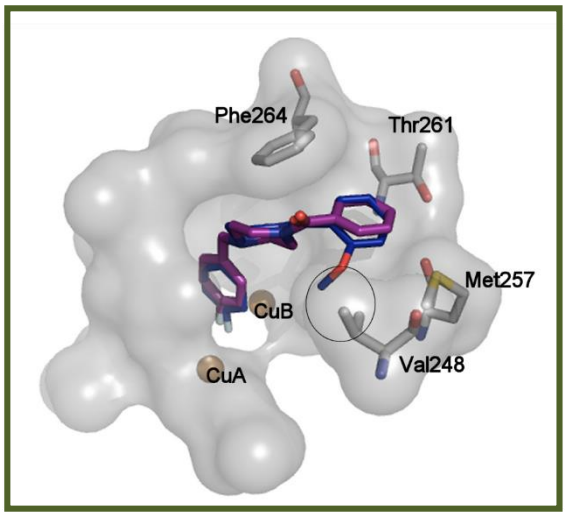

Figure 34. Predicted binding mode of benzamides **57** (purple stick) and **59** (blue stick) within TyM pocket (PDB code 2Y9X). The circle highlights the contact between methyl group and Val248 in the hydrophobic region of the cavity. Copper ions are depicted as brown spheres.[231] The figure was generated using PyMol.[2]

The binding mode of amide **59** in the active site of TyM (figure 34) might lead to the false assumption of a competitive inhibition mechanism. However, we suggest that it could also bind to a peripheral binding site in TyM yet to be elucidated. It was previously highlighted by Deri *et al*.[233] that kojic acid binds in two regions within the enzyme, inside the active site and at the entrance to the active site, giving rise to mixed inhibition kinetics. These results were demonstrated by crystallography as well as by *in silico* simulations. In addition, tropolone, another well-known Ty inhibitor, was also found at the active site entrance of TyM and exhibited mixed inhibition mode.[27] It is assumed that this additional binding mode of compound **59** in the peripheral site of TyM could restrict substrate entrance and product efflux, consequently, the non-competitive inhibition mode is obtained kinetically (see figure 33).[231]

5.2.10 Crystal structure of derivative 65 in comparison with docking studies

Furthermore, to have more informations regarding the binding mode of depicted benzamides, we tried to gain further crystal structures in complex with TyBm. Successfully, compound **65** was co-crystallized in the active site of TyBm at 2.0 Å resolution (figure 35). As expected, the 1-(4-fluorobenzyl) moiety is oriented towards CuA and is stabilized through π-π interactions with His208; a hydrogen bond between carbonyl group of **65** and Arg209 is observed as we have seen for compound **51** in TyBm active site (figure 35). Comparing the positioning of bound amide **51** and

benzamide **65**, the major difference observed is the slight movement of Arg209 (figure 35B). The mobility of Arg209 allows the stabilization of bulky compounds in the active site of TyBm.[231]

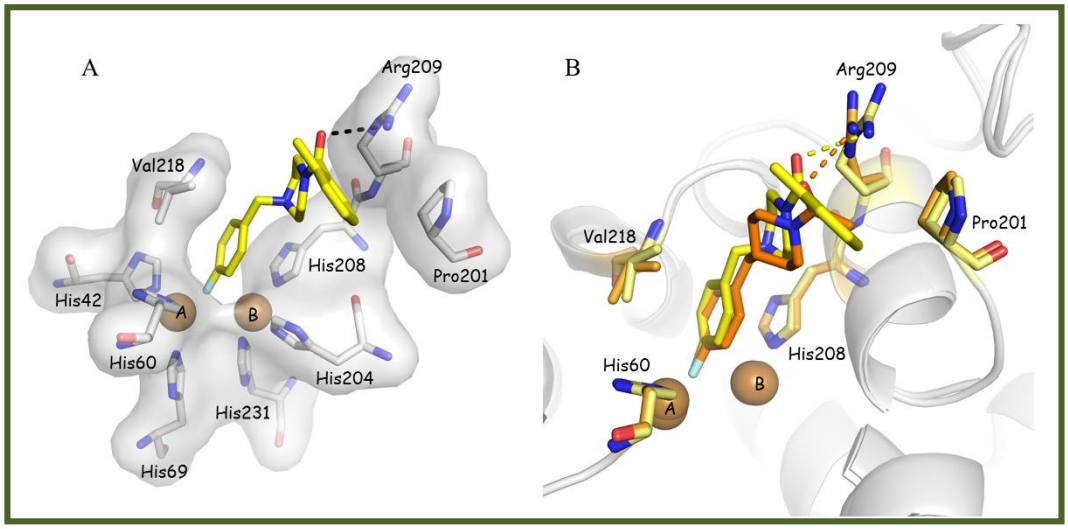

Figure 35. Benzamide **65** in the active site of TyBm. (A) Benzamide **65** (yellow stick) positioned in the active site of TyBm with the oxygen atom of the carbonyl group forming a hydrogen bond with Arg209. (B) Superposition with amide **51** (orange stick). Copper ions are presented as brown spheres and and hydrogen bond interactions by dotted lines.[231] The figure was generated using PyMol.[2]

The two inhibitors **51** and **65** share a very similar binding mode within catalytic site of TyBm, as also suggested by the binding pose of inhibitor **65** docked in the catalytic site of TyM in comparison with analogues **57** and **59** (figure 36).

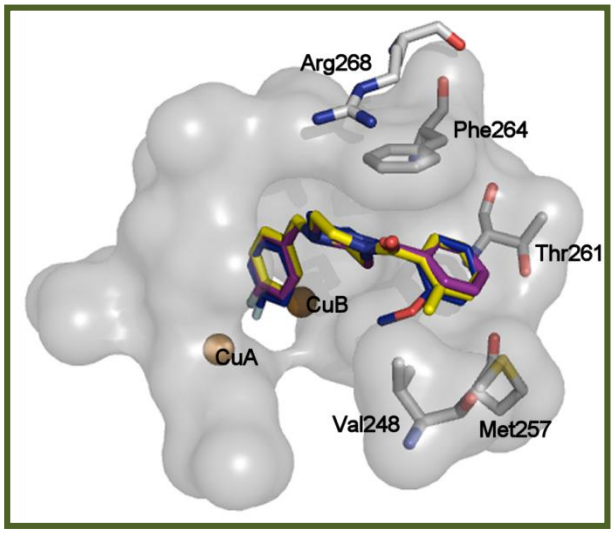

Figure 36: Predicted docking poses of benzamides **65** (yellow stick) into the TyM (PDB code 2Y9X), superimposed to **57** (purple stick) and **59** (blue stick). Copper ions are depicted as brown spheres.[231] The figure was generated using PyMol software.[2]

Considering that the inhibition kinetic suggests that the inhibitor **65** (figure 37) displays a mode of interaction similar to that we found for compound **59** (see figure 33), we can speculate that both **65** and **59** derivatives could hamper the enzymatic activity of TyM through a singular mechanism of interaction that might involve additional and peripheral binding regions.[231]

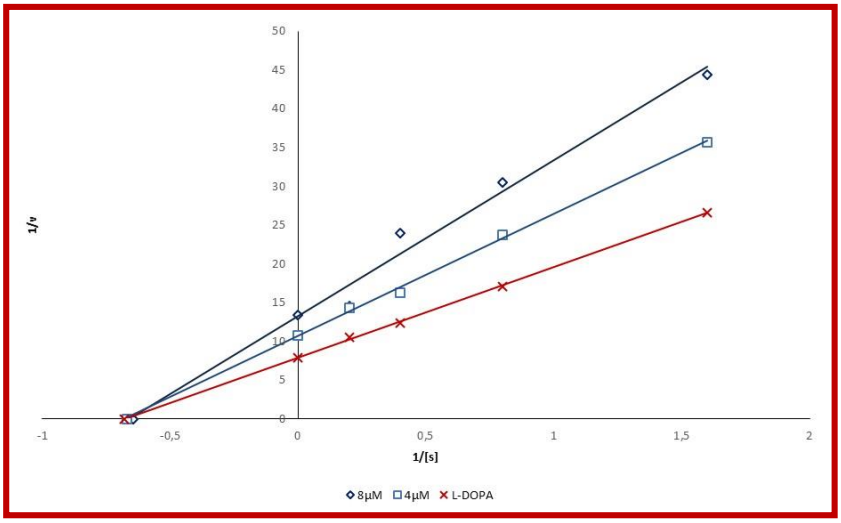

Figure 37: Lineweaver-Burk plots for the inhibition of TyM on diphenolase activity in presence of the active inhibitor **65**.[231]

5.2.11 Insight into the fundamental interactions between derivative 65 and TyM

Taking into consideration the results achieved so far, with the aim to design further possible TyIs by rational approaches, the possible interaction areas of the TyM catalytic site were calculated creating a pharmacophore maps by use of the tool "*Apo Site Grid*", present in the LigandScout vs 4.1 software. In particular, to obtain the Grid maps we considered the best docking pose of compound **65** into the TyM active site (PDB code 2Y9X). Our attention has been turned especially in the benzoyl moiety with the purpose of exploring the wide region in which it is positioned. As depicted in figure 38 A, the grid shows a large hydrophobic area (yellow grid) surrounding the entire molecule, unlike the aromatic map (blue grid) that is instead wider in the para-fluoro benzyl zone, confirming the importance of the presence of an aromatic ring in the catalytic site. A small aromatic zone also appears close to the benzoyl group suggesting that the presence of different or additional aromatic groups may be useful to establish further interactions between the ligands and the protein. Finally, the maps relating to the H-bond donor (green grid) or H-bond acceptor (red grid) suggest that the insertion

of acceptor or donor groups might be favorable on both the aromatic rings of compound **65**. In particular, the insertion of a hydrogen bonding acceptor group in the *ortho* position of the benzoyl ring seems to be more indicated (figure 38 B).

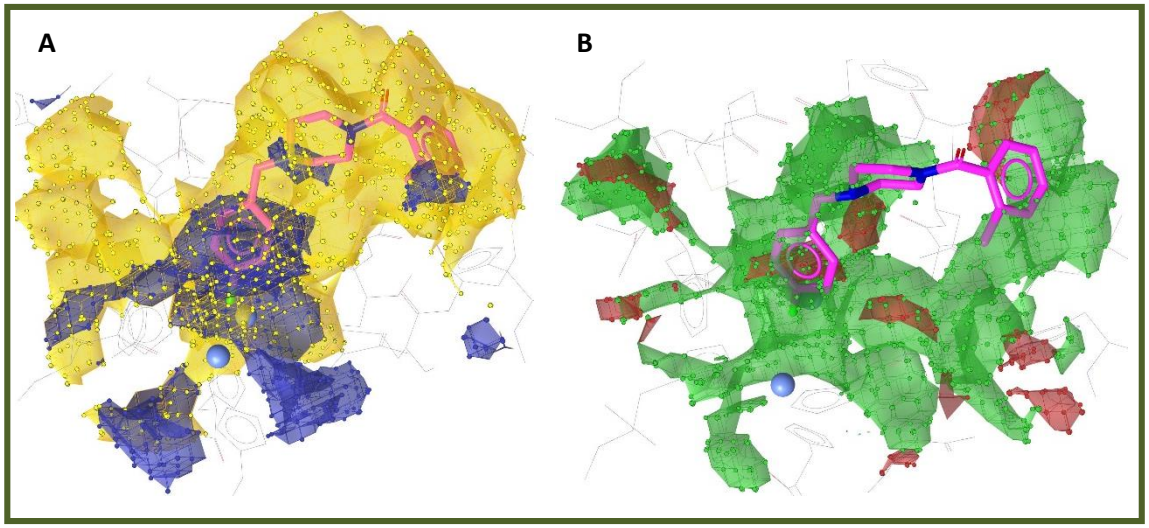

Figure 38: *Apo Site Grid* generated starting from the best docking pose of derivative **66** in the catalytic site of TyM. A) Yellow grid highlights the favorable presence of hydrophobic groups and specifically blue grid indicates aromatic rings. B) Green grid delineates H-bond donor and red grid H-bond acceptor. The picture was generated using Ligand Scout software.[224]

Thus, we designed a new series of compounds with further substituents in *ortho*, *para* and *meta* positions of benzoyl ring considering the grid map obtained. In particular, we chose chlorine and bromine atoms to accomplish the previous series of halogens derivatives (**62-64**) entertaining the hydrophobic interactions (yellow grid) of the grid; nitro group as H-bond acceptor, as suggested by the red grid especially in *ortho* position of benzoyl moiety; amino group as H-bond donor (green grid); trifluoromethyl group considering both the hydrophobic interaction (yellow grid) and the halogen-bond interaction that could be generated (green grid). As generally the presence of substituents in *ortho* and *para* position are favored for inhibitory activity, we also decided to synthesize the 2,4-disubstituted derivatives possessing methyl, methoxy, hydroxy, nitro, amino and trifluoromethyl groups and fluoro, chloro, bromo atoms.

5.2.12 Synthesis of derivatives 71-94

To obtain derivatives **71-83** the same synthetic pathway previously reported was used applying microwave irradiations in alkaline medium for EDIPA. For compounds **84-89**, 1-(4-fluorobenzyl)piperazine was reacted with the suitable benzoic acid furnishing the

corresponding benzamide derivatives via *N,N,N,N*-tetramethyl-*O*-(1*H*-benzotriazol-1-yl)uroniumhexafluorophosphate (HBTU) coupling in the presence of TEA.

Scheme 7

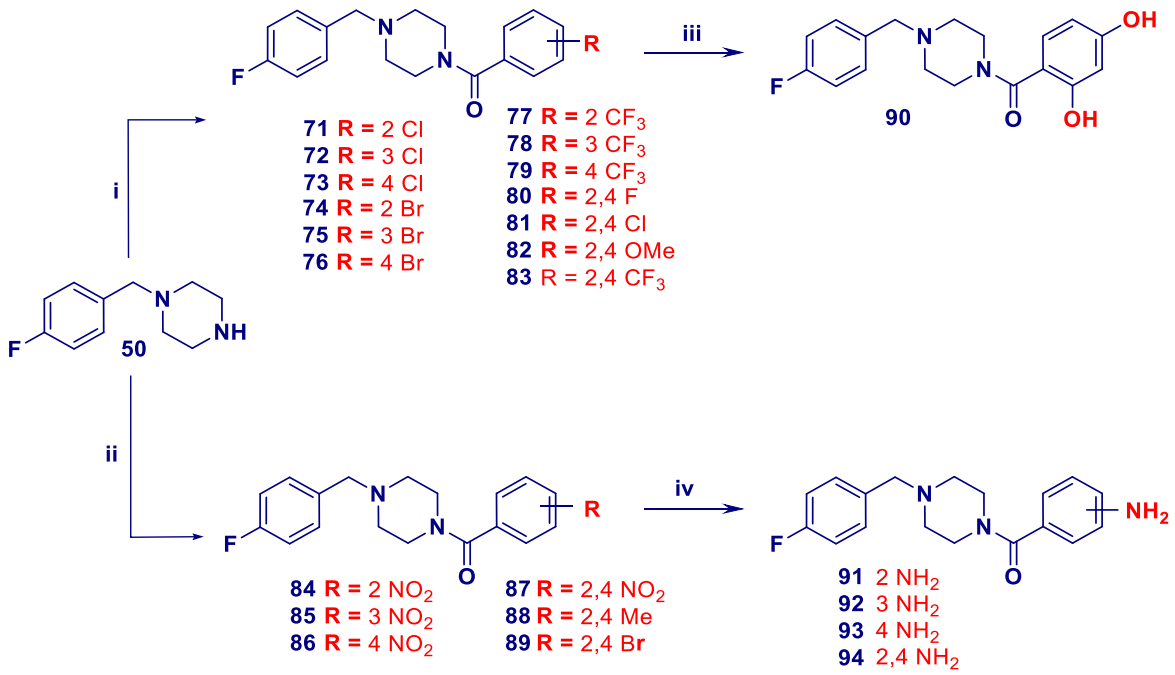

Reagents and conditions: i) Suitable benzoyl chloride, DCM, EDIPA, MW: 10 min, 50 °C, 200 W; ii) suitable benzoic acid, HBTU, TEA, DMF, rt, 24 h; iii) BBr_3, DCM, 0 °C, rt, 24 h; iv) HCl, Zn, EtOH, reflux, 2 h.

The 2,4-hydroxy derivative (**90**) was obtained treating the starting 2,4-methoxy compound (**82**) with boron tribromide. The amino derivatives (**91-94**) instead were achieved by reduction of the suitable nitro compounds (**84-87**) in presence of HCl and zinc.

5.2.13 Biological activity of derivatives 71-94

For all compounds thus obtained we tested the inhibitory activity against TyM and the results are reported in table 4.

Table 4: Inhibitory activity of compounds **71-94** compared to unsubstituted analog **57** and kojic acid of reference.

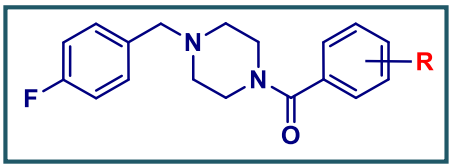

COMPOUND	R	Diphenolase activity IC_{50} (μM)[a]
71	**2 Cl**	3.12 ± 0.04
72	**3 Cl**	5.30 ± 0.40
72	**4 Cl**	3.51 ± 1.24
74	**2 Br**	2.03 ± 0.05
75	**3 Br**	2.40 ± 0.28
76	**4 Br**	4.61 ± 1.83
77	**2-CF_3**	0.48 ± 0.05
78	**3-CF_3**	8.43 ± 0.42
79	**4-CF_3**	3.38 ± 0.07
80	**2,4 F**	1.91 ± 0.13
81	**2,4 Cl**	0.79 ± 0.11
82	**2,4 OMe**	1.40 ± 0.43
83	**2,4-CF_3**	1.63 ± 0.11
84	**2-NO_2**	0.87 ± 0.08
85	**3-NO_2**	3.60 ± 0.07
86	**4-NO_2**	2.05 ± 0.16
87	**2,4 NO_2**	0.96 ± 0.21
88	**2,4 Me**	3.43 ± 0.08
89	**2,4 Br**	1.05 ± 0.09
90	**2,4 OH**	1.49 ± 0.32
91	**2-NH_2**	10.94 ± 0.44
92	**3-NH_2**	3.81 ± 0.56
93	**4-NH_2**	14.66 ± 0.15
94	**2,4 NH_2**	3.67 ± 0.75
57	**H**	13.34 ± 0.73
Kojic acid		17.76 ± 0.18

[a] All compounds were examined in a set of experiments repeated three times;
IC_{50} values of compounds represent the concentration that caused 50% enzyme activity loss.

In general, for all synthesized compounds, a good inhibitory activity was observed with IC_{50} values lower or comparable to that of the unsubstituted analog (**57**) and kojic acid of reference. Particularly interesting was the substitution with nitro and trifluoromethyl groups especially in *ortho* position of the benzoyl ring allowing us to reach nanomolar range with IC_{50} values of 870 and 480 nM respectively. The amino

derivatives instead possess an inhibitory activity comparable to that of unsubstituted analog (**57**) and kojic acid of reference except for the *meta* amino analog (**92**) for which the activity is 3.81 μM.

Considering the disubstitutions, an improvement of inhibitory activity was always observed with IC_{50} values lower or comparable to those of the respective monosubstituted derivatives. In particular, the most active compounds resulted the 2,4-dinitro and 2,4-dichloro analogs with IC_{50} values of 790 and 960 nM respectively.

5.2.14 Docking studies of derivatives 77, 81, 84 and 87

Also for this new series of compounds docking studies were performed. In particular, here are reported the docking poses of the more promising inhibitors.

Considering the monosubstituted derivatives, the best results emerged for compounds **77** and **81**. As always, the 1-(4-fluorobenzyl)piperazine moieties are projected in the catalityc site between the two copper ions, forming π-π interaction with His263. For compound **77** we can observe the formation of different hydrogen bonds: the ionizable NH of piperazine ring keeps hydrogen bond with the carbonylic group of Asn260; the carbonylic group of benzoyl ring mades hydrogen bond with the OH group of Ser282 and the NH group of Val283 (figure 39a). In amide **81** instead, a polar contact between the nitro group of derivative **81** and the guanidine group of Arg268 is observed (figure 39b).

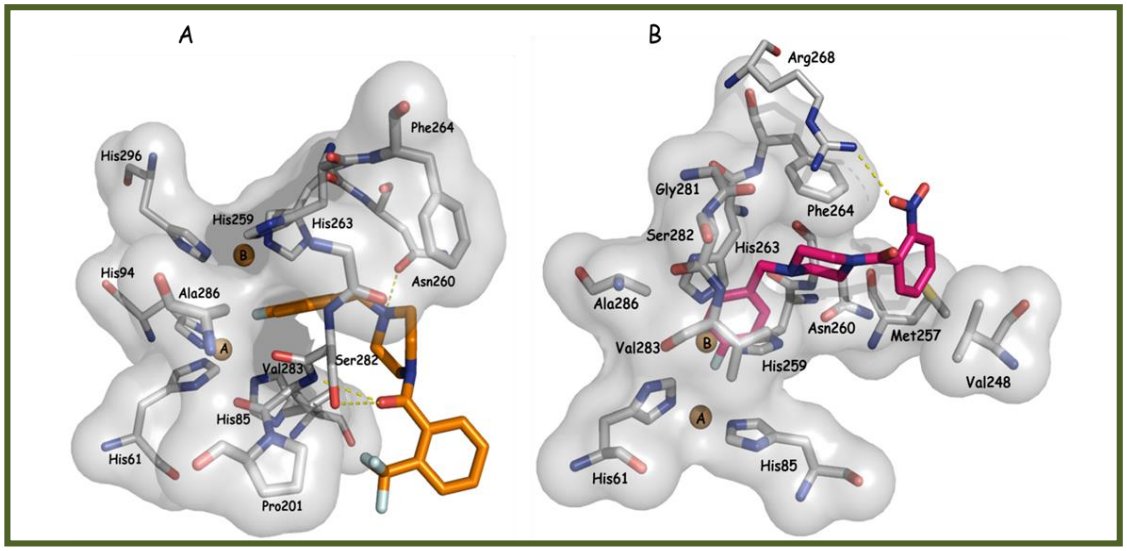

Figure 39: Plausible binding mode of compounds **77** (A) (orange stick) and **81** (B) (magenta stick) in the active site of TyM (PDB code 2Y9X). Key residues of the pocket are presented as grey sticks and hydrogen bond interactions by dotted lines. The interactions between TyM and inhibitors **77** and **81** were examined using PyMol[2] and LIGPLUS[235].
The picture was generated using PyMol.[2]

Taking into account the disubstitued analogs, amides **84** and **87** showed the best results. Apart from the expected π-π interactions between the 1-(4-fluorobenzyl)piperazine moieties and His263, in compound **84** the benzoyl group with the two chlorine atoms is projected in an area characterized by the aminoacids Met257, Gly249 Val248 and Asn260 (figure 40a); in compound **87** the two nitro groups made polar contacts with the guanidine group of Arg268 and the OH group of Thr261 (figure 40b).

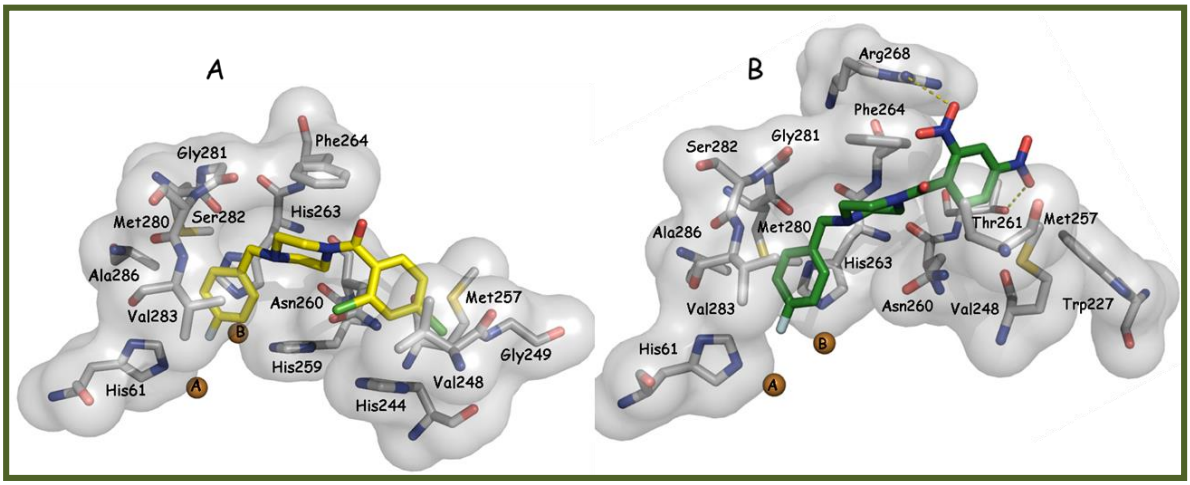

Figure 40: Plausible binding mode of compounds **84** (A) (yellow stick) and **87** (B) (green stick) in the active site of TyM (PDB code 2Y9X). Key residues of the pocket are presented as grey sticks and hydrogen bond interactions by dotted lines. The interactions between TyM and inhibitors **84** and **87** were examined using PyMol[2] and LIGPLUS[235].
The picture was generated using PyMol.[2]

5.2.15 Cytotoxicity effect in B16F10 melanoma cells of derivative 87

In order to have an idea regarding the cytotoxicity effect of our compounds, we attempted to gain the cytotoxicity effect in B16F10 mouse melanoma cells by measuring the cell viability, obtaining it for amide **87**. The preliminary data showed that compound **87** exhibited no cytotoxic effect at its IC_{50} value (0.96 ± 0.21 µM), as demonstrated by the viability of 99.1% in B16F10 cells showing a CC_{50} value of 53.20 µM (graphic 2).

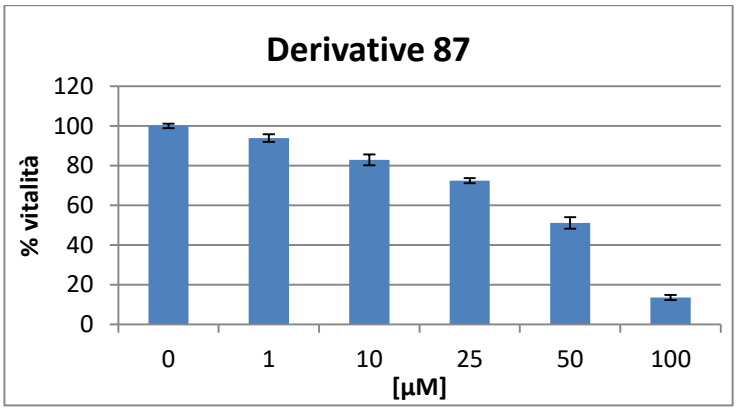

Graphic 2: Effect of compounds **87** on B16F10 melanoma cell viability determined by MTT assay.

The assay has been performed in collaboration with Prof. Antonella Fais at the Department of Life Science and Environment, University of Cagliari.

5.2.16 Modification of the benzoyl ring of derivative 57 with other aromatic or heteroaromatic rings

As last step of our modification on lead compound **57**, we designed a new series of molecules (**95-103**) replacing the phenyl group of benzoyl ring with further aromatic or heteroaromatic rings such as thiophene (**95**), furan (**96**), 1,3-benzodioxole (**98**), 1-naphthalene (**99**), 2-naphthalene (**100**), pyrrole (**101**), indole (**103**), or growing up the length chain of the molecule (**97**, **102**). The choice of the substituents was carried out on the basis of the suggestion from the grid maps previously reported (see figure 38) and different aroyl chlorides and aryl carboxylic acids commercially available. The synthetic pathways employed to obtain this new series of compounds are the same of those already mentioned before and are depicted in scheme 8.

Scheme 8

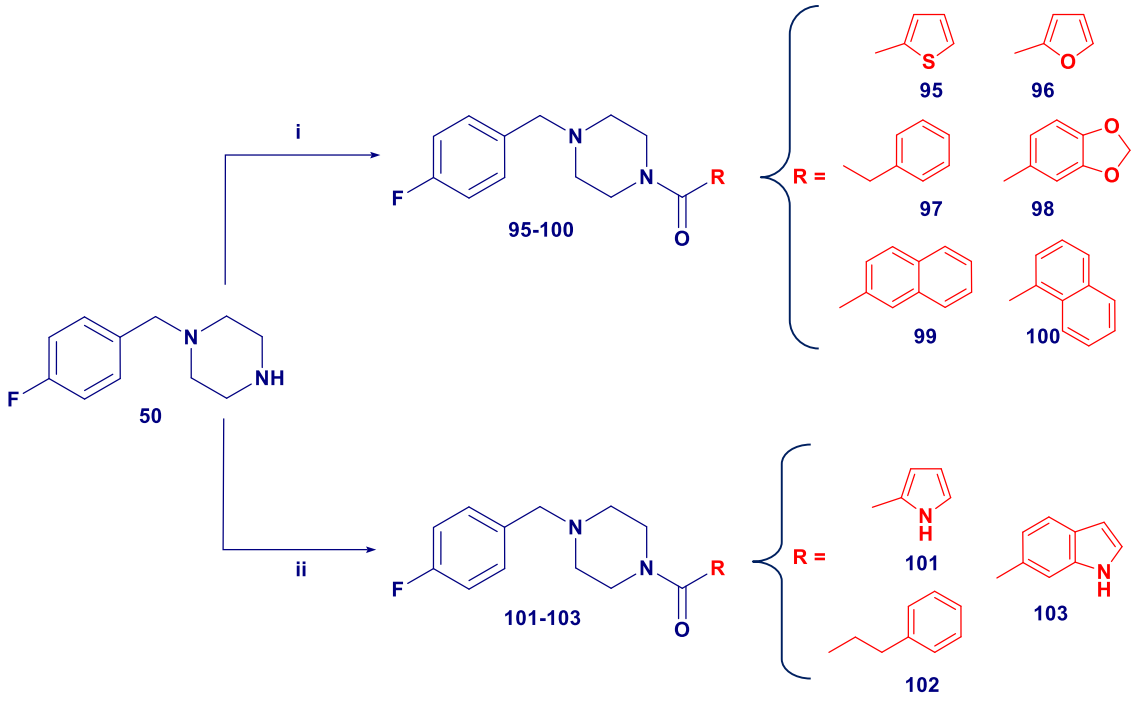

Reagents and conditions: i) Suitable acyl chloride, DCM, EDIPA, MW: 10 min, 50 °C, 200 W; ii) suitable carboxylic acid, HBTU, TEA, DMF, rt, 24 h.

5.2.17 Biological activity of derivatives 95-103

For all obtained compounds, we tested the inhibitory activity against TyM and the results are reported in table 5.

Table 5: Inhibitory activity of compounds **95-103** compared to unsubstituted analog **57** and kojic acid of reference.

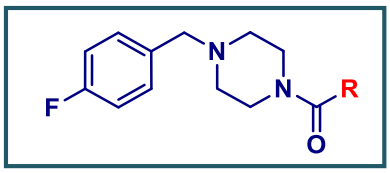

COMPOUND	R	Diphenolase activity IC_{50} (μM)[a]
95	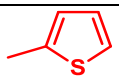	3.49 ± 0.60
96	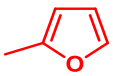	4.84 ± 0.47
97	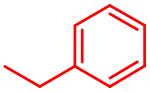	4.28 ± 0.86
98	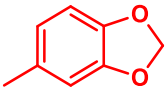	2.68 ± 0.13
99	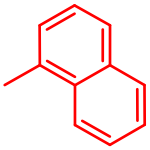	2.54 ± 0.42
100	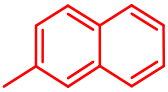	2.62 ± 1.06
101	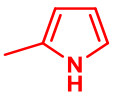	12.01 ± 3.53
102	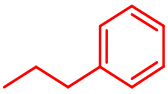	13.17 ± 2.71
103	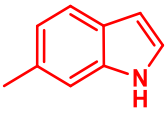	4.52 ± 0.86
57	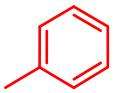	13.34 ± 0.73
Kojic acid		17.76 ± 0.18

[a] All compounds were examined in a set of experiments repeated three times;
IC_{50} values of compounds represent the concentration that caused 50% enzyme activity loss.

In general, a good inhibitory activity was observed for all designed compounds, with IC_{50} values lower or comparable to that of derivative **57** and kojic acid of reference. In particular, the presence of bulky aromatic substituents such as indole, naphthalene or 1,3-benzodioxole rings led to promising results with IC_{50} value between 2 and 4 μM, according to the blue part of the grid reported before (see figure 38). The presence of

furan or thiophene rings conducted to an improvement of inhibitory activity with an IC_{50} value of 4.84 and 3.49 μM respectively, unlike pyrrole analog for which the attributed activity is comparable to that of reference compounds **57** and kojic acid.
Concerning compounds **97** and **102** our idea was to growing up the chain length of the molecules to increase their flexibility and understand if it was possible to gain further contacts with the main amino acids of the pocket. The data suggest that the phenyl derivative (**97**) possesses an inhibitory activity 3-fold up than the benzoyl one (**57**), whereas the propyl analog (**102**) presents an activity comparable to that of reference compound **57**.

5.2.18 Docking studies of derivatives 98-100

Among the series of the amides characterized by different aromatic or heteroaromatic rings, the best results were obtained for derivatives **98-100**. In compound **98** the oxygen atom of benzodioxol ring mades hydrogen bond with the amidic NH_2 of Asn260 (figure 41a); both the naphtoyl rings of compounds **99** and **100** are inserted in an area featured by aminoacids Asn260, Met257, Gly249, Val248; His244 and Leu275, Phe264, Pro277, Gly281 respectively (figure 41b and 41c).

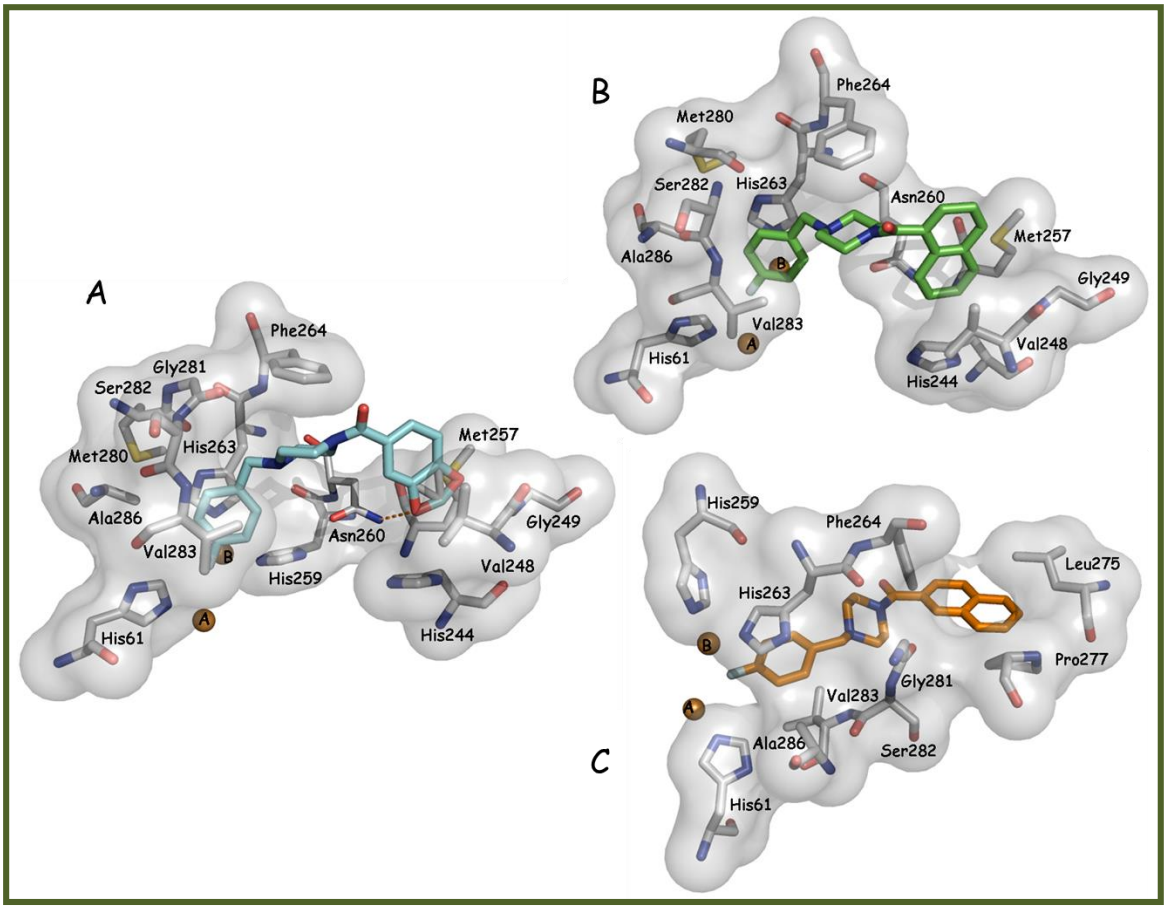

Figure 41: Plausible binding mode of compounds **98** (A) (light blue stick), **99** (B) (green stick) and **100** (C) (orange stick) in the active site of TyM (PDB code 2Y9X). Key residues of the pocket are presented as grey sticks and hydrogen bond interactions by dotted lines. The interactions between TyM and inhibitors **98**, **99** and **100** were examined using PyMol[2] and LIGPLUS[235]. The picture was generated using PyMol.[2]

5.3 Generation of pharmacophore model for the development of new TyM inhibitors

With the aim to identify further TyIs with different chemical behaviors, we decided to create a pharmacophore model starting from the co-crystal structure of one of our previous discovered TyI, 1-[4-(4-fluorobenzyl)piperidin-1-yl]ethanone (**51**) in complex with TyBm (PDB code 5OAE) (see figure 31) through structure-based approaches using LigandScout software vs 4.1. The features derived from both the protein-ligand complex and the enzyme apo-structure were considered, thus generating the apo-site pharmacophore model considering only the buriedness surface and setting the option "Append to existing pharmacophore".

Therefore, we generated the first structure-based pharmacophore model consisting of eight excluded volume spheres and four features: (i) two hydrophobic spheres in yellow and one aromatic feature (blue circle), which project into a pocket defined by

His208, Val218, Ala 221 e Phe227; (ii) one H-bond acceptor targeting Arg209 (figure 42).

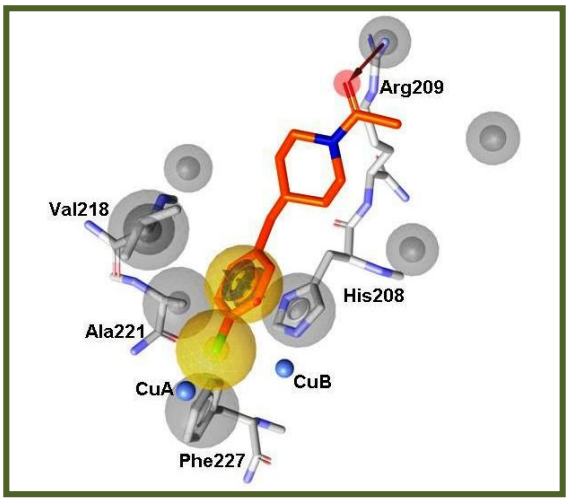

Figure 42: Structure based pharmacophore model generated by LigandScout V4.1 based on TyBm co-crystallized with the inhibitor **51** (orange stick). Chemical features are color-coded: yellow spheres represent hydrophobic features, blue circles represent aromatic features and the red arrows represent H-bond acceptors. Excluded volumes are represented by grey spheres and copper ions by blue spheres. The picture was generated using Ligand Scout.[224]

In order to find other possible interactions with the residues present in the binding pocket, we explored the features deriving from the apo-structure of the protein calculating the entire possible interactions by using the "Create Apo Site Grids" tool implemented in LigandScout 4.1. Among them we found a H-bond donor targeting the Asn205 which was reported to be crucial for Ty activity through the activation of a conserved water molecule. Therefore, the interaction with Asn205 might prevent this activation resulting in inhibition of Ty activity.[232, 233] For this reason, we decided to add to the previous model this H-bond donor interaction with Asn205 and also two hydrophobic features that might contribute to a further stabilization of the ligand in the active site, considering that the Ty binding pocket is essentially hydrophobic (figure 43).

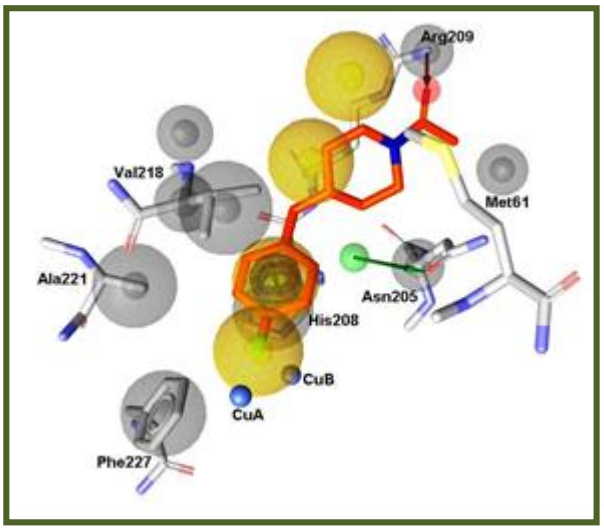

Figure 43: Pharmacophore model generated adding the features from the Apo-Site Pharmacophore. Green arrows represent H-bond donors, red arrows H-bond acceptors, blue circles aromatic features and yellow spheres hydrophobic features. Excluded volumes are represented by grey spheres and copper ions by blue spheres.
The picture was generated using Ligand Scout.[224]

Furthermore, the hydrophobic feature deriving from the fluorine atom was converted into a H-bond acceptor in order to make the model able to retrieve compounds with chemical functionalities that might coordinate the copper ions present in the active site. Excluded volumes were manually added in order to delimit the size and the shape of the binding site. Therefore, the model consists of one aromatic features, one H-bond donor, two H- bond acceptors, two hydrophobic features and thirty-nine excluded volumes (figure 44).

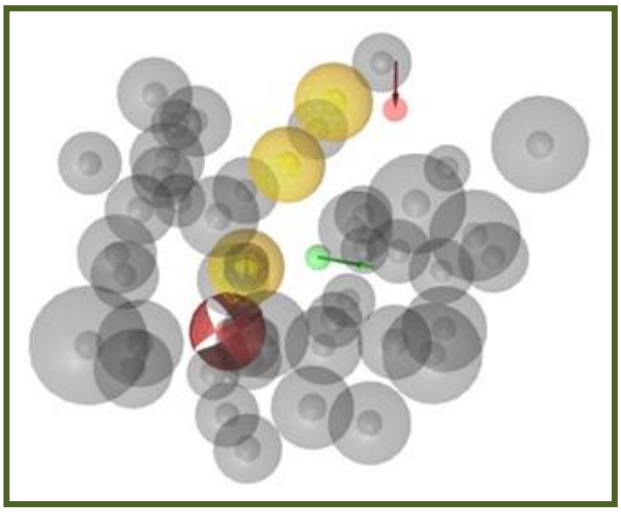

Figure 44: Complete pharmacophore model. The model is characterized by (i) two hydrogen bond acceptors, (ii) one aromatic feature, (iii) three hydrophobic features, (iv) one hydrogen bond donor and thirty-nine excluded volumes. The picture was generated using Ligand Scout.[224]

In order to refine and validate the obtained model, we screened it against a dataset containing 29 active compounds with IC_{50} values between 0-200 µM and 173 low active compounds with IC_{50} values between 100-400 µM. These molecules were extracted from the ChEMBL database which is an Open Data database containing binding, functional and ADMET information for a wide number of bioactive compounds.[237] The dataset was built using a LigandScout KNIME Extensions workflow. The choice to use a dataset containing compound with a low Ty inhibitory activity as negative controls relies on the consideration that the geometry of very low active compounds does not allow the instauration of really good profitable interactions with the target, therefore they can be assimilated to the inactive ones.

For the validation of the pharmacophore model regarding its discrimination power, we considered the enrichment factor (EF) and the area under the curve (AUC) of the Receiver Operating Characteristic (ROC) curve. The EF is defined as the ratio of true positive hit (TP) percentiles in a hit list and the active compounds in the entire database. The AUC of a ROC curve represent a useful parameter to evaluate the ability of a pharmacophore model to discriminate between active and inactive compounds.

In figure 45 is displayed the best pharmacophoric hypothesis that consists of 39 exclusion volumes and six features, of which two were set as optional: (i) one hydrogen bond acceptor, (ii) one aromatic feature, (iii) three hydrophobic features, (iv) one hydrogen bond donor.

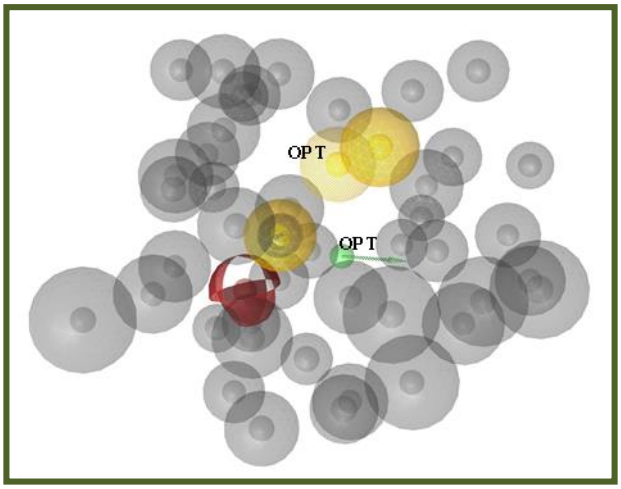

Figure 45: Final pharmacophore model. (i) hydrogen bond acceptor (green), (ii) aromatic feature (blue circle), (iii) hydrophobic features (yellow), (iv) one hydrogen bond donor (red). Optional features are not fully colored and are labeled as "OPT".
The picture was generated using Ligand Scout.[224]

The pharmacophore model thus obtained was finally used as filter to screen compounds from both natural and synthetic sources belonging to two in-house 3D databases: i) a collection of secondary metabolites containing 784 compounds isolated from plants species from mediterranean area; ii) a library of 1214 synthetic compounds synthesized and reported by the Pace research group at University of Vienna, where I performed ten months of my PhD course.

To build our in-house natural product (NP) 3D database, we initially chose 79 plant species present in Mediterranean area (especially from Sicily Island) and reported in the botanical guide "Flora d'Italia" by S. Pignatti.[238] Through a focused bibliographic research, we selected secondary metabolites from the above-mentioned plant species so that the final three-dimensional database contained 784 molecules. The obtained collection was named SiciMet and contained secondary metabolites from different chemical classes (flavonoids, terpenes, coumarins, stilbenes, and chalcones) as naturally occurring TyIs.

Moreover, the 3D database of compounds from synthetic source has been obtained by collecting compounds belonging to different chemical classes (α-methoxymethylketones, pyrazoles, methylendisulfanedil derivetives, phenyl alkyl nitriles, phenylethanones) synthesized and reported by the Pace research group from University of Vienna.

All virtual screening runs were conducted by setting the option "Get best matching conformation" as retrieval mode.

In the first SiCiMet case the search reported 23 hits of which 7 are already reported as Tys. In the second case, the virtual screening led to the identification of 21 hits. Considering the high reactivity of some of the retrieved molecules from the synthetic database, we decide to selected only four hits for the following studies.

5.3.1 Docking studies

The hits thus obtained were subjected to docking studies in order to further investigate their plausible binding-mode within the active site of TyM (PDB code 2Y9X) using GOLD software.[192]

After visual inspection and analysis of the potential interactions between the found hits and the amino acid residues present in the TyM active site, we selected natural compound **104** (1,2-benzenediol, 4-[2-(4-hydroxyphenyl)ethyl], CAS Registry Number 53515-95-0)[239] from the SiciMet database and compounds **105** [1,1'-(methylenedisulfanediyl)bis(4-fluorobenzene)] from synthetic source. Figure 46 displays the plausible binding modes of the two hits **104** and **105** retrieved through the virtual screening process.

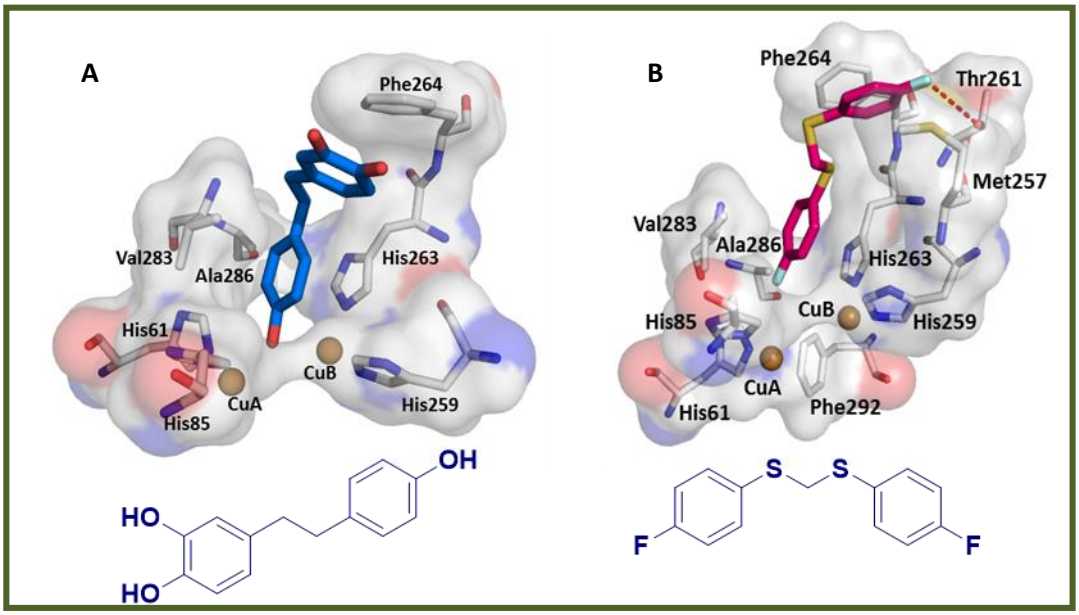

Figure 46: Plausible binding mode of compounds **104** (blue stick, A) and **105** (magenta stick, B) docked into TyM (PDB code 2Y9X). Red dashed lines represent hydrogen bond interactions. The interactions between the retrieved hits and TyM were examined by using LigandScout software.[224] The pictures were generated using PyMol.[2]

The docking results suggested that the *p*-hydroxybenzyl moiety of compound **104** is oriented in a similar fashion to the 4-fluorobenzyl portion of compound **51**, with the aromatic ring stabilized trough π-π interactions with His263 of TyM isoform that corresponds to His208 in TyrBm. In addition, the 2',3'-dihydroxybenzyl portion establishes hydrophobic contacts with the residue Phe264 belonging to hydrophobic wall of TyM catalytic cavity.

Compound **105** fits the hydrophobic pocket of TyM and engages hydrophobic contact with residues Val283, Phe292, Ala286, Phe264 and Met257. We hypothesized that compound **105** could establish additional π-π interaction with His263 as well as H-bond interaction with Thr261.

5.3.2 Synthetic pathways used to obtain compounds 104 and 105

Encouraged by the results of the computational studies, compounds **104** and **105** were synthesized according to the methods reported in literature.

Compound **104** was obtained following the experimental procedures depicted in scheme 9.[240]

Scheme 9

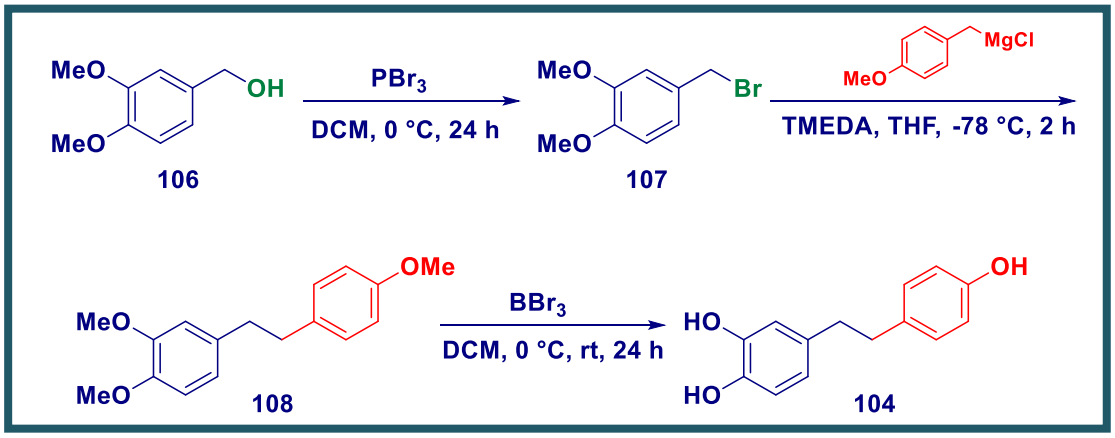

The starting 3,4-dimethoxybenzyl alcohol (**106**) was converted in the corresponding 3,4 dimethoxybenzyl bromide (**107**) in the presence of PBr_3. Compound **107** was then reacted with 4-methoxybenzyl magnesium chloride in the presence of TMEDA to afford the derivative **108** which was subjected to full demethylation with BBr_3 to obtain the desired compound **104**.

Derivative **105** was synthesized as reported in scheme 10 following the experimental procedures reported by Pace *et al*.[241]

Scheme 10

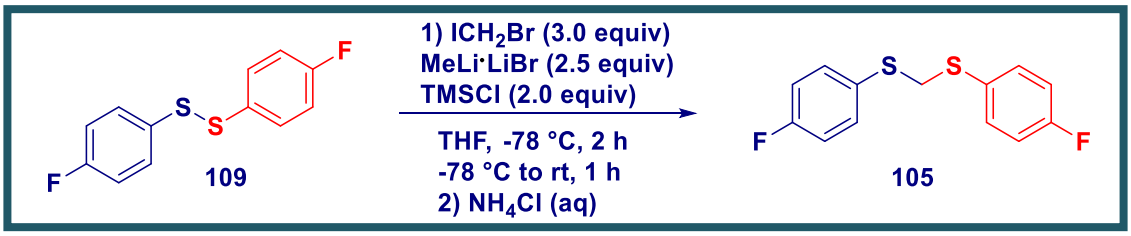

The commercially available diphenyl disulfide **109** was subjected to homologation with $LiCH_2Br$ under Barbier-type conditions (-78 °C, THF) in the presence of TMSCl for 2 h. After that, the reaction mixture was stirred for 1 h at room temperature. The desired compound **105** was obtained after purification through chromatography.

5.3.3 Inhibitory activities of compounds 104 and 105 on TyM

For the two compounds thus obtained, we evaluated the inhibitory activity against TyM. The results of the biochemical screening, reported in table 6, showed that all the compounds inhibit TyM enzymatic activity at micromolar concetration. In particular, compound **105** exhibits the best inhibitory activity with IC_{50} value equal to 48.42 µM.

Table 6: Inhibitory activity of compounds **104** and **105** compared to kojic acid of reference.

COMPOUND	Diphenolase activity IC_{50} (µM)[a]
104	125.96 ± 16.55
105	48.42 ± 0.76
Kojic acid	17.76 ± 0.18

[a] All compounds were examined in a set of experiments repeated three times;
IC_{50} values of compounds represent the concentration that caused 50% enzyme activity loss.

Based on our recent findings,[84, 141] the presence of a fluorine atom at para position of a phenyl moiety influences positively the inhibitory activity against TyM and this could explain the better inhibitory effect of compound **105**.

5.4 Concerning Human Tyrosinase

Actually, it is not available a crystal structure of TyH, thus we collected all the acquired structural information for TyM and TyBm, translating them into the druggable TyH through the employment of the melanogenic TyH-model protein TYRP1. The superposition of the TyH model with TyM and TyBm (figure 47) suggested that all these Tys share similar active sites. Asn205 and Glu195 residues (in TyBm) are crucial for activity through the activation of a conserved water molecule.[242] Favre *et al*. used quantum mechanics to model TyH and showed that their model, deposited in the Protein Model Database, is a reliable structure for future rational inhibitor-design projects.[243]

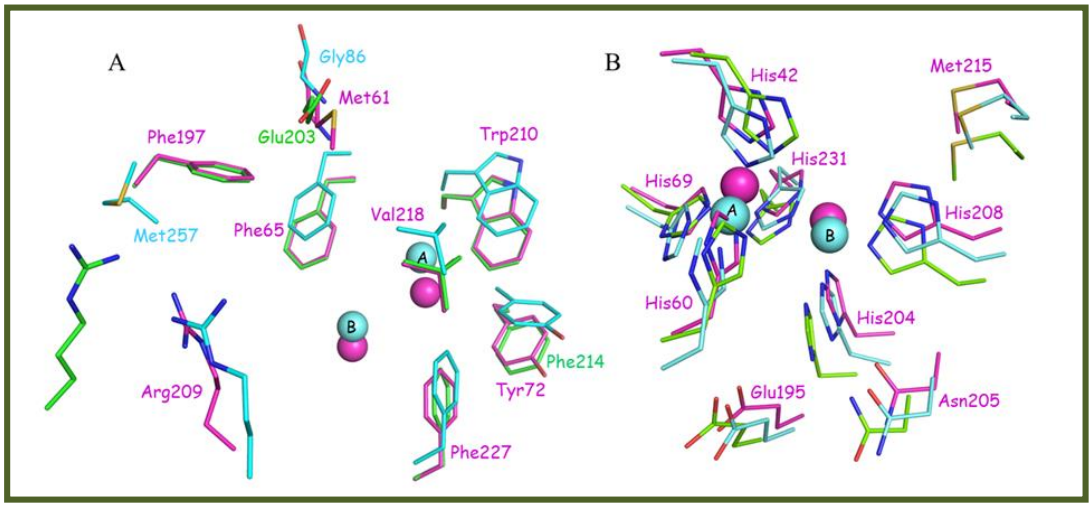

Figure 47: Superposition of the active site of TyBm (pink, PDB 5OAE), TyM (light blue, PDB 2Y9X) and TyH model (green). (A) The entrance to the active site is represented by second shell residues. Residues in TyM and TyH model which are not similar to TyBm are presented by their colors. (B) The active site is represented by conserved amino acids among the different species. Copper ions are represented as spheres colored by organism.[231]

Human TYRP1 was shown to be highly similar to TyBm, with 32% sequence identity and a root-mean-square deviation (RMSD) of 1.6 Å for the 263 aligned amino acids. Furthermore, it was demonstrated that the catalytic domain with the active site is highly similar to those of type 3 copper proteins, especially to that of TyBm.[40, 242]] Superposition of TyBm with bound kojic acid (PDB code 5I38) and TYRP1 with bound kojic acid (PDB code 5M8L) reveals similar orientations of the ligand toward CuA in both enzymes (figure 48). Numerous reports exist on the IC_{50} values of TyH inhibition by ligands such as kojic acid and other natural products that inhibit TyM and TyBm

with similar efficacies.[153, 244, 245] Overall, it is well demonstrated in the literature that inhibitors of TyM and TyBm are relevant in the study of the human enzyme, and therefore the inhibitors developed here could have potential pharmaceutical implications. Clearly, more research is needed to confirm that the inhibitory effects of the most active derivatives might be moved to TyH.[231]

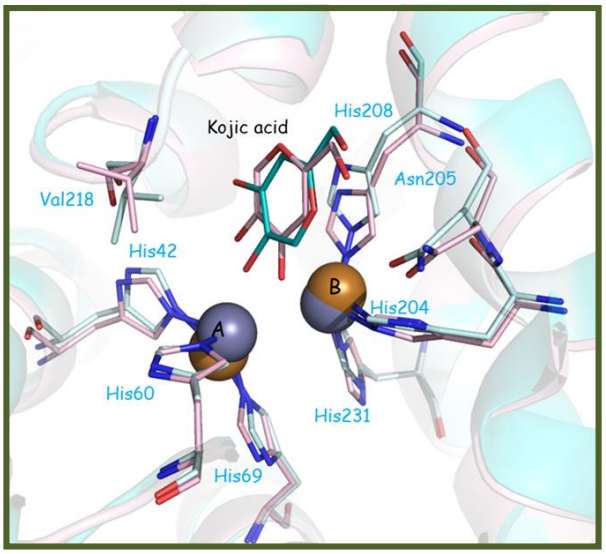

Figure 48: Superposition of the active site of TyBm (light blue) and TRP1 (light pink) with bound kojic acid. The inhibitor binds with similar orientation towards CuA in both TyBm (teal, PDB 5I38) and TYRP1 (pink, PDB 5M8L). Copper and zinc ions are presented as brown and gray spheres, respectively.[231]

5.5 Conclusion

The purpose of this PhD thesis has been focused on the development of new classes of synthetic TyIs bearing 1-(4-fluorobenzyl)piperazine and 4-(4-fluorobenzyl)piperidine scaffolds by rational approaches. A combination of X-ray crystallography and docking simulations studies within the enzymatic cavities of the TyBm and TyM isozymes respectively allowed us to obtain promising TyM inhibitors with various structural modifications clarifying the structure-activity relationships (SARs).

In particular, derivative **18** was used as "lead compound" in order to design the new benzamides obtained using both classical synthetic and microwave-assisted methods, thus improving the yields, reducing reaction times and solvent amount. All compounds were carefully characterized through spectroscopic measurements such as *NMR*.

By means of docking studies we found that the 4-fluorobenzylpiperidine moiety of compound **18** is projected in the catalytic site of TyM between the two copper ions

forming π-π interaction with His263 residue highlighting its important role in inhibitory activity. Our assumption was then confirmed by biological assay and x-ray studies thus we designed a new series of compounds maintaining this portion.

Among this first series of derivatives, compounds **57** resulted a promising TyM inhibitor with IC_{50} value of 13.34 μM suggesting that the combination of the *N*-benzoyl substituent with the piperazine core induced an improvement in the inhibitory effects.

Thus, starting from compound **57** we designed a new series of benzamides possessing both hydrophobic/hydrophilic substituents in *ortho*, *meta* and *para* position of the benzoyl ring in order to explore additional possible interactions in TyM active site. Several of these obtained compounds proved to be very efficient inhibitors exhibiting good activity towards TyM. Particularly interesting was the substitution with nitro and trifluoromethyl groups especially in *ortho* position of the benzoyl ring allowing us to reach nanomolar range with IC_{50} values of 870 and 480 nM respectively. Preliminary assay addressed to evaluate the cytotoxicity effect in B16F10 melanoma cells of our compounds revaled that compound **87** does not show cytotoxic effect at its IC_{50} value (0.96 ± 0.21 μM).

As generally the presence of substituents in *ortho* and *para* position were favored for inhibitory activity, we also decided to synthesize the 2,4-disubstituted derivatives leading to an improvement of inhibitory activity with IC_{50} values between 0.79 and 3.67 μM, lower or comparable to those of the respective monosubstituted ones. In particular, the most active compounds resulted the 2,4-dinitro and 2,4-dichloro analogs with IC_{50} values of 790 and 960 nM respectively.

Furthermore, another structural modification was applied in the phenyl ring of compound **57** benzoyl portion, replacing it with different aromatic or heteroaromatic rings. In general, a good inhibitory activity was observed, with IC_{50} values lower or comparable to that of derivative **57** and kojic acid of reference. In particular, the presence of bulky aromatic substituents such as indole, naphthalene or 1,3-benzodioxole rings led to promising results with IC_{50} values between 2 and 4 μM.

However, another rational approach was employed in order to identify new TyIs with different structural features. In particular, a pharmacophore model was built starting from the inhibitor **57** crystal structure to screen two database concerning compounds from both natural and synthetic sources. Docking studies and biological assays allowed

us to identify two promising TyM inhibitors (**104** and **105**) with IC_{50} values of 125.96 and 48.42 µM respectively.

Overall, the results obtained in this PhD project, could represent a good starting point for the future design of new Tyrosinase inhibitors useful as antimelanogenesis agents.

CHAPTER 6 EXPERIMENTAL SECTION

6.1 Chemistry

All starting materials and reagents commercially available (Sigma-Aldrich Milan, Italy; Alfa Aesar Karlsruhe, Germany) were used without further purification. Microwave-assisted reactions were carried out in a focused Microwave Synthesis System (CEM Technology Ltd Buckingham, UK). Melting points were determined on a Buchi B-545 apparatus (BUCHI Labortechnik AG Flawil, Switzerland) and are uncorrected. Elemental analyses (C, H, N) were carried out on a Carlo Erba Model 1106 Elemental Analyzer (Carlo Erba Milano, Italy); the results confirmed a ≥95% purity. Merck silica gel 60 F254 plates were used for analytical TLC (Merck KGaA, Darmstadt, Germany). Flash Chromatography (FC) was carried out on a Biotage SP1 EXP (Biotage AB Uppsala, Sweden). ^{1}H NMR spectra were measured in chloroform ($CDCl_3$) or in dimethylsulfoxide-d_6 (DMSO-d_6) with a Gemini 300 spectrometer (Varian Inc. Palo Alto, California USA). ^{13}C NMR spectra and mass spectra of selected compounds were measured in chloroform ($CDCl_3$) with a Varian and Mass Spectrometer API 2000 respectively; chemical shifts are expressed in δ (ppm) and coupling constants (J) in Hz.

6.1.1 General procedure for the synthesis of 1-(1-*H*-Benzimidazol-1-yl)-3-chloropropan-1-one (35), 3-Chloro-*N*-(3-methyl-1,2-oxazol-5-yl)propanamide (38a), 3-Chloro-*N*-phenyl-propanamide (38b), Tert-butyl-3-(3-chloropropanoylamino) pyrazole-1-carboxylate (41)

To a solution of the suitable starting compounds (**34**, **37a-b**, **40**) (1 mmol) in THF (5 mL), the 3-chloropropionyl chloride (95 µL, 1 mmol) at 0 °C was added dropwise. For compound **38b** the reaction was carried out in alkaline medium by K_2CO_3 water solution (207 mg, 1.5 mmol). The reaction mixture was stirred at room temperature for 2-16 h, then quenched with a saturated solution of $NaHCO_3$, added water and the aqueous phase extracted with EtOAc (3x10 mL). [141] The collected organic phases were dried over anhydrous Na_2SO_4 and the solvent was removed *in vacuo*. The final compounds (**35**, **38a-b**, **41**) were obtained after purification by FC using the mixture of Cyhex/EtOAc (50:50) as eluent.

1-(1-*H*-Benzimidazol-1-yl)-3-chloropropan-1-one (35)

Yield 25%. White solid. M.p. 145-147 °C. ^{1}H-NMR (DMSO-d_6) (δ): 9.40 (s, 1H, H-3), 7.52 (mc, 2H, ArH), 7.15 (mc, 2H, ArH), 3.86 (t, *J* = 6.5 Hz, 2H, CH_2), 2.83 (t, *J* = 6.5 Hz, 2H, CH_2). Anal. Calcd for ($C_{10}H_9ClN_2O$): C 57.57, H 4.35, N 13.43. Found: C 57.67, H 4.45, N 13.53.

3-Chloro-*N*-(3-methyl-1,2-oxazol-5-yl)propanamide (38a)

Yield 20%. White solid. M.p. 131-133 °C. ^{1}H-NMR (DMSO-d_6) (δ): 11.64 (bs, 1H, NH), 6.13 (s, 1H, ArH), 3.85 (t, *J* = 6.5 Hz, 2H, CH_2), 2.86 (t, *J* = 6.5 Hz, 2H, CH_2), 2.16 (s, 3H, CH_3). Anal. Calcd for ($C_7H_9ClN_2O_2$): C 44.58, H 4.81, N 14.85. Found: C 44.48; H 4.71, N 14.75.

3-Chloro-*N*-phenyl-propanamide (38b)

Yield 46%. White solid. M.p. 115-117 °C. ^{1}H-NMR (DMSO-d_6) (δ): 10.04 (bs, 1H, NH), 7.58 (d, *J* = 8.8 Hz, 2H, ArH), 7.28 (mc, 2H, ArH), 7.05 (mc, 1H, ArH), 3.86 (t, *J* = 6.5 Hz, 2H, CH_2), 2.80 (t, *J* = 6.5 Hz, 2H, CH_2). Anal. Calcd for ($C_9H_{10}ClNO$) C 58.87, H 5.49, N 7.63. Found: C 58.67, H 5.29, N 7.43.

Tert-butyl-3-(3-chloropropanoylamino)pyrazole-1-carboxylate (41)

Yield 25%. White solid. M.p. 89-91 °C. ^{1}H-NMR (DMSO-d_6) (δ): 10.15 (bs, 1H, NH), 7.65 (s, 1H, ArH), 6.65 (s, 1H, ArH), 3.86 (t, *J* = 6.4 Hz, 2H, CH_2), 2.97 (t, *J* = 6.4 Hz, 2H, CH_2), 1.59 (s, 9H, CH_3). Anal. Calcd for ($C_{11}H_{16}ClN_3O_3$) C 48.27, H, 5.89, N 15.35. Found: C 45.37, H 5.99, N 15.45.

6.1.2 General procedure for the synthesis of 1-(1-*H*-Benzimidazol-1-yl)-3-(4-(4-fluorobenzyl) piperidin-1-yl)propan-1-one (36), 3-[4-(4-Fluorobenzyl)piperidin-1-yl]-*N*-(3-methyl-1,2-oxazol-5-yl)propanamide (39a), 3-{4-[(4-Fluorophenyl)methyl] piperidin-1-yl}-*N*-phenyl propanamide (39b) and 3-[4-(4-Fluorobenzyl)piperidin-1-yl]-*N*-(1-*H*-pyrazol-3-yl)propanamide (39c)

The 4-(4-Fluorobenzyl)piperidine (1 mmol) was added to a DMF (2 mL) solution of intermediates (**35**, **38a-b**, **41**) (195 mg, 1 mmol) in alkaline medium by a water solution of K_2CO_3 (276.4 mg, 2 mmol). The obtained mixture was refluxed for 2 h, cooled at room temperature and stirred for 24 h. Then the reaction was quenched with a

satured solution of a $NaHCO_3$, added water and the aqueous phase extracted with EtOAc (3x10 mL).[141] The collected organic phases were dried with anhydrous Na_2SO_4 and the solvent was removed *in vacuo* thus giving desired compounds as crude products which were purified by crystallization with Et_2O.

1-(1-*H*-Benzimidazol-1-yl)-3-(4-(4-fluorobenzyl)piperidin-1-yl)propan-1-one (36)

Yield 46%. White solid. M.p. 108-110 °C. ^{1}H-NMR (DMSO-d_6) (δ): 9.58 (s, 1H, H-2), 7.27 (mc, 8H, ArH), 1.98 (mc, 15H). Anal. Calcd for ($C_{22}H_{24}FN_3O$): C 72.31, H 6.62, N 11.50. Found: C 72.21, H 6.52, N 11.40.

3-[4-(4-Fluorobenzyl)piperidin-1-yl]-*N*-(3-methyl-1,2-oxazol-5-yl)propanamide (39a)

Yield 69%. White solid. M.p. 78-80 °C. ^{1}H NMR (DMSO-d_6) (δ): 7.11 (mc, 4H, ArH), 6.08 (s, 1H, ArH), 2.16 (mc, 15H). Anal. Calcd for ($C_{19}H_{24}FN_3O_2$): C 66.07, H 7.00, N 12.16. Found: C 66.27, H 7.20, N 12.36.

3-{4-[(4-Fluorophenyl)methyl]piperidin-1-yl}-*N*-phenyl-propanamide (39b)

Yield 44%. White solid. M.p. 110-112 °C. ^{1}H-NMR (DMSO-d_6) (δ): 10.12 (bs, 1H, NH), 7.52 (d, J = 7.6 Hz, 2H, ArH), 7.27 (mc, 2H, ArH), 7.16 (mc, 2H, ArH), 7.05 (mc, 3H, ArH), 2.01 (mc, 15H). Anal. Calcd for ($C_{21}H_{25}FN_2O$): C 74.09, H 7.40, N 8.23. Found: C 74.29, H 7.60, N 8.43.

3-[4-(4-Fluorobenzyl)piperidin-1-yl]-*N*-(1-*H*-pyrazol-3-yl)propanamide (39c)

Yield 64%. White solid. M.p. 137-139 °C. ^{1}H-NMR (DMSO-d_6) (δ): 10.55 (bs, 1H, NH), 7.55 (s, 1H, ArH), 7.13 (mc, 8H, ArH), 6.44 (s, 1H, ArH), 2.08 (mc, 15H). Anal. Calcd for ($C_{18}H_{23}FN_4O$): C 65.43, H 7.02, N 16.96. Found: C 65.53, H 7.12, N 17.06.

6.1.3 Amino group Boc-protection of 3-aminopirazole (37c)

To a solution of 3-aminopirazole (**37c**) (83 mg, 1 mmol) in dioxane (10 mL), a mixture of di-tert-butyl dicarbonate (240 mg, 1.1 mmol) in Et_3N (277 µl, 2 mmol) was added. The obtained mixture reaction was stirred at room temperature for 1 h. Then, the solvent was removed *in vacuo*, the residue was dissolved in H_2O (15 mL) and extracted with EtOAc (3x10 mL).[141] The organic phase was dried over Na_2SO_4 and the solvent was

removed under reduced pressure to obtain the desired intermediate (**40**). In turn, the intermediate was used for the next step without further purification.

6.1.4 Amino group Boc-deprotection of tert-butyl-3-(3-chloropropanoylamino) pyrazole-1-carboxylate (42)

A mixture of TFA and DCM (1:1, 2 mL) was added slowly to a solution of protected-derivative (**42**) (430 mg, 1 mmol) in DCM at 0 °C. The reaction mixture was stirred for 1 h at room temperature and successively quenched with water (3 mL) and saturated solution of $NaHCO_3$ (5 mL).[141] The aqueous phase was extracted with EtOAc (3×10 mL) and the organic layer thus obtained was dried over Na_2SO_4. The solvent was removed *in vacuo* and the crude product was purified by FC (DCM/MeOH 90:10) and recrystallized by treatment with Et_2O to give the desired final product (**39c**).

6.1.5 Synthesis of 3-{4-[(4-Fluorophenyl)methyl]piperidin-1-yl}propane nitrile (44)

To a stirred solution of 4-(4-Fluorobenzyl)piperidine (**43**) (400 mg, 2.1 mmol) in DCM (4.7 mL) was added 3-bromopropane nitrile (281 mg, 2.1 mmol) and TEA (0.6 mL, 4.2 mmol) and the reaction was carried out for 6 h. The mixture was quenched with water and the aqueous phase extracted with DCM (3x5 mL).[141] The organic phase thus obtained was dried over Na_2SO_4 and the solvent removed under reduced pressure to give the final compound (**44**) as a yellow oily without further purification.

Yield 90%. Oily residue. ^{1}H-NMR ($CDCl_3$) (δ): 7.09 (mc, 2H, ArH), 6.95 (mc, 2H, ArH), 2.86 (mc, 2H, 2CH), 2.67 (mc, 2H, CH_2), 2.49 (mc, 4H, $2CH_2$), 2.00 (mc, 2H, 2CH), 1.62 (mc, 2H, 2CH), 1.50 (mc, 1H, CH), 1.27 (mc, 2H, 2CH). Anal. Calcd for ($C_{15}H_{19}FN_2$): C 73.14, H 7.77, N 11.37. Found: C 73.54, H 8.17, N 11.77.

6.1.6 Synthesis of 3-[4-(4-Fluorobenzyl)piperidin-1-yl]-1-phenyl-4-butan-2-one (45)

To a solution of benzyl-magnesium-chloride (1M) (2.4 mL, 2.4 mmol) in Et_2O, the intermediate (**44**) (303 mg, 1.2 mmol) in Et_2O (1 mL) was added. The reaction mixture was refluxed for 2 h and then quenched with an aqueous satured ammonium chloride solution.[141] The aqueous phase was extracted with Et_2O and the organic phase thus obtained was dried over Na_2SO_4. The solvent was removed under reduced pressure to give the final compound (**45**) as a yellow oily residue.

Yield 92%. Oily residue. ^{1}H-NMR ($CDCl_3$) (δ): 7.27 (mc, 3H, ArH), 7.09 (mc, 2H, ArH), 6.95 (mc, 2H, ArH), 4.68 (s, 2H, CH_2), 2.85 (mc, 2H, CH_2), 2.65 (mc, 2H, CH_2), 2.48 (mc, 4H, $2CH_2$), 1.98 (mc, 2H, 2CH), 1.62 (mc, 2H, 2CH), 1.50 (mc, 1H, CH), 1.27 (mc, 2H, 2CH). Anal. Calcd for ($C_{22}H_{26}FNO$): C 77.84, H 7.72, N 4.13. Found: C 78.74, H 7.62, N 4.03.

6.1.7 Synthesis of 4-[(4-Fluorophenyl)methyl]-1-methylpiperidine (47)

To a stirred mixture of 4-(4-Fluorobenzyl)piperidine (**43**) (192 mg, 2.8 mmol) and paraformaldehyde (30 mg, 3.1 mmol), formic acid (46 mg, 7 mmol) was added dropwise at 0 °C. The reaction mixture was heated at reflux for 13 h and then quenched by addition of HCl 37% (1 mL). The solvent was removed under reduce pressure and the residue was dissolved in water (5 mL). The solution was made alkaline by the addition of NaOH 2N and extracted with Et_2O (3x5 mL).[230] The organic phase was dried over Na_2SO_4 and the solvent removed under reduced pressure to give the final compound (**47**) as yellow oily residue without further purification.

Yield 71%. Oily residue. ^{1}H-NMR ($CDCl_3$) (δ): 7.08 (mc, 2H, ArH), 6.93 (mc, 2H, ArH), 2.84 (mc, 2H, 2CH), 2.50 (d, J = 7.0 Hz, 2H, CH_2), 2.25 (s, 3H, CH_3), 1.87 (mc, 2H, 2CH), 1.62 (mc, 2H, 2CH), 1.46 (mc, 1H, CH), 1.31 (mc, 2H, 2CH). Anal. Calcd for ($C_{13}H_{18}FN$): C 75.33, H 8.75, N 6.76. Found: C 75.73, H 9.15, N 7.16.

6.1.8 Synthesis of 1-Ethyl-4-(4-fluorobenzyl)piperidine (48)

A mixture of iodoethane (218 mg, 1.4 mmol) in MeCN (3.5 mL) was added dropwise to a stirred solution of 4-(4-Fluorobenzyl)piperidine (**43**) (250 mg, 1.4 mmol) and K_2CO_3 (387 mg, 2.8 mmol) in MeCN (7 mL). The resulting mixture was heated at reflux for 2 h. The suspended solid was filtered off and the solvent removed under reduce pressure to afford a crude white solid material. At this residue was added water (5 mL) and the solution extracted with Et_2O (3x5 mL).[230] The organic phase was washed many times with a saturated solution of $NaHCO_3$ (3x5 mL) and then dried over Na_2SO_4. The solvent was removed under reduced pressure to give the final compound (**48**) as a yellow oily residue without further purification.

Yield 79%. Oily residue. ^{1}H-NMR ($CDCl_3$) (δ): 7.07 (mc, 2H, ArH), 6.91 (mc, 2H, ArH), 2.90 (mc, 2H, 2CH), 2.50 (d, J = 7.0 Hz, 2H, CH_2), 2.34 (mc, 2H, CH_2), 1.81 (mc, 2H, 2CH), 1.61 (mc, 2H, 2CH), 1.46 (mc, 1H, CH), 1.29 (mc, 2H, 2CH), 1.06 (mc, 3H, CH_3). Anal. Calcd for ($C_{14}H_{20}FN$): C 75.98, H 9.11, N 6.33. Found: C 76.38, H 9.51, N 6.73.

6.1.9 Synthesis of 1-(5,6-dimethoxy-1*H*-indol-3-il)ethanone (46)

The 5,6-dimethoxyindole (**49**) (1 mmol) was added to a solution of phosphorus (V) oxychloride (0.92 mL, 10 mmol) in dimethylacetamide (2.79 mL, 30 mmol) and the resulting mixture was stirred at room temperature for 24 h. Then, the reaction mixture was basified by adding a solution of sodium hydroxide (4N) and extracted with EtOAc (3x10 mL).[141] The organic phase was dried over Na_2SO_4 and the solvent removed under reduced pressure leading to crude product. The final compound (**46**) was obtained by crystallization with Et_2O.

Yield 74%. Yellow powder. M.p. 132 °C. ^{1}H-NMR (DMSO-d_6) (δ): 11.61 (bs, 1H, NH), 8.08 (d, J = 1.8 Hz, 1H, ArH), 7.63 (d, J = 1.8 Hz, 1H, ArH), 6.95 (d, J = 1.8 Hz, 1H, ArH,), 3.75 (s, 6H, OCH_3), 2.41 (s, 3H, CH_3CO). Anal. Calcd for ($C_{12}H_{15}NO_3$): C 65.74, H 5.98, N 6.39. Found: C 65.84, H 6.08, N 6.49.

6.1.10 General procedure for the synthesis of 1-[4-(4-Fluorobenzyl)piperidin-1-yl]ethanone (51), 1-[4-(4-Fluorobenzyl)piperidin-1-yl]propan-1-one (52), 1-[4-(4-Fluorobenzyl)piperidin-1-yl]-2-methylpropan-1-one (53), [4-(4-Fluorobenzyl) piperidin-1-yl](phenyl)methanone (54), 1-{4-[(4-Fluorophenyl)methyl]piperazin-1-yl}propan-1-one (55), 1-{4-[(4-Fluorophenyl)methyl]piperazin-1-yl}-2-methylpropan-1-one (56), {4-[(4-Fluorophenyl)methyl]piperazin-1-yl}-phenyl-methanone (57)

The suitable acyl chloride (1.5 mmol) was dissolved in DMF (1 mL). Then the 4-(4-Fluorobenzyl)piperidine (**43**) or 1-(4-Fluorobenzyl)piperazine (**50**) (1.5 mmol) was added slowly in the presence of K_2CO_3 (0.75 mmol) as alkaline catalyst. The reaction was carried out using microwave irradiations under the following conditions: 5 min, 100 °C, 200 Psi. The reaction mixture was quenched by addition of a saturated solution of $NaHCO_3$ (10 mL) and the aqueous phase was extracted with EtOAc (3x5 mL).[231] The organic phase thus obtained was washed with brine (3x5 mL) and dried with anhydrous Na_2SO_4. The solvent was removed under reduced pressure and the final

products **51-57** were obtained after purification by chromatographic column (Cyhex/EtOAc 30:70).

1-[4-(4-Fluorobenzyl)piperidin-1-yl]ethanone (51)

Yield 15%. White solid. M.p. 59-60 °C. ^{1}H-NMR ($CDCl_3$) (δ): 7.02 (mc, 4H, ArH), 4.60 (mc, 1H, CH), 3.78 (mc, 1H, CH), 2.97 (mc, 1H, CH), 2.51 (mc, 3H, CH), 2.08 (s, 3H, CH_3), 1.67 (mc, 3H, CH), 1.14 (mc, 2H, CH). Anal. Calcd for ($C_{14}H_{18}FNO$): C 71.46, H 7.71, N 5.95. Found: C 71.86, H 8.11, N 6.35.

1-[4-(4-Fluorobenzyl)piperidin-1-yl]propan-1-one (52)

Yield 23%. Oily residue. ^{1}H-NMR ($CDCl_3$) (δ): 7.02 (mc, 4H, ArH), 4.61 (mc, 1H, CH), 3.82 (mc, 1H, CH), 2.93 (mc, 1H, CH), 2.51 (mc, 3H, CH), 2.34 (q, J = 7.6 Hz, 2H, CH_2), 1.70 (mc, 3H, CH), 1.13 (t, J = 7.6 Hz, 3H, CH_3), 1.10 (mc, 2H, CH). Anal. Calcd for ($C_{15}H_{20}FNO$): C 72.26, H 8.09, N 5.62. Found: C 72.66, H 8.49, N 6.02.

1-[4-(4-Fluorobenzyl)piperidin-1-yl]-2-methylpropan-1-one (53)

Yield 31%. Oily residue. ^{1}H-NMR ($CDCl_3$) (δ): 7.02 (mc, 4H, ArH), 4.63 (mc, 1H, CH), 3.91 (mc, 1H, CH), 2.96 (mc, 1H, CH), 2.80 (mc, 1H, CH), 2.51 (mc, 3H, CH), 1.68 (mc, 3H, CH), 1.13 (mc, 2H, CH), 1.11 (mc, 6H, CH_3). Anal. Calcd for ($C_{16}H_{22}FNO$): C 72.97, H 8.42, N 5.32. Found: C 72.57, H 8.02, N 4.92.

[4-(4-Fluorobenzyl)piperidin-1-yl](phenyl)methanone (54)

Yield 37%. Oily residue. ^{1}H-NMR ($CDCl_3$) (δ): 7.16 (mc, 9H, ArH), 4.70 (mc, 1H, CH), 3.71 (mc, 1H, CH), 2.73 (mc, 4H, CH), 1.69 (mc, 3H, CH), 1.27 (mc, 2H, CH). Anal. Calcd for ($C_{19}H_{20}FNO$): C 76.74, H 6.78, N 4.71. Found: C 76.34, H 8.38, N 4.31.

1-{4-[(4-Fluorophenyl)methyl]piperazin-1-yl}propan-1-one (55)

Yield: 33%. Oily residue. ^{1}H-NMR ($CDCl_3$) (δ): 7.29 (mc, 2H, ArH), 7.01 (mc, 2H, ArH), 3.63 (mc, 2H, CH_2), 3.45 (mc, 4H, CH_2), 2.40 (mc, 4H, CH_2), 2.31 (q, J = 6.5 Hz, 2H, CH_2), 1.14 (t, J = 6.5 Hz, 3H, CH_3). Anal. Calcd for ($C_{14}H_{19}FN_20$): C 67.18, H 7.65, N 11.19. Found: C 66.78, H 7.25, N 10.79.

1-{4-[(4-Fluorophenyl)methyl]piperazin-1-yl}-2-methylpropan-1-one (56)

Yield: 53%. Oily residue. ^{1}H-NMR ($CDCl_3$) (δ): 7.30 (mc, 2H, ArH), 7.01 (mc, 2H, ArH), 3.64 (mc, 2H, CH_2), 3.49 (mc, 4H, CH_2), 2.77 (mc, 1H, CH), 2.41 (mc, 4H, CH_2), 1.12 (d, *J* = 6.5 Hz, 6H, CH_3). Anal. Calcd for ($C_{15}H_{21}FN_2O$): C 68.16, H 8.01, N 10.6. Found: C 68.06, H 7.91, N 10.5.

{4-[(4-Fluorophenyl)methyl]piperazin-1-yl}-phenyl-methanone (57)

Yield: 16%. White solid. M.p. 78-80 °C. ^{1}H-NMR ($CDCl_3$) (δ): 7.39 (s, 5H, ArH), 7.27 (mc, 2H, ArH), 6.98 (mc, 2H, ArH), 3.78 (mc, 1H, CH_2), 3.45 (mc, 4H, CH_2), 2.50 (mc, 2H, CH_2), 2.36 (mc, 2H, CH_2), 1.71 (s, 1H, CH_2). Anal. Calcd for ($C_{18}H_{19}FN_2O$): C 72.46, H 6.42, N 9.39. Found: C 72.06, H 6.02, N 8.99.

6.1.11 Synthesis of derivative 1-[4-(4-Fluorobenzyl) piperazin-1-yl]ethanone (58)

To a solution of 1-(4-Fluorobenzyl)piperazine (**50**) (2.05 mmol) and TEA (3.28 mmol) in THF (7 mL) the acetyl chloride (2.05 mmol) was added. The reaction mixture was stirred at room temperature for 10 min under nitrogen atmosphere. Then, the obtained precipitate was turned away by filtration and the solution was evaporated under reduced pressure to give the final compound **58** as crude product, which has been purified by chromatographic column (Cyhex /EtOAc 20:80).[231]

Yield: 20%. Oily residue. ^{1}H-NMR ($CDCl_3$) (δ): 7.29 (mc, 2H, ArH), 7.00 (mc, 2H, ArH), 3.63 (mc, 2H, CH_2), 3.47 (mc, 4H, CH_2), 2.42 (mc, 4H, CH_2), 2.09 (s, 3H, CH_3). Anal. Calcd for ($C_{13}H_{17}FN_2O$): C 66.08, H 7.25, N 11.86. Found: C 66.48, H 7.65, N 12.26.

6.1.12 General procedure for the synthesis of [4-(4-Fluorobenzyl)piperazin-1-yl]methanone derivatives (59-61)

To a solution of 1-(4-Fluorobenzyl)piperazine (**50**) (0.5 mmol) in DCM (4 mL) the N,N-diisopropylethylamine (0.75 mmol) and the suitable benzoyl chloride (0.5 mmol) were added. The reaction mixture was stirred at room temperature for 5 h. After turning off the reaction by addition of MeOH (2 mL), water was added and the mixture was extracted with DCM (3x5 mL).[231] The obtained organic phase was washed many times with brine (3x5 mL) and was dried with anhydrous Na_2SO_4. The solvent was removed

under reduced pressure and the final products (**59-61**) were purified by crystallization with Et_2O.

[4-(4-Fluorobenzyl)piperazin-1-yl](2-methoxyphenyl)methanone (59)

Yield 40%. White solid. M.p. 78-79 °C. ^{1}H-NMR ($CDCl_3$) (*δ*): 7.29 (mc, 4H, ArH), 6.95 (mc, 4H, ArH), 3.82 (mc, 3H, OCH_3; 1H, CH_2), 3.48 (s, 2H, CH_2), 3.25 (mc, 2H, CH_2), 2.40 (mc, 4H, CH_2), 1.62 (mc, 1H, CH_2). Anal. Calcd for ($C_{19}H_{21}FN_2O_2$): C 69.49, H 6.45, N 8.53. Found: C 69.29, H 6.25, N 8.33.

[4-(4-Fluorobenzyl)piperazin-1-yl](3-methoxyphenyl)methanone (60)

Yield 60%. Oily residue. ^{1}H-NMR ($CDCl_3$) *(δ)*: 7.31 (mc, 4H, ArH), 6.98 (mc, 4H, ArH), 3.82 (mc, 3H, OCH_3; 2H, CH_2), 3.61 (mc, 4H, CH_2), 2.56 (mc, 4H, CH_2). Anal. Calcd for ($C_{19}H_{21}FN_2O_2$): C 69.49, H 6.45, N 8.53. Found: C 69.29, H 6.25, N 8.33.

[4-(4-Fluorobenzyl)piperazin-1-yl](4-methoxyphenyl)methanone (61)

Yield 67%. White solid. M.p. 120-121 °C. ^{1}H-NMR ($CDCl_3$) (δ): 7.33 (mc, 4H, ArH), 6.95 (mc, 4H, ArH), 3.83 (mc, 3H, OCH_3; 1H, CH_2), 3.52 (mc, 4H, CH_2), 2.44 (mc, 4H, CH_2), 1.64 (mc, 1H, CH_2). Anal. Calcd for: ($C_{19}H_{21}FN_2O_2$) C 69.49, H 6.45, N 8.53. Found: C 69.79, H 6.75, N 8.83.

6.1.13 General procedure for the synthesis of [4-(4-Fluorobenzyl)piperazin-1-yl]methanone derivatives (62-67, 71-83, 95-100)

To a solution of 1-(4-Fluorobenzyl)piperazine (**50**) (0.5 mmol) in DCM (2 mL) the N,N-diisopropylethylamine (0.75 mmol) and the suitable benzoyl chloride (0.5 mmol) were added. The reaction was carried out under microwave irradiation 10 min, 50 °C, 200 Psi. After turning off the reaction by addition of MeOH (2 mL), water was added and the mixture was extracted with DCM (3x5 mL).[231] The obtained organic phase was washed many times with brine (3x5 mL) and was dried with anhydrous Na_2SO_4. The solvent was removed under reduced pressure and the final products (**62-67, 71-83, 95-100**) were purified by crystallization with Et_2O or by chromatographic column (DCM/MeOH 98:02).

[4-(4-Fluorobenzyl)piperazin-1-yl](2-fluorophenyl)methanone (62)

Yield 34%. White solid. M.p. 78-79 °C. ^{1}H-NMR ($CDCl_3$) (δ): 7.20 (mc, 8H, ArH), 3.83 (bs, 2H, CH_2), 3.52 (bs, 2H, CH_2), 3.35 (bs, 2H, CH_2), 2.47 (mc, 4H, CH_2). Anal. Calcd for ($C_{18}H_{18}F_2N_2O$): C 68.34, H 5.74, N 8.86. Found: C 68.14, H 5.54, N 8.66.

[4-(4-Fluorobenzyl)piperazin-1-yl](3-fluorophenyl)methanone (63)

Yield 43%. Oily residue. ^{1}H-NMR ($CDCl_3$) (δ): 7.25 (mc, 4H, ArH), 7.01 (mc, 4H, ArH), 3.83 (bs, 2H, CH_2), 3.71 (bs, 2H, CH_2), 3.39 (mc, 4H, CH_2), 2.38 (mc, 4H, CH_2). Anal. Calcd for ($C_{18}H_{18}F_2N_2O$): C 68.34, H 5.74, N 8.86. Found: C 68.24, H 5.64, N 8.76.

[4-(4-Fluorobenzyl)piperazin-1-yl](4-fluorophenyl)methanone (64)

Yield 46%. White solid. M.p. 112-113 °C. ^{1}H-NMR ($CDCl_3$) (δ): 7.34 (mc, 4H, ArH), 7.05 (mc, 4H, ArH), 3.75 (mc, 1H, CH_2), 3.50 (mc, 3H, CH_2), 2.40 (mc, 2H, CH_2), 1.59 (mc, 3H, CH_2), 1.25 (s, 1H, CH_2). Anal. Calcd for ($C_{18}H_{18}F_2N_2O$): C 68.34, H 5.74, N 8.86. Found: C 68.74, H 6.14, N 9.26.

[4-(4-Fluorobenzyl)piperazin-1-yl](2-methylphenyl)methanone (65)

Yield 56%. White solid. M.p. 72-73 °C. ^{1}H-NMR ($CDCl_3$) (δ): 7.23 (mc, 6H, ArH), 6.98 (mc, 2H, ArH), 3.83 (mc, 2H, CH_2), 3.48 (s, 2H, CH_2), 3.23 (mc, 2H, CH_2), 2.52 (mc, 2H, CH_2), 2.30 (s, 3H, CH_3), 2.28 (mc, 1H, CH_2), 1.74 (mc, 1H, CH_2). Anal. Calcd for ($C_{19}H_{21}FN_2O$): C 73.05, H 6.78, N 8.97. Found: C 73.15, H 6.88, 9.07.

[4-(4-Fluorobenzyl)piperazin-1-yl](3-methylphenyl)methanone (66)

Yield 80%. Oily residue. ^{1}H-NMR ($CDCl_3$) (δ): 7.21 (mc, 4H, ArH), 7.01 (mc, 4H, ArH), 3.60 (mc, 6H, CH_2), 2.41 (mc, 4H, CH_2), 2.36 (s, 3H, CH_3). Anal. Calcd for ($C_{19}H_{21}FN_2O$): C 73.05, H 6.78, N 8.97. Found: C 73.15, H 6.88, N 9.07.

[4-(4-Fluorobenzyl)piperazin-1-yl](4-methylphenyl)methanone (67)

Yield 60%. White solid. M.p. 114-115 °C. ^{1}H-NMR ($CDCl_3$) (δ): 7.25 (mc, 6H, ArH), 7.00 (mc, 2H, ArH), 3.75 (mc, 1H, CH_2), 3.49 (mc, 4H, CH_2), 2.43 (mc, 4H, CH_2), 2.37 (s, 3H,

CH_3), 1.70 (s, 1H, CH_2). Anal. Calcd for ($C_{19}H_{21}FN_2O$): C 73.05, H 6.78, N 8.97. Found: C 73.25, H 6.98, N 9.17.

[4-(4-Fluorobenzyl)piperazin-1-yl](2-chlorophenyl)methanone (71)

Yield 60%. White solid. M.p. 94-95 °C. ^{1}H-NMR ($CDCl_3$) (δ): 7.32 (mc, 6H, ArH), 7.00 (mc, 2H, ArH), 3.81 (mc, 2H, CH_2), 3.49 (s, 2H, CH_2), 3.22 (mc, 2H, CH_2), 2.41 (mc, 4H, CH_2). Anal. Calcd for ($C_{18}H_{18}ClFN_2O$): C 65.00, H 5.50, N 8.40. Found: C 65.20, H 5.60, N 8.50.

[4-(4-Fluorobenzyl)piperazin-1-yl](3-chlorophenyl)methanone (72)

Yield 70%. Oily residue. ^{1}H-NMR ($CDCl_3$) (δ): 7.33 (mc, 6H, ArH), 7.01 (mc, 2H, ArH), 3.78 (mc, 2H, CH_2), 3.50 (s, 2H, CH_2), 3.41 (mc, 2H, CH_2), 2.51 (mc, 2H, CH_2), 2.37 (mc, 2H, CH_2). Anal. Calcd for ($C_{18}H_{18}ClFN_2O$): C 65.00, H 5.50, N 8.40. Found: C 65.30, H 5.70, N 8.60.

[4-(4-Fluorobenzyl)piperazin-1-yl](4-chlorophenyl)methanone (73)

Yield 50%. White solid. M.p. 81-82 °C. ^{1}H-NMR ($CDCl_3$) (δ): 7.32 (mc, 6H, ArH), 7.00 (mc, 2H, ArH), 3.82 (mc, 2H, CH_2), 3.49 (s, 2H, CH_2), 3.22 (mc, 2H, CH_2), 2.47 (mc, 4H, CH_2). Anal. Calcd for ($C_{18}H_{18}ClFN_2O$): C 65.00, H 5.50, N 8.40. Found: C 65.40, H 5.90, N 8.80.

[4-(4-Fluorobenzyl)piperazin-1-yl](2-bromophenyl)methanone (74)

Yield 50%. White solid. M.p. 86 °C. ^{1}H-NMR ($CDCl_3$) (δ): 7.56 (mc, 1H, ArH), 7.30 (mc, 5H, ArH), 6.99 (mc, 2H, ArH), 3.82 (mc, 2H, CH_2), 3.49 (s, 2H, CH_2), 3.23 (mc, 2H, CH_2), 2.44 (mc, 4H, CH_2). Anal. Calcd for ($C_{18}H_{18}BrFN_2O$): C 57.30, H 4.80, N 7.40. Found: C 57.40, H 4.90, N 7.50.

[4-(4-Fluorobenzyl)piperazin-1-yl](3-bromophenyl)methanone (75)

Yield 60%. Oily residue. ^{1}H-NMR ($CDCl_3$) (δ): 7.54 (mc, 1H, ArH), 7.28 (mc, 5H, ArH), 7.01 (mc, 2H, ArH), 3.77 (mc, 2H, CH_2), 3.49 (s, 2H, CH_2), 3.40 (mc, 2H, CH_2), 2.51 (mc,

2H, CH_2), 2.37 (mc, 2H, CH_2). Anal. Calcd for ($C_{18}H_{18}BrFN_2O$): C 57.30, H 4.80, N 7.40. Found: C 57.40, H 4.90, N 7.50.

[4-(4-Fluorobenzyl)piperazin-1-yl](4-bromophenyl)methanone (76)

Yield 55%. White solid. M.p. 87 °C. ^{1}H-NMR ($CDCl_3$) (δ): 7.53 (mc, 1H, ArH), 7.30 (mc, 5H, ArH), 7.00 (mc, 2H, ArH), 3.76 (mc, 2H, CH_2), 3.49 (s, 2H, CH_2), 3.40 (mc, 2H, CH_2), 2.40 (mc, 4H, CH_2). Anal. Calcd for ($C_{18}H_{18}BrFN_2O$): C 57.30, H 4.80, N 7.40. Found: C 57.20, H 4.70, N 7.30.

[4-(4-Fluorobenzyl)piperazin-1-yl](2-trifluoromethyl)methanone (77)

Yield 90%. Oily residue. ^{1}H-NMR ($CDCl_3$) (δ): 7.69 (d, J = 7.3 Hz, 1H, ArH), 7.53 (mc, 2H, ArH), 7.28 (mc, 3H, ArH), 6.99 (mc, 2H, ArH), 3.81 (t, J = 5.0 Hz, 2H, CH_2), 3.48 (s, 2H, CH_2), 3.16 (t, J = 5.0 Hz, 2H, CH_2), 2.50 (mc, 2H, CH_2), 2.29 (mc, 2H, CH_2). Anal. Calcd for ($C_{19}H_{18}F_4N_2O$): C 62.29, H 4.95, N 7.65. Found: C 62.09, H 4.75, N 7.45.

[4-(4-Fluorobenzyl)piperazin-1-yl](3-trifluoromethyl)methanone (78)

Yield 92%. Oily residue. ^{1}H-NMR ($CDCl_3$) (δ): 7.67 (mc, 2H, ArH), 7.56 (mc, 2H, ArH), 7.27 (mc, 2H, ArH), 7,00 (mc, 2H, ArH), 3.79 (mc, 2H, CH_2), 3.50 (s, 2H, CH_2), 3.39 (mc, 2H, CH_2), 2.45 (mc, 4H, CH_2). Anal. Calcd for ($C_{19}H_{18}F_4N_2O$): C 62.29, H 4.95, N 7.65. Found: C 62.19, H 4.85, N 7.55.

[4-(4-Fluorobenzyl)piperazin-1-yl](4-trifluoromethyl)methanone (79)

Yield 87%. White solid. M.p. 82.8-84.5 °C. ^{1}H-NMR ($CDCl_3$) (δ): 7.66 (d, J = 8.2 Hz, 2H, ArH), 7.50 (d, J = 8.2 Hz, 2H, ArH), 7.27 (mc, 2H, ArH), 7.00 (mc, 2H, ArH), 3.80 (mc, 2H, CH_2), 3.50 (s, 2H, CH_2), 3.37 (mc, 2H, CH_2), 2.44 (mc, 4H, CH_2). Anal. Calcd for ($C_{19}H_{18}F_4N_2O$): C 62.29, H 4.95, N 7.65. Found: C 62.09, H 4.75, N 7.45.

[4-(4-Fluorobenzyl)piperazin-1-yl](2,4-difluorophenyl)methanone (80)

Yield 50%. White solid. M.p. 88 °C. ^{1}H-NMR ($CDCl_3$) (δ): 7.34 (mc, 3H, ArH), 6.91 (mc, 4H, ArH), 3.79 (mc, 2H, CH_2), 3.49 (s, 2H, CH_2), 3.32 (mc, 2H, CH_2), 2.44 (mc, 4H, CH_2). Anal. Calcd for ($C_{18}H_{17}F_3N_2O$): C 64.66, H 5.13, N 8.38. Found: C 64.76, H 5.23, N 8.48.

[4-(4-Fluorobenzyl)piperazin-1-yl](2,4-dichlorophenyl)methanone (81)

Yield 65%. Oily residue. ^{1}H-NMR ($CDCl_3$) (δ): 7.41 (mc, 1H, ArH), 7.24 (mc, 4H, ArH), 7.00 (mc, 2H, ArH), 3.80 (mc, 2H, CH_2), 3.49 (s, 2H, CH_2), 3.24 (mc, 2H, CH_2), 2.47 (mc, 3H, CH_2), 2.32 (mc, 1H, CH_2). Anal. Calcd for ($C_{18}H_{17}Cl_2FN_2O$): C 58.87, H 4.67, N 7.63. Found: C 58.97, H 4.77, N 7.83.

[4-(4-Fluorobenzyl)piperazin-1-yl](2,4-dimethoxyphenyl)methanone (82)

Yield 50 %. White solid. M.p. 97 °C. ^{1}H-NMR ($CDCl_3$) (δ): 7.22 (mc, 3H, ArH), 6.99 (mc, 2H, ArH), 6.46 (mc, 2H, ArH), 3.80 (s, 3H, CH_3), 3.79 (mc, 2H, CH_2), 3.78 (s, 3H, CH_3), 3.47 (s, 2H, CH_2), 3.25 (mc, 2H, CH_2), 2.39 (mc, 4H, CH_2). Anal. Calcd for ($C_{20}H_{23}FN_2O_3$): C 67.00, H 6.50, N 7.80. Found: C 67.10, H 6.60, N 7.90.

[2,4-bis(trifluoromethyl)phenyl][4-(4-fluorobenzyl)piperazin-1-yl]methanone (83)

Yield 80%. White solid. m.p. 75-77 °C. ^{1}H-NMR ($CDCl_3$) (δ): 7.86 (mc, 2H, ArH), 7.65 (mc, 1H, ArH), 7.38 (mc, 2H, ArH), 7.07 (m, 2H, ArH), 3.50 (s, 2H, CH_2), 3.43 (mc, 4H, CH_2), 2.52 (mc, 4H, CH_2). Anal. Calcd for ($C_{20}H_{17}F_7N_2O$:) C 55.31, H 3.94, N 6.45. Found: C 55.21, H 3.84, N 6.35.

[4-(4-Fluorobenzyl)piperazin-1-yl](thiophen-2-yl)methanone (95)

Yield 85%. Oily residue. ^{1}H-NMR ($CDCl_3$) (δ): 7.43 (dd, *J* = 5.0, 1.0 Hz, 1H, ArH), 7.27 (mc, 3H, ArH), 7.02 (mc, 3H, ArH), 3.74 (t, *J* = 5.0 Hz, 4H, CH_2), 3.50 (s, 2H, CH_2), 2.46 (t, *J* = 5.0 Hz, 4H, CH_2). Anal. Calcd for: ($C_{16}H_{17}FN_2OS$) C 63.14, H 5.63, N 9.20. Found: C 63.04, H 5.53, N 9.12.

[4-(4-Fluorobenzyl)piperazin-1-yl](furan-2-yl)methanone (96)

Yield 65%. White solid. M.p. 128.9-130.9 °C. ^{1}H-NMR ($CDCl_3$) (δ): 7.46 (mc, 1H, ArH), 7.28 (t, *J* = 8.7 Hz, 2H, ArH), 7.01 (t, *J* = 8.7 Hz, 2H, ArH), 6.97 (mc, 1H, ArH), 6.45 (mc, 1H, ArH), 3.80 (mc, 4H, CH_2), 3.50 (s, 2H, CH_2), 2.48 (t, *J* = 5.0 Hz, 4H, CH_2). ^{13}C-NMR ($CDCl_3$) (δ): 163.07 (CF), 159.05 (CO), 147.98, 143.56, 133.35, 131.11, 116.23, 115.05, 111.21, 62.06, 52.96. MS (ESI): m/z: 289.0 [M+H$^+$]. Anal. Calcd for ($C_{16}H_{17}FN_2O_2$): C 66.65, H 5.94, N 9.72. Found: C 66.25, H 5.54, N 9.32.

1-[4-(4-Fluorobenzyl)piperazin-1-yl]-2-phenylethanone (97)

Yield 96%. Oily residue. ^{1}H-NMR ($CDCl_3$) (δ): 7.30 (mc, 2H, ArH), 7.23 (mc, 5H, ArH), 6.98 (t, *J* = 8.6 Hz, 2H, ArH), 3.72 (s, 2H, CH_2), 3.65 (t, *J* = 4.6 Hz, 2H, CH_2), 3.42 (mc, 4H, CH_2), 2.39 (t, *J* = 4.8 Hz, 2H, CH_2), 2.22 (t, *J* = 4.8 Hz, 2H, CH_2). Anal. Calcd for: ($C_{19}H_{21}FN_2O$) C 73.05, H 6.78, N 8.97; Found: C 73.25, H 6.88, N 8.87.

1,3-Benzodioxol-5-yl[4-(4-fluorobenzyl)piperazin-1-yl]methanone (98)

Yield 74%. White solid. M.p. 106-106.6 °C. ^{1}H-NMR ($CDCl_3$) (*δ*): 7.28 (t, *J* = 8.7 Hz, 2H, ArH), 7.00 (t, *J* = 8.7 Hz, 2H, ArH), 6.91 (mc, 2H, ArH), 6.82 (d, *J* = 7.8 Hz, 1H, ArH), 5.99 (s, 2H, CH_2), 3.62 (mc, 4H, CH_2), 3.49 (s, 2H, CH_2), 2.43 (mc, 4H, CH_2). ^{13}C-NMR ($CDCl_3$) (*δ*): 169.77 (CO), 163.07 (CF), 148.76, 147.56, 133.31, 130.59, 129.42, 121.56, 115.13, 108.16, 108.06, 101.38, 62.06, 53.04, 44.46. MS (ESI): m/z: 342.9 [M+H$^+$]. Anal. Calcd for ($C_{16}H_{17}FN_2O_2$): C 66.65, H 5.94, N 9.72. Found: C 66.55, H 5.84, N 9.62.

[4-(4-Fluorobenzyl)piperazin-1-yl](naphthalen-2-yl)methanone (99)

Yield 75%. White solid. M.p. 120.5-121.4 °C. ^{1}H-NMR ($CDCl_3$) (*δ*): 7.87 (mc, 4H, ArH), 7.50 (mc, 3H, ArH), 7.28 (t, *J* = 8.5 Hz, 2H, ArH), 7.00 (t, *J* = 8.5 Hz, 2H, ArH), 3.84 (mc, 2H, CH_2), 3.51 (s, 2H, CH_2), 3.48 (mc, 2H, CH_2), 2.40 (mc, 4H, CH_2). ^{13}C-NMR ($CDCl_3$) (*δ*): 170.31 (CO), 163.07 (C-F), 133.65, 133.30, 132.70, 130.56, 130.50, 128.37, 128.28, 127.78, 127.05, 126.90, 126.87, 126.68, 124.31, 115.23, 115.06, 62.07, 53.22, 52.88. MS (ESI): m/z: 348.9 [M+H$^+$]. Anal. Calcd for ($C_{22}H_{21}FN_2O$): C 75.84, H 6.08, N 8.04. Found: C 75.74, H 5.98, N 7.94.

[4-(4-Fluorobenzyl)piperazin-1-yl](naphthalen-1-yl)methanone (100)

Yield 88%. Oily residue. ^{1}H-NMR ($CDCl_3$) (*δ*): 7.87 (mc, 3H, ArH), 7.47 (mc, 4H, ArH), 7.25 (t, *J* = 8.7 Hz, 2H, ArH), 6.98 (t, *J* = 8.7 Hz, 2H, ArH), 3.95 (mc, 2H, CH_2), 3.48 (s, 2H, CH_2), 3.19 (t, *J* = 5.0 Hz, 2H, CH_2), 2.58 (t, *J* = 5.0 Hz, 2H, CH_2), 2.26 (q, *J* = 5.0 Hz, 2H, CH_2). Anal. Calcd for ($C_{22}H_{21}FN_2O$): C 75.84, H 6.08, N 8.04. Found: C 75.74, H 5.98., N 7.94.

6.1.14 General procedure to synthesize [4-(4-Fluorobenzyl)piperazin-1-yl]methanone derivatives (84-89, 101-103)

A mixture of the suitable carboxylate derivative (1 mmol), N,N,N',N'-tetramethyl-O-(1*H*-benzotriazol-1-yl)uranium hexafluorophosphate (HBTU) (1 mmol, 380 mg) in DMF (4 mL) was stirred at room temperature for 1 h. Then, a solution of the 1-(4-Fluorobenzyl)pyperazine (**50**) (1 mmol) in TEA (1 mmol, 140 µL) was added dropwise. The reaction mixture was left overnight and then quenched with water (10 mL) and extracted with DCM (3x5 mL).[246] The organic phase was dried with Na_2SO_4 and the solvent was removed *in vacuo*. The residues were then purified by crystallization with Et_2O or by chromatographic column (DCM/MeOH 98:02), leading to the final compounds (**84-89, 101-103**).

[4-(4-Fluorobenzyl)piperazin-1-yl](2-nitrophenyl)methanone (84)

Yield 70%. Bright yellow solid. M.p. 101-102 °C. ^{1}H-NMR ($CDCl_3$) (δ): 8.18 (d, *J* = 7.7 Hz, 1H, ArH), 7.69 (t, *J* = 7.7 Hz, 1H, ArH), 7.55 (t, *J* = 7.7 Hz, 1H, ArH), 7.38 (d, *J* = 7.7 Hz, 1H, ArH), 7.27 (t, *J* = 8.5 Hz, 2H, ArH), 6.99 (t, *J* = 8.5 Hz, 2H, ArH), 3.83 (mc, 2H, CH_2), 3.49 (s, 2H, CH_2), 3.21 (t, *J* = 5.1 Hz, 2H, CH_2), 2.57 (mc, 2H, CH_2), 2.35 (mc, 2H, CH_2). Anal. Calcd for ($C_{18}H_{18}FN_3O_3$): C 63.00, H 5.30, N 12.20. Found: C 63.40, H 5.70, N 12.60.

[4-(4-Fluorobenzyl)piperazin-1-yl](3-nitrophenyl)methanone (85)

Yield 76%. Bright yellow solid. M.p. 110-112 °C. ^{1}H-NMR ($CDCl_3$) (δ): 8.28 (mc, 1H, ArH), 7.74 (d, *J* = 7.4 Hz, 1H, ArH), 7.62 (mc, 1H, ArH), 7,28 (mc, 3H, ArH), 7.00 (mc, 2H, ArH), 3.80 (mc, 2H, CH_2), 3.51 (s, 2H, CH_2), 3.39 (mc, 2H, CH_2), 2.55 (mc, 2H, CH_2), 2.26 (mc, 2H, CH_2). Anal. Calcd for ($C_{18}H_{18}FN_3O_3$): C 63.00, H 5.30, N 12.20. Found: C 63.10, H 5.40, N 12.30.

[4-(4-Fluorobenzyl)piperazin-1-yl](4-nitrophenyl)methanone (86)

Yield 80%. Bright yellow solid. M.p. 123-124 °C. ^{1}H-NMR ($CDCl_3$) (δ): 8.27 (d, *J* = 8.6 Hz, 2H, ArH), 7.56 (d, *J* = 8.6 Hz, 2H, ArH), 7.27 (t, *J* = 8.7 Hz, 2H, ArH), 7.00 (t, *J* = 8.7 Hz, 2H, ArH), 3.80 (mc, 2H, CH_2), 3.51 (s, 2H, CH_2), 3.36 (mc, 2H, CH_2), 2.53 (mc, 2H, CH_2),

2.37 (mc, 2H, CH_2). Anal. Calcd for ($C_{18}H_{18}FN_3O_3$): C 63.00, H 5.30, N 12.20. Found: C 63.20, H 5.50, N 12.40.

[4-(4-Fluorobenzyl)piperazin-1-yl](2,4-dinitrophenyl)methanone (87)

Yield 62%. Yellow solid. M.p. 169-171 °C. ^{1}H-NMR ($CDCl_3$) (δ): 9.01 (s, 1H, ArH), 8.54 (d, *J* = 8.3 Hz, 1H, ArH), 7.61 (d, *J* = 8.3 Hz, 1H, ArH), 7.28 (mc, 2H, ArH), 7.00 (t, *J* = 8.7 Hz, 2H, ArH), 3.84 (mc, 2H, CH_2), 3.52 (s, 2H, CH_2), 3.21 (t, *J* = 5.0 Hz, 2H, CH_2), 2.58 (mc, 2H, CH_2), 2.38 (mc, 2H, CH_2). ^{13}C-NMR ($CDCl_3$) (δ): 164.14 (CO), 163.12 (CF), 147.95, 145.74, 138.22, 133.10, 130.50, 129.59, 128.65, 120.44, 115.21, 61.91, 52.11, 46.91. MS (ESI): m/z: 388.8 [M+H$^+$]. Anal. Calcd for ($C_{18}H_{17}FN_4O_5$): C 55.67, H 4.41, N 14.43. Found: C 55.57, H 4.31, N 14.33.

[4-(4-Fluorobenzyl)piperazin-1-yl](2,4-dimethylphenyl)methanone (88)

Yield 56%. White solid. M.p. 247-249 °C. ^{1}H-NMR ($CDCl_3$) (δ): 7.66 (mc, 2H, ArH), 7.13 (t, *J* = 8.6 Hz, 2H, ArH), 7.02 (mc, 3H, ArH), 4.15 (mc, 2H, CH_2), 4.00 (mc, 1H, CH_2), 3.73 (mc, 1H, CH_2), 3.56 (mc, 2H, CH_2), 3.30 (mc, 1H, CH_2), 2.71 (mc, 3H, CH_2), 2.31 (s, 3H, CH_3), 2.23 (s, 3H, CH_3). ^{13}C-NMR ($CDCl_3$) (δ): 170.24 (CO), 162.81 (CF), 139.86, 134.45, 133.46, 131.55, 126.80, 116.65, 60.36, 51.31, 21.20, 19.00. MS (ESI): m/z: 327.0 [M+H$^+$]. Anal. Calcd for ($C_{20}H_{23}FN_2O$): C 73.59, H 7.10, N 8.58. Found: C 73.49, H 7.00, N 8.48.

[4-(4-Fluorobenzyl)piperazin-1-yl](2,4-dibromophenyl)methanone (89)

Yield 80%. Oily residue. ^{1}H-NMR ($CDCl_3$) (δ): 7.73 (mc, 1H, ArH), 7.49 (d, *J* = 8.2 Hz, 1H, ArH), 7.27 (mc, 2H, ArH), 7.12 (d, *J* = 8.2 Hz 1H, ArH), 7.00 (mc, 2H, ArH), 3.80 (t, *J* = 5.2 Hz, 2H, CH_2), 3.50 (s, 2H, CH_2), 3.23 (mc, 2H, CH_2), 2.45 (mc, 3H, CH_2), 2.33 (mc, 1H, CH_2). Anal. Calcd for ($C_{18}H_{17}Br_2FN_2O$): C 47.40, H 3.76, N 6.14. Found: C 47.50, H 3.86, N 6.24.

[4-(4-Fluorobenzyl)piperazin-1-yl](1*H*-pyrrol-2-yl)methanone (101)

Yield 40%. White solid. M.p. 140.6-141.8 °C. ^{1}H-NMR ($CDCl_3$) (δ): 9.58 (bs, 1H, NH), 7.29 (t, *J* = 8.5 Hz, 2H, ArH), 7.02 (t, *J* = 8.5 Hz, 2H, ArH), 6.90 (mc, 1H, ArH), 6.49 (mc, 1H, ArH), 6.23 (mc, 1H, ArH), 3.85 (mc, 4H, CH_2), 3.50 (s, 2H, CH_2), 2.48 (t, *J* = 5.0 Hz, 4H,

CH_2). ^{13}C-NMR ($CDCl_3$) (δ): 163.07 (CF), 161.11 (CO), 133.38, 130.50, 124.62, 120.84, 115.11, 112.02, 109.41, 62.10, 52.97. MS (ESI): m/z: 288.0 [M+H$^+$]. Anal. Calcd for ($C_{18}H_{17}FN_4O_5$): C 66.88, H 6.31, N 14.62. Found: C 66.68, H 6.11, N 14.42.

1-[4-(4-Fluorobenzyl)piperazin-1-yl]-3-phenylpropan-1-one (102)

Yield 100%. Oily residue. ^{1}H-NMR ($CDCl_3$) (δ): 7.24 (mc, 7H, ArH), 7.00 (t, *J* = 8.7 Hz, 2H, ArH), 3.62 (t, *J* = 4.8 Hz, 2H, CH_2), 3.45 (s, 2H, CH_2), 3.38 (t, *J* = 5.0 Hz, 2H, CH_2), 2.96 (t, *J* = 7.8 Hz, 2H, CH_2), 2.61 (t, *J* = 7.8 Hz, 2H, CH_2), 2.38 (t, *J* = 5.0 Hz, 2H, CH_2), 2.28 (t, *J* = 4.8 Hz, 2H, CH_2). Anal. Calcd for ($C_{20}H_{23}FN_2O$): C 73.59, H 7.10, N 8.58; Found: C 73.69, H 7.20, N 8.68.

[4-(4-Fluorobenzyl)piperazin-1-yl](1*H*-indol-6-yl)methanone (103)

Yield 50%. Brown solid. M.p. 141-142 °C. ^{1}H-NMR ($CDCl_3$) (δ): 9.31 (bs, 1H, NH), 7.59 (d, *J* = 8.1 Hz, 1H, ArH), 7.47 (s, 1H, ArH), 7.27 (t, *J* = 8.7 Hz, 2H, ArH), 7.21 (mc, 1H, ArH), 7.11 (d, *J* = 8.1, 1H, ArH), 7.00 (t, *J* = 8.7 Hz, 2H, ArH), 6.50 (mc, 1H, ArH), 3.60 (mc, 4H, CH_2), 3.49 (s, 2H, CH_2), 2.43 (mc, 4H, CH_2). Anal. Calcd for ($C_{20}H_{20}FN_3O$): C 71.20, H 5.97, N 12.45. Found: C 71.10, H 5.87, N 12.35.

6.1.15 General procedure to synthetize 4-(4-Fluorobenzyl)piperazin-1-yl] (hydroxyphenyl) methanone derivatives (68-70, 90) and 4-[2-(4-hydroxyphenyl) ethyl]-1,2-benzenediol (104)

To a solution of the suitable derivatives (**59-61**, **82**) (0.4 mmol) in DCM (3 mL) BBr_3 (6 mmol) was added at 0 °C under nitrogen atmosphere. The reaction mixture was stirred for 24 h at room temperature, then a small amount of MeOH (1.5 mL) was added at 0 °C.[247] The solvent was removed at reduced pressure and the obtained residue was extracted with EtOAc (3x5 mL). The organic phase thus obtained was washed with a saturated solution of $NaHCO_3$ (3x5 mL) and subsequently was dried with anhydrous Na_2SO_4. The solvent was removed at reduced pressure and the final products (**68-70**, **90**) were purified by crystallization with MeOH.

[4-(4-Fluorobenzyl)piperazin-1-yl](2-hydroxyphenyl)methanone (68)

Yield 50%. White solid. M.p. 167-169 °C . ^{1}H-NMR ($CDCl_3$) (δ): 9.63 (bs, 1H, OH), 7.33 (mc, 4H, ArH), 6.93 (mc, 4H, ArH), 3.78 (mc, 4H, CH_2), 3.52 (s, 2H, CH_2), 2.48 (mc, 2H,

CH_2), 1.60 (mc, 2H, CH_2). Anal. Calcd for ($C_{18}H_{19}FN_2O_2$): C 68.77, H 6.09, N 8.91. Found: C 68.97, H 6.29, N 9.11.

[4-(4-Fluorobenzyl)piperazin-1-yl](3-hydroxyphenyl)methanone (69)

Yield 57%. White solid. M.p. 175-177 °C. ^{1}H-NMR ($CDCl_3$) (δ): 7.54 (bs, 1H, OH), 7.27 (mc, 4H, ArH), 6.99 (mc, 2H, ArH), 6.81 (mc, 2H, ArH), 3.79 (mc, 1H, CH_2), 3.46 (mc, 4H, CH_2), 2.43 (mc, 3H, CH_2), 1.69 (mc, 2H, CH_2). Anal. Calcd for ($C_{18}H_{19}FN_2O_2$): C 68.77, H 6.09, N 8.91. Found: C 68.87, H 6.19, N 9.01.

[4-(4-Fluorobenzyl)piperazin-1-yl](4-hydroxyphenyl)methanone (70)

Yield 70%. White solid. M.p. 170-172 °C. ^{1}H-NMR ($CDCl_3$) (δ): 7.27 (mc, 4H, ArH), 7.01 (mc, 2H, ArH), 6.74 (mc, 2H, ArH), 3.66 (mc, 4H, CH_2), 2.45 (mc, 2H, CH_2),1.65 (mc, 4H, $2CH_2$). Anal. Calcd for ($C_{18}H_{19}FN_2O_2$): C 68.77, H 6.09, N 8.91; Found: C 68.87, H 6.19, N 9.01.

[4-(4-fluorobenzyl)piperazin-1-yl](2,4-dihydroxyphenyl)methanone (90)

Yield 60%. Oily residue. ^{1}H-NMR ($CDCl_3$) (δ): 7.27 (t, *J* = 8.5 Hz, 2H, ArH), 7.07 (d, *J* = 8.5 Hz, 1H, ArH), 6.99 (t, *J* = 8.5 Hz, 2H, ArH), 6.37 (mc, 1H, ArH), 6.27 (d, *J* = 8.5 Hz, 1H, ArH), 3.69 (mc, 4H, CH_2), 3.50 (s, 2H, CH_2), 2.48 (mc, 4H, $2CH_2$). Anal. Calcd for ($C_{18}H_{19}FN_2O_3$): C 65.44, H 5.80, N 8.48; Found: C 65.54, H 5.90, N 8.58.

4-[2-(4-hydroxyphenyl)ethyl]-1,2-benzenediol (104)

Yield 64%. White solid. M.p. 150-152 °C. ^{1}H NMR ($CDCl_3$) (δ): 8.03 (bs, 1H, OH), 7.62 (bs, 1H, OH), 7.60 (bs, 1H, OH), 7.02 (m, 2H, ArH), 6.73 (m, 2H, ArH), 6.70 (d, *J* = 8.0 Hz, 1H, Ar), 6.69 (d, *J* = 2.1 Hz, 1H, ArH), 6.52 (dd, *J* = 8.0, 2.1 Hz, 1H, Ar), 2.74 (m, 2H, CH_2), 2.71 (m, 2H, CH_2). ^{13}C NMR ($CDCl_3$) (δ): 156.3, 145.7, 143.9, 134.6, 133.7, 130.2, 120.5, 116.4, 115.88, 115.85, 38.4, 38.1 Anal. Calcd for ($C_{14}H_{14}O_3$): C 73.03, H 6.13; Found: C 73.43, H 6.53.

6.1.16 General procedure to synthetize 4-(4-Fluorobenzyl)piperazin-1-yl] (aminophenyl) methanone derivatives (91-94)

To a solution of the suitable nitro-derivatives (**84-87**) (0.2 mmol) in EtOH (1.5 mL) and HCl (1 mL), Zn powder (432 mg, 6.6 mmol) was added slowly. The reaction mixture was refluxed for 2 h and then added NaOH (2N).[248] The obtained residue was extracted with EtOAc (3x5 mL). The organic phase thus obtained was dried with anhydrous Na_2SO_4. The solvent was removed at reduced pressure and the desired amino-analogues (**91-94**) were purified by crystallization with EtOH.

[4-(4-Fluorobenzyl)piperazin-1-yl](2-aminophenyl)methanone (91)

Yield 80%. Oily residue. ^{1}H-NMR ($CDCl_3$) (δ): 7.27 (mc, 2H, ArH), 7.14 (mc, 1H, ArH), 7.04 (mc, 3H, ArH), 6.68 (mc, 2H, ArH), 4.31 (bs, 2H, NH_2), 3.62 (mc, 4H, CH_2), 3.48 (s, 2H, CH_2), 2.43 (mc, 4H, CH_2). Anal. Calcd for ($C_{18}H_{20}FN_3O$): C 68.99, H 6.43, N 13.41. Found: C 69.09, H 6.53, N 13.51.

[4-(4-Fluorobenzyl)piperazin-1-yl](3-aminophenyl)methanone (92)

Yield 85%. Oily residue. ^{1}H-NMR ($CDCl_3$) (δ): 7.26 (mc, 3H, ArH), 6.99 (mc, 2H, ArH), 6.69 (mc, 3H, ArH), 3.75 (mc, 2H, CH_2), 3.48 (s, 2H, CH_2), 3.43 (mc, 2H, CH_2), 2.45 (mc, 4H, CH_2). Anal. Calcd for ($C_{18}H_{20}FN_3O$): C 68.99, H 6.43, N 13.41. Found: C 69.19, H 6.63, N 13.61.

[4-(4-Fluorobenzyl)piperazin-1-yl](4-aminophenyl)methanone (93)

Yield 80%. White solid. M.p. 146-148 °C. ^{1}H-NMR ($CDCl_3$) (δ): 7.27 (mc, 4H, ArH), 7.00 (t, J = 8.8 Hz, 2H, ArH), 6.63 (d, J = 8.8 Hz, 2H, ArH), 3.85 (mc, 2H, CH_2), 3.62 (mc, 2H, CH_2), 3.48 (s, 2H, CH_2), 2.43 (mc, 4H, CH_2). ^{13}C-NMR ($CDCl_3$) (δ): 170.85 (CO), 163.20 (CF), 148.21, 133.57, 130.72, 129.46, 125.36, 115.22, 114.30, 62.27, 53.21. MS (ESI): m/z: 314.0 [M+H$^+$]. Anal. Calcd for ($C_{18}H_{20}FN_3O$): C 68.99, H 6.43, N 13.41. Found: C 69.29, H 6.73, N 13.71.

[4-(4-fluorobenzyl)piperazin-1-yl](2,4-diaminophenyl)methanone (94)

Yield 74%. Oily residue. ^{1}H-NMR ($CDCl_3$) (δ): 7.25 (mc, 2H, ArH), 7.01 (mc, 2H, ArH), 6.88 (mc, 1H, ArH), 6.00 (mc, 2H, ArH), 3.61 (t, J = 5.0 Hz, 4H, CH_2), 3.47 (s, 2H, CH_2),

2.42 (t, *J* = 5.0 Hz, 4H, CH_2). Anal. Calcd for ($C_{18}H_{21}FN_4O$): C 65.84, H 6.45, N 17.06. Found: C 65.74, H 6.35, N 16.96.

6.1.17 Synthesis of derivative 4-(bromomethyl)-1,2-dimethoxybenzene (107)

DCM (4 mL) was put into a flask, cooled to 0 °C and afterwards 3,4-dimethoxybenzylalcohol (**106**) (500 mg, 3.0 mmol) was added followed by the addition of PBr_3 (964 mg, 3.6 mmol). The reaction was stirred for 20 h and then quenched using ice. The obtained residue was extracted using CH_2Cl_2 (3x5 mL).[249] The organic phase thus obtained was dried with anhydrous Na_2SO_4. The solvent was removed at reduced pressure to obtain the desired compound (**107**) in good yields without further purification.

Yield 87%. Yellow solid. M.p. 57-58 °C. ^{1}H-NMR ($CDCl_3$) (δ): 6.94 (mc, 2H, ArH), 6.81 (mc, 1H, ArH), 4.50 (s, 2H, CH_2), 3.90 (s, 3H, OCH_3), 3.88 (s, 3H, OCH_3). Anal. Calcd for ($C_9H_{11}BrO_2$): C 46.78, H 4.80. Found: C 46.88, H 4.90.

6.1.18 Synthesis of 1,2-dimethoxy-4-[2-(4-methoxyphenyl)ethyl]benzene (108)

THF (1 mL) was put into a small three-neck flask and TMEDA (300 µl, 2.0 mmol) was added. The solution was stirred and cooled to -78 °C. 4-Methoxybenzylmagnesium chloride solution in THF (2.0 mmol, 0.25 M) was then added slowly followed by slow addition of derivative **107** (1.0 mmol). The reaction mixture was stirred at -78 °C for 2 h and then quenched with H_20 (5 mL).[240] The obtained residue was extracted using EtOAc (3x5 mL). The organic phase thus obtained was dried with anhydrous Na_2SO_4 and the solvent removed at reduced pressure. The desired compound was obtained after purification by FC using the mixture of Cyhex/EtOAc (90:10) as eluent.

Yield 50%. Oily residue. ^{1}H NMR ($CDCl_3$) (δ): 7.09 (m, 2H, ArH), 6.83 (m, 2H, ArH), 6.79 (d, *J* = 8.1 Hz, 1H, ArH), 6.72 (dd, *J* = 8.1, 1.9 Hz, 1H, ArH), 6.65 (d, *J* = 1.9 Hz, 1H, ArH), 3.86 (s, 3H, OCH_3), 3.84 (s, 3H, OCH_3), 3.79 (s, 3H, OCH_3), 2.85 (s, 4H, CH_2). ^{13}C NMR ($CDCl_3$) (δ): 157.8, 148.6, 147.1, 134.4, 133.8, 129.4, 120.2, 113.6, 111.8, 111.1, 55.8, 55.7, 55.2, 37.7, 37.2. Anal. Calcd for ($C_{17}H_{20}O_3$): C 74.97, H 7.40. Found: C 74.87, H 7.60.

6.1.19 Synthesis of derivative 1,1'-(methylenedisulfanediyl)bis(4-fluorobenzene) (105)

To a cooled (-78 °C) solution of bis(4-fluorophenyl)disulfide (**109**) (200 mg, 0.79 mmol) in dry THF was added trimethylsilyl chloride (0.20 mL, 1.58 mmol) and bromoiodomethane (0.18 mL, 2.37 mmol). After 2 min, an ethereal solution of MeLi-LiBr (1.32 mL, 1.97 mmol, 1.5 M) was added dropwise over 5 min. The resulting solution was stirred for 2 h at that temperature and, after removing the cooling bath the mixture was stirred for 1 additional hour at rt. Saturated aq. NH_4Cl was added (2 mL) and then, the organic phase was extracted with Et_2O (2x5 mL), washed with water (5 mL) and brine (10 mL).[241] The organic phase was dried (anhydrous Na_2SO4), filtered and, after removal of the solvent under reduced pressure, the so-obtained crude mixture was subjected to chromatography silica gel (n-hexane-DCM, 95:05) to afford pure compound.

Yield 83%. Oily residue. ^{1}H NMR ($CDCl_3$) (δ): 7.41 (m, 4H, ArH), 7.02 (m, 4H, ArH), 4.22 (s, 2H, SCH_2S). ^{13}C NMR ($CDCl_3$) (δ): 162.5, 134.0, 129.5, 116.2, 43.2. Anal. Calcd for ($C_{13}H_{10}F_2S_2$): C 58.19, H 3.76. Found: C 58.09, H 3.66.

6.2 Docking analysis

The crystal structure of *Agaricus bisporus* Mushroom Tyrosinase in complex with inhibitor tropolone was retrieved from the RCSB Protein Data Bank (PDB code 2Y9X). The ligand and water molecules were discarded and the hydrogens were added to the protein by Discovery Studio 2.5.[250] The ligand structure was constructed using Discovery Studio 2.5.5 and energy minimized using the Smart Minimizer protocol (1000 steps) which combines the Steepest Descent and the Conjugate Gradient methods. CHARMm force field was used for energy minimization steps The minimized ligand was docked in their corresponding proteins by means of Gold Suite 5.0.1. The region of interest used by the Gold program[191] was defined in order to contain the residues within 15 Å from the original position of the ligand in the X-ray structure. The side chains of residues His244, Met257, Val248, His251, Asn260, Thr261, Leu275, Phe264 and Arg 268 were allowed to rotate according to the internal rotamer libraries in GOLD Suite 5.0.1. A scaffold constraint (penalty = 10.0) was used to restrict the solutions in which the 4-fluorophenyl fragment was able to close-in its binding pose upon the

cocrystal structure of the active portion of inhibitor **18**. GoldScore was chosen as fitness function. The standard default settings were used in all calculations and the ligands were submitted to 100 genetic algorithm runs. The "allow early termination" command was deactivated. Results differing by less than 0.75 Å in ligand-all atom RMSD, were clustered together. The conformations with the highest GoldScore fitness values were chosen both for analysis and representation The molecular model of the docked compound was displayed using Pymol software.[2]

6.3 Mushroom tyrosinase inhibition assay

Mushroom tyrosinase (EC 1.14.18.1) was purchased from Sigma Chemical Co. (St. Louis, MO, USA). Tyrosinase inhibition was assayed according to the method of Masamoto[251] with minor modifications.[252] Briefly, aliquots (0.05 mL) of sample at various concentrations (5 – 300 µM) were mixed with 0.5 mL of L- tyrosine or L-DOPA solution (1.25 mM), 0.9 mL of sodium acetate buffer solution (0.05 M, pH 6.8) and preincubated at 25 °C for 10 min. Then 0.05 mL of an aqueous solution of mushroom tyrosinase (333 U/mL) was added last to the mixture. The linear increase in absorbance (Abs) at 475 nm was measured after 30 or 5 minutes of incubation time in the reaction mixture containing L-DOPA. The inhibitory activity of samples is expressed as inhibition percentage and calculated as follows:

Inhibition % = [(A-B)-(C-D)]/[A-B]/100

A: Abs acetate buffer and enzyme

B: Abs acetate buffer

C: Abs acetate buffer, test sample and enzyme

D: Abs acetate buffer and test sample

The concentrations leading to 50% activity lost (IC_{50}) were also calculated by interpolation of the dose-response curves. Kojic acid [5-hydroxy-2-(hydroxymethyl)-4H-pyran-4-one], a fungal secondary metabolite used as skin whitening agent, was employed as a positive standard (8 – 35 µM). A spectrophotometer (Shimadzu UV-1601) was used for mushroom tyrosinase inhibition assay and kinetic analysis of the tyrosinase inhibition.

6.4 Kinetic analysis of the tyrosinase inhibition

The reaction mixture consisted of four different concentrations of L-DOPA (0.6–5 mM) as substrate and mushroom tyrosinase in acetate buffer (0.05 M, pH 6.8). Three different concentrations of compound **18**, **59**, **65** (2,4,8 μM) were added to the reaction mixture. Michaelis–Menten constant (Km) and maximal velocity (Vmax) of the tyrosinase were determined by Lineweaver–Burk plots.

APPENDIX

TELESCOPED *C1-C2* HOMOLOGATIONS OF IMINES SURROGATES EN ROUTE TO FUNCTIONALIZED CF_3-AZIRIDINES

Supervisor:
Prof. Vittorio PACE

Department of Pharmaceutical Chemistry, Faculty of Life Sciences

universität wien

JANUARY 2017-NOVEMBER 2017

AIM OF THE WORK

Carbenoids are organometallic compounds employed in organic synthesis in order to realize a homologation event *via* the introduction of a reactive fragment featuring a precise substitution pattern. The concept is well contextualized taking into account functionalized methylenic units (*e.g.* MCH_2X, M = metal, X = halogen) which act as nucleophilic synthons enabling the transfer of the CH_2X unit into a proper electrophilic partner. The overall result is the formation of a new carbon-carbon bond, in which the so-added portion presents an additional element of substitution (*i.e.* C-X).

Carbenoids posses ambiphilic character, acting as nucleophile (a negative charge is localized at carbon) or electrophile (the carbon brings a positive charge), due to the concomitant presence of an electron-withdrawing *or* an electron-donating group linked at the same *metallated* carbon atom. The predominance of one of these characters depends on the nature of the metal and temperature of reaction, rendering these species unique within the class of organometallic reagents.

In this Appendix we document an unprecedented telescoped *C1* or *C2* homologation of imines surrogates to aziridines derivatives (α-halo and α-halomethyl) through a single synthetic operation.

CHAPTER 1 CARBENOIDS

1.1 Introduction

Carbenoids are classical reagents employed in homologation reactions, which are synthetic operations enabling the formation of a new carbon-carbon or carbon-heteroatom bond through the addition of methylene unit (*e.g.* $-CH_2X$, X = Halogen, CN, OR).[253] The typical homologative transformation is the Arndt-Eistert reaction leading to α-diazoketone starting from a carboxylic acid derivative and diazomethane.[254-256] However, due to the safety concerns of diazomethane, safer alternative have been developed such as the Witting,[257] Corey-Chaykovsky,[258] Morita-Baylis-Hillman[259] and Köbrich[260] reactions (scheme 1).

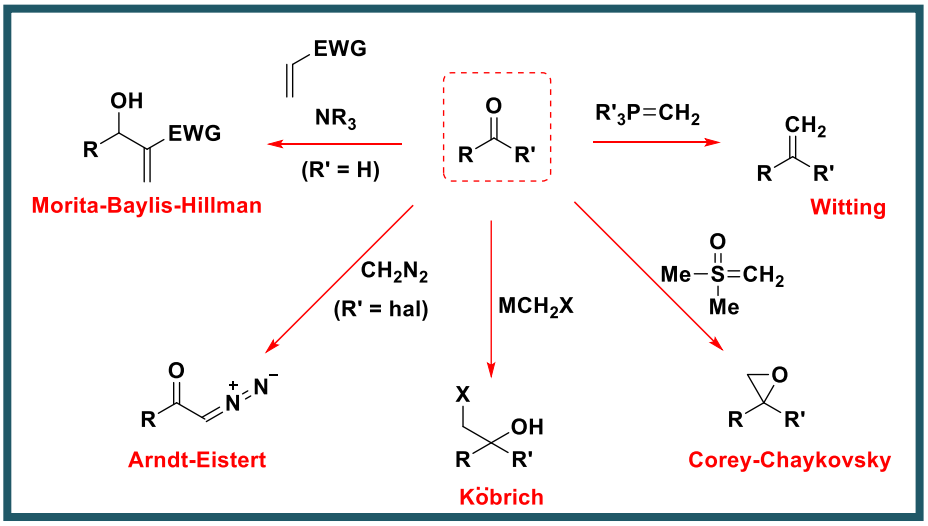

Scheme 1: Classical homologation reactions. Scheme modified from reference [261].

The term carbenoid introduced by the pioneers of the field - Closs[262] and Moss[263] - indicates an organometallic compound containing a metal atom (*e.g.* Li, Mg) and at least one electronegative element (*e.g.* halogen) linked at the *same* carbon, presenting a reactivity profile "*qualitatively analogous to those of carbenes without necessarily being free divalent carbon species*".[263] A peculiar feature of carbenoids is their ambiphilic character, since they can act as nucleophile (a negative charge is localized at carbon) or electrophile (the carbon brings a positive charge), due to the concomitant presence of an electron-withdrawing or an electron-donating groups linked at the same metallated carbon atom (scheme 2). The predominance of one of these characters depends on the reaction conditions, in particular:

- **Nature of the metal**: Electron-positive metals (*e.g.* Li, Mg) confer predominatly nucleophilic character, while switching to less positive metals (*e.g.* Zn, Rh), the electrophilic behavior prevails.
- **Temperature**: Low temperatures slightly promote nucleophilic behavior, whereas high temperatures the electrophilic one.[264]

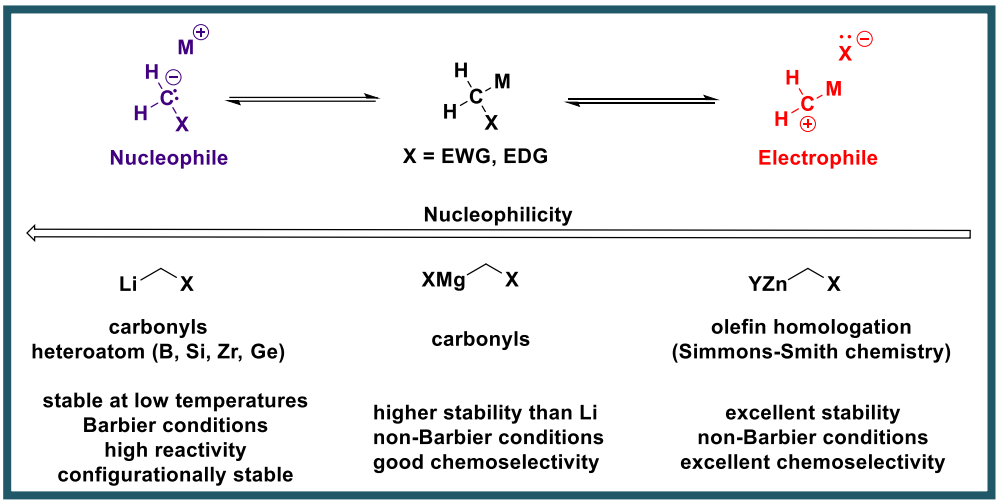

Scheme 2: Carbenoids ambiphilic characters. Scheme modified from reference [253].

Thus, carbenoids can be conveniently employed in two conceptually distinct different homologation protocols:

- **Nucleophilic addition**: Eventually followed by elimination (*i.e.* formal nucleophilic substitution);
- **Cyclopropanation-type process**: Exemplified by the Simmons-Smith-type chemistry for the olefin homologation.[261, 265]

The main limitation in the use of carbenoids reagents is the thermal instability, resulting in a degradation process through α-elimination, due to an internal coordination of the metal with the halogen, finally leading to a free carbene and a metal halide salt. Therefore, it is important to find a good compromise between stability and reactivity in order to obtain the best results in homologation processes. The approaches that can be used to avoid this degradation pathway were suggested in seminal studies by Köbrich,[266] Villieiras,[267] Barluenga[268-270] and Matteson.[271, 272] Conducting the reactions under Barbier-type conditions, at low temperatures (-78 °C is considered a good compromise between thermal stability and reactivity of carbenoids),

in the presence of lithium halide and Lewis basic ethereal-type solvents, it is possible to practically circumvent the α-elimination process. The lithium halide (*e.g.* LiBr) coordinates the halogen atom of carbenoid, disrupting the internal Li-X interaction responsible for the α-elimination.[267, 273] According to these studies, Pace highlighted that LiBr is important not only for the stabilizing effect due to the internal coordination, but it also eliminates the competitive attack of MeLi to an electrophilic substrate in a reaction mixture.[274-277] Furthermore LiBr, behaving as a mild Lewis acid, promotes the attack of the formed carbenoid to the electrophilic species.[277] Lewis basic ethereal-type solvents (*e.g.* THF, Et_2O), by coordinating the carbenoids metal atom, further contribute to suppress the undesired α-elimination.[278] However, a strongly polar solvent such as hexamethylphosporamide (HMPA) favors the degradation process because its oxygen atom solvent coordinates the carbenoid lithium atom, thus enabling the cleavage of the carbon-lithium bond (scheme 3).[261, 267]

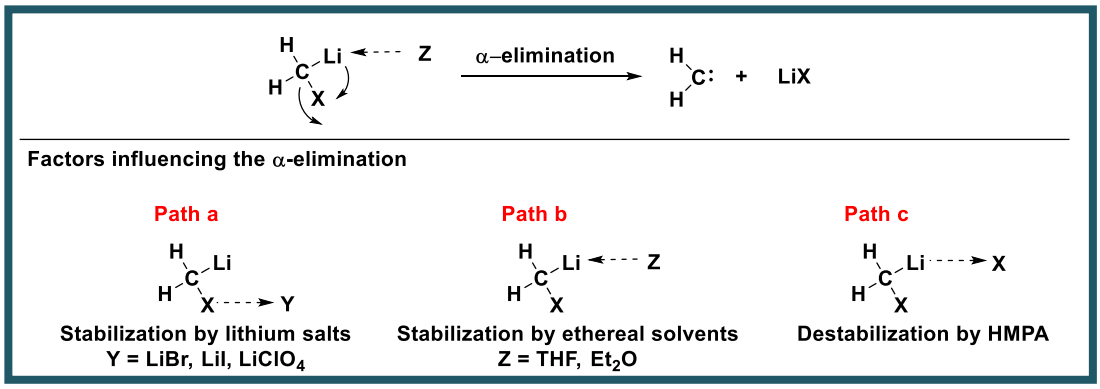

Scheme 3: α-Elimination process and approaches employed to avoid it.
Scheme modified from reference [261].

1.2 Classical methods for preparing carbenoids species

In this context, the correct preparation of carbenoids becomes crucial for applications in synthetic processes. The classical methods used for their preparation are the same of those employed for general organometallic reagents and can be classified as follows: metal-halide exchange; metal-proton exchange (*i.e.* deprotonation); metal-sulfinyl exchange; metal-tin exchange.[278-280]

1.2.1 Metal-halide exchange

Although MeLi and *n*-BuLi are very good lithium sources for accomplishing halide-lithium exchange processes,[269] the commercially available MeLi-LiBr complex in Et_2O recently emerged as the reactive of choice for preparing $LiCH_2Cl$ starting from ICH_2Cl (scheme 4).[274, 275, 281] The nature of dihalomethane used is important because it influences the efficacy of the process. ICH_2Cl is favorited due to the extremely easy iodine-lithium exchange,[278] although the cheaper $BrCH_2Cl$ is also employed especially in industry.[282, 283] Considering the stochiometric ratio, the dihalomethane and organolithium reagents can be used in a ratio of 1:1 because the reaction proceeds quantitatively. Nevertheless, it is preferred to use a small excess (0.2-0.4 equiv) of dihalomethane because of the possibility of the competitive attack of the alkyllithium to the electrophile or variations in its concentration.[284] In this kind of reaction, the alkyllithium has to be added very slowly in the reaction mixture containing both the electrophile and dihalomethane, in such a way that the carbenoid reacts immediately after its formation. Moreover, the nature of the electrophile influences the process because it is required that the dihalomethane reacts faster with the organolithium reagent than the electrophile.[261]

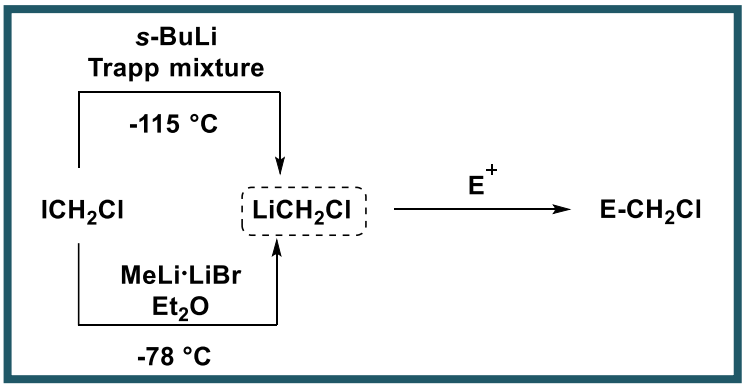

Scheme 4: Carbenoids generation through metal-halide exchange.
Scheme modified from reference [261].

It is possible also to prepare magnesium halocarbenoids through magnesium-iodine exchange in presence of ICH_2Cl and, for example, *i-Pr*MgCl as reported by Knochel, Marek and co-workers.[279, 285] Magnesium carbenoids are more stable than lithium ones, thus they can be generated at -78 °C, adding the electrophile subsequently (scheme 5).

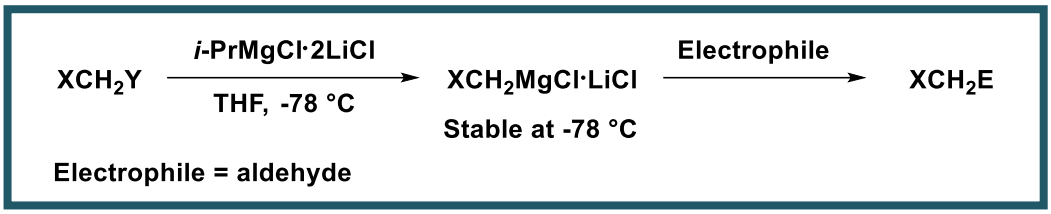

Scheme 5: Magnesium carbenoids generation through metal-halide exchange. Scheme modified from reference [261].

Magnesium carbenoids can represent a good alternative to lithium ones when a strong electrophile is employed, such as aldehyde. Otherwise, with weaker electrophile (*e.g.* Weinreb amides) the reaction does not work as reported by Pace *et al*.[274]

1.2.2 Metal-proton exchange

This approach is rather used for preparing dihalomethylcarbenoids such as $LiCHCl_2$,[286] $LiCHBr_2$[286] and $LiCHI_2$,[287, 288] starting from the suitable dihalomethane in the presence of a lithium amide base (*e.g.* LDA, $LNCy_2$, LTMP or LiHDMS) which extracts the proton of dihalomethane (scheme 6).

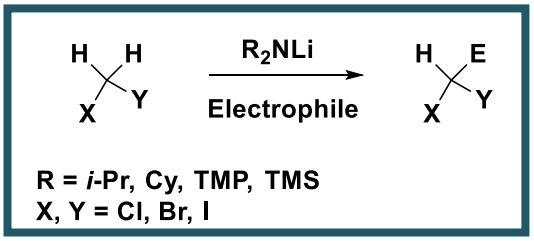

Scheme 6: Carbenoids generation through metal-proton exchange. Scheme modified from reference [261].

In this kind of approach it is not mandatory the use of Barbier-type conditions as highlighted by Bull and coworkers,[287, 288] and generally the nature of the base does not affect the chemocontrol of reactions.[261]

1.2.3 Metal-sulfinyl exchange

This method allows the preparation of both lithium and magnesium carbenoids, as reported by Hoffmann[289] and Blakemore[290] respectively. In scheme 7 it is presented the carbenoids' generation employing this method: the aryl group is placed on the sulfinyl group; the sulfur group suffers inversion of stereochemistry, although in some cases can depend on the carbenoid generated.

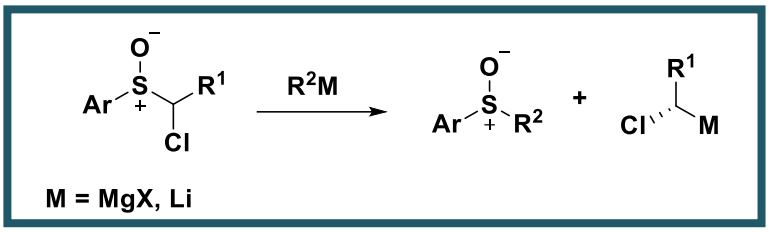

Scheme 7: Carbenoids generation through metal-sulfinyl exchange.
Scheme modified from reference [264].

The α-halosulfoxides have to be prepared previously as reported by Blakemore,[291] Ellman,[292] Bolm[293] and Yamakawa.[294]

1.2.4 Metal-tin exchange

This method is sensible to the nature of alkyllithium species. Indeed, MeLi leads better results compared to *n*-BuLi, which conducts to the formation of undesired impurities. That can may depend on the greater basicity of *n*-BuLi. In 2008, Hammerschmidt *et al*.[295] identified a good method for preparing chiral chloromethyllithium from chloromethylstannane-[D_1] and MeLi under Appel conditions (PPh_3/CCl_4).[296] The homochiral tributylstannyl[D_1]-methanol is the precursor of chloromethylstannane-[D_1] (scheme 8).

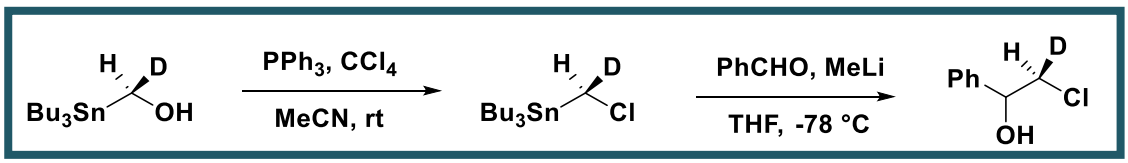

Scheme 8: Carbenoids generation through metal-tin exchange.
Scheme modified from reference [261].

If the reaction is carried out at -78 °C, adding the electrophile after 30 minutes, the carbenoid stability is lower but the chiral information is preserved.[261]

1.3 Lithium carbenoids homologation reactions: electrophilic partners

1.3.1 Weinreb amides

The homologation reactions of Weinreb amides with carbenoids allow the formation of different α-haloketones (α-amino, α,β-unsatured) as reported in scheme 9, highlighting the synthetic pathway described by Pace *et al*.[274, 275] This method excludes unwanted processes such as overaddition of organometallic reagents,

Michael-type processes, unlike esters in which is preferred the double addition of carbenoids leading to carbinol instead of α-haloketones.[253]

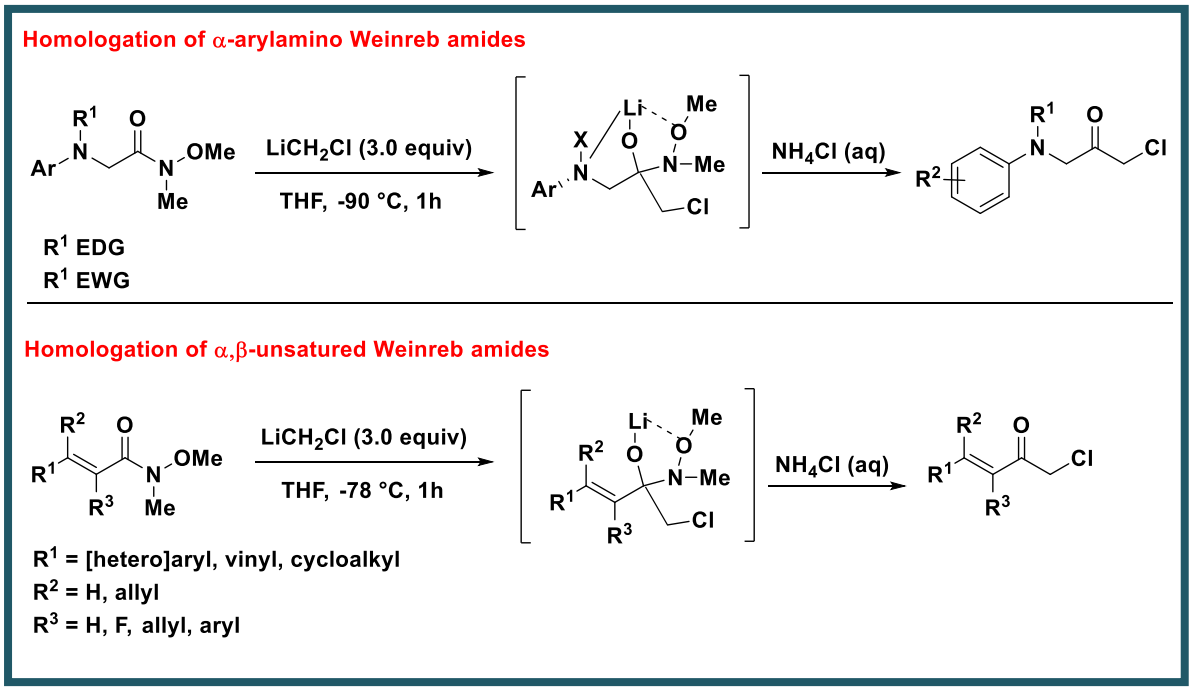

Scheme 9: α-Amino and α,β-unsatured haloketones formation by Weinreb amides homologation reactions. Scheme modified from reference [264].

These differences seem due to the higher stability of the (isolable) tetrahedral intermediate formed by Weinreb amides than that produced by esters.[253]

Furthermore, we employed this strategy for different purposes:

- Synthesis of Nelfinavir, an important HIV inhibitor,[297] as depicted in scheme 10;

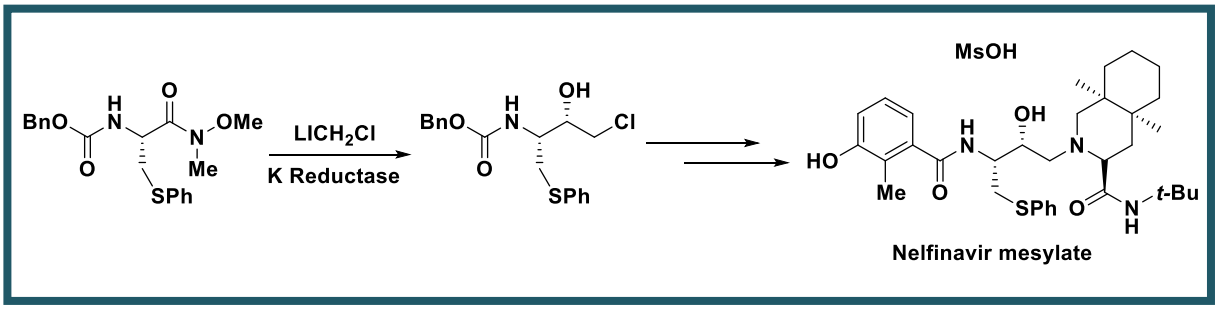

Scheme 10: Synthesis of Nelfinavir employing Weinreb amides. Scheme modified from reference [264].

- Synthesis of α-cyanoketones, as reported in scheme 11.[298]

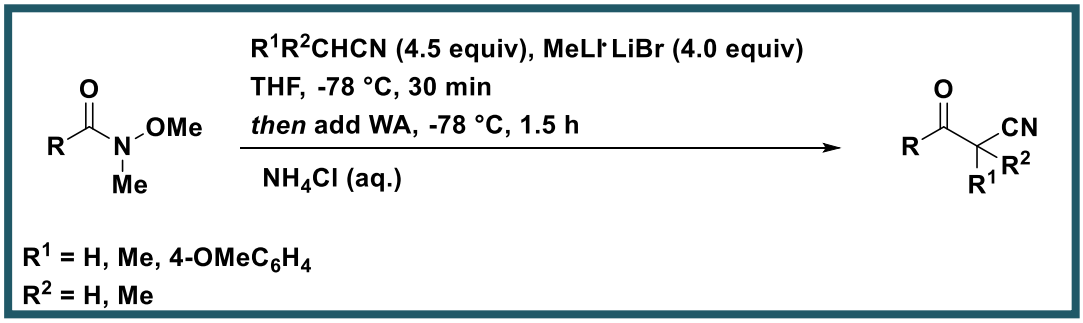

Scheme 11: Synthesis of α-cyanoketones employing Weinreb amides.
Scheme modified from reference [264].

- Synthesis of α-oxyketones[299] and β-oxothioethers[300] as depicted in scheme 12.

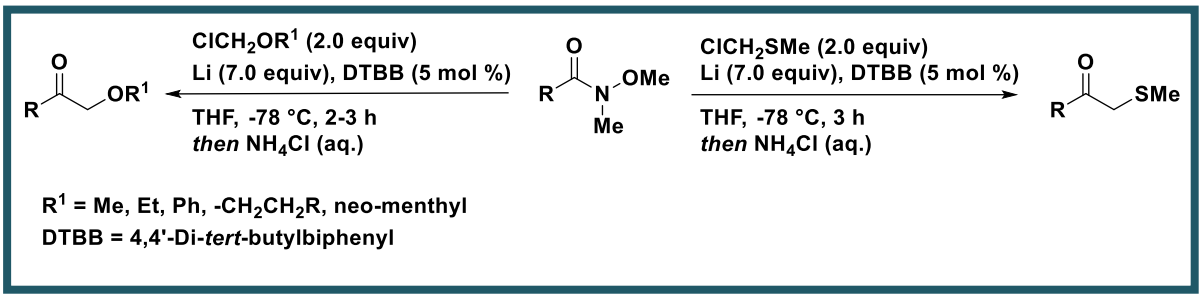

Scheme 12: Synthesis of α-oxyketones and β-oxothioethers employing Weinreb amides.
Scheme modified from reference [264].

- Synthesis of α-aryl and α-alkyl-selenomethyl ketones as reported in scheme 13.[301]

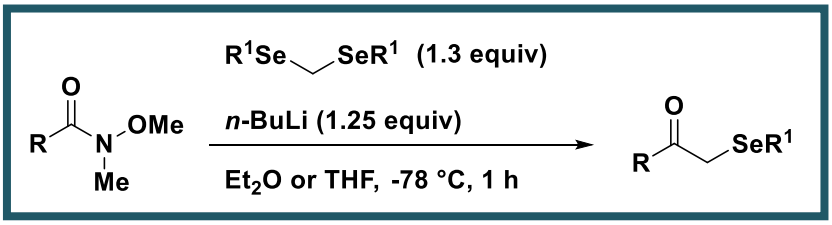

Scheme 13: Synthesis of α-aryl and α-alkyl-selenomethyl ketones employing Weinreb amides.
Scheme modified from reference [264].

1.3.2 α,β-Unsatured ketones

Generally, the addition of halocarbenoids to the carbonyl group of ketones can lead to: 1) halohydrin by acidic quenching; 2) epoxide by ring closure, increasing temperature to rt: 3) homologation of cyclic system to the (*n*+1) cycle; 4) Simmon-Smith-type cyclopropanation process (scheme 14).

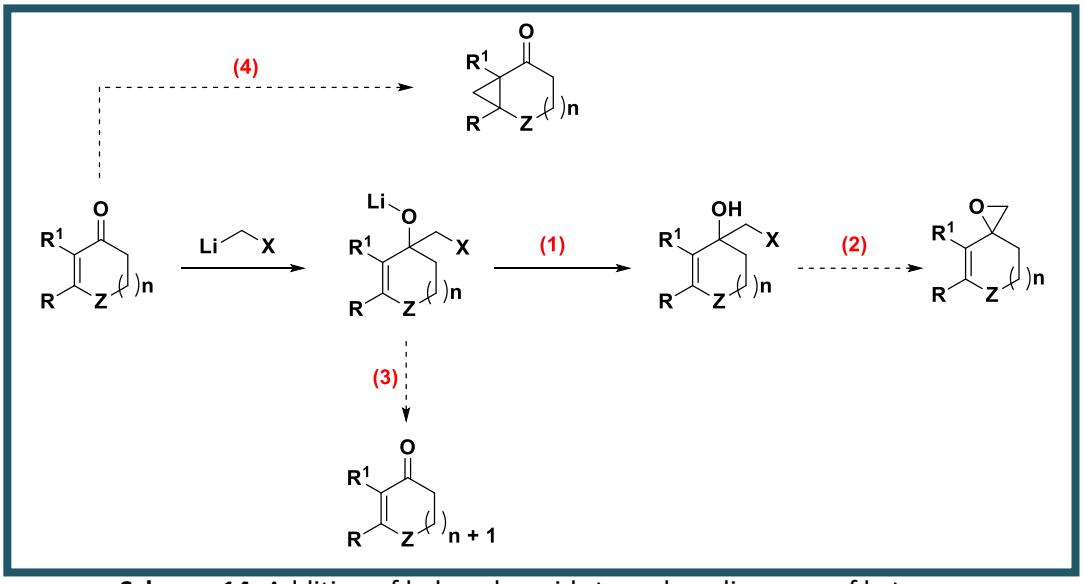

Scheme 14: Addition of halocarbenoids to carbonylic group of ketones.
Scheme modified from reference [253].

Isatins are particular cyclic unsatured carbonylic compounds. The presence of lactamic group makes the C3 highly electrophilic, thus halocarbenoids react with precise chemoselectivity also in the presence of NH lactam proton. This is particularly interesting because several authors reported the difficulties of homologation in systems presenting free amidic or aminic NH groups. As depicted in scheme 15, the isatins homologation with lithium carbenoids leads to ring-closure of the formed halohydrin, finally conducting to spiro-epoxyoxindoles.[264]

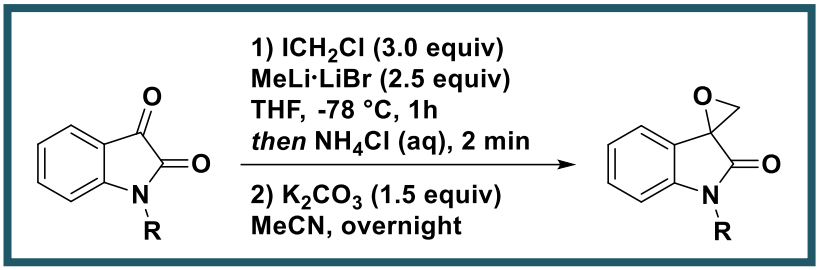

Scheme 15: Spiro-epoxyoxindoles generation from isatins and lithium halocarbenoids.
Scheme modified from reference [264].

Recently, Pace and co-workers reported the surprising formation of full-quaternary α-aldehydes, by reaction of α,β-unsatured ketones and lithium halocarbenoids, instead of the expected vinyl epoxides (scheme 16).[302]

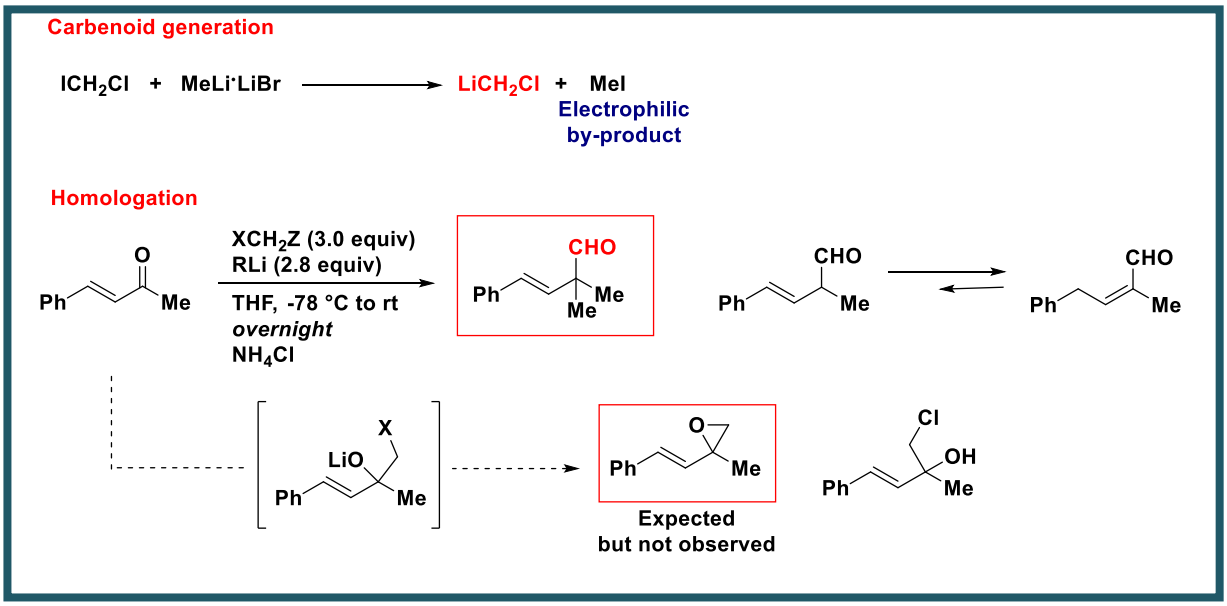

Scheme 16: Surprising full-quaternary α-aldehydes formation instead of vinyl epoxides. Scheme modified from reference [264].

The presence of an additional carbon in the full-quaternary α-aldehydes, was assumed to be due to the formation of the MeI byproduct during carbenoids generation with MeLi-LiBr. Changing MeLi-LiBr with *n*-BuLi, PhLi or $TMSCH_2Li$, the corresponding α-tertiary aldehydes were formed. It is possible to obtain similar results generating $LiCH_2Cl$ by Sn/Li exchange.[264]

1.3.3 Heterocumulenes

Pace and co-workers reported the chemoselective formation of α-haloacetamides from isocyanates and halocarbenoids as depicted in scheme 17.[281]

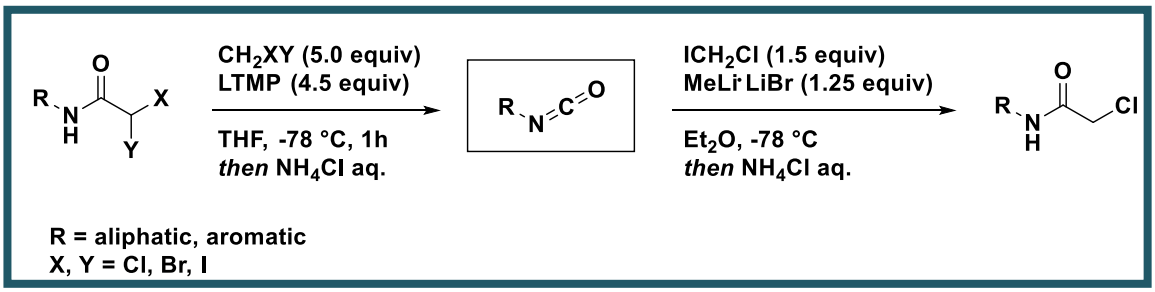

Scheme 17: α-Haloacetamides generation from isocyanates and halocarbenoids. Scheme modified from reference [264].

This tactic – using more general organolithiums - is applicable to several isothiocyanates for the synthesis of thioamides (scheme 18).[264]

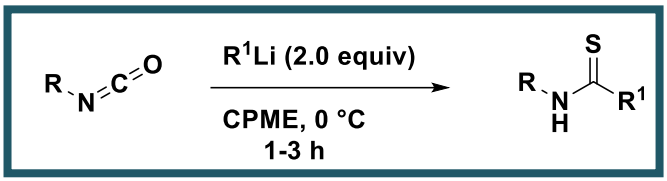

Scheme 18: Thioamides generation from isothiocyanates and halocarbenoids. Scheme modified from reference [264].

1.3.4 Imines

The homologation reaction of imine derivatives in the presence of lithium halocarbenoids generates the corresponding aziridine cycle by ring-closure. Savoia *et al*. reported the generation of aziridine starting from imine derived from 2-pyridinecarboxaldehyde and (*S*)-valinol, as depicted in scheme 19.[303]

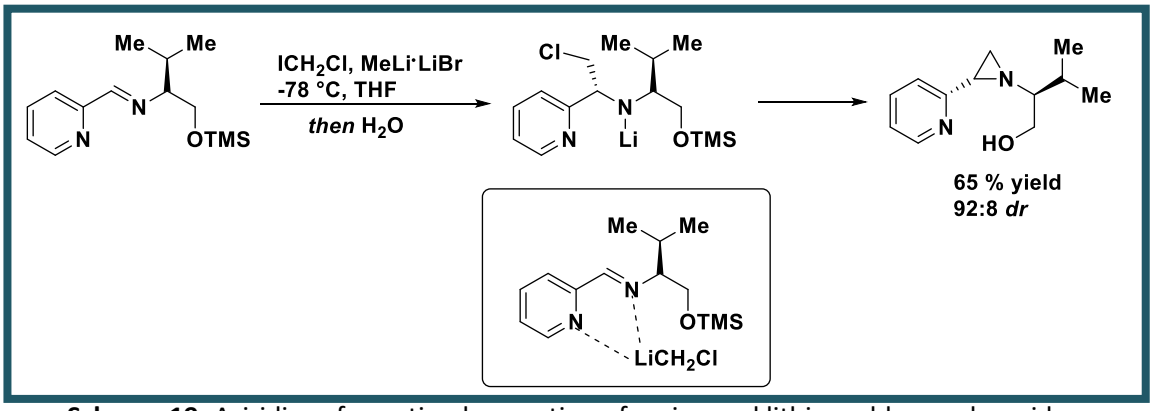

Scheme 19: Aziridines formation by reaction of amine and lithium chlorocarbenoids. Scheme modified from reference [261].

Concellón *et al*. reported aziridines generation starting from sulfonyl-protected imines and lithium iodocarbenoids, as depicted in scheme 20. They highlighted that the generation of aziridines was not possible by using ICH_2Cl instead of CH_2I_2.[304, 305]

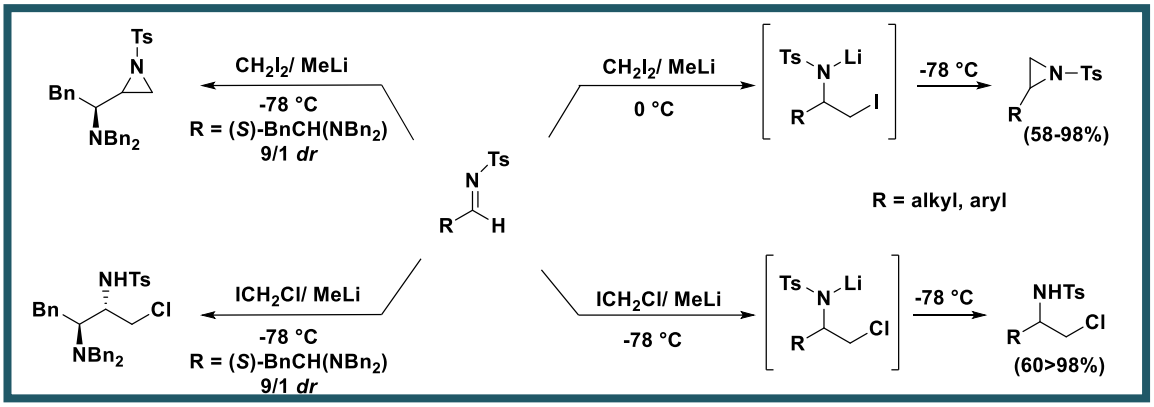

Scheme 20: Aziridines generation by sulfonyl-protected imines and lithium iodocarbenoids. Scheme modified from reference [261].

1.3.5 Disulfides and Diselenides

Recently, Pace and co-workers reported the homologation of disulfides to the corresponding dithioacetals employing lithium carbenoids (scheme 21).[241]

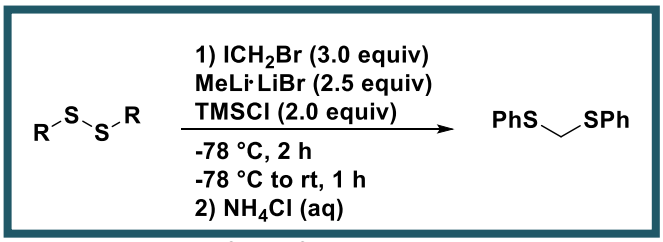

Scheme 21: Homologation of disulfides to the corresponding dithioacetals. Scheme modified from reference [264].

In this process, the chemoselectivity is manteined in the presence of different groups such as halides, heterocycles, esters and secondary amines. This method can be also employed for the homologation of an asymmetric disulfide and aryl or alkyl diselenides.[241]

1.4 Fluorocarbenoids

Fluorocarbenoids are chemical species extremely instable even at very low temperature. Hammerschmidt generated LiCHDF under Barbier-type conditions *via* Sn/Li exchange on a fluoromethylstannane prepared in two steps from paraformaldehyde. However, this methodology was mainly studied for stereochemical aspects and not preparative synthetic insights were presented.[306] In 2017 Pace and R. Luisi directed their efforts to the generation and use of $LiCH_2F$ at preparative scale. They tried to generate this specie through both sulfoxide-lithium and sulfoxide-lithium exchange, resulting in modest yields. Remarkably, through iodine-lithium exchange

conducted on the commercially available fluoroiodomethane, they could properly generate the carbenoid and therefore use it in synthetic processes. The following conditions were pivotal for the success of the transformation (scheme 22):

- MeLi·LiBr was used as the optimal lithiating agent;
- Requirement for Barbier-type conditions;
- Precise stoichiometry of the reaction: electrophile : MeLi·LiBr : ICH_2F = 1 : 1.5 : 2;
- Use of a solvent mixture of THF: Et_2O 1:1 v/v.[307, 308]

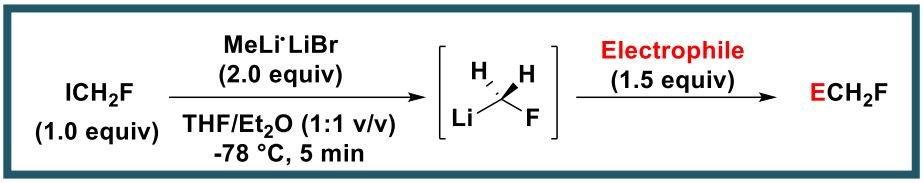

Scheme 22: Generation of fluorolithiumcarbenoids employing iodine-lithium exchange. Scheme modified from reference [264].

This approach demonstrated to be an excellent strategy of fluoromethylation, since it was useful for homologation of several substrates including carbonyls, Weinreb amide and imines.[264]

1.5 Carbenoids and microfluidic techniques

In the last years, the employment of flow methodologies became an interesting tool in order to minimize the degradative α-elimination during the carbenoids generation. Luisi *et al*. noticed the usefulness of such an approach for the preparation of the thermolabile $LiCH_2Cl$, followed by the trapping with electrophiles at considerable high temperatures (up to -20 °C).[309] Sedelmeier and coworkers generated $LiCHCl_2$, using DCM and *n*-butyllithium at -30 °C, followed by the successive addition of aldehydes or boronic esters in order to access the corresponding α-chloro analogues.[310]

1.6 Aziridines

Aziridine is the smallest nitrogen-containing saturated heterocycle exhibiting a particular reactivity due to the ring strain.[311] The pK_a value for aziridines conjugate acid is 7.9, indeed they have a lower basicity than acylic aliphatic amines due to the higher *s* character of the nitrogen electron pair.[312] This motif is found in different synthetic and natural compounds possessing antitumor, antimicrobial and

antibacterial activities. It can be used for the synthesis of biologically active molecules such as amino acids, β-lactams and alkaloids. Some indicative example of natural occurring aziridines (figure 1) with biological activities are:

- Mitosanes isolates from the *Streptomyces verticillatus*. The aziridine ring acts as DNA alkylating agent.[313]
- Azinomycines, DNA cross-linker due to the nucleophilic opening of the aziridine operated by the N-7 of the purines bases.[287]

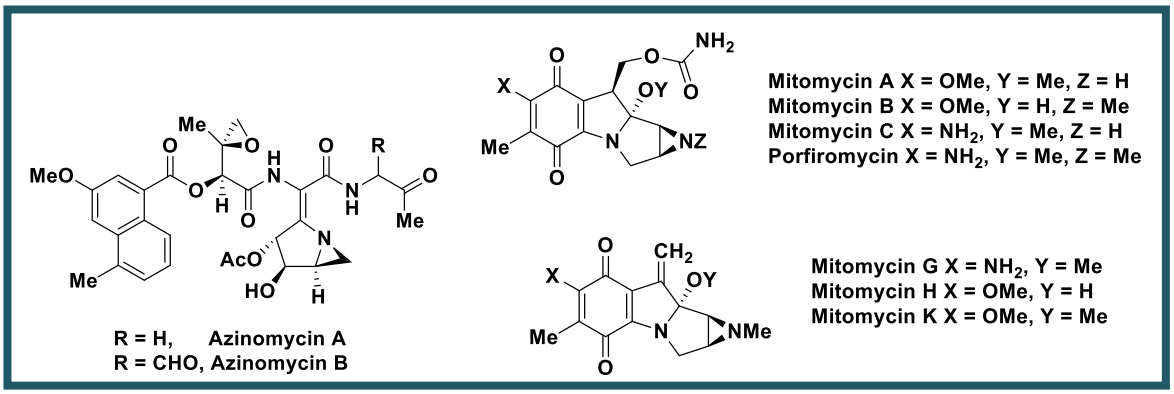

Figure 1: Natural products containing aziridine nucleus. Picture modified from reference [311].

Furthermore, the nitrogen mustards are a synthetic products able to alkylate the DNA because of their aptitude to form aziridinium ions (figure 2).[314]

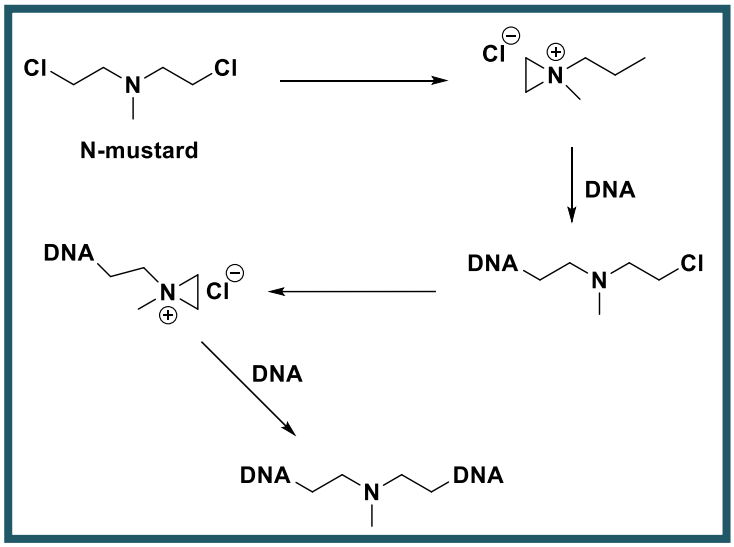

Figure 2: N-mustards activities. Scheme modified from reference [314].

CHAPTER 2 RESULTS AND DISCUSSION

2.1 *C1* or *C2* homologations of imines to aziridines through a single synthetic operation

The simplicity of ring closure operations on formal β-substituted CF_3-containing amines emerged as a classical tool to access the targeted scaffolds.[315] The retrosynthetic analysis shown in scheme 23 indicates analogues of (CF_3-imines) as common precursors for the requested intermediate easily accessible *via* the homologation of imines.[316] Accordingly, classical homologative transformations such as the aza-Darzens[317] or the Corey-Chaiykovski[318] reactions have been thoroughly employed for this purpose: however, as a common feature, the homologation event is limited to the transfer of *one* single carbon unit. We realized that accomplishing *two* consecutive homologations within the same process would enable the introduction of additional elements of complexity, with the final goal of reaching densely functionalized aziridine derivatives through a single chemical step. Although the advancements in the field illustrated in the work by Novak[319] showcase the construction of the aziridine ring with efficiency, tactics suited for the simultaneous aziridine formation – functionalization are still unprecedented and their design would contribute to assembling this important. In this context, our group documented that homologation processes mediated by lithium carbenoids might forge complex molecular architectures in an extremely convenient and effective way by simply tuning the reaction conditions, thus making flexible and divergent the strategy to the target (scheme 23).[302]

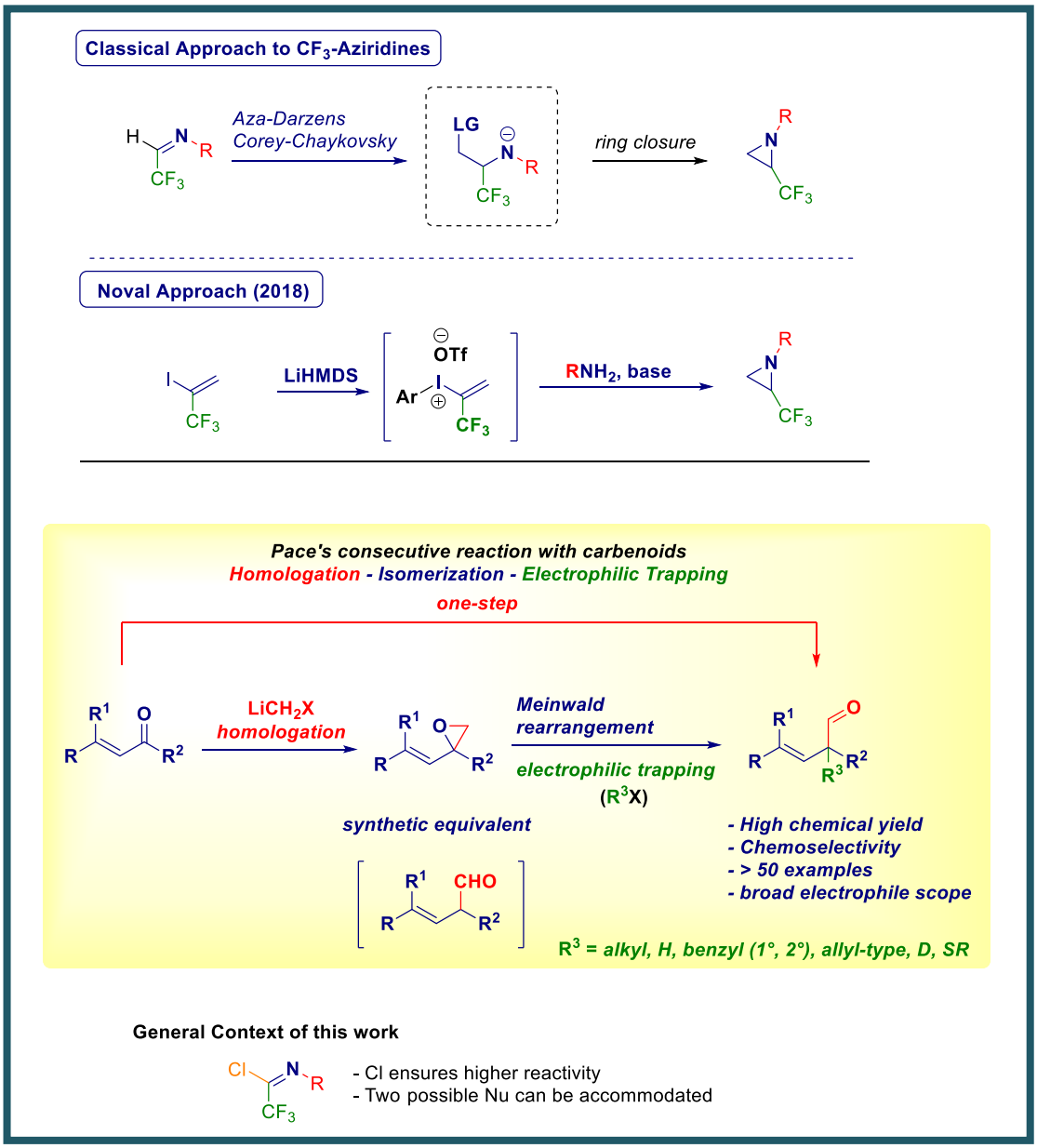

Scheme 23: Approaches to CF_3-Aziridines.

Our synthetic plan started by individuating the easily accessible chlorotrifluoroimidate as the proper imine surrogate placeholder on which conducting-targeting the bis-functionalization process. Its intrinsic higher reactivity (compared to a normal imine) conferred by the chlorine not only would ensure the smooth addition of the homologating agent but, more importantly, would be the key to switch the mechanism from a nucleophilic addition to a nucleophilic addition-elimination (*i.e.* substitution) pathway. The starting chlorotrifluoroimidate have been prepared using the synthetic procedure reported by Uneyama and coworkers (scheme 24).[320] The reaction was carried out coupling the suitable aniline with PPh_3 and trifluoroacetic acid in DCE and

CCl_4, in presence of trietylamine at reflux overnight. The so-obtained crude mixture was subjected to chromatography to afford pure compounds.

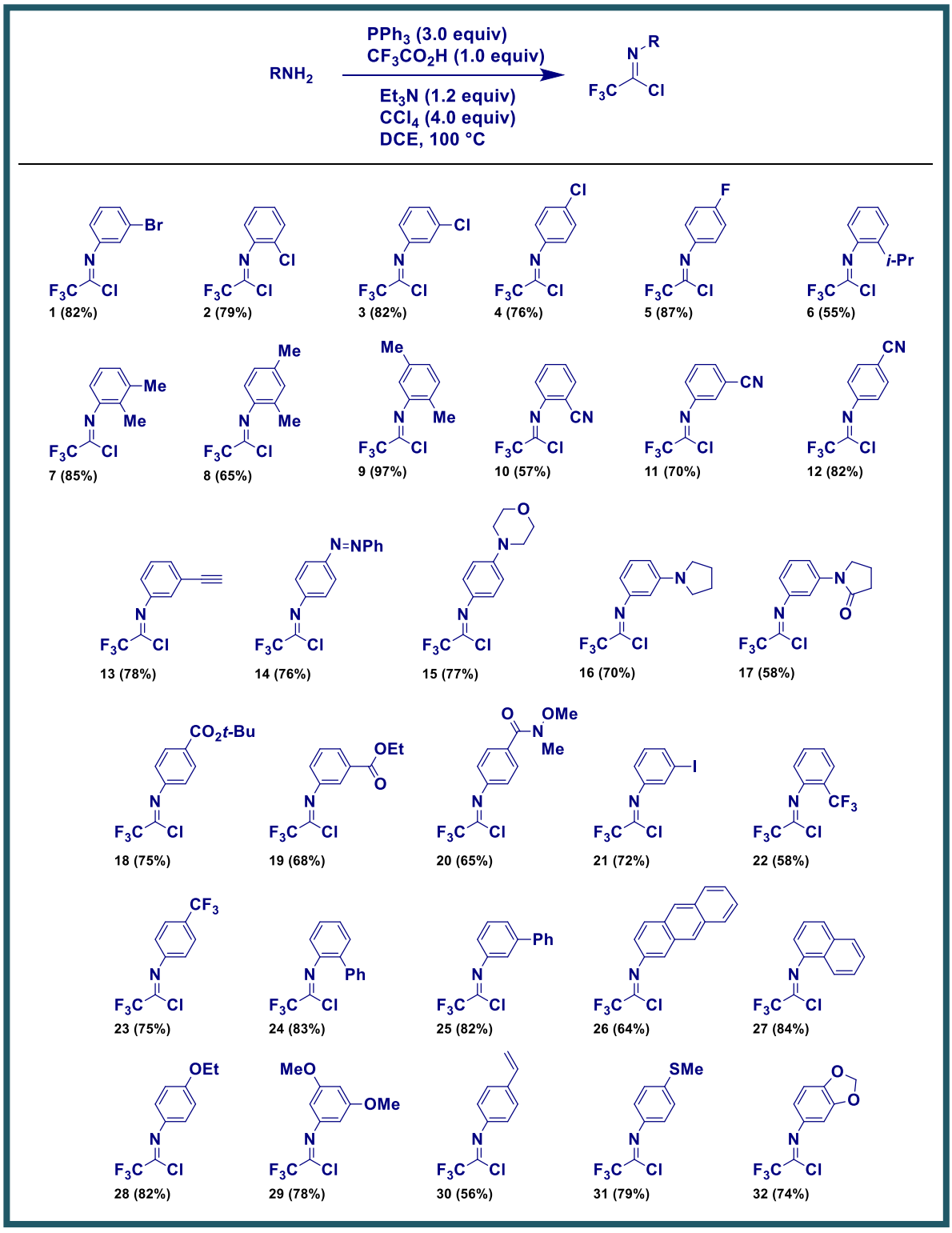

Scheme 24: Synthesis of chlorotrifluoroimidate 1-32.

We commenced our investigations reacting the electrophilic haloimidate **1** with $LiCH_2Cl$ (1.3 equiv) under standard homologation conditions: the α-chloroaziridine **33** was formed as the unique product in an excellent 90% yield. By increasing the loading of carbenoid to 1.8 equiv, the chloromethylaziridine **54** was obtained as the major product (70%) together with **33** (30%), thus confirming the initial hypothesis that **1** can act as a placeholder for two additions. Chemoselectivity could be maximized by using 2.8 equiv of $LiCH_2Cl$, therefore forming **54** as the exclusive product (table 1).

Table 1: Different homologation pathways.

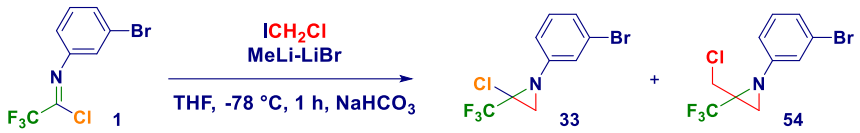

Entry	Solvent	Lithiation time (min)	$LiCH_2Cl$ equiv	Ratio **33**:**54**	Yield of **54** (%)
1	THF	60	1.3	100:0	0
2	THF	60	1.8	33:77	70
3	THF	60	2.8	0:100	91

Overall, these indications suggest the possibility to achieve with full chemocontrol three different products by simply tuning two elemental parameters: the nature of the carbenoid and the stoichiometry of the process, being the former *a condition sine qua non* to observe this reactivity. In fact, as noticed in seminal studies by Uneyama the addition of normal organometallics (*e.g.* Grignard reagents) proceeds through the simple substitution of the leaving chlorine to afford a simple CF_3-imine. Three additional aspects are worth to mention: a) employing a more stable (but less nucleophilic) magnesium carbenoid does not induce any transformation (*i.e.* full recovery of **1**); b) no concomitant Cl-Li exchange on **1** during the Barbier-conditions carbenoid generation event was noticed. c) regardless the targeted substrate, the reaction is extremely fast (completion within 1 h) in agreement with commonly observed halomethylithium-mediated chemistry for which the homologation must occur as fast as possible to ensure the stability of the reagents.[302]

With this condition in hand, we screened the scope of the reaction targeting separately the two possible class of products: α-chloroaziridines and α-chloromethylaziridines. Accordingly, by using the quasi-stoichiometric ratio a series of α-chloroaziridines (scheme 25) were accessed in high to excellent yields starting from the corresponding chlorotrifluoromethylimidates easily prepared according to the well suited Uneyama's procedure[320] (scheme 24). The protocol turned to be highly versatile and of general applicability, as documented by the structural diversity of the synthesized aziridines. The following points underline the potentialities of the methodology: 1) various substitution across the aromatic ring is permitted, without noticeable differences in the position of the decorating element; 2) no concomitant halogen-lithium exchange occurs in systems featuring analogue substituents, including bromine, chlorine or even fluorine; 3) *ortho*-substitution is not influenced by sterical factors. The excellent chemocontrol achieved during the transformation is evidenced in substrates featuring sensitive moieties to the organometallic environment. Noteworthy, nitrile-containing substrates cleanly undergo the homologation, as well as, alkynyl-, diazo or aminic ones. The formidable electrophilic behaviour of chlorotrifluoromethylimidates is showcased in the simultaneous presence of notoriously reactive functionalities to carbenoids such as esters or even a Weinreb amide.

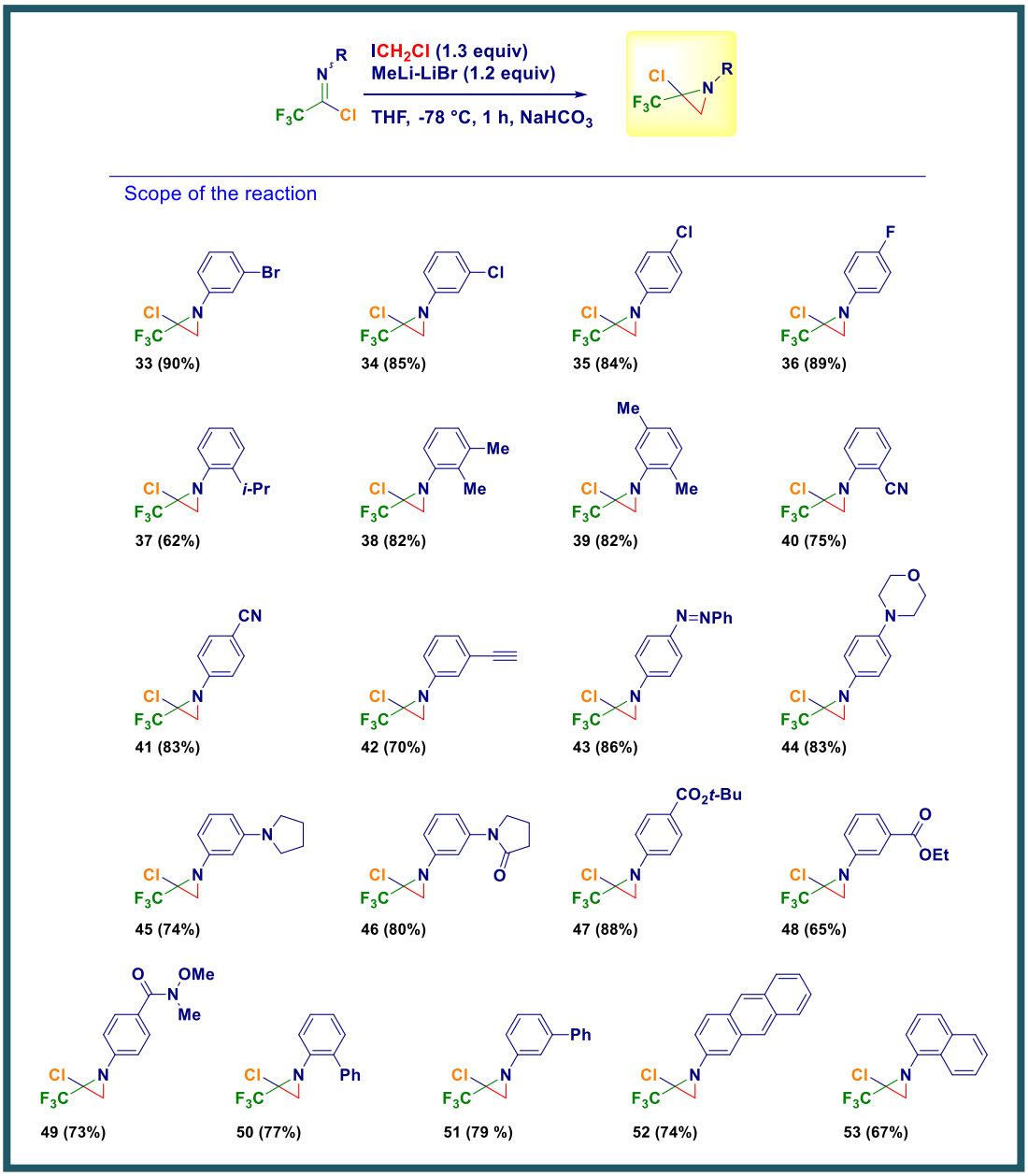

Scheme 25: Synthesis of α-chloroaziridine 33-53.

Subsequently, we addressed the more ambitious *C2* homologation to the α-halomethyl-trifluoromethylaziridines (scheme 26) by simply increasing the carbenoid, loading up to 2.8 equiv, as indicated in table 1. With much of our delight, chemoselectivity aspects emerged in C*1* homologations can be fully transferred. Halogens of different nature (including iodine or a trifluoromethyl) can be embodied into the reactive electrophiles giving exclusively the bis-homologated products. Again, sterical factors on the aromatic ring, as well as, a plethora of chemical functionalities decorating the nuclei do not interfere the efficiency. Not only an alkyne but also an alkene is tolerated: this is quite remarkable since olefins are often employed in

carbenoids-mediated homologations (Simmons-Smith-type chemistry).[265] In analogy to the above discussed examples, nitriles and esters can also be placed on the aromatic nuclei, as well as, thio-, aminic, diazo or acetal-substituted materials.

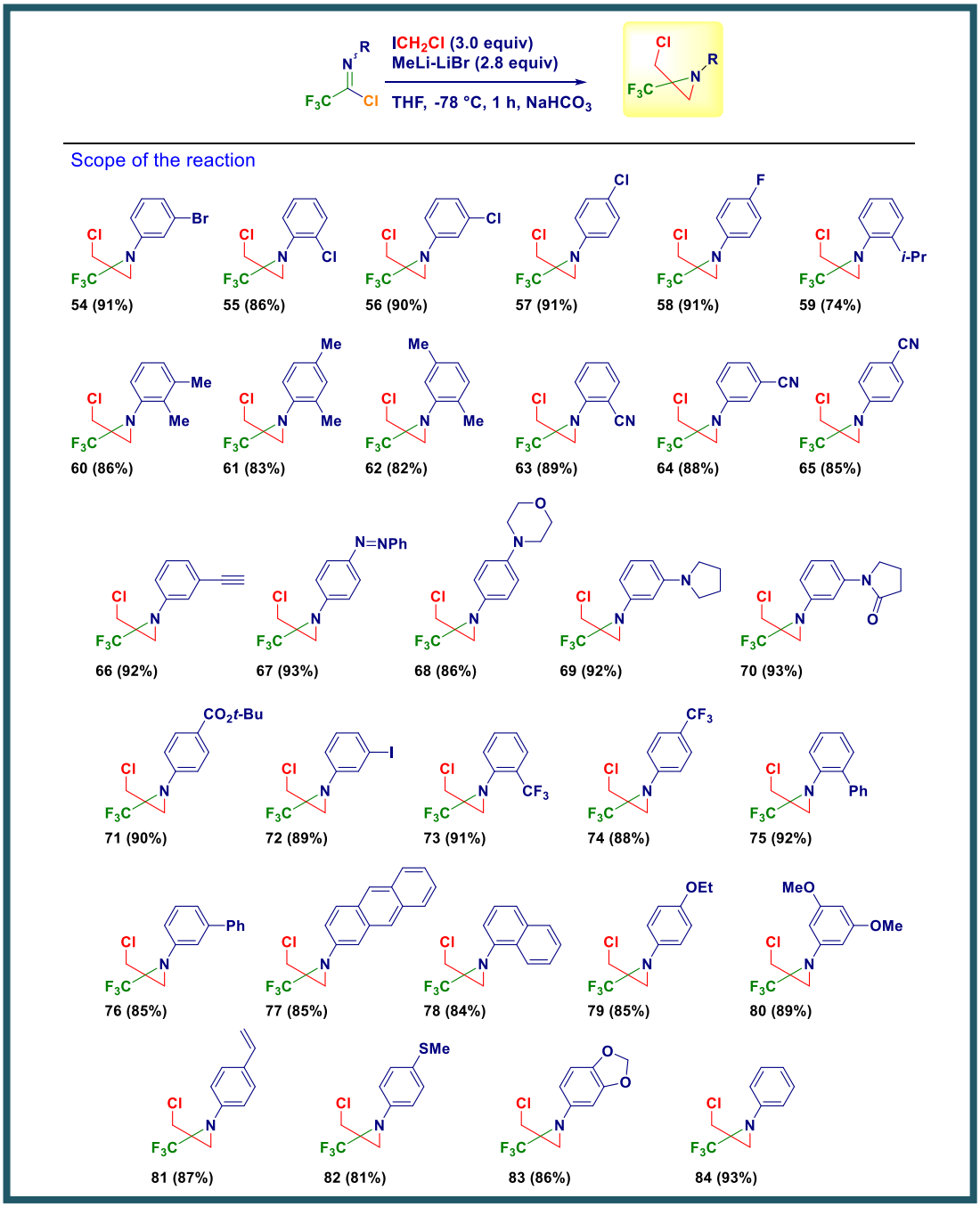

Scheme 26: Synthesis of chloromethylaziridine 54-84.

The conceptual introduction emerged from this study is further straightened by the novelty (*i.e.* unknown) of the synthesized scaffolds. Indeed, geminal substituted CF_3-aziridine are rare entities and, perhaps condensing in a very short three-carbon carbon

skeleton many electrophilic sites (namely: chloromethyl, quaternary carbon and aziridine's methylene) constitutes a formidable synthetic goal. For sake of comparison and considering the isosterical phenomena existing between aziridine and epoxides, analogous germinal trifluoromethyl-epihalohydrines – to the best of our knowledge - have not been reported (scheme 27). In this regard, the intrinsic tamed reactivity of aziridines compared to epoxides may play a crucial role in furnishing additional stability to our substrates.[317]

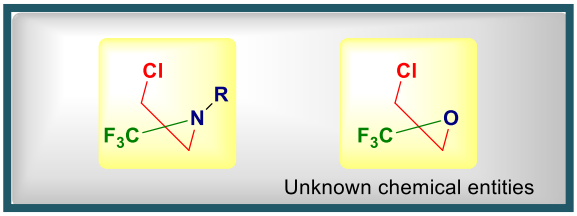

Scheme 27: CF_3-Halomethylaziridines reactivity compared to CF_3-epihalohydrins.

The mechanistic understanding of the experimentally observed transformations was pivotal to gain full insights into the tactic. The addition of the first equivalent of $LiCH_2Cl$ generates the tetrahedral intermediate in the form of a lithium amide: the metal can coordinate the inserted chlorine *via* the formation of an internal five-membered chelate with the final result of activating the methylenic unit towards the nucleophilic displacement promoted by the Li amide.[321] Overall, the *C1* homologation event – in agreement with the experimental evidence - produces the α-chloroaziridine.[317, 318]

On the other hand, the use of the homologating agent in excess (2.8 equiv) *via* a similar pathway conducts to α-chloroaziridine which undergo an internal elimination of chlorine, furnishing a highly reactive azirinium ion. Such an electrophilic species would then suffer the attack of the second equivalent of carbenoid, finally leading to α-chloromethylaziridines (scheme 28).

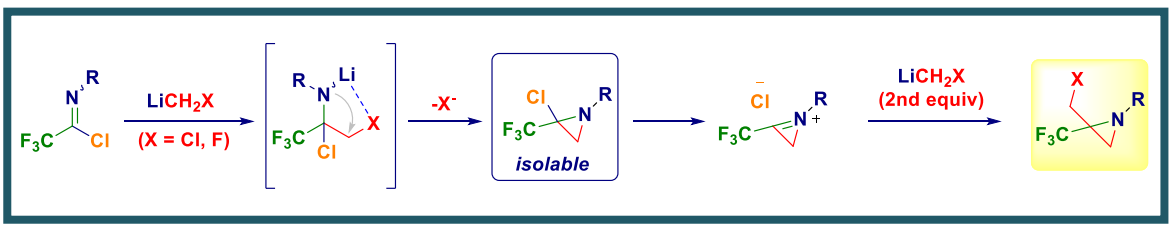

Scheme 28: Reaction mechanism.

Should such a mechanistic hypothesis valid, the addition of a second nucleophilic agent could be envisaged.

Considering our interest in fluorinated carbenoids, we designed a highly effective strategy enabling the homologation of chloro-trifluoroimidates with $LiCH_2Cl$ (*first nucleophile*), followed by a second homologation with our recently introduced $LiCH_2F$ (*second nucleophile*).[322] Pleasingly, *via* a single synthetic operation, we introduced two different carbenoids, therefore accessing in high yields the α-fluoromethylaziridines **85-91** (scheme 29). This outcome is particularly relevant from a conceptual perspective, since the addition of two different halomethylcarbenoids within the same sequence is unprecedented.

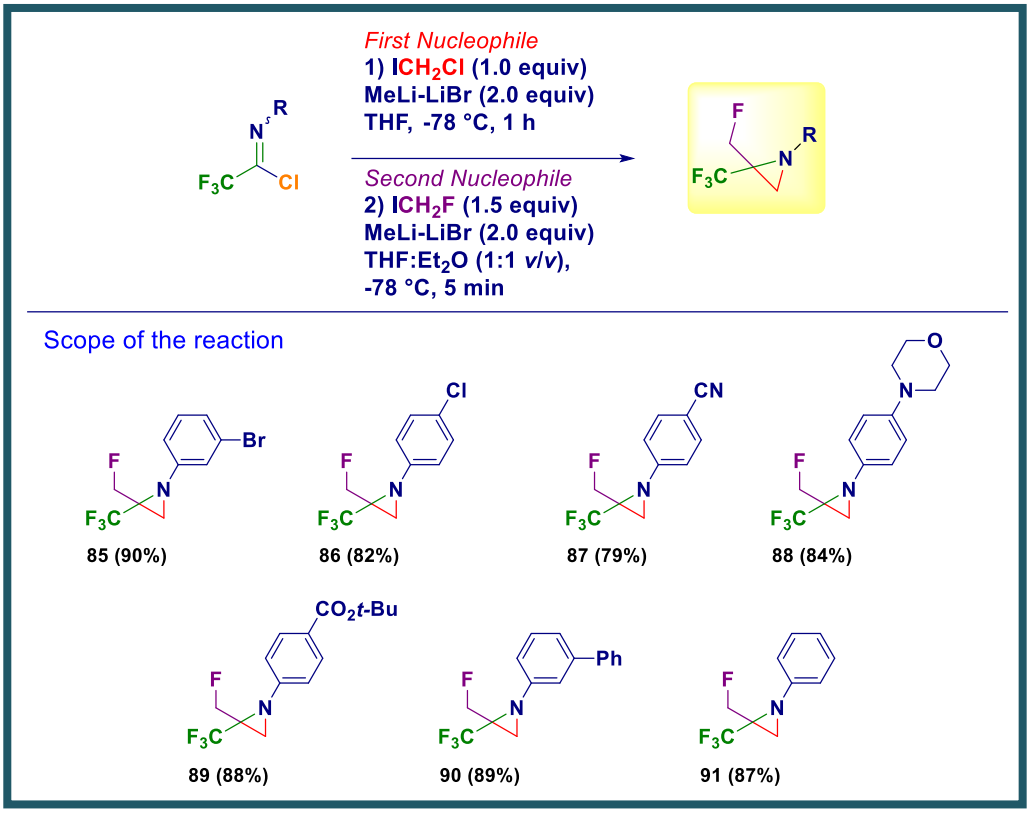

Scheme 29: Synthesis of α-fluoromethylaziridines 85-91.

2.1.1 α-Halomethyl-trifluoromethyl aziridines as useful synthons in preparative chemistry

The reactivity of these not previously known synthesized scaffolds was then evaluated with the purpose of introducing them as useful synthons in preparative chemistry. Substituents on the aromatic nuclei serve as useful platforms for selective reactions: 1) the sulfide to sulfoxide oxidation with periodic acid under Fe(III)-catalysis[323] (scheme

30a) or, 2) the Wacker-type Pd-oxidation of an alkyne to a methyl ketone[324] (scheme 30b). The latter reaction constitutes an expedient tool for preparing the carbonyl-type halomethyl-aziridine **94**.[325] The electrophilic activation of the aziridinyl ring with allyl iodide in the presence of Ag(I) enables the subsequent addition of a nucleophilic amine for the synthesis of an interesting quaternary trifluoromethyl diamine[326] (scheme 30c).

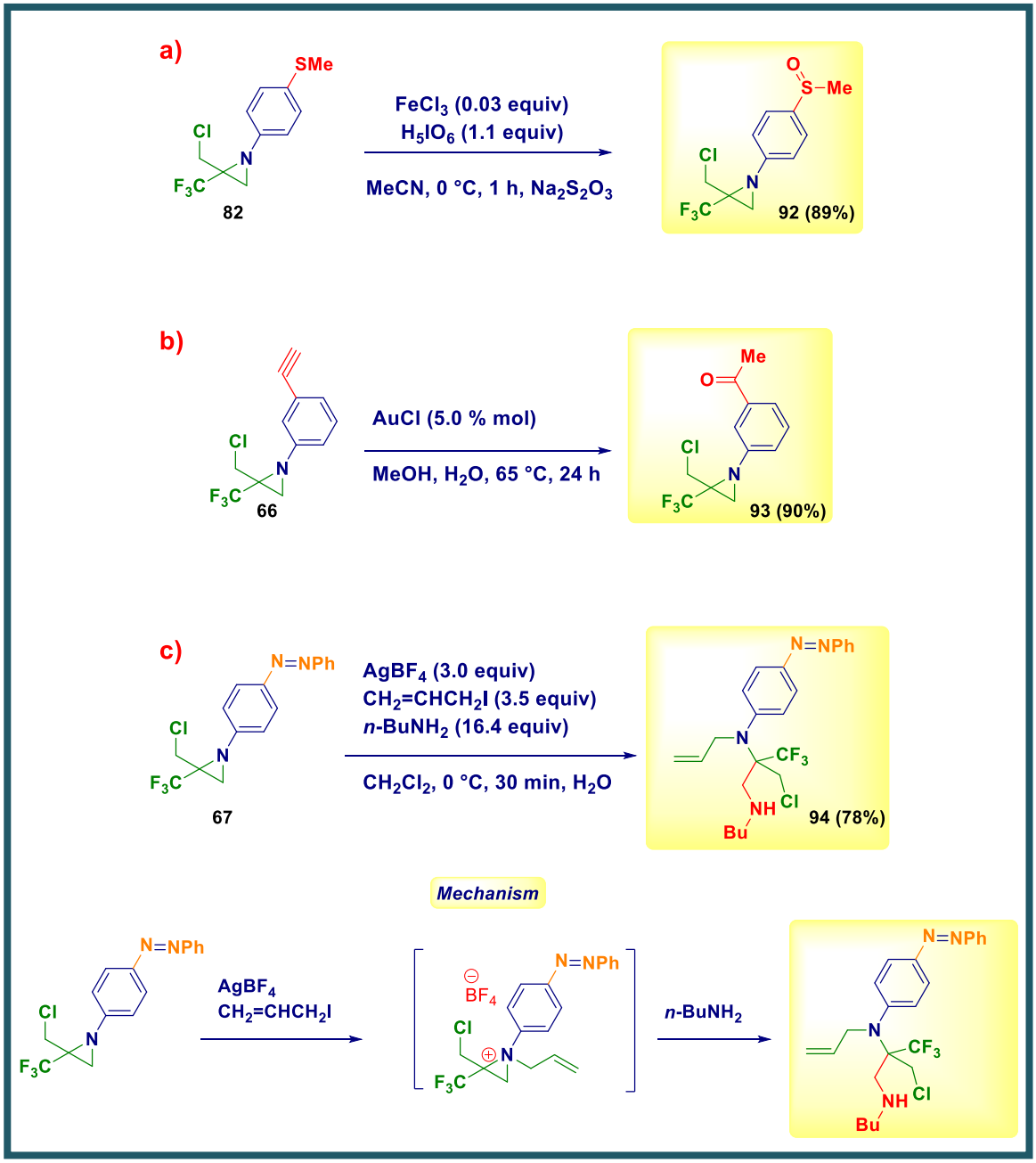

Scheme 30: α-Halomethyl-trifluoromethyl aziridines as useful synthons in preparative chemistry.

2.1.2 X ray analisys of compounds 43 and 67

X ray analisys of our compounds were performed in collaboration with Dr. A. Roller (Institute of Inorganic Chemistry, University of Vienna) and two representative examples of α-chloroaziridine (**43**) and chloromethylaziridine (**67**) respectively are dispayed in figure 3.

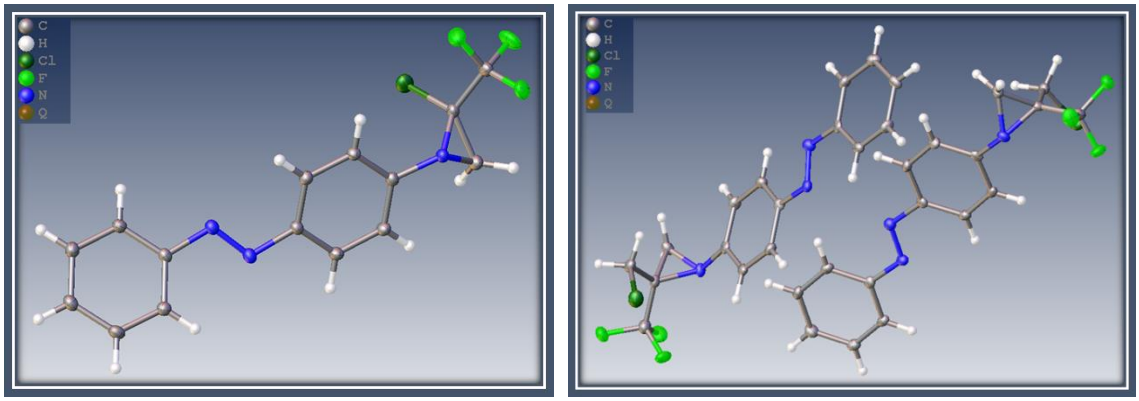

Figure 3: X ray analisys of compounds 43 and 67.

2.2 Conclusion

In summa, we have conceived a conceptually novel telescoped transformation enabling the addition of two (eventually distinct) homologating halomethyl carbenoids to electrophilic imines surrogates for the chemoselective synthesis of α-chloroaziridines and α-chloromethylaziridines, by simply selecting the nature of the carbenoid and the stoichiometry of the protocol. Robust efficiency and superb chemocontrol are uniformly observed thus, allowing a flexible and easy access to previously unkown – densely functionalized – carbon arrays.

CHAPTER 3 EXPERIMENTAL SECTION

3.1 General methods

Melting points were determined on a Reichert–Kofler hot-stage microscope and are uncorrected. Mass spectra were obtained on a Shimadzu QP 1000 instrument (EI, 70 eV) and on a Bruker maXis 4G instrument (ESI-TOF, HRMS). ^{1}H, ^{13}C, ^{19}F and ^{15}N NMR spectra were recorded with a Bruker Avance III 400 spectrometer (400 MHz for ^{1}H, 100 MHz for ^{13}C, 377 MHz for ^{19}F, 40 MHz for ^{15}N) and with a Bruker DRX spectrometer (200 MHz for ^{1}H, 50 MHz for ^{13}C) at 297 K. The center of the solvent signal was used as an internal standard which was related to TMS with δ 7.26 ppm (^{1}H in $CDCl_3$), δ 77.00 ppm (^{13}C in $CDCl_3$). ^{15}N NMR spectra were referenced against external nitromethane (0.0 ppm), ^{19}F NMR spectra by absolute referencing via *Ξ* ratio. Spin-spin coupling constants (*J*) are given in Hz. In nearly all cases, full and unambiguous assignment of all resonances was performed by combined application of standard NMR techniques, such as APT, HSQC, HMBC, COSY and NOESY experiments in collaboration with Prof. W. Holzer (Department of Pharmaceutical Chemistry, University of Vienna).

THF was distilled over Na/benzophenone. Chemicals were purchased from Sigma-Aldrich, Acros, Alfa Aesar, Fluorochem and TCI Europe, otherwise specified. Solutions were evaporated under reduced pressure with a rotary evaporator. TLC was carried out on aluminium sheets precoated with silica gel 60F254 (Macherey-Nagel, Merck); the spots were visualized under UV light (λ = 254 nm) and/or $KMnO_4$ (aq.) was used as revealing system.

3.1.1 General Procedure 1 and spectral data of Chlorotrifluoroimidates 1-32

Scheme 24 - To a solution of Ph_3P (3.0 equiv) in DCE was added CCl_4 (4.0 equiv), Et_3N (1.2 equiv) and TFA (1.0 equiv) at 0 °C and the mixture was stirred for 10 minutes. After the solution was cooled to room temperature, suitable aniline (1.0 equiv) was added. The mixture was then refluxed overnight. Solvent was removed under reduce pressure, and the residue was diluted and washed with *n*-hexane several times and filtered. The filtrate was concentrated under reduced pressure, the so-obtained crude mixture was subjected to chromatography (silica gel) to afford pure compounds.[320]

***N*-(3-Bromophenyl)-2,2,2- trifluoroethanimidoyl chloride (1)[327]**

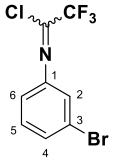

By following the General Procedure **1**, starting from **3-bromoaniline** (1000 mg, 5.8 mmol, 1.0 equiv), TFA (662 mg, 0.4 mL, 5.8 mmol, 1.0 equiv), Ph_3P (4560 mg, 17.4 mmol, 3.0 equiv), Et_3N (704 mg, 1.0 mL, 6.9 mmol, 1.2 equiv), CCl_4 (3568 mg, 2.2 mL, 23.2 mmol, 4.0 equiv) and DCE (20 mL), the desired product **1** was obtained in 82% yield (1362 mg) as a yellow oil after chromatography on silica gel (98:02 *v/v*, *n*-hexane/diethyl ether).

^{1}H NMR (400 MHz, $CDCl_3$) δ: 7.44 (m, 1H, Ph H-4), 7.31 (t, *J* = 8.0 Hz, 1H, Ph H-5), 7.26 (t, *J* = 1.9 Hz, 1H, Ph H-2), 7.02 (m, 1H, Ph H-6).

^{13}C NMR (100 MHz, $CDCl_3$) δ: 144.7 (Ph C-1), 133.8 (q, *J* = 43.4 Hz, $\underline{C}CF_3$), 130.5 (Ph C-5), 130.2 (Ph C-4), 123.4 (Ph, C-2), 122.8 (Ph C-3), 119.1 (Ph C-6), 116.7 (q, *J* = 277.4 Hz, CF_3).

^{19}F NMR (376 MHz, $CDCl_3$) δ: -71.7 (s, CF_3).

HRMS (ESI), *m/z*: calcd. for $C_8H_5BrClF_3N^+$: 285.9240 $[M+H]^+$; found: 285.9242.

***N*-(2-Chlorophenyl)-2,2,2-trifluoroethanimidoyl chloride (2)[328]**

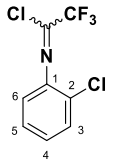

By following the General Procedure **1**, starting from **2-chloroaniline** (1000 mg, 7.8 mmol, 1.0 equiv), TFA (893 mg, 0.6 mL, 7.8 mmol, 1.0 equiv), Ph_3P (6160 mg, 23.5 mmol, 3.0 equiv), Et_3N (951 mg, 1.3 mL, 9.4 mmol, 1.2 equiv), CCl_4 (4818 mg, 3.0 mL, 31.3 mmol, 4.0 equiv) and DCE (20 mL), the desired product **2** was obtained in 79% yield (1491 mg) as a colorless oil after chromatography on silica gel (98:02 *v/v*, *n*-hexane/diethyl ether).

^{1}H NMR (400 MHz, $CDCl_3$) δ: 7.48 (dd, *J* = 8.0, 1.3 Hz, 1H, Ph H-3), 7.33 (m, 1H, Ph H-5), 7.23 (m, 1H, Ph H-4), 6.96 (dd, *J* = 7.9, 1.6 Hz, 1H, Ph H-6).

^{13}C NMR (100 MHz, $CDCl_3$) δ: 141.7 (Ph C-1), 135.9 (q, *J* = 43.6 Hz, $\underline{C}CF_3$), 130.2 (Ph C-3), 127.6 (Ph C-4), 127.4 (Ph C-5), 124.5 (Ph C-2), 120.8 (Ph C-6), 116.7 (q, *J* = 277.5 Hz, CF_3).

^{19}F NMR (376 MHz, $CDCl_3$) δ: -71.6 (s, CF_3).

HRMS (ESI), *m/z*: calcd. for $C_8H_5Cl_2F_3N^+$: 241.9746 $[M+H]^+$; found: 241.9748.

N-(3-Chlorophenyl)-2,2,2-trifluoroethanimidoyl chloride (3)[327]

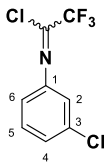

By following the General Procedure **1**, starting from **3-chloroaniline** (1000 mg, 7.8 mmol, 1.0 equiv), TFA (893 mg, 0.6 mL, 7.8 mmol, 1.0 equiv), Ph_3P (6160 mg, 23.5 mmol, 3.0 equiv), Et_3N (951 mg, 1.3 mL, 9.4 mmol, 1.2 equiv), CCl_4 (4818 mg, 3.0 mL, 31.3 mmol, 4.0 equiv) and DCE (20 mL), the desired product **3** was obtained in 82% yield (1548 mg) as a yellow oil after chromatography on silica gel (80:20 *v/v*, *n*-hexane/diethyl ether).

^{1}H NMR (400 MHz, $CDCl_3$) δ: 7.38 (t, *J* = 7.9 Hz, 1H, Ph H-5), 7.29 (ddd, *J* = 8.1, 1.9, 1.0 Hz, 1H, Ph H-4), 7.10 (m, 1H, Ph H-2), 6.96 (ddd, *J* = 7.9, 1.9, 1.0 Hz, 1H, Ph H-6).

^{13}C NMR (100 MHz, $CDCl_3$) δ: 144.6 (Ph C-1), 135.0 (Ph C-3), 133.8 (q, *J* = 43.5 Hz, $\underline{C}CF_3$), 130.3 (Ph C-5), 127.3 (Ph C-4), 120.6 (Ph C-2), 118.6 (Ph C-6), 116.7 (q, *J* = 277.5 Hz, CF_3).

^{19}F NMR (376 MHz, $CDCl_3$) δ: -71.7 (s, CF_3).

HRMS (ESI), *m/z*: calcd. for $C_8H_5Cl_2F_3N^+$: 241.9746 $[M+H]^+$; found: 241.9749.

N-(4-Chlorophenyl)-2,2,2-trifluoroethanimidoyl chloride (4)[329]

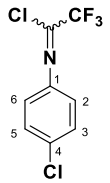

By following the General Procedure **1**, starting from **4-chloroaniline** (1000 mg, 7.8 mmol, 1.0 equiv), TFA (893 mg, 0.6 mL, 7.8 mmol, 1.0 equiv), Ph_3P (6160 mg, 23.5 mmol, 3.0 equiv), Et_3N (951 mg, 1.3 mL, 9.4 mmol, 1.2 equiv), CCl_4 (4818 mg, 3.0 mL, 31.3 mmol, 4.0 equiv) and DCE (20 mL), the desired product **4** was obtained in 76% yield (1434 mg) as a bright yellow oil after chromatography on silica gel (80:20 *v/v*, *n*-hexane/diethyl ether).

^{1}H NMR (400 MHz, $CDCl_3$) δ: 7.42 (m, 2H, Ph H-3,5), 7.08 (m, 2H, Ph H-2,6).

^{13}C NMR (100 MHz, $CDCl_3$) δ: 141.7 (Ph C-1), 133.3 (Ph C-4), 132.7 (q, *J* = 43.4 Hz, $\underline{C}CF_3$), 129.4 (Ph C-3,5), 122.3 (Ph C-2,6), 116.7 (q, *J* = 277.3 Hz, CF_3).

^{19}F NMR (376 MHz, $CDCl_3$) δ: -71.6 (s, CF_3).

HRMS (ESI), *m/z*: calcd. for $C_8H_5Cl_2F_3N^+$: 241.9746 $[M+H]^+$; found: 241.9747.

N-(4-Fluorophenyl)-2,2,2-trifluoroethanimidoyl chloride (5)[329]

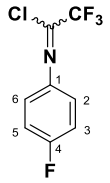

By following the General Procedure **1**, starting from **4-fluoroaniline** (1000 mg, 8.9 mmol, 1.0 equiv), TFA (689 mg, 0.7 mL, 8.9 mmol, 1.0 equiv), Ph_3P (7070 mg, 27.0 mmol, 3.0 equiv), Et_3N (1091 mg, 1.5 mL, 10.8 mmol, 1.2 equiv), CCl_4 (4148 mg, 2.6 mL, 27.0 mmol, 4.0 equiv) and DCE (20 mL), the desired product **5** was obtained in 87% yield (1746 mg) as a colorless oil after chromatography on silica gel (90:10 *v/v*, *n*-hexane/diethyl ether).

^{1}H NMR (400 MHz, $CDCl_3$) δ: 7.14 (m, 4H, Ar-H).

^{13}C NMR (100 MHz, $CDCl_3$) δ: 164.2 (Ar), 159.3 (Ar), 123.4 (Ar), 123.2 (Ar), 116.8 (CF_3), 116.4 (Ar), 115.9 (Ar).

HRMS (ESI), *m/z*: calcd. for $C_8H_5ClF_4N^+$: 224.9968 $[M+H]^+$; found: 224.9969.

2,2,2-Trifluoro-*N*-(2-isopropylphenyl)ethanimidoyl chloride (6)

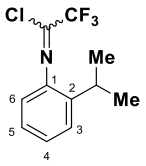

By following the General Procedure **1**, starting from **2-(propan-2-yl)aniline** (1000 mg, 7.4 mmol, 1.0 equiv), TFA (843 mg, 0.6 mL, 7.4 mmol, 1.0 equiv), Ph_3P (5800 mg, 22.2 mmol, 3.0 equiv), Et_3N (897 mg, 1.2 mL, 8.9 mmol, 1.2 equiv), CCl_4 (4547 mg, 2.9 mL, 29.6 mmol, 4.0 equiv) and DCE (20 mL), the desired product **6** was obtained in 55% yield (1016 mg) as a colorless oil after chromatography on silica gel (98:02 *v/v*, *n*-hexane/diethyl ether).

^{1}H NMR (400 MHz, $CDCl_3$) δ: 7.38 (m, 1H, Ph H-3), 7.29 (m, 1H, Ph H-4), 7.25 (m, 1H, Ph H-5), 6.91 (m, 1H, Ph H-6), 3.0 (sept, *J* = 6.9 Hz, 1H, C<u>H</u>CH_3), 1.22 (d, *J* = 6.9 Hz, 6H, CHC<u>H</u>$_3$).

^{13}C NMR (100 MHz, $CDCl_3$) δ: 141.5 (Ph C-1), 140.1 (Ph C-2), 132.0 (q, *J* = 42.9 Hz, <u>C</u>CF_3), 127.5 (Ph C-4), 126.2 (Ph C-3,5), 118.6 (Ph C-6), 116.8 (q, *J* = 277.0 Hz, CF_3), 28.8 (<u>C</u>HCH_3), 22.7 (CH<u>C</u>H_3).

^{19}F NMR (376 MHz, $CDCl_3$) δ: -71.5 (s, CF_3).

HRMS (ESI), *m/z*: calcd. for $C_{11}H_{12}ClF_3N^+$: 250.0605 $[M+H]^+$; found: 250.0603.

N-(2,3-Dimethylphenyl)-2,2,2-trifluoroethanimidoyl chloride (7)

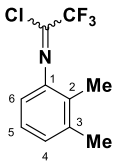

By following the General Procedure **1**, starting from **2,3-dimethylaniline** (1000 mg, 8.2 mmol, 1.0 equiv), TFA (941 mg, 0.6 mL, 8.2 mmol, 1.0 equiv), Ph_3P (6452 mg, 24.6 mmol, 3.0 equiv), Et_3N (996 mg, 1.4 mL, 9.8 mmol, 1.2 equiv), CCl_4 (5045 mg, 3.2 mL, 32.8 mmol, 4.0 equiv) and DCE (20 mL), the desired product **7** was obtained in 85% yield (1642 mg) as a colorless oil after chromatography on silica gel (80:20 *v/v*, *n*-hexane/diethyl ether).

^{1}H NMR (400 MHz, $CDCl_3$) δ: 7.18 (m, 1H, Ph H-5), 7.13 (m, 1H, Ph H-4), 6.82 (d, *J* = 7.6 Hz, 1H, Ph H-6), 2.36 (s, 3H, 3-CH_3), 2.12 (s, 3H, 2-CH_3).

^{13}C NMR (100 MHz, $CDCl_3$) δ: 142.7 (Ph C-1), 138.1 (Ph C-3), 131.9 (q, *J* = 42.7 Hz, <u>C</u>CF_3), 128.5 (Ph C-4), 127.7 (Ph C-2), 125.8 (Ph C-5), 116.8 (q, *J* = 277.0 Hz, CF_3), 116.2 (Ph C-6), 20.0 (3-CH_3), 13.8 (2-CH_3).

^{19}F NMR (376 MHz, $CDCl_3$) δ: -71.4 (s, CF_3).

HRMS (ESI), *m/z*: calcd. for $C_{10}H_{10}ClF_3N^+$: 236.0448 $[M+H]^+$; found: 236.0446.

N-(2,4-Dimethylphenyl)-2,2,2-trifluoroethanimidoyl chloride (8)[330]

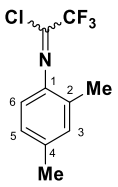

By following the General Procedure **1**, starting from **2,4-dimethylaniline** (1000 mg, 8.2 mmol, 1.0 equiv), TFA (941 mg, 0.6 mL, 8.2 mmol, 1.0 equiv), Ph_3P (6452 mg, 24.6 mmol, 3.0 equiv), Et_3N (996 mg, 1.4 mL, 9.8 mmol, 1.2 equiv), CCl_4 (5045 mg, 3.2 mL, 32.8 mmol, 4.0 equiv) and DCE (20 mL), the desired product **8** was obtained in 65% yield (1256 mg) as a yellow oil after chromatography on silica gel (80:20 *v/v*, *n*-hexane/diethyl ether).

^{1}H NMR (400 MHz, $CDCl_3$) δ: 7.13 (m, 1H, Ph H-3), 7.09 (m, 1H, Ph H-5), 6.95 (d, *J* = 8.1 Hz, 1H, Ph H-6), 2.38 (s, 3H, 4-CH_3), 2.21 (s, 3H, 2-CH_3).

^{13}C NMR (100 MHz, $CDCl_3$) δ: 139.9 (Ph C-1), 137.2 (Ph C-4), 131.5 (Ph C-3), 131.1 (q, *J* = 42.9 Hz, $\underline{C}CF_3$), 130.0 (Ph C-2), 126.9 (Ph C-5), 118.6 (Ph C-6), 116.9 (q, *J* = 276.9 Hz, CF_3), 20.9 (4-CH_3), 17.4 (2-CH_3).

^{19}F NMR (376 MHz, $CDCl_3$) δ: -71.4 (s, CF_3).

HRMS (ESI), *m/z*: calcd. for $C_{10}H_{10}ClF_3N^+$: 236.0448 $[M+H]^+$; found: 236.0446.

N-(2,5-Dimethylphenyl)-2,2,2-trifluoroethanimidoyl chloride (9)

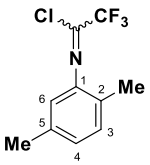

By following the General Procedure **1**, starting from **2,5-dimethylaniline** (1000 mg, 8.2 mmol, 1.0 equiv), TFA (935 mg, 0.6 mL, 8.2 mmol, 1.0 equiv), Ph_3P (6452 mg, 24.6 mmol, 3.0 equiv), Et_3N (991 mg, 1.3 mL, 9.8 mmol, 1.2 equiv), CCl_4 (5045 mg, 3.2 mL, 32.8 mmol, 4.0 equiv) and DCE (20 mL), the desired product **9** was obtained in 97% yield (1880 mg) as a colorless oil after chromatography on silica gel (*n*-hexane).

^{1}H NMR (400 MHz, $CDCl_3$) δ: 7.18 (d, *J* = 7.8 Hz, 1H, Ph H-3), 7.04 (dd, *J* = 7.8, 1.5 Hz, 1H, Ph H-4), 6.77 (d, *J* = 1.5 Hz, 1H, Ph H-6), 2.38 (s, 3H, 5-CH_3), 2.16 (s, 3H, 2-CH_3).

^{13}C NMR (100 MHz, $CDCl_3$) δ: 142.7 (Ph C-1), 136.2 (Ph C-5), 132.1 (q, *J* = 42.9 Hz, $\underline{C}CF_3$), 130.6 (Ph C-3), 127.7 (Ph C-4), 125.8 (Ph C-2), 118.7 (Ph C-6), 116.8 (q, *J* = 277.2 Hz, CF_3), 20.9 (5-CH_3), 16.9 (2-CH_3).

^{19}F NMR (376 MHz, $CDCl_3$) δ: -71.5 (s, CF_3).

HRMS (ESI), *m/z*: calcd. for $C_{10}H_{10}ClF_3N^+$: 236.0448 $[M+H]^+$; found: 236.0449.

N-(2-Cyanophenyl)-2,2,2-trifluorethanimidoyl chloride (10)[329]

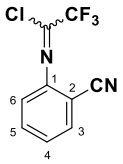

By following the General Procedure **1**, starting from **2-aminobenzonitrile** (1000 mg, 8.5 mmol, 1.0 equiv), TFA (965 mg, 0.7 mL, 8.5 mmol, 1.0 equiv), Ph_3P (6657 mg, 25.4 mmol, 3.0 equiv), Et_3N (1027 mg, 1.4 mL, 10.2 mmol, 1.2 equiv), CCl_4 (5205 mg, 3.3 mL, 33.8 mmol, 4.0 equiv) and DCE (20 mL), the desired product **10** was obtained in 57% yield (1127 mg) as a colorless oil after chromatography on silica gel (98:02 *v/v*, *n*-hexane/diethyl ether).

^{1}H NMR (400 MHz, $CDCl_3$) δ: 7.75 (m, 1H, Ph H-3), 7.68 (m, 1H, Ph H-5), 7.40 (m, 1H, Ph H-4), 7.12 (m, 1H, Ph H-6).

^{13}C NMR (100 MHz, $CDCl_3$) δ: 146.3 (Ph C-1), 137.4 (q, *J* = 44.1 Hz, $\underline{C}CF_3$), 133.7 (Ph C-5), 133.4 (Ph C-3), 127.2 (Ph C-4), 119.7 (Ph C-6), 116.5 (q, *J* = 278.2 Hz, CF_3), 115.3 (C≡N), 104.7 (Ph C-2).

^{19}F NMR (376 MHz, $CDCl_3$) δ: -71.6 (s, CF_3).

HRMS (ESI), *m/z*: calcd. for $C_9H_5ClF_3N_2^+$: 233.0088 $[M+H]^+$; found: 233.0086.

N-(3-Cyanophenyl)-2,2,2-trifluorethanimidoyl chloride (11)

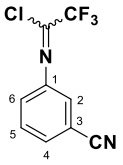

By following the General Procedure **1**, starting from **3-aminobenzonitrile** (1000 mg, 8.5 mmol, 1.0 equiv), TFA (965 mg, 0.7 mL, 8.5 mmol, 1.0 equiv), Ph_3P (6657 mg, 25.4 mmol, 3.0 equiv), Et_3N (1027 mg, 1.4 mL, 10.2 mmol, 1.2 equiv), CCl_4 (5205 mg, 3.3 mL, 33.8 mmol, 4.0 equiv) and DCE (20 mL), the desired product **11** was obtained in 70% yield (1384 mg) as a colorless oil after chromatography on silica gel (98:02 *v/v*, *n*-hexane/diethyl ether).

^{1}H NMR (400 MHz, $CDCl_3$) δ: 7.61 (m, 1H, Ph H-4), 7.58 (m, 1H, Ph H-5), 7.36 (m, 1H, Ph H-2), 7.30 (m, 1H, Ph H-6).

^{13}C NMR (100 MHz, $CDCl_3$) δ: 144.3 (Ph C-1), 135.3 (q, *J* = 43.7 Hz, $\underline{C}CF_3$), 130.7 (Ph C-4), 130.3 (Ph C-5), 124.8 (Ph C-6), 123.7 (Ph C-2), 117.7 (C≡N), 116.6 (q, *J* = 277.7 Hz, CF_3), 113.6 (Ph C-3).

^{19}F NMR (376 MHz, $CDCl_3$) δ: -71.7 (s, CF_3).

HRMS (ESI), *m/z*: calcd. for $C_9H_5ClF_3N_2^+$: 233.0088 $[M+H]^+$; found: 233.0087.

N-(4-Cyanophenyl)-2,2,2-trifluoroethanimidoyl chloride (12)[327]

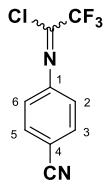

By following the General Procedure **1**, starting from **4-aminobenzonitrile** (1000 mg, 8.5 mmol, 1.0 equiv), TFA (965 mg, 0.6 mL, 8.5 mmol, 1.0 equiv), Ph_3P (6656 mg, 25.4 mmol, 3.0 equiv), Et_3N (1027 mg, 1.4 mL, 10.2 mmol, 1.2 equiv), CCl_4 (5205 mg, 3.3 mL, 33.8 mmol, 4.0 equiv) and DCE (20 mL), the desired product **12** was obtained in 82% yield (1621 mg) as a white solid (m.p.: 44-45 °C) after chromatography on silica gel (80:20 *v/v*, *n*-hexane/diethyl ether).

^{1}H NMR (400 MHz, $CDCl_3$) δ: 7.73 (m, 2H, Ph H-3,5), 7.10 (m, 2H, Ph H-2,6).

^{13}C NMR (100 MHz, $CDCl_3$) δ: 147.3 (Ph C-1), 135.3 (q, *J* = 43.9 Hz, $\underline{C}CF_3$), 133.3 (Ph C-3,5), 120.6 (Ph C-2,6), 118.0 (C≡N), 116.5 (q, *J* = 277.8 Hz, CF_3), 110.8 (Ph C-4).

^{15}N NMR (40 MHz, $CDCl_3$) δ: -53.0 (PhN).

^{19}F NMR (376 MHz, $CDCl_3$) δ: -71.8 (s, CF_3).

HRMS (ESI), *m/z*: calcd. for $C_9H_4ClF_3N_2Na^+$: 254.9907 $[M+H]^+$; found: 254.9902.

N-(3-Ethynylphenyl))-2,2,2-trifluoroethanimidoyl chloride (13)

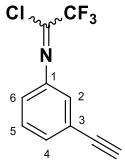

By following the General Procedure **1**, starting from **3-ethynylaniline** (1000 mg, 8.5 mmol, 1.0 equiv), TFA (969 mg, 0.6 mL, 8.5 mmol, 1.0 equiv), Ph_3P (6688 mg, 25.5 mmol, 3.0 equiv), Et_3N (1032 mg, 1.4 mL, 10.2 mmol, 1.2 equiv), CCl_4 (5230 mg, 3.3 mL, 34.0 mmol, 4.0 equiv) and DCE (20 mL), the desired product **13** was obtained in 78% yield (1535 mg) as a colorless oil after chromatography on silica gel (90:10 *v/v*, *n*-hexane/diethyl ether).

^{1}H NMR (400 MHz, $CDCl_3$) δ: 7.42 (m, 1H, Ph H-4), 7.40 (m, 1H, Ph H-5), 7.21 (m, 1H, Ph H-2), 7.06 (m, 1H, Ph H-6), 3.13 (s, 1H, C≡CH).

^{13}C NMR (100 MHz, $CDCl_3$) δ: 143.6 (Ph C-1), 133.3 (q, *J* = 43.1 Hz, $\underline{C}CF_3$), 130.9 (Ph C-4), 129.3 (Ph C-5), 123.8 (Ph C-2), 123.4 (Ph C-3), 120.9 (Ph C-6), 116.7 (q, *J* = 277.3 Hz, CF_3), 82.4 ($\underline{C}\equiv CH$), 78.4 ($C\equiv\underline{C}H$).

^{19}F NMR (376 MHz, $CDCl_3$) δ: -71.7 (s, CF_3).

HRMS (ESI), *m/z*: calcd. for $C_{10}H_6ClF_3N^+$: 232.0135 $[M+H]^+$; found: 232.0137.

2,2,2-Trifluoro-*N*-[4-(phenyldiazenyl)phenyl]ethanimidoyl chloride (14)

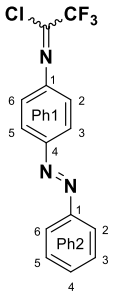

By following the General Procedure **1**, starting from **4-(phenyldiazenyl)aniline** (1000 mg, 5.1 mmol, 1.0 equiv), TFA (578 mg, 0.4 mL, 5.1 mmol, 1.0 equiv), Ph_3P (3990 mg, 15.2 mmol, 3.0 equiv), Et_3N (616 mg, 0.8 mL, 6.1 mmol, 1.2 equiv), CCl_4 (3119 mg, 2.0 mL, 20.3 mmol, 4.0 equiv) and DCE (20 mL), the desired product **14** was obtained in 76% yield (1200 mg) as an orange solid (m.p.: 75-77 °C) after chromatography on silica gel (90:10 *v/v*, *n*-hexane/diethyl ether).

^{1}H NMR (400 MHz, $CDCl_3$) δ: 8.02 (m, 2H, ArH), 7.94 (m, 1H, ArH), 7.54 (m, 3H, ArH), 7.24 (m, 3H, ArH).

^{13}C NMR (100 MHz, $CDCl_3$) δ: 152.6 (Ar), 131.3 (Ar), 129.1 (Ar), 128.8 (Ar), 123.9 (Ar), 122.9 (Ar), 121.3 (Ar), 120.5 (Ar).

HRMS (ESI), *m/z*: calcd. for $C_{14}H_{10}ClF_3N_3^+$: 311.0437 $[M+H]^+$; found: 311.0435.

2,2,2-Trifluoro-*N*-[4-(4-morpholinyl)phenyl]ethanimidoyl chloride (15)

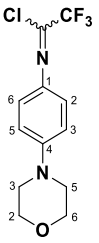

By following the General Procedure **1**, starting from **4-(morpholin-4-yl)aniline** (1000 mg, 5.6 mmol, 1.0 equiv), TFA (640 mg, 0.4 mL, 5.6 mmol, 1.0 equiv), Ph_3P (4410 mg, 16.8 mmol, 3.0 equiv), Et_3N (681 mg, 0.9 mL, 6.7 mmol, 1.2 equiv), CCl_4 (3451 mg, 2.2

mL, 22.4 mmol, 4.0 equiv) and DCE (20 mL), the desired product **15** was obtained in 77% yield (1262 mg) as a white solid (m.p.: 52-54 °C) after chromatography on silica gel (98:02 *v/v*, *n*-hexane/diethyl ether).

^{1}H NMR (400 MHz, $CDCl_3$) δ: 7.36 (m, 2H, Ph H-2,6), 6.93 (m, 2H, Ph H-3,5), 3.87 (m, 4H, morph H-2,6), 3.24 (m, 4H, morph H-3,5).

^{13}C NMR (100 MHz, $CDCl_3$) δ: 151.1 (Ph C-4), 133.8 (Ph C-1), 126.5 (q, *J* = 43.0 Hz, $\underline{C}CF_3$), 124.8 (Ph C-2,6), 117.1 (q, *J* = 276.3 Hz, CF_3), 114.8 (Ph C-3,5), 66.7 (morph C-2,6), 48.4 (morph C-3,5).

^{19}F NMR (376 MHz, $CDCl_3$) δ: -71.1 (s, CF_3).

HRMS (ESI), *m/z*: calcd. for $C_{12}H_{13}ClF_3N_2O^+$: 293.0663 $[M+H]^+$; found: 293.0665.

2,2,2-Trifluoro-*N*-[3-(1-pyrrolidinyl)phenyl]ethanimidoyl chloride (16)

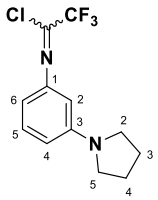

By following the General Procedure **1**, starting from **3-(pyrrolidin-1-yl)aniline** (1000 mg, 6.2 mmol, 1.0 equiv), TFA (704 mg, 0.5 mL, 6.2 mmol, 1.0 equiv), Ph_3P (4800 mg, 18.5 mmol, 3.0 equiv), Et_3N (1310 mg, 1.8 mL, 12.9 mmol, 1.2 equiv), CCl_4 (3800 mg, 2.4 mL, 24.6 mmol, 4.0 equiv) and DCE (20 mL), the desired product **16** was obtained in 70% yield (1200 mg) as a yellow oil after chromatography on silica gel (95:05 *v/v*, *n*-hexane/diethyl ether).

^{1}H NMR (400 MHz, $CDCl_3$) δ: 7.25 (m, 1H, Ph H-5), 6.48 (m, 1H, Ph H-4), 6.35 (m, 1H, Ph H-6), 6.20 (m, 1H, Ph H-2), 3.29 (m, 4H, pyrr H-2,5), 2.02 (m, 4H, pyrr H-3,4).

^{13}C NMR (100 MHz, $CDCl_3$) δ: 148.4 (Ph C-3), 144.6 (Ph C-1), 131.2 (q, *J* = 42.7 Hz, $\underline{C}CF_3$), 129.5 (Ph C-5), 116.8 (q, *J* = 277.1 Hz, CF_3), 110.5 (Ph C-4), 106.8 (Ph C-6), 103.3 (Ph C-2), 47.6 (pyrr C-2,5), 25.4 (pyrr C-3,4).

^{19}F NMR (376 MHz, $CDCl_3$) δ: -71.5 (s, CF_3).

^{15}N NMR (40 MHz, $CDCl_3$) δ: -305.9 (pyrrolidine N), PhN was not found.

HRMS (ESI), *m/z*: calcd. for $C_{12}H_{13}ClF_3N_2^+$: 277.0714 $[M+H]^+$; found: 277.0716.

2,2,2-Trifluoro-*N*-[3-(2-oxo-1-pyrrolidinyl)phenyl]ethanimidoyl chloride (17)

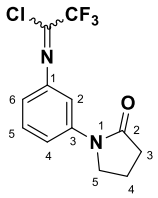

By following the General Procedure **1**, starting from **1-(3-aminophenyl)pyrrolidin-2-one** (1000 mg, 5.7 mmol, 1.0 equiv), TFA (650 mg, 0.4 mL, 5.7 mmol, 1.0 equiv), Ph_3P (4500 mg, 17.1 mmol, 3.0 equiv), Et_3N (692 mg, 0.9 mL, 6.8 mmol, 1.2 equiv), CCl_4 (3500 mg, 2.2 mL, 22.8 mmol, 4.0 equiv) and DCE (20 mL), the desired product **17** was obtained in 58% yield (961 mg) as a yellow oil after chromatography on silica gel (60:40 *v/v*, *n*-hexane/diethyl ether).

^{1}H NMR (400 MHz, $CDCl_3$) δ: 7.55 (m, 1H, Ph H-4), 7.45 (m, 1H, Ph H-2), 7.42 (m, 1H, Ph H-5), 6.86 (m, 1H, Ph H-6), 3.88 (m, 2H, pyrr H-5), 2.64 (m, 2H, pyrr H-3), 2.19 (m, 2H, pyrr H-4).

^{13}C NMR (100 MHz, $CDCl_3$) δ: 174.4 (pyrr C-2), 144.0 (Ph C-1), 140.3 (Ph C-3), 132.6 (q, *J* = 43.1 Hz, $\underline{C}CF_3$), 129.5 (Ph C-5), 118.1 (Ph C-4), 116.8 (q, *J* = 277.3 Hz, CF_3), 116.1 (Ph C-6), 111.8 (Ph C-2), 48.6 (pyrr C-5), 32.8 (pyrr C-3), 17.9 (pyrr C-4).

^{19}F NMR (376 MHz, $CDCl_3$) δ: -71.6 (s, CF_3).

^{15}N NMR (40 MHz, $CDCl_3$) δ: -247.9 (pyrrolidine N), PhN was not found.

HRMS (ESI), *m/z*: calcd. for $C_{12}H_{11}ClF_3N_2O^+$: 291.0507 $[M+H]^+$; found: 291.0504.

2-Methyl-2-propanyl 4-[(1-chloro-2,2,2-trifluoroethylidene)amino]benzoate (18)

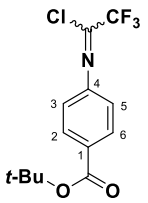

By following the General Procedure **1**, starting from ***tert*-butyl-4-aminobenzoate** (1000 mg, 5.2 mmol, 1.0 equiv), TFA (590 mg, 0.4 mL, 5.2 mmol, 1.0 equiv), Ph_3P (4068 mg, 15.5 mmol, 3.0 equiv), Et_3N (628 mg, 0.9 mL, 6.2 mmol, 1.2 equiv), CCl_4 (3181 mg, 2.0 mL, 20.7 mmol, 4.0 equiv) and DCE (20 mL), the desired product **18** was obtained in 75% yield (1200 mg) as a colorless oil after chromatography on silica gel (98:02 *v/v*, *n*-hexane/diethyl ether).

^{1}H NMR (400 MHz, $CDCl_3$) δ: 8.07 (m, 2H, Ph H-2,6), 7.05 (m, 2H, Ph H-3,5), 1.60 (s, 9H, CCH_3).

^{13}C NMR (100 MHz, $CDCl_3$) δ: 164.8 (C=O), 147.1 (Ph C-4), 133.9 (q, *J* = 43.4 Hz, $\underline{C}CF_3$), 130.7 (Ph C-1), 130.6 (Ph C-2,6), 119.7 (Ph C-3,5), 116.7 (q, *J* = 277.4 Hz, CF_3), 81.4 ($\underline{C}Me_3$), 28.2 ($C\underline{Me}_3$).

^{19}F NMR (376 MHz, $CDCl_3$) δ: -71.7 (s, CF_3).

HRMS (ESI), *m/z*: calcd. for $C_{13}H_{14}ClF_3NO_2^+$: 308.0660 $[M+H]^+$; found: 308.0662

Ethyl 3-[(1-chloro-2,2,2-trifluoroethylidone)amino]benzoate (19)

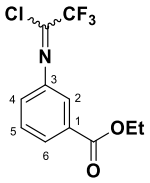

By following the General Procedure **1**, starting from **ethyl-3-aminobenzoate** (1000 mg, 0.9 mL, 6.0 mmol, 1.0 equiv), TFA (684 mg, 0.5 mL, 6.0 mmol, 1.0 equiv), Ph_3P (4700 mg, 18.0 mmol, 3.0 equiv), Et_3N (429 mg, 1.0 mL, 7.2 mmol, 1.2 equiv), CCl_4 (3692 mg, 2.3 mL, 24.0 mmol, 4.0 equiv) and DCE (20 mL), the desired product **19** was obtained in 68% yield (1140 mg) as a yellow oil after chromatography on silica gel (90:10 *v/v*, *n*-hexane/diethyl ether).

^{1}H NMR (400 MHz, $CDCl_3$) δ: 7.99 (m, 1H, Ph H-6), 7.75 (m, 1H, Ph H-2), 7.52 (m, 1H, Ph H-5), 7.25 (m, 1H, Ph H-4), 4.40 (q, *J* = 7.1 Hz, 2H, $OC\underline{H}_2CH_3$), 1.41 (t, *J* = 7.1 Hz, 3H, $OCH_2C\underline{H}_3$).

^{13}C NMR (100 MHz, $CDCl_3$) δ: 165.6 (C=O), 143.7 (Ph C-3), 133.5 (q, *J* = 43.3 Hz, $\underline{C}CF_3$), 131.8 (Ph C-1), 129.3 (Ph C-5), 128.3 (Ph C-6), 124.7 (Ph C-4), 121.5 (Ph C-2), 116.7 (q, *J* = 277.4 Hz, CF_3), 61.4 ($O\underline{C}H_2CH_3$), 14.3 ($OCH_2\underline{C}H_3$).

^{19}F NMR (376 MHz, $CDCl_3$) δ: -71.7 (s, CF_3).

^{15}N NMR (40 MHz, $CDCl_3$) δ: -52.9 (PhN).

HRMS (ESI), *m/z*: calcd. for $C_{11}H_{10}ClF_3NO_2^+$: 280.0347 $[M+H]^+$; found: 280.0345.

2,2,2-trifluoro-*N*-{4-[methoxy(methyl)carbamoyl]phenyl}ethanimidoyl chloride (20)

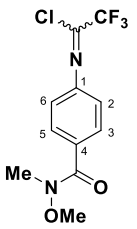

By following the General Procedure **1**, starting from **4-amino-*N*-methoxy-*N*-methylbenzamide** (600 mg, 3.3 mmol, 1.0 equiv), TFA (380 mg, 0.3 mL, 3.3 mmol, 1.0 equiv), Ph_3P (2620 mg, 10.0 mmol, 3.0 equiv), Et_3N (404 mg, 0.5 mL, 4.0 mmol, 1.2 equiv), CCl_4 (2049 mg, 1.3 mL, 13.3 mmol, 4.0 equiv) and DCE (20 mL), the desired product **20** was obtained in 65% yield (632 mg) as a yellow oil after chromatography on silica gel (50:50 *v/v*, *n*-hexane/diethyl ether).

^{1}H NMR (400 MHz, $CDCl_3$) δ: 7.80 (m, 2H, Ph H-3,5), 7.09 (m, 2H, Ph H-2,6), 3.57 (s, 3H, OCH_3), 3.38 (s, 3H, NCH_3).

HRMS (ESI), *m/z*: calcd. for $C_{11}H_{11}ClF_3N_2O_2^+$: 295.0456 $[M+H]^+$; found: 295.0458.

2,2,2-Trifluoro-*N*-(3-iodophenyl)ethanimidoyl chloride (21)[327]

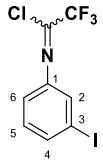

By following the General Procedure **1**, starting from **3-iodoaniline** (1000 mg, 0.5 mL, 4.6 mmol, 1.0 equiv), TFA (521 mg, 0.4 mL, 4.6 mmol, 1.0 equiv), Ph_3P (3590 mg, 13.7 mmol, 3.0 equiv), Et_3N (554 mg, 0.8 mL, 5.5 mmol, 1.2 equiv), CCl_4 (2830 mg, 1.8 mL, 18.4 mmol, 4.0 equiv) and DCE (20 mL), the desired product **21** was obtained in 72% yield (1104 mg) as a colorless oil after chromatography on silica gel (*n*-hexane).

^{1}H NMR (400 MHz, $CDCl_3$) δ: 7.64 (m, 1H, Ph H-4), 7.44 (m, 1H, Ph H-2), 7.17 (m, 1H, Ph H-5), 7.05 (m, 1H, Ph H-6).

^{13}C NMR (100 MHz, $CDCl_3$) δ: 144.5 (Ph C-1), 136.2 (Ph C-4), 133.6 (q, *J* = 43.3 Hz, $\underline{C}CF_3$), 130.6 (Ph C-5), 129.1 (Ph C-2), 119.7 (Ph C-6), 116.6 (q, *J* = 277.4 Hz, CF_3), 93.9 (Ph C-3).

^{19}F NMR (376 MHz, $CDCl_3$) δ: -71.7 (s, CF_3).

HRMS (ESI), *m/z*: calcd. for $C_8H_5ClF_3IN^+$: 333.9102 $[M+H]^+$; found: 333.9104.

2,2,2-Trifluoro-*N*-[2-(trifluoromethyl)phenyl]ethanimidoyl chloride (22)[330]

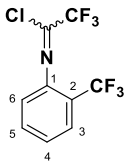

By following the General Procedure **1**, starting from **2-(trifluoromethyl)aniline** (1000 mg, 6.2 mmol, 1.0 equiv), TFA (708 mg, 0.5 mL, 6.2 mmol, 1.0 equiv), Ph_3P (4886 mg, 18.6 mmol, 3.0 equiv), Et_3N (754 mg, 1.0 mL, 7.5 mmol, 1.2 equiv), CCl_4 (3820 mg, 2.4

mL, 24.8 mmol, 4.0 equiv) and DCE (20 mL), the desired product **22** was obtained in 58% yield (991 mg) as a yellow oil after chromatography on silica gel (98:02 *v/v*, *n*-hexane/diethyl ether).

^{1}H NMR (400 MHz, $CDCl_3$) δ: 7.74 (m, 1H, Ph H-3), 7.61 (m, 1H, Ph H-5), 7.38 (m, 1H, Ph H-4), 6.96 (m, Ph H-6).

^{13}C NMR (100 MHz, $CDCl_3$) δ: 142.2 (Ph H-1), 136.1 (q, *J* = 43.4 Hz, $\underline{C}CF_3$), 132.7 (Ph C-5), 126.8 (q, *J* = 5.0 Hz, Ph C-3), 126.5 (Ph C-4), 123.0 (q, *J* = 273.1 Hz, $PhCF_3$), 120.8 (q, *J* = 31.6 Hz, Ph C-2), 119.3 (Ph C-6), 116.5 (q, *J* = 277.7 Hz, CF_3).

^{19}F NMR (376 MHz, $CDCl_3$) δ: -72.0 (s, CF_3).

HRMS (ESI), *m/z*: calcd. for $C_9H_5ClF_6N^+$: 276.0009 $[M+H]^+$; found: 276.0012.

2,2,2-Trifluoro-*N*-[4-(trifluoromethyl)phenyl]ethanimidoyl chloride (23)[331]

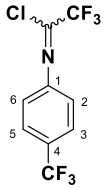

By following the General Procedure **1**, starting from **4-(trifluoromethyl)aniline** (1000 mg, 6.2 mmol, 1.0 equiv), TFA (707 mg, 0.5 mL, 6.2 mmol, 1.0 equiv), Ph_3P (4878 mg, 18.6 mmol, 3.0 equiv), Et_3N (753 mg, 1.0 mL, 7.4 mmol, 1.2 equiv), CCl_4 (3815 mg, 2.4 mL, 24.8 mmol, 4.0 equiv) and DCE (20 mL), the desired product **23** was obtained in 75% yield (1277 mg) as a yellow oil after chromatography on silica gel (80:20 *v/v*, *n*-hexane/diethyl ether).

^{1}H NMR (400 MHz, $CDCl_3$) δ: 7.71 (m, 2H, Ph H-3,5), 7.13 (m, 2H, Ph H-2,6).

^{13}C NMR (100 MHz, $CDCl_3$) δ: 146.7 (Ph C-1), 134.7 (q, *J* = 43.6 Hz, $\underline{C}CF_3$), 129.2 (q, *J* = 33.0 Hz, Ph C-4), 126.6 (q, *J* = 3.7 Hz, Ph C-3,5), 123.8 (q, *J* = 272.0 Hz, $PhCF_3$), 120.3 (Ph C-2), 116.6 (q, *J* = 277.6 Hz, CF_3).

^{19}F NMR (376 MHz, $CDCl_3$) δ: -71.8 (s, CF_3), -62.5 (s, $PhCF_3$).

HRMS (ESI), *m/z*: calcd. for $C_9H_5ClF_6N^+$: 276.0009 $[M+H]^+$; found: 276.0007.

N-(2-Biphenylyl)-2,2,2-trifluoroethanimidoyl chloride (24)[332]

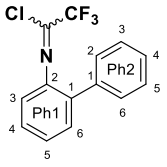

By following the General Procedure **1**, starting from **biphenyl-2-amine** (1000 mg, 5.9 mmol, 1.0 equiv), TFA (674 mg, 0.5 mL, 5.9 mmol, 1.0 equiv), Ph_3P (4640 mg, 17.7 mmol, 3.0 equiv), Et_3N (716 mg, 0.1 mL, 7.1 mmol, 1.2 equiv), CCl_4 (3630 mg, 2.3 mL, 23.6 mmol, 4.0 equiv) and DCE (20 mL), the desired product **24** was obtained in 83% yield (1389 mg) as a yellow oil after chromatography on silica gel (98:02 *v/v*, *n*-hexane/diethyl ether).

^{1}H NMR (400 MHz, $CDCl_3$) δ: 7.53 (m, 1H, Ph1 H-6), 7.45 (m, 3H, Ph1 H-4, Ph2 H-3,5), 7.41 (m, 1H, Ph1 H-5), 7.40 (m, 3H, Ph2 H-2,4,6), 7.04 (m, 1H, Ph1 H-3).

^{13}C NMR (100 MHz, $CDCl_3$) δ: 141.8 (Ph1 C-2), 138.0 (Ph2 C-1), 133.1 (Ph1 C-1), 133.0 (q, *J* = 43.2 Hz, $\underline{C}CF_3$), 130.6 (Ph1 C-6), 129.0 (Ph2 C-2,6), 128.2 (Ph2 C-3,5), 128.0 (Ph1 C-4), 127.6 (Ph2 C-4), 127.1 (Ph1 C-5), 119.1 (Ph1 C-3), 116.6 (q, *J* = 277.4 Hz, CF_3).

^{15}N NMR (40 MHz, $CDCl_3$) δ: -48.6 (PhN).

^{19}F NMR (376 MHz, $CDCl_3$) δ: -71.7 (s, CF_3).

HRMS (ESI), *m/z*: calcd. for $C_{14}H_{10}ClF_3N^+$: 284.0448 $[M+H]^+$; found: 284.0446.

N-(3-Biphenylyl)-2,2,2-trifluoroethanimidoyl chloride (25)

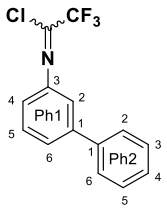

By following the General Procedure **1**, starting from **biphenyl-3-amine** (1000 mg, 5.9 mmol, 1.0 equiv), TFA (674 mg, 0.5 mL, 5.9 mmol, 1.0 equiv), Ph_3P (4600 mg, 17.7 mmol, 3.0 equiv), Et_3N (1254 mg, 1.7 mL, 12.4 mmol, 1.2 equiv), CCl_4 (3630 mg, 2.3 mL, 23.6 mmol, 4.0 equiv) and DCE (20 mL), the desired product **25** was obtained in 82% yield (1372 mg) as a yellow oil after chromatography on silica gel (95:05 *v/v*, *n*-hexane/diethyl ether).

^{1}H NMR (400 MHz, $CDCl_3$) δ: 7.74 (m, 2H, Ph2 H-2,6), 7.66 (m, 1H, Ph1 H-6), 7.61 (m, 3H, Ph1 H-5, Ph2 H-3,5), 7.54 (m, 1H, Ph2 H-4), 7.50 (m, 1H, Ph1 H-2), 7.24 (m, 1H, Ph1 H-4).

^{13}C NMR (100 MHz, $CDCl_3$) δ: 143.9 (Ph1 C-3), 142.4 (Ph1 C-1), 139.9 (Ph2 C-1), 132.1 (q, *J* = 43.1 Hz, $\underline{C}CF_3$), 129.5 (Ph1 C-5), 128.8 (Ph2 C-3,5), 127.8 (Ph2 C-4), 127.1 (Ph2 C-2,6), 126.0 (Ph2 C-6), 119.4 (Ph2 C-2), 119.2 (Ph2 C-4), 117.0 (q, *J* = 277.1 Hz, CF_3).

^{19}F NMR (376 MHz, $CDCl_3$) δ: -71.3 (s, CF_3).

^{15}N NMR (40 MHz, $CDCl_3$) δ: -51.3 (PhN).

HRMS (ESI), *m/z*: calcd. for $C_{14}H_{10}ClF_3N^+$: 284.0448 $[M+H]^+$; found: 284.0446.

N-(2-Anthryl)-2,2,2-trifluoroethanimidoyl chloride (26)

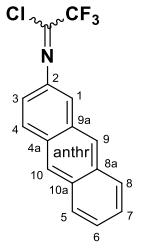

By following the General Procedure **1**, starting from **anthracen-2-amine** (1000 mg, 5.2 mmol, 1.0 equiv), TFA (590 mg, 0.4 mL, 5.2 mmol, 1.0 equiv), Ph_3P (4068 mg, 15.5 mmol, 3.0 equiv), Et_3N (628 mg, 0.9 mL, 6.2 mmol, 1.2 equiv), CCl_4 (3181 mg, 2.0 mL, 20.7 mmol, 4.0 equiv) and DCE (20 mL), the desired product **26** was obtained in 64% yield (1024 mg) as a yellow solid (m.p.: 135-137 °C) after chromatography on silica gel (98:02 *v/v*, *n*-hexane/diethyl ether).

^{1}H NMR (400 MHz, $CDCl_3$) δ: 8.45 (m, 1H, anthr H-10), 8.44 (m, 1H, anthr H-9), 8.08 (d, *J* = 9.0 Hz, 1H, anthr H-4), 8.01 (m, 2H, anthr H-5,8), 7.73 (d, *J* = 2.0 Hz, 1H, anthr H-1), 7.50 (m, 2H, anthr H-6,7), 7.28 (dd, *J* = 9.0, 2.0 Hz, 1H, anthr H-3).

^{13}C NMR (100 MHz, $CDCl_3$) δ: 140.2 (anthr C-2), 132.3 (anthr C-8a), 132.1 (anthr C-10a), 131.0 (anthr C-9a), 130.2 (anthr C-4a), 129.7 (anthr C-4), 128.2 (anthr C-8), 128.0 (anthr C-5), 126.9 (anthr C-9), 126.5 (anthr C-10), 126.0 (anthr C-7), 125.9 (anthr C-6), 120.2 (anthr C-3), 118.6 (anthr C-1), 116.9 (q, *J* = 277.2 Hz, CF_3).

^{19}F NMR (376 MHz, $CDCl_3$) δ: -71.4 (s, CF_3).

HRMS (ESI), *m/z*: calcd. for $C_{16}H_{10}ClF_3N^+$: 308.0448 $[M+H]^+$; found:308.0446.

2,2,2,-Trifluoro-*N*-(1-naphthalenyl)ethanimidoyl chloride(27)[327]

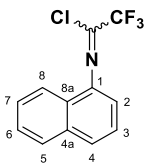

By following the General Procedure **1**, starting from **naphtalen-1-amine** (1000 mg, 6.9 mmol, 1.0 equiv), TFA (796 mg, 0.5 mL, 6.9 mmol, 1.0 equiv), Ph_3P (5430 mg, 20.7 mmol, 3.0 equiv), Et_3N (838 mg, 1.2 mL, 8.3 mmol, 1.2 equiv), CCl_4 (4245 mg, 2.6 mL, 27.6 mmol, 4.0 equiv) and DCE (20 mL), the desired product **27** was obtained in 84% yield (1500 mg) as a yellow oil after chromatography on silica gel (98:02 *v/v*, *n*-hexane/diethyl ether).

^{1}H NMR (400 MHz, $CDCl_3$) δ: 7.92 (m, 1H, naphth H-5), 7.91 (m, 1H, naphth H-8), 7.84 (m, 1H, naphth H-4), 7.60 (m, 1H, naphth H-6), 7.59 (m, 1H, naphth H-7), 7.54 (m, 1H, naphth H-3), 7.24 (m, 1H, naphth H-2).

^{13}C NMR (100 MHz, $CDCl_3$) δ: 139.7 (naphth C-1), 133.9 (naphth C-4a), 132.9 (q, *J* = 43.0 Hz, $\underline{C}CF_3$), 128.1 (naphth C-5), 127.7 (naphth C-4), 126.8 (naphth C-6), 126.7 (naphth C-7), 126.2 (naphth C-8a), 125.1 (naphth C-3), 122.7 (naphth C-8), 117.0 (q, *J* = 277.3 Hz, CF_3), 115.1 (naphtha C-2).

^{19}F NMR (376 MHz, $CDCl_3$) δ: -71.1 (s, CF_3).

^{15}N NMR (40 MHz, $CDCl_3$) δ: -54.3 (PhN).

HRMS (ESI), *m/z*: calcd. for $C_{12}H_8ClF_3N^+$: 258.0292 $[M+H]^+$; found: 258.0294.

N-(4-Ethoxyphenyl)-2,2,2-trifluoroethanimidoyl chloride (28)

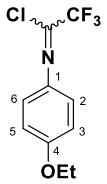

By following the General Procedure **1**, starting from **4-ethoxyaniline** (1000 mg, 7.3 mmol, 1.0 equiv), TFA (832 mg, 0.6 mL, 7.3 mmol, 1.0 equiv), Ph_3P (5744 mg, 21.9 mmol, 3.0 equiv), Et_3N (886 mg, 1.2 mL, 8.8 mmol, 1.2 equiv), CCl_4 (4491 mg, 2.8 mL, 29.2 mmol, 4.0 equiv) and DCE (20 mL), the desired product **28** was obtained in 82% yield (1500 mg) as a bright yellow oil after chromatography on silica gel (80:20 *v/v*, *n*-hexane/diethyl ether).

^{1}H NMR (400 MHz, $CDCl_3$) δ: 7.31 (m, 2H, Ph H-2,6), 6.95 (m, 2H, Ph H-3,5), 4.07 (q, *J* = 7.0 Hz, 2H, $OC\underline{H}_2CH_3$), 1.44 (t, *J* = 7.0 Hz, 3H, $OCH_2C\underline{H}_3$).

^{13}C NMR (100 MHz, $CDCl_3$) δ: 159.0 (Ph C-4), 135.2 (Ph C-1), 127.9 (q, *J* = 43.1 Hz, $\underline{C}CF_3$), 124.4 (Ph C-2,6), 117.0 (q, *J* = 276.6 Hz, CF_3), 114.7 (Ph C-3,5), 63.8 ($O\underline{C}H_2CH_3$), 14.7 ($OCH_2\underline{C}H_3$).

^{19}F NMR (376 MHz, $CDCl_3$) δ: -71.3 (s, CF_3).

HRMS (ESI), *m/z*: calcd. for $C_{10}H_{10}ClF_3NO^+$: 252.0398 $[M+H]^+$; found: 252.0399.

N-(3,5-Dimethoxyphenyl)-2,2,2- trifluoroethanimidoyl chloride (29)

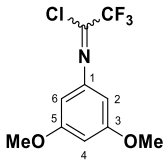

By following the General Procedure **1**, starting from **3,5-dimethoxyaniline** (1000 mg, 6.5 mmol, 1.0 equiv), TFA (744 mg, 0.5 mL, 6.5 mmol, 1.0 equiv), Ph_3P (5130 mg, 19.6 mmol, 3.0 equiv), Et_3N (792 mg, 1.1 mL, 7.8 mmol, 1.2 equiv), CCl_4 (4011 mg, 2.5 mL, 26.1 mmol, 4.0 equiv) and DCE (20 mL), the desired product **29** was obtained in 78% yield (1357 mg) as an orange solid (m.p.: 76-78 °C) after chromatography on silica gel (90:10 *v/v*, *n*-hexane/diethyl ether).

^{1}H NMR (400 MHz, $CDCl_3$) δ: 6.40 (t, *J* = 2.2 Hz, 1H, Ph H-4), 6.22 (d, *J* = 2.2 Hz, 2H, Ph H-2,6), 3.79 (s, 6H, OCH_3).

^{13}C NMR (100 MHz, $CDCl_3$) δ: 161.2 (Ph C-3,5), 145.3 (Ph C-1), 132.5 (q, *J* = 43.0 Hz, $\underline{C}CF_3$), 116.8 (q, *J* = 277.2 Hz, CF_3), 99.1 (Ph C-4), 98.4 (Ph C-2,6), 55.3 (OCH_3).

^{19}F NMR (376 MHz, $CDCl_3$) δ: -71.7 (s, CF_3).

HRMS (ESI), *m/z*: calcd. for $C_{10}H_{10}ClF_3NO_2^+$: 268.0347 $[M+H]^+$; found: 268.0345.

N-(4-Ethenylphenyl)-2,2,2-trifluoroethanimidoyl chloride (30)

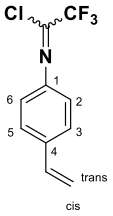

By following the General Procedure **1**, starting from **4-ethenylaniline** (1000 mg, 8.4 mmol, 1.0 equiv), TFA (957 mg, 0.6 mL, 8.4 mmol, 1.0 equiv), Ph_3P (6600 mg, 25.2 mmol, 3.0 equiv), Et_3N (1019 mg, 1.4 mL, 10.1 mmol, 1.2 equiv), CCl_4 (5168 mg, 3.2 mL, 33.6 mmol, 4.0 equiv) and DCE (20 mL), the desired product **30** was obtained in 56% yield (1099 mg) as an orange oil after chromatography on silica gel (90:10 *v/v*, *n*-hexane/diethyl ether).

^{1}H NMR (400 MHz, $CDCl_3$) δ: 7.49 (m, 2H, Ph H-3,5), 7.13 (m, 2H, Ph H-2,6), 6.74 (dd, *J* = 17.6, 10.9 Hz, 1H, $C\underline{H}=CH_2$), 5.81 (d, *J* = 17.6 Hz, 1H, $CH=C\underline{H}_2$ trans), 5.33 (d, *J* = 10.9 Hz, 1H, $CH=C\underline{H}_2$ cis).

^{13}C NMR (100 MHz, $CDCl_3$) δ: 142.5 (Ph C-1), 137.1 (Ph C-4), 135.8 (<u>C</u>H=CH_2), 131.4 (q, *J* = 43.1 Hz, <u>C</u>CF_3), 126.9 (Ph C-3,5), 121.3 (Ph C-2,6), 116.8 (q, *J* = 277.1 Hz, CF_3), 114.8 (CH=<u>C</u>H_2).

^{15}N NMR (40 MHz, $CDCl_3$) δ: -53.3 (PhN).

^{19}F NMR (376 MHz, $CDCl_3$) δ: -71.5 (s, CF_3).

HRMS (ESI), *m/z*: calcd. for $C_{10}H_8ClF_3N^+$: 234.0292 $[M+H]^+$; found: 234.0294.

2,2,2-Trifluoro-*N*-[4-(methylsulfanyl)phenyl]ethanimidoyl chloride (31)

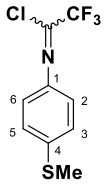

By following the General Procedure **1**, starting from **4-(methylsulfanyl)aniline** (1000 mg, 7.2 mmol, 1.0 equiv), TFA (891 mg, 0.5 mL, 7.2 mmol, 1.0 equiv), Ph_3P (5665 mg, 21.6 mmol, 3.0 equiv), Et_3N (874 mg, 1.2 mL, 8.6 mmol, 1.2 equiv), CCl_4 (4430 mg, 2.8 mL, 28.8 mmol, 4.0 equiv) and DCE (20 mL), the desired product **31** was obtained in 79% yield (1443 mg) as a white solid (m.p.:124-125 °C) after chromatography on silica gel (80:20 *v/v*, *n*-hexane/diethyl ether).

^{1}H NMR (400 MHz, $CDCl_3$) δ: 7.30 (m, 2H, Ph H-3,5), 7.15 (m, 2H, Ph H-2,6), 2.51 (s, 3H, SCH_3).

^{13}C NMR (100 MHz, $CDCl_3$) δ: 139.8 (Ph C-1), 139.0 (Ph C-4), 130.6 (q, *J* = 43.0 Hz, <u>C</u>CF_3), 126.7 (Ph C-3,5), 122.2 (Ph C-2,6), 116.9 (q, *J* = 276.9 Hz, CF_3), 15.6 (SCH_3).

^{19}F NMR (376 MHz, $CDCl_3$) δ: -71.4 (s).

HRMS (ESI), *m/z*: calcd. for $C_9H_8ClF_3N^+$: 254.0013 $[M+H]^+$; found: 254.0015.

***N*-(1,3-Benzodioxol-5-yl)-2,2,2-trifluoroethanimidoyl chloride (32)**

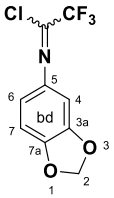

By following the General Procedure **1**, starting from **1,3-benzodioxol-5-amine** (1000 mg, 7.3 mmol, 1.0 equiv), TFA (832 mg, 0.6 mL, 7.3 mmol, 1.0 equiv), Ph_3P (5700 mg, 21.9 mmol, 3.0 equiv), Et_3N (886 mg, 1.2 mL, 8.8 mmol, 1.2 equiv), CCl_4 (4492 mg, 2.8

mL, 29.2 mmol, 4.0 equiv) and DCE (20 mL), the desired product **32** was obtained in 74% yield (1359 mg) as a colorless oil after chromatography on silica gel (90:10 *v/v*, *n*-hexane/diethyl ether).

^{1}H NMR (400 MHz, $CDCl_3$) δ: 6.88 (d, *J* = 2.0 Hz, 1H, bd H-4), 6.86 (d, *J* = 8.3 Hz, 1H, bd H-7), 6.80 (dd, *J* = 8.3, 2.0 Hz, 1H, bd H-6), 6.03 (s, 2H, CH_2).

^{13}C NMR (100 MHz, $CDCl_3$) δ: 148.1 (bd C-3a), 147.6 (bd C-7a), 136.6 (bd C-5), 128.9 (q, *J* = 43.1 Hz, $\underline{C}CF_3$), 117.0 (bd C-6), 116.9 (q, *J* = 277.0 Hz, CF_3), 108.3 (bd C-7), 103.4 (bd C-4), 101.8 (bd C-2).

^{19}F NMR (376 MHz, $CDCl_3$) δ: -71.3 (s, CF_3).

HRMS (ESI), *m/z*: calcd. for $C_9H_6ClF_3NO_2^+$: 252.0034 $[M+H]^+$; found: 252.0036.

3.1.2 General Procedure 2 and spectral data of Chloroaziridines 33-53

Scheme 25- To a cooled (-78 °C) solution of trifluoromethylchloroimidate (1.0 equiv) in dry THF was added chloroiodomethane (1.3 equiv). After 2 min, an ethereal solution of MeLi-LiBr (1.2 equiv, 1.5 M) was added dropwise, using a syringe pump (flow: 0.200 mL/min). The resulting solution was stirred for 1 h. Then 10% aq solution $NaHCO_3$ (2 mL/mmol substrate) was added and the reaction mixture was extracted with Et_2O (2 x 5 mL) and washed with water (5 mL) and brine (10 mL). The organic phase was dried over anhydrous Na_2SO_4, filtered and, after removal of the solvent under reduced pressure, the so-obtained crude mixture was subjected to chromatography (neutral alumina BG2) to afford pure compounds.

1-(3-Bromophenyl)-2-chloro-2-(trifluoromethyl)aziridine (33)

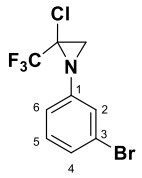

By following the General Procedure **2**, starting from ***N*-(3-bromophenyl)-2,2,2-trifluoroethanimidoyl chloride** (400 mg, 1.4 mmol, 1.0 equiv), ICH_2Cl (321 mg, 0.1 mL, 1.8 mmol, 1.3 equiv), MeLi-LiBr complex (1.5 M, 1.1 mL, 1.7 mmol, 1.2 equiv) and THF (8 mL), the desired product **33** was obtained in 90% yield (379 mg) as a yellow oil after chromatography on neutral alumina BG2 (*n*-hexane).

^{1}H NMR (400 MHz, $CDCl_3$) δ: 7.28 (ddd, *J* = 8.0, 1.9, 1.0 Hz, 1H, Ph H-4), 7.20 (t, *J* = 8.0 Hz, 1H, Ph H-5), 7.10 (t, *J* = 2.0 Hz, 1H, Ph H-2), 6.90 (ddd, J = 8.0, 2.1, 1.0 Hz, 1H, Ph H-6), 3.01 (s, 1H, NCH_2), 2.49 (q, *J* = 0.9 Hz, 1H, NCH_2).

^{13}C NMR (100 MHz, $CDCl_3$) δ: 145.9 (Ph C-1), 130.3 (Ph C-5), 127.6 (Ph C-4), 123.9 (Ph C-2), 122.6 (Ph C-3), 121.2 (q, *J* = 274.9 Hz, CF_3), 119.8 (Ph C-6), 56.8 ($\underline{C}CF_3$), 37.1 (NCH_2).

^{19}F NMR (376 MHz, $CDCl_3$) δ: -76.4 (s, CF_3).

^{15}N NMR (40 MHz, $CDCl_3$) δ: -316.8 (aziridine N).

HRMS (ESI), *m/z*: calcd. for $C_9H_7BrClF_3N^+$: 299.9370 $[M+H]^+$; found: 299.9372.

2-Chloro-1-(3-chlorophenyl)-2-(trifluoromethyl)aziridine (34)

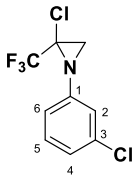

By following the General Procedure **2**, starting from ***N*-(3-chlorophenyl)-2,2,2-trifluoroethanimidoyl chloride** (500 mg, 2.0 mmol, 1.0 equiv), ICH_2Cl (459 mg, 0.2 mL, 2.6 mmol, 1.3 equiv), MeLi-LiBr complex (1.5 M, 1.6 mL, 2.4 mmol, 1.2 equiv) and THF (10 mL), the desired product **34** was obtained in 85% yield (445 mg) as a colorless oil after chromatography on neutral alumina BG2 (*n*-hexane).

^{1}H NMR (400 MHz, $CDCl_3$) δ: 7.27 (t, *J* = 8.0 Hz, 1H, Ph H-5), 7.13 (ddd, *J* = 8.0, 2.1, 1.0 Hz, 1H, Ph H-4), 6.95 (t, *J* = 2.1 Hz, 1H, Ph H-2), 6.86 (ddd, *J* = 8.0, 2.1, 1.0 Hz, 1H, Ph H-6), 3.01 (s, 1H, NCH_2), 2.50 (q, *J* = 0.9 Hz, 1H, NCH_2).

^{13}C NMR (100 MHz, $CDCl_3$) δ: 145.8 (Ph C-1), 134.7 (Ph C-3), 130.0 (Ph C-5), 124.6 (Ph C-4), 121.2 (q, *J* = 275.4 Hz, CF_3), 121.1 (Ph C-2), 119.3 (Ph C-6), 57.0 (q, *J* = 43.2 Hz, $\underline{C}CF_3$), 37.1 (NCH_2).

^{19}F NMR (376 MHz, $CDCl_3$) δ: -76.4 (s, CF_3).

^{15}N NMR (40 MHz, $CDCl_3$) δ: -316.9 (aziridine N).

HRMS (ESI), *m/z*: calcd. for $C_9H_7Cl_2F_3N^+$: 255.9902 $[M+H]^+$; found: 255.9901.

2-Chloro-1-(4-chlorophenyl)-2-(trifluoromethyl)aziridine (35)

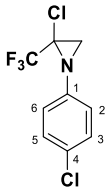

By following the General Procedure **2**, starting from ***N*-(4-chlorophenyl)-2,2,2-trifluoroethanimidoyl chloride** (250 mg, 1.0 mmol, 1.0 equiv), ICH_2Cl (236 mg, 0.1 mL,

1.3 mmol, 1.3 equiv), MeLi-LiBr complex (1.5 M, 0.8 mL, 1.2 mmol, 1.2 equiv) and THF (5 mL), the desired product **35** was obtained in 84% yield (215 mg) as a yellow oil after chromatography on neutral alumina BG2 (95:05 *v/v*, *n*-hexane/diethyl ether).

^{1}H NMR (400 MHz, $CDCl_3$) δ: 7.31 (m, 2H, Ph H-3,5), 6.89 (m, 2H, Ph H-2,6), 3.01 (s, 1H, NCH_2), 2.47 (q, *J* = 1.0 Hz, 1H, NCH_2).

^{13}C NMR (100 MHz, $CDCl_3$) δ: 143.2 (Ph C-1), 129.9 (Ph C-4), 129.1 (Ph C-3,5), 122.2 (Ph C-2,6), 121.3 (q, *J* = 275.5 Hz, CF_3), 57.1 (q, *J* = 42.7 Hz, $\underline{C}CF_3$), 37.1 (NCH_2).

^{19}F NMR (376 MHz, $CDCl_3$) δ: -76.4 (s, CF_3).

^{15}N NMR (40 MHz, $CDCl_3$) δ: -317.8 (aziridine N).

HRMS (ESI), *m/z*: calcd. for $C_9H_7Cl_2F_3N^+$: 255.9902 $[M+H]^+$; found: 255.9904.

2-Chloro-1-(4-fluorophenyl)-2-(trifluoromethyl)aziridine (36)

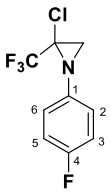

By following the General Procedure **2**, starting from ***N*-(4-fluorophenyl)-2,2,2-trifluoroethanimidoyl chloride** (393 mg, 1.7 mmol, 1.0 equiv), ICH_2Cl (388 mg, 0.2 mL, 2.2 mmol, 1.3 equiv), MeLi-LiBr complex (1.5 M, 1.4 mL, 2.0 mmol, 1.2 equiv) and THF (8 mL), the desired product **36** was obtained in 89% yield (363 mg) as a yellow oil after chromatography on neutral alumina BG2 (90:10 *v/v*, *n*-hexane/diethyl ether).

^{1}H NMR (400 MHz, $CDCl_3$) δ: 7.03 (m, 2H, Ph H-3,5), 6.91 (m, 2H, Ph H-2,6), 3.00 (s, 1H, NCH_2), 2.47 (q, *J* = 0.9 Hz, 1H, NCH_2).

^{13}C NMR (100 MHz, $CDCl_3$) δ: 159.9 (d, *J* = 243.0 Hz, Ph C-4), 140.5 (d, *J* = 2.7 Hz, Ph C-1), 122.2 (d, *J* = 8.2 Hz, Ph C-2,6), 121.4 (q, *J* = 275.3 Hz, CF_3), 115.8 (d, *J* = 23.0 Hz, Ph C-3,5), 57.3 (q, *J* = 42.7 Hz, $\underline{C}CF_3$), 37.1 (NCH_2).

^{19}F NMR (376 MHz, $CDCl_3$) δ: -118.8 (m, PhF), -76.4 (s, CF_3).

^{15}N NMR (40 MHz, $CDCl_3$) δ: -318.8 (aziridine N).

HRMS (ESI), *m/z*: calcd. for $C_9H_7ClF_4N^+$: 240.0198 $[M+H]^+$; found: 240.0199.

2-Chloro-1-(2-isopropylphenyl)-2-(trifluoromethyl)aziridine (37)

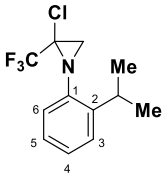

By following the General Procedure **2**, starting from **2,2,2-trifluoro-*N*-(2-isopropylphenyl)ethanimidoyl chloride** (500 mg, 2.0 mmol, 1.0 equiv), ICH_2Cl (459 mg, 0.2 mL, 2.6 mmol, 1.3 equiv), MeLi-LiBr complex (1.5 M, 1.6 mL, 2.4 mmol, 1.2 equiv) and THF (10 mL), the desired product **37** was obtained in 62% yield (327 mg) as a yellow oil after chromatography on neutral alumina BG2 (98:02 *v/v*, *n*-hexane/diethyl ether).

^{1}H NMR (400 MHz, $CDCl_3$) δ: 7.34 (m, 1H, Ph H-3), 7.18 (m, 1H, Ph H-4), 7.17 (m, 1H, Ph H-5), 6.79 (m, 1H, Ph H-6), 3.33 (sept, *J* = 6.8 Hz, 1H, C<u>H</u>CH_3), 2.92 (s, 1H, NCH_2), 2.60 (s, 1H, NCH_2), 1.32 (d, *J* = 6.8 Hz, 3H, CHC<u>H</u>$_3$, attached to C at 22.8 ppm), 1.22 (d, *J* = 6.8 Hz, 3H, CHC<u>H</u>$_3$, attached to C at 23.5 ppm).

^{13}C NMR (100 MHz, $CDCl_3$) δ: 142.9 (Ph C-2), 140.7 (Ph C-1), 126.2 (Ph C-3), 126.1 (Ph C-5), 125.3 (Ph C-4), 121.7 (q, *J* = 276.3 Hz, CF_3), 120.0 (Ph C-6), 58.3 (q, *J* = 42.4 Hz, <u>C</u>CF_3), 35.2 (NCH_2), 26.8 (<u>C</u>HCH_3), 23.5 (CH<u>C</u>H_3), 22.8 (CH<u>C</u>H_3).

^{19}F NMR (376 MHz, $CDCl_3$) δ: -75.2 (s, CF_3).

^{15}N NMR (40 MHz, $CDCl_3$) δ: -318.9 (aziridine N).

HRMS (ESI), *m/z*: calcd. for $C_{12}H_{14}ClF_3N^+$: 264.0761 $[M+H]^+$; found: 264.0763.

2-Chloro-1-(2,3-dimethylphenyl)-2-(trifluoromethyl)aziridine (38)

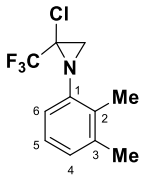

By following the General Procedure **2**, starting from ***N*-(2,3-dimethylphenyl)-2,2,2-trifluoroethanimidoyl chloride** (500 mg, 2.1 mmol, 1.0 equiv), ICH_2Cl (482 mg, 0.2 mL, 2.7 mmol, 1.3 equiv), MeLi-LiBr complex (1.5 M, 1.7 mL, 2.5 mmol, 1.2 equiv) and THF (10 mL), the desired product **38** was obtained in 82% yield (430 mg) as a colorless oil after chromatography on neutral alumina BG2 (98:02 *v/v*, *n*-hexane/diethyl ether).

^{1}H NMR (400 MHz, $CDCl_3$) δ: 7.06 (m, 2H, Ar), 6.67 (m, 1H, Ar), 2.92 (s, 1H, NCH_2), 2.57 (s, 1H, NCH_2), 2.34 (s, 3H, CH_3), 2.28 (s, 3H, CH_3).

^{13}C NMR (100 MHz, $CDCl_3$) δ: 142.6 (Ar), 137.9 (Ar), 130.8 (Ar), 126.6 (Ar), 125.7 (Ar), 124.6 (CF_3), 117.6 (Ar), 58.3 ($\underline{C}CF_3$), 35.4 (NCH_2), 20.3 (CH_3), 13.5 (CH_3).

HRMS (ESI), *m/z*: calcd. for $C_{11}H_{12}ClF_3N^+$: 250.0605 $[M+H]^+$; found: 250.0607.

2-Chloro-1-(2,5-dimethylphenyl)-2-(trifluoromethyl)aziridine (39)

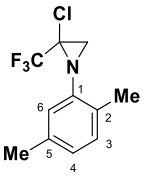

By following the General Procedure **2**, starting from ***N*-(2,5-dimethylphenyl)-2,2,2-trifluoroethanimidoyl chloride** (500 mg, 2.1 mmol, 1.0 equiv), ICH_2Cl (482 mg, 0.2 mL, 2.7 mmol, 1.3 equiv), MeLi-LiBr complex (1.5 M, 1.7 mL, 2.5 mmol, 1.2 equiv) and THF (10 mL), the desired product **39** was obtained in 82% yield (430 mg) as a yellow oil after chromatography on neutral alumina BG2 (98:02 *v/v*, *n*-hexane/diethyl ether).

^{1}H NMR (400 MHz, $CDCl_3$) δ: 7.09 (d, *J* = 7.6 Hz, 1H, Ph H-3), 6.90 (d, *J* = 7.6 Hz, 1H, Ph H-4), 6.60 (s, 1H, Ph H-6), 2.90 (s, 1H, NCH_2), 2.56 (s, 1H, NCH_2), 2.32 (s, 3H, 5-CH_3), 2.31 (s, 3H, 2-CH_3).

^{13}C NMR (100 MHz, $CDCl_3$) δ: 142.4 (Ph C-1), 136.2 (Ph C-5), 130.8 (Ph C-3), 129.0 (Ph C-2), 125.4 (Ph C-4), 121.8 (q, *J* = 276.1 Hz, CF_3), 120.5 (Ph C-6), 58.1 (q, *J* = 42.6 Hz, $\underline{C}CF_3$), 35.2 (NCH_2), 21.0 (5-CH_3), 17.5 (2-CH_3).

^{19}F NMR (376 MHz, $CDCl_3$) δ: -74.9 (s, CF_3).

^{15}N NMR (40 MHz, $CDCl_3$) δ: -317.7 (aziridine N).

HRMS (ESI), *m/z*: calcd. for $C_{11}H_{12}ClF_3N^+$: 250.0605 $[M+H]^+$; found: 250.0603.

2-[2-Chloro-2-(trifluoromethyl)-1-azidirinyl]benzonitrile (40)

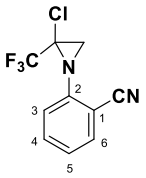

By following the General Procedure **2**, starting from ***N*-(2-cyanophenyl)-2,2,2-trifluoroethanimidoyl chloride** (360 mg, 1.5 mmol, 1.0 equiv), ICH_2Cl (344 mg, 0.3 mL, 2.0 mmol, 1.3 equiv), MeLi-LiBr complex (1.5 M, 1.2 mL, 1.8 mmol, 1.2 equiv) and THF (6 mL), the desired product **40** was obtained in 75% yield (277 mg) as a yellow oil after chromatography on neutral alumina BG2 (80:20 *v/v*, *n*-hexane/diethyl ether).

^{1}H NMR (400 MHz, $CDCl_3$) δ: 7.63 (dd, *J* = 7.8, 1.5 Hz, 1H, Ph H-6), 7.56 (m, 1H, Ph H-4), 7.22 (m, 1H, Ph H-5), 7.07 (m, 1H, Ph H-3), 3.30 (s, 1H, NCH_2), 2.81 (q, *J* = 1.0 Hz, 1H, NCH_2).

^{13}C NMR (100 MHz, $CDCl_3$) δ: 147.1 (Ph C-2), 133.8 (Ph C-6), 133.3 (Ph C-4), 124.4 (Ph C-5), 122.1 (Ph C-3), 121.1 (q, *J* = 276.3 Hz, CF_3), 116.3 (C≡N), 104.9 (Ph C-1), 57.1 (q, *J* = 43.5 Hz, $\underline{C}CF_3$), 38.7 (NCH_2).

^{19}F NMR (376 MHz, $CDCl_3$) δ: -75.8 (s, CF_3).

^{15}N NMR (40 MHz, $CDCl_3$) δ: -315.5 (aziridine N).

HRMS (ESI), *m/z*: calcd. for $C_{10}H_7ClF_3N_2^+$: 247.0244 $[M+H]^+$; found: 247.0246.

4-[2-Chloro-2-(trifluoromethyl)-1-azidirinyl]benzonitrile (41)

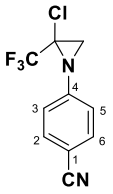

By following the General Procedure **2**, starting from ***N*-(4-cyanophenyl)-2,2,2-trifluoroethanimidoyl chloride** (500 mg, 2.1 mmol, 1.0 equiv), ICH_2Cl (482 mg, 0.2 mL, 2.7 mmol, 1.3 equiv), MeLi-LiBr complex (1.5 M, 1.7 mL, 2.5 mmol, 1.2 equiv) and THF (10 mL), the desired product **41** was obtained in 83% yield (430 mg) as a yellow oil after chromatography on neutral alumina BG2 (70:30 *v/v*, *n*-hexane/diethyl ether).

^{1}H NMR (400 MHz, $CDCl_3$) δ: 7.63 (m, 2H, Ph H-2,6), 7.03 (m, 2H, Ph H-3,5), 3.10 (s, 1H, NCH_2), 2.55 (q, *J* = 1.0 Hz, 1H, NCH_2).

^{13}C NMR (100 MHz, $CDCl_3$) δ: 148.5 (Ph C-4), 133.2 (Ph C-2,6), 121.5 (Ph C-3,5), 121.0 (q, *J* = 275.8 Hz, CF_3), 118.6 (C≡N), 108.0 (Ph C-1), 56.7 (q, *J* = 43.4 Hz, $\underline{C}CF_3$), 37.4 (q, *J* = 0.9 Hz, NCH_2).

^{19}F NMR (376 MHz, $CDCl_3$) δ: -76.4 (s, CF_3).

^{15}N NMR (40 MHz, $CDCl_3$) δ: -313.9 (aziridine N).

HRMS (ESI), *m/z*: calcd. for $C_{10}H_7ClF_3N_2^+$: 247.0244 $[M+H]^+$; found: 247.0242.

2-Chloro-1-(3-ethynylphenyl)-2-(trifluoromethyl)aziridine (42)

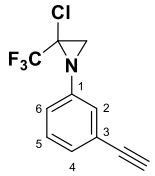

By following the General Procedure **2**, starting from ***N*-(3-ethynylphenyl))-2,2,2-trifluoroethanimidoyl chloride** (1000 mg, 4.3 mmol, 1.0 equiv), ICH_2Cl (986 mg, 0.4 mL, 5.6 mmol, 1.3 equiv), MeLi-LiBr complex (1.5 M, 3,5 mL, 5.2 mmol, 1.2 equiv) and THF (20 mL), the desired product **42** was obtained in 70% yield (739 mg) as a yellow oil after chromatography on neutral alumina BG2 (90:10 *v/v*, *n*-hexane/diethyl ether).

^{1}H NMR (400 MHz, $CDCl_3$) δ: 7.29 (m, 1H, Ph H-5), 7.28 (m, Ph H-4), 7.07 (m, 1H, Ph H-2), 6.96 (m, 1H, Ph H-6), 3.10 (s, 1H, ≡CH), 3.01 (s, 1H, NCH_2), 2.50 (q, *J* = 1.0 Hz, 1H, NCH_2).

^{13}C NMR (100 MHz, $CDCl_3$) δ: 144.6 (Ph C-1), 129.0 (Ph C-5), 128.3 (Ph C-4), 124.2 (Ph C-2), 123.0 (Ph C-3), 121.7 (Ph C-6), 121.3 (q, *J* = 275.5 Hz, CF_3), 82.9 (C≡CH), 77.8 (C≡CH), 57.0 (q, *J* = 42.9 Hz, CCF_3), 36.9 (NCH_2).

^{19}F NMR (376 MHz, $CDCl_3$) δ: -76.4 (s, CF_3).

^{15}N NMR (40 MHz, $CDCl_3$) δ: -317.2 (aziridine N).

HRMS (ESI), *m/z*: calcd. for $C_{11}H_8ClF_3N^+$: 246.0292 $[M+H]^+$; found: 246.0292.

2-Chloro-1-{4-[(E)-phenyldiazenyl]phenyl}-2-(trifluoromethyl)aziridine (43)

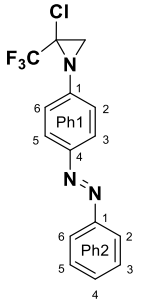

By following the General Procedure **2**, starting from **2,2,2-trifluoro-*N*-[4-(phenyldiazenyl)phenyl]ethanimidoyl chloride** (500 mg, 1.6 mmol, 1.0 equiv), ICH_2Cl (367 mg, 0.5 mL, 2.1 mmol, 1.3 equiv), MeLi-LiBr complex (1.5 M, 1.3 mL, 1.9 mmol, 1.2 equiv) and THF (10 mL), the desired product **43** was obtained in 86% yield (448 mg) as an orange solid (m.p.: 110-112 °C) after chromatography on neutral alumina BG2 (95:05 *v/v*, *n*-hexane/diethyl ether).

^{1}H NMR (400 MHz, $CDCl_3$) δ: 7.94 (m, 2H, Ph1 H-3,5), 7.90 (m, 2H, Ph2 H-2,6), 7.52 (m, 2H, Ph2 H-3,5), 7.48 (m, 1H, Ph2 H-4), 7.09 (m, 2H, Ph1 H-2,6), 3.09 (s, 1H, NCH_2), 2.58 (br s, 1H, NCH_2).

^{13}C NMR (100 MHz, $CDCl_3$) δ: 152.7 (Ph2 C-1), 149.6 (Ph1 C-4), 147.0 (Ph1 C-1), 130.9 (Ph2 C-4), 129.1 (Ph2 C-3,5), 123.9 (Ph1 C-3,5), 121.4 (Ph1 C-2,6, Ph2 C-2,6), 121.3 (q, *J* = 275.7 Hz, CF_3), 57.1 (q, *J* = 43.0 Hz, $\underline{C}CF_3$), 37.3 (NCH_2).

^{19}F NMR (376 MHz, $CDCl_3$) δ: -76.3 (s, CF_3).

^{15}N NMR (40 MHz, $CDCl_3$) δ: -315.3 (aziridine N).

HRMS (ESI), *m/z*: calcd. for $C_{15}H_{12}ClF_3N_3^+$: 326.0666 $[M+H]^+$; found: 326.0667.

4-{4-[2-Chloro-2-(trifluoromethyl)-1-azidirinyl]phenyl}morpholine (44)

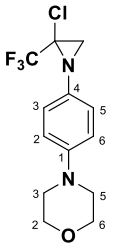

By following the General Procedure **2**, starting from **2,2,2-trifluoro-*N*-[4-(4-morpholinyl)phenyl]ethanimidoyl chloride** (500 mg, 1.7 mmol, 1.0 equiv), ICH_2Cl (390 mg, 0.2 mL, 2.2 mmol, 1.3 equiv), MeLi-LiBr complex (1.5 M, 1.4 mL, 2.0 mmol, 1.2 equiv) and THF (10 mL), the desired product **44** was obtained in 83% yield (433 mg) as a brown solid (m.p.: 105-106 °C) after chromatography on neutral alumina BG2 (60:40 *v/v*, *n*-hexane/diethyl ether).

^{1}H NMR (400 MHz, $CDCl_3$) δ: 6.88 ('s', 4H, Ph H-2,3,5,6), 3.86 (m, 4H, morph H-2,6), 3.12 (m, 4H, morph H-3,5), 2.94 (s, 1H, NCH_2), 2.44 (s, 1H, NCH_2).

^{13}C NMR (100 MHz, $CDCl_3$) δ: 148.4 (Ph C-1), 137.4 (Ph C-4), 121.7 (Ph C-3,5), 121.5 (q, *J* = 275.1 Hz, CF_3), 116.4 (Ph C-2,6), 66.9 (morph C-2,6), 57.7 (q, *J* = 42.5 Hz, $\underline{C}CF_3$), 49.7 (morph C-3,5), 36.7 (NCH_2).

^{19}F NMR (376 MHz, $CDCl_3$) δ: -76.3 (s, CF_3).

^{15}N NMR (40 MHz, $CDCl_3$) δ: -319.7 (morpholine N), -319.5 (aziridine N).

HRMS (ESI), *m/z*: calcd. for $C_{13}H_{15}ClF_3N_2O^+$: 307.0820 $[M+H]^+$; found: 307.0817.

1-{3-[2-Chloro-2-(trifluoromethyl)-1-azidirinyl]phenyl}pyrrolidine (45)

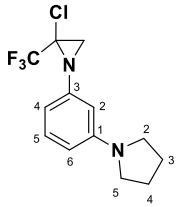

By following the General Procedure **2**, starting from **(1*Z*)-2,2,2-trifluoro-*N*-[3-(pyrrolidinyl)phenyl]ethanimidoyl chloride** (400 mg, 1.4 mmol, 1.0 equiv), ICH_2Cl (321 mg, 0.1 mL, 1.8 mmol, 1.3 equiv), MeLi-LiBr complex (1.5 M, 1.1 mL, 1.7 mmol, 1.2 equiv) and THF (8 mL), the desired product **45** was obtained in 74% yield (301 mg) as a yellow oil after chromatography on neutral alumina BG2 (90:10 *v/v*, *n*-hexane/chloroform).

^{1}H NMR (400 MHz, $CDCl_3$) δ: 7.16 (m, 1H, Ph H-5), 6.37 (m, 1H, Ph H-6), 6.27 (m, 1H, Ph H-4), 6.13 (br s, 1H, Ph H-2), 3.30 (m, 4H, pyrr H-2,5), 2.94 (s, 1H, NCH_2), 2.50 (s, 1H, NCH_2), 2.01 (m, 4H, pyrr H-3,4).

^{13}C NMR (100 MHz, $CDCl_3$) δ: 148.4 (Ph C-1), 145.4 (Ph C-3), 129.5 (Ph C-5), 121.5 (q, *J* = 275.3 Hz, CF_3), 108.2 (br, Ph C-6), 108.0 (br, Ph C-4), 104.1 (Ph C-2), 57.3 (m, $\underline{C}CF_3$), 47.7 (pyrr C-2,5), 36.6 (NCH_2), 25.4 (pyrr C-3,4).

^{19}F NMR (376 MHz, $CDCl_3$) δ: -76.3 (s, CF_3).

^{15}N NMR (40 MHz, $CDCl_3$) δ: -316.7 (aziridine N), -306.7 (pyrrolidine N).

HRMS (ESI), *m/z*: calcd. for $C_{13}H_{15}ClF_3N_2^+$: 291.0870 $[M+H]^+$; found: 291.0872.

1-{3-[2-Chloro-2-(trifluoromethyl)-1-azidirinyl]phenyl}-2-pyrrolidinone (46)

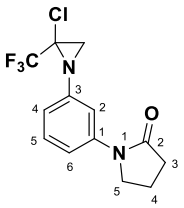

By following the General Procedure **2**, starting from **(1*Z*)-2,2,2-trifluoro-*N*-[3-(2-oxo-1-pyrrolidinyl)phenyl]ethanimidoyl chloride** (228 mg, 0.8 mmol, 1.0 equiv), ICH_2Cl (183 mg, 0.1 mL, 1.0 mmol, 1.3 equiv), MeLi-LiBr complex (1.5 M, 0.6 mL, 1.0 mmol, 1.2 equiv) and THF (5 mL), the desired product **46** was obtained in 80% yield (195 mg) as a colorless oil after chromatography on neutral alumina BG2 (50:50 *v/v*, *n*-hexane/chloroform).

^{1}H NMR (400 MHz, $CDCl_3$) δ: 7.42 (m, 1H, Ph H-2), 7.32 (m, 1H, Ph H-5), 7.31 (m, 1H, Ph H-6), 6.76 (m, 1H, Ph H-4), 3.87 (m, 2H, pyrr H-5), 3.00 (s, 1H, NCH_2), 2.62 (m, 2H, pyrr H-3), 2.53 (s, 1H, NCH_2), 2.17 (m, 2H, pyrr H-4).

^{13}C NMR (100 MHz, $CDCl_3$) δ: 174.4 (pyrr C-2), 145.0 (Ph C-3), 140.2 (Ph C-1), 129.2 (Ph C-5), 121.4 (q, *J* = 275.3 Hz, CF_3), 117.1 (Ph C-4), 115.3 (Ph C-6), 112.1 (Ph C-2), 48.7 (pyrr C-5), 37.0 (NCH_2), 32.9 (pyrr C-3), 17.9 (pyrr C-4).

^{19}F NMR (376 MHz, $CDCl_3$) δ: -76.3 (s, CF_3).

^{15}N NMR (40 MHz, $CDCl_3$) δ: -316.4 (aziridine N), pyrrolidine N was not found.

HRMS (ESI), *m/z*: calcd. for $C_{13}H_{13}ClF_3NO^+$: 305.0663 $[M+H]^+$; found: 305.0660.

2-Methyl-2-propanyl 4-[2-chloro-2-(trifluoromethyl)-1-aziridinyl]benzoate (47)

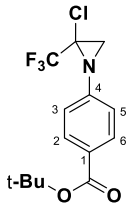

By following the General Procedure **2**, starting from **2-methyl-2-propanyl-4-{[1-chloro-2,2,2-trifluoroethylidene]amino}benzoate** (500 mg, 1.6 mmol, 1.0 equiv), ICH_2Cl (367 mg, 0.2 mL, 2.1 mmol, 1.3 equiv), MeLi-LiBr complex (1.5 M, 1.3 mL, 1.9 mmol, 1.2 equiv) and THF (10 mL), the desired product **47** was obtained in 88% yield (453 mg) as a colorless oil after chromatography on neutral alumina BG2 (95:05 *v/v*, *n*-hexane/diethyl ether).

^{1}H NMR (400 MHz, $CDCl_3$) δ: 7.98 (m, 2H, Ph H-2,6), 6.98 (m, 2H, Ph H-3,5), 3.05 (s, 1H, NCH_2), 2.53 (q, *J* = 1.0 Hz, 1H, NCH_2), 1.59 (s, 9H, CCH_3).

^{13}C NMR (100 MHz, $CDCl_3$) δ: 165.2 (C=O), 148.2 (Ph C-4), 130.6 (Ph C-2,6), 128.2 (Ph C-1), 121.2 (q, *J* = 275.6 Hz, CF_3), 120.5 (Ph C-3,5), 81.0 ($\underline{C}Me_3$), 56.9 (q, *J* = 43.1 Hz, $\underline{C}CF_3$), 37.2 (NCH_2), 28.2 ($C\underline{Me}_3$).

^{19}F NMR (376 MHz, $CDCl_3$) δ: -76.4 (s, CF_3).

^{15}N NMR (40 MHz, $CDCl_3$) δ: -315.1 (aziridine N).

HRMS (ESI), *m/z*: calcd. for $C_{14}H_{16}ClF_3NO_2Na^+$: 345.0636 $[M+Na]^+$; found: 345.0638.

Ethyl 3-[2-chloro-2-(trifluoromethyl)-1-azidirinyl]benzoate (48)

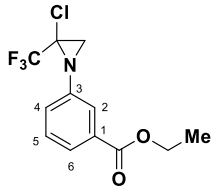

By following the General Procedure **2**, starting from **ethyl-3-{(1*Z*)-1-chloro-2,2,2-trifluoroethylidone]amino}benzoate** (522 mg, 1.9 mmol, 1.0 equiv), ICH_2Cl (436 mg, 0.2 mL, 2.5 mmol, 3.0 equiv), MeLi-LiBr complex (1.5 M, 1.5 mL, 2.3 mmol, 1.2 equiv) and THF (10 mL), the desired product **48** was obtained in 65% yield (363 mg) as a colorless oil after chromatography on neutral alumina BG2 (70:30 *v/v*, *n*-hexane/chloroform).

^{1}H NMR (400 MHz, $CDCl_3$) δ: 7.84 (m, 1H, Ph H-6), 7.59 (m, 1H, Ph H-2), 7.42 (m, 1H, Ph H-5), 7.17 (m, 1H, Ph H-4), 4.39 (q, *J* = 7.1 Hz, 2H, OCH_2), 3.05 (s, 1H, NCH_2), 2.56 (s, 1H, NCH_2), 1.40 (t, *J* = 7.1 Hz, 3H, CH_3).

^{13}C NMR (100 MHz, $CDCl_3$) δ: 166.0 (C=O), 144.8 (Ph C-3), 131.6 (Ph C-1), 129.0 (Ph C-5), 125.8 (Ph C-4), 125.6 (Ph C-6), 121.4 (Ph C-2), 61.2 (OCH_2), 37.1 (NCH_2), 14.3 (CH_3), CF_3 and $\underline{C}CF_3$ were not found.

^{19}F NMR (376 MHz, $CDCl_3$) δ: -76.4 (s, CF_3).

HRMS (ESI), *m/z*: calcd. for $C_{12}H_{12}ClF_3NO_2^+$: 294.0503 $[M+H]^+$; found: 294.0500.

4-[2-Chloro-2-(trifluoromethyl)-1-azidirinyl]-*N*-methoxy-*N*-methylbenzamide (49)

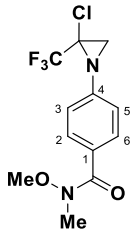

By following the General Procedure **2**, starting from **2,2,2-trifluoro-*N*-{4-[methoxy (methyl)carbamoyl]phenyl}ethanimidoyl chloride** (190 mg, 0.6 mmol, 1.0 equiv), ICH_2Cl (137 mg, 0.1 mL, 0.8 mmol, 1.3 equiv), MeLi-LiBr complex (1.5 M, 0.5 mL, 0.7 mmol, 1.2 equiv) and THF (4 mL), the desired product **49** was obtained in 73% yield (135 mg) as a colorless oil after chromatography on neutral alumina BG2 (98:02 *v/v*, *n*-hexane/diethyl ether).

^{1}H NMR (400 MHz, $CDCl_3$) δ: 7.73 (m, 2H, Ph H-2,6), 6.98 (m, 2H, Ph H-3,5), 3.55 (s, 3H, OCH_3), 3.36 (s, 3H, CH_3), 3.05 (s, 1H, NCH_2), 2.53 (s, 1H, NCH_2).

^{13}C NMR (100 MHz, $CDCl_3$) δ: 169.1 (C=O), 146.6 (Ph C-4), 129.9 (Ph C-1), 129.6 (Ph C-2,6), 121.3 (q, *J* = 275.5 Hz, CF_3), 120.3 (Ph C-3,5), 61.0 (OCH_3), 57.1 ($\underline{C}CF_3$), 37.1 (NCH_2), 33.8 (NCH_3).

^{19}F NMR (376 MHz, $CDCl_3$) δ: -76.4 (s, CF_3).

^{15}N NMR (40 MHz, $CDCl_3$) δ: -315.8 (aziridine N).

HRMS (ESI), *m/z*: calcd. for $C_{12}H_{13}ClF_3N_2O_2^+$: 309.0612 $[M+H]^+$; found: 309.0610.

1-(2-Biphenylyl)-2-chloro-2-(trifluoromethyl)aziridine (50)

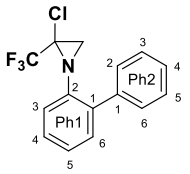

By following the General Procedure **2**, starting from ***N*-(2-biphenylyl)-2,2,2-trifluoroethanimidoyl chloride** (500 mg, 1.8 mmol, 1.0 equiv), ICH_2Cl (413 mg, 0.2 mL, 2.3 mmol, 1.3 equiv), MeLi-LiBr complex (1.5 M, 1.4 mL, 2.2 mmol, 1.2 equiv) and THF (10 mL), the desired product **50** was obtained in 77% yield (413 mg) as a yellow oil after chromatography on neutral alumina BG2 (*n*-hexane).

^{1}H NMR (400 MHz, $CDCl_3$) δ: 7.50 (m, 2H, Ph2 H-2,6), 7.44 (m, 2H, Ph2 H-3,5), 7.36 (m, 1H, Ph2 H-4), 7.35 (m, 1H, Ph1 H-4), 7.34 (m, 1H, Ph1 H-6), 7.22 (m, 1H, Ph1 H-5), 7.05 (m, 1H, Ph1 H-3), 2.67 (s, 1H, NCH_2), 1.96 (q, *J* = 0.9 Hz, 1H, NCH_2).

^{13}C NMR (100 MHz, $CDCl_3$) δ: 141.5 (Ph1 C-2), 138.7 (Ph2 C-1), 134.4 (Ph1 C-1), 131.2 (Ph1 C-6), 129.5 (Ph2 C-2,6), 128.2 (Ph2 C-3,5), 127.6 (Ph1 C-4), 127.3 (Ph1 C-4), 124.3 (Ph1 C-5), 121.6 (Ph1 C-3), 121.3 (q, *J* = 275.8 Hz, CF_3), 58.7 (q, *J* = 42.9 Hz, $\underline{C}CF_3$), 38.1 (NCH_2).

^{19}F NMR (376 MHz, $CDCl_3$) δ: -76.1 (s, CF_3).

^{15}N NMR (40 MHz, $CDCl_3$) δ: -318.5 (aziridine N).

HRMS (ESI), *m/z*: calcd. for $C_{15}H_{12}ClF_3N^+$: 298.0605 $[M+H]^+$; found: 298.0604.

1-(3-Biphenylyl)-2-chloro-2-(trifluoromethyl)azidirine (51)

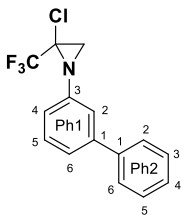

By following the General Procedure **2**, starting from ***N*-(3-biphenylyl)-2,2,2-trifluoroethanimidoyl chloride** (500 mg, 1.8 mmol, 1.0 equiv), ICH_2Cl (413 mg, 0.2 mL, 2.3 mmol, 1.3 equiv), MeLi-LiBr complex (1.5 M, 1.4 mL, 2.2 mmol, 1.2 equiv) and THF (10 mL), the desired product **51** was obtained in 79% yield (423 mg) as a yellow oil after chromatography on neutral alumina BG2 (90:10 *v/v*, *n*-hexane/chloroform).

^{1}H NMR (400 MHz, $CDCl_3$) δ: 7.60 (m, 2H, Ph2 H-2,6), 7.47 (m, 2H, Ph2 H-3,5), 7.42 (m, 1H, Ph1 H-5), 7.39 (m, 1H, Ph1 H-6), 7.38 (m, 1H, Ph2 H-4), 7.17 (m, 1H, Ph1 H-2), 6.96 (m, 1H, Ph1 H-4), 3.05 (s, 1H, NCH_2), 2.56 (s, 1H, NCH_2).

^{13}C NMR (100 MHz, $CDCl_3$) δ: 145.0 (Ph1 C-3), 142.3 (Ph1 C-1), 140.5 (Ph2 C-1), 129.4 (Ph1 C-5), 128.8 (Ph2 C-3,5), 127.6 (Ph2 C-4), 127.2 (Ph2 C-2,6), 123.3 (Ph1 C-6), 121.4 (q, *J* = 275.4 Hz, CF_3), 119.7 (Ph1 C-4), 119.6 (Ph1 C-2), 57.2 (q, *J* = 42.8 Hz, $\underline{C}CF_3$), 37.0 (NCH_2).

^{19}F NMR (376 MHz, $CDCl_3$) δ: -76.3 (s, CF_3).

^{15}N NMR (40 MHz, $CDCl_3$) δ: -316.8 (aziridine N).

HRMS (ESI), *m/z*: calcd. for $C_{15}H_{12}ClF_3N^+$: 298.0605 $[M+H]^+$; found: 298.0607.

1-(2-Anthryl)-2-chloro-2-(trifluoromethyl)aziridine (52)

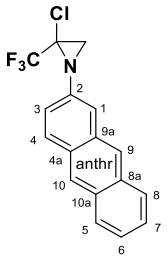

By following the General Procedure **2**, starting from ***N*-(2-anthryl)-2,2,2-trifluoroethanimidoyl chloride** (260 mg, 0.8 mmol, 1.0 equiv), ICH_2Cl (183 mg, 0.1 mL, 1.0 mmol, 1.3 equiv), MeLi-LiBr complex (1.5 M, 0.6 mL, 1.0 mmol, 1.2 equiv) and THF (5 mL), the desired product **52** was obtained in 74% yield (190 mg) as an orange solid (m.p.: 178-180 °C) after chromatography on neutral alumina BG2 (98:02 *v/v*, *n*-hexane/diethyl ether).

^{1}H NMR (400 MHz, $CDCl_3$) δ: 8.40 (s, 1H, anthr H-10), 8.34 (s, 1H, anthr H-9), 7.99 (m, 1H, anthr H-4), 7.98 (m, 1H, anthr H-5), 7.97 (m, 1H, anthr H-8), 7.48 (m, 1H, anthr H-7), 7.45 (m, 1H, anthr H-6), 7.41 (d, *J* = 2.1 Hz, 1H, Ph H-1), 7.22 (dd, *J* = 9.0, 2.1 Hz, 1H, anthr H-3), 3.12 (s, 1H, NCH_2), 2.69 (s, 1H, NCH_2).

^{13}C NMR (100 MHz, $CDCl_3$) δ: 142.0 (anthr C-2), 132.2 (anthr C-8a), 131.6 (anthr C-9a), 131.2 (anthr C-10a), 129.5 (anthr C-4a), 129.4 (anthr C-4) 128.2 (anthr C-5), 127.8 (anthr C-8), 126.5 (anthr C-10), 125.8 (anthr C-7), 125.2 (anthr C-6), 125.1 (anthr C-9),

122.1 (anthr C-3), 121.5 (q, *J* = 275.4 Hz, CF_3), 115.8 (anthr C-1), 57.3 (q, *J* = 42.6 Hz, $\underline{C}CF_3$), 37.0 (NCH_2).

^{19}F NMR (376 MHz, $CDCl_3$) δ: -76.2 (s, CF_3).

^{15}N NMR (40 MHz, $CDCl_3$) δ: -315.8 (aziridine N).

HRMS (ESI), *m/z*: calcd. for $C_{17}H_{12}ClF_3N^+$: 322.0605 $[M+H]^+$; found: 322.0606.

2-Chloro-1-(1-ethynylphenyl)-2-(trifluoromethyl)aziridine (53)

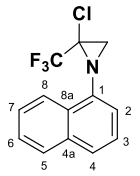

By following the General Procedure **2**, starting from **2,2,2-trifluoro-*N*-(1-naphthalenyl)ethanimidoyl chloride** (500 mg, 1.9 mmol, 1.0 equiv), ICH_2Cl (436 mg, 0.2 mL, 2.5 mmol, 1.3 equiv), MeLi-LiBr complex (1.5 M, 1.5 mL, 2.3 mmol, 1.2 equiv) and THF (10 mL), the desired product **53** was obtained in 67% yield (346 mg) as a colorless oil after chromatography on neutral alumina BG2 (98:02 *v/v*, *n*-hexane/diethyl ether).

^{1}H NMR (400 MHz, $CDCl_3$) δ: 8.19 (m, 1H, napth H-8), 7.88 (m, 1H, napth H-5), 7.68 (m, 1H, napth H-4), 7.56 (m, 1H, napth H-7), 7.55 (m, napth H-6), 7.41 (m, 1H, napth H-3), 6.95 (m, 1H, napth H-2), 3.12 (s, 1H, NCH_2), 2.77 (s, 1H, NCH_2).

^{13}C NMR (100 MHz, $CDCl_3$) δ: 140.5 (napth C-1), 134.1 (napth C-4a), 128.6 (napth C-8a), 128.2 (napth C-5), 126.5 (napth C-6), 126.2 (napth C-7), 125.4 (napth C-4), 125.2 (napth C-3), 122.4 (q, *J* = 2.0 Hz, napth C-8) 121.8 (q, *J* = 276.2 Hz, CF_3), 116.0 (napth C-2), 58.3 (q, *J* = 42.4 Hz, $\underline{C}CF_3$), 35.7 (NCH_2).

^{19}F NMR (376 MHz, $CDCl_3$) δ: -74.8 (s, CF_3).

^{15}N NMR (40 MHz, $CDCl_3$) δ: -318.9 (aziridine N).

HRMS (ESI), *m/z*: calcd. for $C_{13}H_{10}ClF_3N^+$: 272.0448 $[M+H]^+$; found: 272.0448.

3.1.3 General Procedure 3 and spectral data of Chloromethylaziridines 54-84

Scheme 26 - To a cooled (-78 °C) solution of trifluoromethylchloroimidate (1.0 equiv) in dry THF was added chloroiodomethane (3.0 equiv). After 2 min, an ethereal solution of MeLi-LiBr (2.8 equiv, 1.5 M) was added dropwise, using a syringe pump (flow: 0.200 mL/min). The resulting solution was stirred for 1 h. Then 10% aq solution $NaHCO_3$ (2 mL/mmol substrate) was added and the reaction mixture was extracted with Et_2O (2 x 5 mL) and washed with water (5 mL) and brine (10 mL). The organic phase was dried

over anhydrous Na_2SO_4, filtered and, after removal of the solvent under reduced pressure, the so-obtained crude mixture was subjected to chromatography (neutral alumina BG2) to afford pure compounds.

1-(3-Bromophenyl)-2-(chloromethyl)-2-(trifluoromethyl)aziridine (54)

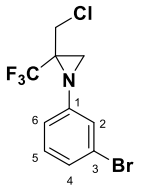

By following the General Procedure **3**, starting from ***N*-(3-bromophenyl)-2,2,2-trifluoroethanimidoyl chloride** (400 mg, 1.4 mmol, 1.0 equiv), ICH_2Cl (741 mg, 0.3 mL, 4.2 mmol, 3.0 equiv), MeLi-LiBr complex (1.5 M, 2.6 mL, 3.9 mmol, 2.8 equiv) and THF (8 mL), the desired product **54** was obtained in 91% yield (400 mg) as a yellow oil after chromatography on neutral alumina BG2 (*n*-hexane).

^{1}H NMR (400 MHz, $CDCl_3$) δ: 7.22 (m, 1H, Ph H-4), 7.16 (m, 1H, Ph H-5), 7.10 (m, 1H, Ph H-2), 6.91 (m, 1H, Ph H-6), 3.75 (A-part of an AB-system, $^2J_{AB}$ = 13.0 Hz, 1H, CH_2Cl), 3.42 (B-part of an AB system, $^2J_{AB}$ = 13.0 Hz, 1H, CH_2Cl), 2.83 (s, 1H, NCH_2), 2.44 (q, *J* = 1.4 Hz, 1H, NCH_2).

^{13}C NMR (100 MHz, $CDCl_3$) δ: 147.3 (Ph C-1), 130.7 (Ph C-5), 127.1 (Ph C-4), 123.5 (Ph C-2), 123.5 (q, *J* = 277.4 Hz, CF_3), 123.0 (Ph C-3), 119.4 (Ph C-6), 44.8 (q, *J* = 35.1 Hz, $\underline{C}CF_3$), 39.5 (CH_2Cl), 34.0 (q, *J* = 2.1 Hz, NCH_2).

^{19}F NMR (376 MHz, $CDCl_3$) δ: -72.3 (s, CF_3).

^{15}N NMR (40 MHz, $CDCl_3$) δ: -316.2 (aziridine N).

HRMS (ESI), *m/z*: calcd. for $C_{10}H_9BrClF_3N^+$: 313.9553 $[M+H]^+$; found: 313.9555.

2-(Chloromethyl)-1-(2-chlorophenyl)-2-(trifluoromethyl)aziridine (55)

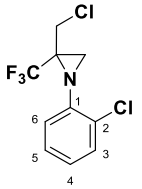

By following the General Procedure **3**, starting from ***N*-(2-chlorophenyl)-2,2,2-trifluoroethanimidoyl chloride** (500 mg, 2.0 mmol, 1.0 equiv), ICH_2Cl (1058 mg, 0.4 mL, 6.0 mmol, 3.0 equiv), MeLi-LiBr complex (1.5 M, 3.7 mL, 5.6 mmol, 2.8 equiv) and THF

(10 mL), the desired product **55** was obtained in 86% yield (464 mg) as a yellow oil after chromatography on neutral alumina BG2 (*n*-hexane).

^{1}H NMR (400 MHz, $CDCl_3$) δ: 7.37 (dd, *J* = 8.0, 1.4 Hz, 1H, Ph H-3), 7.23 (m, 1H, Ph H-5), 7.05 (m, 1H, Ph H-4), 6.91 (dd, *J* = 8.0, 1.4 Hz, 1H, Ph H-6), 4.18 (dd, *J* = 13.0, 0.9 Hz, 1H, CH_2Cl), 3.16 (d, *J* = 13.0 Hz, 1H, CH_2Cl), 2.90 (s, 1H, NCH_2), 2.57 (s, 1H, NCH_2).

^{13}C NMR (100 MHz, $CDCl_3$) δ: 142.7 (Ph C-1), 130.4 (Ph C-3), 127.8 (Ph C-5), 127.0 (Ph C-2), 124.9 (Ph C-4), 123.8 (q, *J* = 278.0 Hz, CF_3), 121.5 (Ph C-6), 46.0 (q, *J* = 35.1 Hz, $\underline{C}CF_3$), 39.0 (CH_2Cl), 33.7 (NCH_2).

^{19}F NMR (376 MHz, $CDCl_3$) δ: -71.7 (s, CF_3).

^{15}N NMR (40 MHz, $CDCl_3$) δ: -314.5 (aziridine N).

HRMS (ESI), *m/z*: calcd. for $C_{10}H_9Cl_2F_3N^+$: 270.0059 $[M+H]^+$; found: 270.0060.

2-(Chloromethyl)-1-(3-chlorophenyl)-2-(trifluoromethyl)aziridine (56)

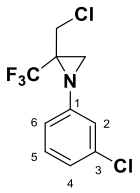

By following the General Procedure **3**, starting from ***N*-(3-chlorophenyl)-2,2,2-trifluoroethanimidoyl chloride** (500 mg, 2.0 mmol, 1.0 equiv), ICH_2Cl (1058 mg, 0.4 mL, 6.0 mmol, 3.0 equiv), MeLi-LiBr complex (1.5 M, 3.7 mL, 5.6 mmol, 2.8 equiv) and THF (10 mL), the desired product **56** was obtained in 90% yield (486 mg) as a colorless oil after chromatography on neutral alumina BG2 (*n*-hexane).

^{1}H NMR (400 MHz, $CDCl_3$) δ: 7.23 (t, *J* = 8.0 Hz, 1H, Ph H-5), 7.07 (ddd, *J* = 8.0, 2.0, 0.9 Hz, 1H, Ph H-4), 6.95 (t, *J* = 2.1 Hz, 1H, Ph H-2), 6.86 (ddd, *J* = 8.0, 2.1, 1.0 Hz, 1H, Ph H-6), 3.76 (A-part of an AB-system, $^{2}J_{AB}$ = 13.0 Hz, 1H, CH_2Cl), 3.42 (B-part of an AB system, $^{2}J_{AB}$ = 13.0 Hz, 1H, CH_2Cl), 2.83 (s, 1H, NCH_2), 2.44 (q, *J* = 1.4 Hz, 1H, NCH_2).

^{13}C NMR (100 MHz, $CDCl_3$) δ: 147.2 (Ph C-1), 135.1 (Ph C-3), 130.4 (Ph C-5), 124.2 (Ph C-4), 123.5 (q, *J* = 277.5 Hz, CF_3), 120.7 (Ph C-2), 118.9 (Ph C-6), 44.7 (q, *J* = 35.1 Hz, $\underline{C}CF_3$), 39.5 (CH_2Cl), 34.0 (q, *J* = 1.5 Hz, NCH_2).

^{19}F NMR (376 MHz, $CDCl_3$) δ: -72.3 (s, CF_3).

^{15}N NMR (40 MHz, $CDCl_3$) δ: -316.2 (aziridine N).

HRMS (ESI), *m/z*: calcd. for $C_{10}H_9Cl_2F_3N^+$: 270.0059 $[M+H]^+$; found: 270.0056.

2-(Chloromethyl)-1-(4-chlorophenyl)-2-(trifluoromethyl)aziridine (57)

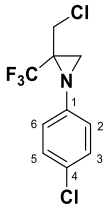

By following the General Procedure **3**, starting from ***N*-(4-chlorophenyl)-2,2,2-trifluoroethanimidoyl chloride** (250 mg, 1.0 mmol, 1.0 equiv), ICH_2Cl (547 mg, 0.2 mL, 3.1 mmol, 3.0 equiv), MeLi-LiBr complex (1.5 M, 1.8 mL, 2.9 mmol, 2.8 equiv) and THF (5 mL), the desired product **57** was obtained in 91% yield (246 mg) as a yellow oil after chromatography on neutral alumina BG2 (85:15 *v/v*, *n*-hexane/diethyl ether).

^{1}H NMR (400 MHz, $CDCl_3$) δ: 7.27 (m, 2H, Ph H-3,5), 6.90 (m, 2H, Ph H-2,6), 3.71 (A-part of an AB-system, $^2J_{AB}$ = 13.0 Hz ,1H, CH_2Cl), 3.43 (B-part of an AB-system, $^2J_{AB}$ = 13.0 Hz ,1H, CH_2Cl), 2.83 (d, *J* = 0.6 Hz, 1H, NCH_2), 2.42 (q, *J* = 1.4 Hz, 1H, NCH_2).

^{13}C NMR (100 MHz, $CDCl_3$) δ: 144.4 (Ph C-1), 129.4 (Ph C-3,5), 129.3 (Ph C-4), 123.6 (q, *J* = 277.4 Hz, CF_3), 121.9 (Ph C-2,6), 44.7 (q, *J* = 34.8 Hz, $\underline{C}CF_3$), 39.6 (CH_2Cl), 34.0 (q, *J* = 1.6 Hz, NCH_2).

^{19}F NMR (376 MHz, $CDCl_3$) δ: -72.2 (s, CF_3).

^{15}N NMR (40 MHz, $CDCl_3$) δ: -317.4 (aziridine N).

HRMS (ESI), *m/z*: calcd. for $C_{10}H_9Cl_2F_3N^+$: 270.0059 $[M+H]^+$; found: 270.0059.

2-(Chloromethyl)-1-(4-fluorophenyl)-2-(trifluoromethyl)aziridine (58)

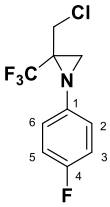

By following the General Procedure **3**, starting from ***N*-(4-fluorophenyl)-2,2,2-trifluoroethanimidoyl chloride** (393 mg, 1.7 mmol, 1.0 equiv), ICH_2Cl (900 mg, 0.4 mL, 5.1 mmol, 3.0 equiv), MeLi-LiBr complex (1.5 M, 3.2 mL, 4.8 mmol, 2.8 equiv) and THF (8 mL), the desired product **58** was obtained in 91% yield (392 mg) as a yellow oil after chromatography on neutral alumina BG2 (90:10 *v/v*, *n*-hexane/diethyl ether).

^{1}H NMR (400 MHz, $CDCl_3$) δ: 7.00 (m, 2H, Ph H-3,5), 6.92 (m, 2H, Ph H-2,6), 3.70 (dd, *J* = 13.0, 0.6 Hz, 1H, CH_2Cl), 3.42 (d, *J* = 13.0 Hz, 1H, CH_2Cl), 2.82 (d, *J* = 0.8 Hz, 1H, NCH_2), 2.42 (q, *J* = 1.5 Hz, 1H, NCH_2).

^{13}C NMR (100 MHz, $CDCl_3$) δ: 159.5 (d, *J* = 242.8 Hz, Ph C-4), 141.6 (d, *J* = 2.5 Hz, Ph C-1), 123.7 (q, *J* = 277.0 Hz, CF_3), 121.8 (d, *J* = 8.1 Hz, Ph C-2,6), 116.1 (d, *J* = 22.8 Hz, Ph C-3,5), 44.8 (q, *J* = 34.8 Hz, $\underline{C}CF_3$), 39.6 (CH_2Cl), 34.3 (q, *J* = 1.8 Hz, NCH_2).

^{19}F NMR (376 MHz, $CDCl_3$) δ: -119.2 (m, PhF), -72.2 (s, CF_3).

^{15}N NMR (40 MHz, $CDCl_3$) δ: -318.5 (aziridine N).

HRMS (ESI), *m/z*: calcd. for $C_{10}H_9ClF_4N^+$: 254.0354 $[M+H]^+$; found: 254.0355.

2-(Chloromethyl)-1-(2-isopropylphenyl)-2-(trifluoromethyl)aziridine (59)

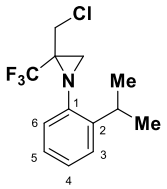

By following the General Procedure **3**, starting from **2,2,2-trifluoro-*N*-(2-isopropylphenyl)ethanimidoyl chloride** (500 mg, 2.0 mmol, 1.0 equiv), ICH_2Cl (1058 mg, 0.4 mL, 6.0 mmol, 3.0 equiv), MeLi-LiBr complex (1.5 M, 3.7 mL, 5.6 mmol, 2.8 equiv) and THF (10 mL), the desired product **59** was obtained in 74% yield (411 mg) as a yellow oil after chromatography on neutral alumina BG2 (98:02 *v/v*, *n*-hexane/diethyl ether).

^{1}H NMR (400 MHz, $CDCl_3$) δ: 7.29 (m, 1H, Ph H-3), 7.14 (m, 1H, Ph H-5), 7.13 (m, 1H, Ph H-4), 6.78 (m, 1H, Ph H-6), 3.85 (A-part of an AB-system, $^2J_{AB}$ = 13.0 Hz, 1H, CH_2Cl), 3.26 (sept, *J* = 6.8 Hz, 1H, $C\underline{H}Me_2$), 3.12 (B-part of an AB-system, $^2J_{AB}$ = 13.0 Hz, 1H, CH_2Cl), 2.80 (s, 1H, NCH_2), 2.56 (s, 1H, NCH_2), 1.26 (d, *J* = 6.8 Hz, 3H, $CHC\underline{H}_3$, attached to C at 22.3 ppm), 1.21 (d, *J* = 6.8 Hz, 3H, $CHC\underline{H}_3$, attached to C at 23.7 ppm).

^{13}C NMR (100 MHz, $CDCl_3$) δ: 142.4 (Ph C-2), 141.8 (Ph C-1), 126.6 (Ph C-5), 126.3 (Ph C-3), 124.9 (Ph C-4), 123.9 (CF_3), 119.8 (Ph C-6), 45.6 (q, *J* = 35.0 Hz, $\underline{C}CF_3$), 39.1 (CH_2Cl), 32.8 (NCH_2), 26.8 ($\underline{C}HCH_3$), 23.7 ($CH\underline{C}H_3$), 22.3 ($CH\underline{C}H_3$).

^{19}F NMR (376 MHz, $CDCl_3$) δ: -71.9 (s, CF_3).

^{15}N NMR (40 MHz, $CDCl_3$) δ: -316.3 (aziridine N).

HRMS (ESI), *m/z*: calcd. for $C_{13}H_{16}ClF_3N^+$: 278.0918 $[M+H]^+$; found: 278.0919.

2-(Chloromethyl)-1-(2,3-dimethylphenyl)-2-(trifluoromethyl)aziridine (60)

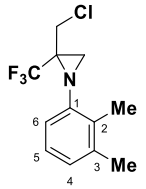

By following the General Procedure **3**, starting from ***N*-(2,3-dimethylphenyl)-2,2,2-trifluoroethanimidoyl chloride** (500 mg, 2.1 mmol, 1.0 equiv), ICH_2Cl (1111 mg, 0.5 mL, 6.3 mmol, 3.0 equiv), MeLi-LiBr complex (1.5 M, 3.9 mL, 5.9 mmol, 2.8 equiv) and THF (10 mL), the desired product **60** was obtained in 86% yield (476 mg) as a colorless oil after chromatography on neutral alumina BG2 (98:02 *v/v*, *n*-hexane/diethyl ether).

^{1}H NMR (400 MHz, $CDCl_3$) δ: 7.05 (m, 1H, Ph H-5), 6.94 (m, 1H, Ph H-4), 6.65 (m, 1H, Ph H-6), 3.82 (dd, *J* = 12.9, 1.1 Hz, 1H, CH_2Cl), 3.10 (dq, d *J* = 12.9 Hz, q *J* = 0.*8* Hz, 1H, CH_2Cl), 2.79 (d, *J* = 1.1 Hz, 1H, NCH_2), 2.53 (s, 1H, NCH_2), 2.28 (s, 3H, Ph 3-C$\underline{H}_3$), 2.20 (s, 3H, Ph 2-C$\underline{H}_3$).

^{13}C NMR (100 MHz, $CDCl_3$) δ: 143.4 (Ph C-1), 138.2 (Ph C-3), 130.2 (Ph C-2), 126.2 (Ph C-4), 126.1 (Ph C-5), 124.1 (q, *J* = 277.9 Hz, CF_3), 117.4 (Ph C-6), 45.5 (q, *J* = 34.8 Hz, $\underline{C}CF_3$), 38.9 (CH_2Cl), 33.0 (q, *J* = 1.8 Hz, NCH_2), 20.4 (Ph 3-$\underline{C}H_3$), 13.5 (Ph 2-$\underline{C}H_3$).

^{19}F NMR (376 MHz, $CDCl_3$) δ: -71.4 (s, CF_3).

^{15}N NMR (40 MHz, $CDCl_3$) δ: -314.6 (aziridine N).

HRMS (ESI), *m/z*: calcd. for $C_{12}H_{14}ClF_3N^+$: 264.0761 $[M+H]^+$; found: 264.0763.

2-(Chloromethyl)-1-(2,4-dimethylphenyl)-2-(trifluoromethyl)aziridine (61)

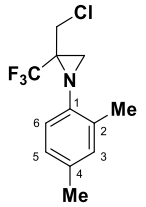

By following the General Procedure **3**, starting from ***N*-(2,4-dimethylphenyl)-2,2,2-trifluoroethanimidoyl chloride** (500 mg, 2.1 mmol, 1.0 equiv), ICH_2Cl (1111 mg, 0.5 mL, 6.3 mmol, 3.0 equiv), MeLi-LiBr complex (1.5 M, 3.9 mL, 5.9 mmol, 2.8 equiv) and THF (10 mL), the desired product **61** was obtained in 83% yield (459 mg) as a bright yellow oil after chromatography on neutral alumina BG2 (98:02 *v/v*, *n*-hexane/diethyl ether).

^{1}H NMR (400 MHz, $CDCl_3$) δ: 6.99 (m,1H, Ph H-3), 6.95 (m, 1H, Ph H-5), 6.67 (m, 1H, Ph H-6), 3.83 (dd, *J* = 12.0, 1.0 Hz, 1H, CH_2Cl), 3.13 (d, *J* = 12.9 Hz, 1H, CH_2Cl), 2.77 (s, 1H, NCH_2), 2.52 (s, 1H, NCH_2), 2.28 (s, 3H, Ph 4-C$\underline{H}_3$), 2.26 (s, 3H, Ph 2-C$\underline{H}_3$).

^{13}C NMR (100 MHz, $CDCl_3$) δ: 140.8 (Ph C-1), 133.9 (Ph C-4), 132.0 (Ph C-3), 131.6 (Ph C-2), 127.3 (Ph C-5), 124.2 (q, *J* = 277.6 Hz, CF_3), 119.4 (Ph C-6), 43.7 (q, $\underline{C}CF_3$), 38.8 (CH_2Cl), 32.8 (NCH_2), 20.6 (Ph 4-$\underline{C}H_3$), 17.7 (Ph 2-$\underline{C}H_3$).

^{19}F NMR (376 MHz, $CDCl_3$) δ: -71.7 (s, CF_3).

^{15}N NMR (40 MHz, $CDCl_3$) δ: -316.6 (aziridine N).

HRMS (ESI), *m/z*: calcd. for $C_{12}H_{14}ClF_3N^+$: 264.0761 $[M+H]^+$; found: 264.0762.

2-(Chloromethyl)-1-(2,5-dimethylphenyl)-2-(trifluoromethyl)aziridine (62)

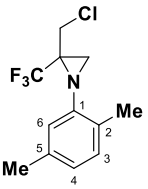

By following the General Procedure **3**, starting from ***N*-(2,5-dimethylphenyl)-2,2,2-trifluoroethanimidoyl chloride** (500 mg, 2.1 mmol, 1.0 equiv), ICH_2Cl (1111 mg, 0.5 mL, 6.3 mmol, 3.0 equiv), MeLi-LiBr complex (1.5 M, 3.9 mL, 5.9 mmol, 2.8 equiv) and THF (10 mL), the desired product **62** was obtained in 82% yield (454 mg) as a yellow oil after chromatography on neutral alumina BG2 (98:02 *v/v*, *n*-hexane/diethyl ether).

^{1}H NMR (400 MHz, $CDCl_3$) δ: 7.06 (m, 1H, Ar), 6.84 (m, 1H, Ar), 6.59 (s, 1H, Ar), 3.87 (m, 1H, CH_2Cl), 3.11 (m, 1H, CH_2Cl), 2.79 (s, 1H, NCH_2), 2.53 (s, 1H, NCH_2), 2.30 (s, 3H, CH_3), 2.24 (s, 3H, CH_3).

^{13}C NMR (100 MHz, $CDCl_3$) δ: 131.1 (Ar), 130.8 (Ar), 125.0 (Ar), 120.3 (Ar), 38.9 (CH_2Cl), 32.9 (NCH_2), 22.5 (CH_3), 19.8 (CH_3).

HRMS (ESI), *m/z*: calcd. for $C_{12}H_{14}ClF_3N^+$: 264.0761 $[M+H]^+$; found: 264.0761.

2-[2-(Chloromethyl)-2-(trifluoromethyl)-1-azidirinyl]benzonitrile (63)

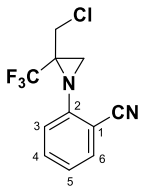

By following the General Procedure **3**, starting from ***N*-(2-cyanophenyl)-2,2,2-trifluorethanimidoyl chloride** (360 mg, 1.5 mmol, 1.0 equiv), ICH_2Cl (794 mg, 0.3 mL, 4.5 mmol, 3.0 equiv), MeLi-LiBr complex (1.5 M, 2.8 mL, 4.2 mmol, 2.8 equiv) and THF (6 mL), the desired product **63** was obtained in 89% yield (321 mg) as a yellow oil after chromatography on neutral alumina BG2 (80:20 *v/v*, *n*-hexane/diethyl ether).

^{1}H NMR (400 MHz, $CDCl_3$) δ: 7.59 (m, 1H, Ph H-6), 7.51 (m, 1H, Ph H-4), 7.14 (m, 1H, Ph H-5), 7.03 (m, 1H, Ph H-3), 4.07 (dd, *J* = 13.1, 0.7 Hz, 1H, CH_2Cl), 3.63 (d, *J* = 13.1 Hz, 1H, CH_2Cl), 3.02 (s, 1H, NCH_2), 2.78 (q, *J* = 1.4 Hz, 1H, NCH_2).

^{13}C NMR (100 MHz, $CDCl_3$) δ: 149.1 (Ph C-2), 134.0 (Ph C-6), 133.8 (Ph C-4), 123.8 (Ph C-5), 123.3 (q, *J* = 278.8 Hz, CF_3), 120.8 (Ph C-3), 116.6 (CN), 104.7 (Ph C-1), 45.8 (q, *J* = 34.7 Hz, $\underline{C}CF_3$), 39.4 (CH_2Cl), 33.9 (NCH_2).

^{19}F NMR (376 MHz, $CDCl_3$) δ: -71.0 (s, CF_3).

^{15}N NMR (40 MHz, $CDCl_3$) δ: -315.3 (aziridine N).

HRMS (ESI), *m/z*: calcd. for $C_{11}H_9ClF_3N_2^+$: 261.0400 $[M+H]^+$; found: 261.0401.

3-[2-(Chloromethyl)-2-(trifluoromethyl)-1-aziridine]benzonitrile (64)

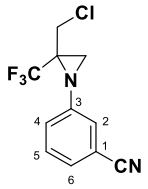

By following the General Procedure **3**, starting from ***N*-(3-cyanophenyl)-2,2,2-trifluoroethanimidoyl chloride** (495 mg, 2.1 mmol, 1.0 equiv), ICH_2Cl (1111 mg, 0.5 mL, 6.3 mmol, 3.0 equiv), MeLi-LiBr complex (1.5 M, 4.0 mL, 5.9 mmol, 2.8 equiv) and THF (10 mL), the desired product **64** was obtained in 88% yield (482 mg) as a yellow oil after chromatography on neutral alumina BG2 (70:30 *v/v*, *n*-hexane/diethyl ether).

^{1}H NMR (400 MHz, $CDCl_3$) δ: 7.67 (m, 1H, Ar), 7.52 (m, 1H, Ar), 7.40 (m, 1H, Ar), 7.21 (m, 1H, Ar), 3.71 (m, 1H, CH_2Cl), 3.56 (m, 1H, CH_2Cl), 2.87 (s, 1H, NCH_2), 2.60 (s, 1H, NCH_2).

^{13}C NMR (100 MHz, $CDCl_3$) δ: 130.2 (Ar), 129.6 (Ar), 127.6 (Ar), 125.6 (Ar), 124.3 (Ar), 120.0 (Ar), 119.5 (CN), 39.5 (CH_2Cl), 32.8 (NCH_2).

HRMS (ESI), *m/z*: calcd. for $C_{11}H_9ClF_3N_2^+$: 261.0401 $[M+H]^+$; found: 261.0403.

4-[2-(Chloromethyl)-2-(trifluoromethyl)-1-azidirinyl]benzonitrile (65)

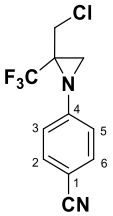

By following the General Procedure **3**, starting from ***N*-(4-cyanophenyl)-2,2,2-trifluoroethanimidoyl chloride** (500 mg, 2.1 mmol, 1.0 equiv), ICH_2Cl (1111 mg, 0.5 mL, 6.3 mmol, 3.0 equiv), MeLi-LiBr complex (1.5 M, 4.0 mL, 5.7 mmol, 2.8 equiv) and THF (10 mL), the desired product **65** was obtained in 85% yield (465 mg) as a colorless oil after chromatography on neutral alumina BG2 (70:30 *v/v*, *n*-hexane/diethyl ether).

^{1}H NMR (400 MHz, $CDCl_3$) δ: 7.59 (m, 2H, Ph H-2,6), 7.05 (m, 2H, Ph H-3,5), 3.74 (A-part of an AB-system, $^2J_{AB}$ = 13.0 Hz, 1H, CH_2Cl), 3.57 (B-part of an AB-system, $^2J_{AB}$ = 13.0 Hz, 1H, CH_2Cl), 2.88 (s, 1H, NCH_2), 2.52 (q, *J* = 1.4 Hz, 1H, NCH_2).

^{13}C NMR (100 MHz, $CDCl_3$) δ: 150.2 (Ph C-4), 133.5 (Ph C-2,6), 123.2 (q, *J* = 278.1 Hz, CF_3), 121.0 (Ph C-3,5), 118.6 (CN), 107.3 (Ph C-1), 45.0 (q, *J* = 34.9 Hz, $\underline{C}CF_3$), 39.4 (CH_2Cl), 33.8 (q, *J* = 1.9 Hz, NCH_2).

^{19}F NMR (376 MHz, $CDCl_3$) δ: -71.8 (s, CF_3).

^{15}N NMR (40 MHz, $CDCl_3$) δ: -314.2 (aziridine N).

HRMS (ESI), *m/z*: calcd. for $C_{11}H_9ClF_3N_2^+$: 261.0401 $[M+H]^+$; found: 261.0402.

2-(Chloromethyl)-1-(3-ethynylphenyl)-2-(trifluoromethyl)aziridine (66)

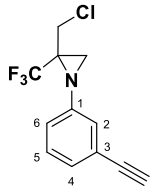

By following the General Procedure **3**, starting from ***N*-(3-ethynylphenyl)-2,2,2-trifluoroethanimidoyl chloride** (1000 mg, 4.3 mmol, 1.0 equiv), ICH_2Cl (2275 mg, 1.0 mL, 12.9 mmol, 3.0 equiv), MeLi-LiBr complex (1.5 M, 8.0 mL, 12.0 mmol, 2.8 equiv) and THF (20 mL), the desired product **66** was obtained in 92% yield (1027 mg) as an orange oil after chromatography on neutral alumina BG2 (90:10 *v/v*, *n*-hexane/diethyl ether).

^{1}H NMR (400 MHz, $CDCl_3$) δ: 7.26 (m, 1H, Ph H-5), 7.22 (m, 1H Ph H-4), 7.06 (m, 1H, Ph H-2), 6.97 (m, 1H, Ph H-6), 3.75 (A-part of an AB-system, $^2J_{AB}$ = 13.0 Hz, 1H, CH_2Cl), 3.38 (B-part of an AB-system, $^2J_{AB}$ = 13.0 Hz, 1H, CH_2Cl), 3.09 (s, 1H, ≡CH) 2.83 (s, 1H, NCH_2), 2.44 (q, *J* = 1.4 Hz, 1H, NCH_2).

^{13}C NMR (100 MHz, $CDCl_3$) δ: 145.8 (Ph C-1), 129.4 (Ph C-5), 127.8 (Ph C-4), 123.8 (Ph C-2), 123.6 (q, *J* = 277.4 Hz, CF_3), 123.3 (Ph C-3), 121.4 (Ph C-6), 82.9 ($\underline{C}$≡CH), 77.8 (C≡$\underline{C}$H), 44.6 (q, *J* = 34.9 Hz, $\underline{C}CF_3$), 39.6 (CH_2Cl), 33.9 (q, *J* = 1.8 Hz, NCH_2).

^{19}F NMR (376 MHz, $CDCl_3$) δ: -72.4 (s, CF_3).

^{15}N NMR (40 MHz, $CDCl_3$) δ: -316.4 (aziridine N).

HRMS (ESI), *m/z*: calcd. for $C_{12}H_{10}ClF_3N^+$: 260.0448 $[M+H]^+$; found: 260.0449.

2-(Chloromethyl)-1-{4-[(*E*)-phenyldiazenyl]phenyl}-2-(trifluoromethyl)aziridine (67)

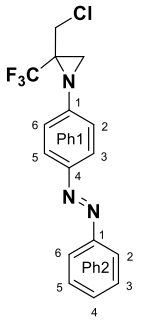

By following the General Procedure **3**, starting from **2,2,2-trifluoro-*N*-[4-(phenyldiazenyl)phenyl]ethanimidoyl chloride** (500 mg, 1.6 mmol, 1.0 equiv), ICH_2Cl (847 mg, 0.4 mL, 4.8 mmol, 3.0 equiv), MeLi-LiBr complex (1.5 M, 3.0 mL, 4.5 mmol, 2.8 equiv) and THF (10 mL), the desired product **67** was obtained in 93% yield (505 mg) as an orange solid (m.p.: 88-90 °C) after chromatography on neutral alumina BG2 (95:05 *v/v*, *n*-hexane/diethyl ether).

^{1}H NMR (400 MHz, $CDCl_3$) δ: 7.91 (m, 2H, Ph1 H-3,5), 7.89 (m, 2H, Ph2 H-2,6), 7.52 (m, 2H, Ph2 H-3,5), 7.46 (m, 1H, Ph2 H-4), 7.09 (m, 2H, Ph1 H-2,6), 3.82 (A-part of an AB-system, $^2J_{AB}$ = 13.0 Hz, 1H, CH_2Cl), 3.48 (B-part of an AB-system, $^2J_{AB}$ = 13.0 Hz, 1H, CH_2Cl), 2.91 (s, 1H, NCH_2), 2.53 (q, *J* = 1.3 Hz, 1H, NCH_2).

^{13}C NMR (100 MHz, $CDCl_3$) δ: 152.7 (Ph2 C-1), 149.3 (Ph1 C-4), 148.5 (Ph1 C-1), 130.8 (Ph2 C-4), 129.1 (Ph2 C-3,5), 124.3 (Ph1 C-3,5), 123.6 (q, *J* = 277.5 Hz, CF_3), 122.7 (Ph2 C-2,6), 120.9 (Ph1 C-2,6), 44.9 (q, *J* = 34.8 Hz, $\underline{C}CF_3$), 39.6 (CH_2Cl), 34.1 (q, *J* = 1.8 Hz, NCH_2).

^{19}F NMR (376 MHz, $CDCl_3$) δ: -72.2 (s, CF_3).

^{15}N NMR (40 MHz, $CDCl_3$) δ: -314.5 (aziridine N), diazene Ns not determined.

HRMS (ESI), *m/z*: calcd. for $C_{16}H_{14}ClF_3N_3^+$: 340.0823 $[M+H]^+$; found: 340.0824.

4-{4-[2-(Chloromethyl)-2-(trifluoromethyl)-1-azidirinyl]phenyl}morpholine (68)

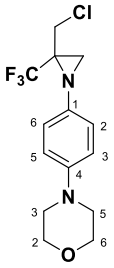

By following the General Procedure **3**, starting from **2,2,2-trifluoro-*N*-[4-(4-morpholinyl)phenyl]ethanimidoyl chloride** (500 mg, 1.7 mmol, 1.0 equiv), ICH_2Cl (900 mg, 0.4 mL, 5.1 mmol, 3.0 equiv), MeLi-LiBr complex (1.5 M, 3.2 mL, 4.8 mmol, 2.8 equiv) and THF (10 mL), the desired product **68** was obtained in 86% yield (469 mg) as a brown solid (m.p.: 89-91 °C) after chromatography on neutral alumina BG2 (60:40 *v/v*, *n*-hexane/diethyl ether).

^{1}H NMR (400 MHz, $CDCl_3$) δ: 6.88 (m, 2H, Ph H-3,5), 6.85 (m, 2H, Ph H-2,6), 3.85 (m, 4H, morph H-2,6), 3.70 (A-part of an AB-system, $^2J_{AB}$ = 13.0 Hz, 1H, CH_2Cl), 3.33 (B-part of an AB-system, $^2J_{AB}$ = 13.0 Hz, 1H, CH_2Cl), 3.10 (m, 4H, morph H-3,5), 2.78 (s, 1H, NCH_2), 2.38 (q, *J* = 1.4 Hz, 1H, NCH_2).

^{13}C NMR (100 MHz, $CDCl_3$) δ: 148.1 (Ph C-1), 138.3 (Ph C-4), 123.8 (q, *J* = 277.0 Hz, CF_3), 121.5 (Ph C-3,5), 116.8 (Ph C-2,6), 66.9 (morph C-2,6), 49.8 (morph C-3,5), 44.7 (q, *J* = 34.7 Hz, $\underline{C}CF_3$), 39.7 (CH_2Cl), 34.0 (q, *J* = 1.6 Hz, NCH_2).

^{19}F NMR (376 MHz, $CDCl_3$) δ: -72.4 (s, CF_3).

^{15}N NMR (40 MHz, $CDCl_3$) δ: -319.8 (morph N), -318.3 (aziridine N).

HRMS (ESI), *m/z*: calcd. for $C_{14}H_{17}ClF_3N_2O^+$: 321.0976 $[M+H]^+$; found: 321.0974.

1-{3-[2-(Chloromethyl)-2-(trifluoromethyl)-1-azidirinyl]phenyl}pyrrolidine (69)

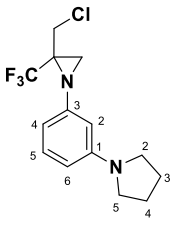

By following the General Procedure **3**, starting from **(1*Z*)-2,2,2-trifluoro-*N*-[3-(pyrrolidinyl)phenyl]ethanimidoyl chloride** (400 mg, 1.4 mmol, 1.0 equiv), ICH_2Cl (741 mg, 0.3 mL, 4.2 mmol, 3.0 equiv), MeLi-LiBr complex (1.5 M, 2.6 mL, 3.9 mmol, 2.8 equiv) and THF (8 mL), the desired product **69** was obtained in 92% yield (392 mg) as a yellow oil after chromatography on neutral alumina BG2 (90:10 *v/v*, *n*-hexane/diethyl ether).

^{1}H NMR (400 MHz, $CDCl_3$) δ: 7.11 (m, 1H, Ph H-5), 6.31 (m, Ph H-6), 6.22 (m, 1H, Ph H-4), 6.13 (br s, 1H, Ph H-2), 3.80 (dd, *J* = 12.9, 1.1 Hz, 1H, CH_2Cl), 3.29 (m, 1H, CH_2Cl), 3.28 (m, 4H, pyrr H-2,5), 2.78 (d, *J* = 1.1 Hz, 1H, NCH_2), 2.41 (q, *J* = 1.4 Hz, 1H, NCH_2), 2.01 (m, 4H, pyrr H-3,4).

^{13}C NMR (100 MHz, $CDCl_3$) δ: 148.7 (Ph C-1), 146.8 (Ph C-3), 129.9 (Ph C-5), 123.9 (q, *J* = 277.1 Hz, CF_3), 107.9 (Ph C-6), 107.6 (Ph C-4), 103.8 (Ph C-2), 47.8 (pyrr C-2,5), 44.3 (q, *J* = 35.0 Hz, $\underline{C}CF_3$), 40.0 (CH_2Cl), 34.0 (NCH_2), 25.4 (pyrr C-3,4).

^{19}F NMR (376 MHz, $CDCl_3$) δ: -72.8 (s, CF_3).

^{15}N NMR (40 MHz, $CDCl_3$) δ: -314.3 (aziridine N), -306.3 (pyrrolidine N).

HRMS (ESI), *m/z*: calcd. for $C_{14}H_{17}ClF_3N_2^+$: 305.1027 $[M+H]^+$; found: 305.1025.

1-{3-[2-(Chloromethyl)-2-(trifluoromethyl)-1-azidirinyl]phenyl}-2-pyrrolidinone (70)

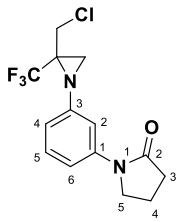

By following the General Procedure **3**, starting from **(1*Z*)-2,2,2-trifluoro-*N*-[3-(2-oxo-1-pyrrolidinyl)phenyl]ethanimidoyl chloride** (228 mg, 0.8 mmol, 1.0 equiv), ICH_2Cl (423 mg, 0.2 mL, 2.4 mmol, 3.0 equiv), MeLi-LiBr complex (1.5 M, 1.5 mL, 2.2 mmol, 2.8 equiv) and THF (5 mL), the desired product **70** was obtained in 93% yield (237 mg) as a colorless oil after chromatography on neutral alumina BG2 (50:50 *v/v*, *n*-hexane/chloroform).

^{1}H NMR (400 MHz, $CDCl_3$) δ: 7.42 (m, 1H, Ph H-2), 7.28 (m, 1H, Ph H-5), 7.25 (m, 1H, Ph H-6), 6.75 (m, 1H, Ph H-4), 3.86 (m, 2H, pyrr H-5), 3.76 (A-part of an AB-system, $^{2}J_{AB}$ = 13.0 Hz, 1H, CH_2Cl), 3.40 (B-part of an AB-system, $^{2}J_{AB}$ = 13.0 Hz, 1H, CH_2Cl), 2.83 (s, 1H, NCH_2), 2.62 (m, 2H, pyrr H-3), 2.45 (q, *J* = 1.4 Hz, 1H, NCH_2), 2.17 (m, 2H, pyrr H-4).

^{13}C NMR (100 MHz, $CDCl_3$) δ: 174.4 (pyrr C-2), 146.3 (Ph C-3), 140.5 (Ph C-1), 129.6 (Ph C-5), 123.7 (q, *J* = 277.1 Hz, CF_3), 116.6 (Ph C-4), 114.9 (Ph C-6), 112.1 (Ph C-2), 48.6 (pyrr C-5), 39.8 (CH_2Cl), 34.1 (NCH_2), 32.8 (pyrr C-3), 17.9 (pyrr C-4).

^{19}F NMR (376 MHz, $CDCl_3$) δ: -72.4 (s, CF_3).

^{15}N NMR (40 MHz, $CDCl_3$) δ: -315.4 (aziridine N), -247.9 (pyrrolidinone N).

HRMS (ESI), *m/z*: calcd. for $C_{15}H_{12}ClF_3N^+$: 319.0820 $[M+H]^+$; found: 319.0820.

2-Methyl-2-propanyl 4-[2-(chloromethyl)-2-(trifluoromethyl)-1-aziridinyl]benzoate (71)

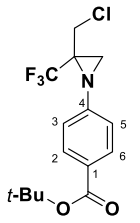

By following the General Procedure **1**, starting from **2-methyl-2-propanyl 4-{[1-chloro-2,2,2-trifluoroethylidene]amino}benzoate** (500 mg, 1.6 mmol, 1.0 equiv), ICH_2Cl (847 mg, 0.4 mL, 4.8 mmol, 3.0 equiv), MeLi-LiBr complex (1.5 M, 3.0 mL, 4.5 mmol, 2.8 equiv) and THF (10 mL), the desired product **71** was obtained in 90% yield (483 mg) as a colorless oil after chromatography on neutral alumina BG2 (95:05 *v/v*, *n*-hexane/diethyl ether).

^{1}H NMR (400 MHz, $CDCl_3$) δ: 7.94 (m, 2H, Ph H-2,6), 6.97 (m, 2H, Ph H-3,5), 3.75 (A-part of an AB-system, $^2J_{AB}$ = 13.0 Hz, 1H, CH_2Cl), 3.41 (B-part of an AB-system, $^2J_{AB}$ = 13.0 Hz, 1H, CH_2Cl), 2.86 (s, 1H, NCH_2), 2.48 (q, *J* = 1.4 Hz, 1H, NCH_2), 1.58 (s, 9H, CCH_3).

^{13}C NMR (100 MHz, $CDCl_3$) δ: 165.2 (C=O), 149.7 (Ph C-4), 130.9 (Ph C-2,6), 127.7 (Ph C-1), 123.5 (q, *J* = 277.6 Hz, CF_3), 120.0 (Ph C-3,5), 81.0 ($\underline{C}Me_3$), 44.7 (q, *J* = 34.9 Hz, $\underline{C}CF_3$), 39.5 (CH_2Cl), 33.9 (q, *J* = 1.9 Hz, NCH_2), 28.2 ($C\underline{Me}_3$).

^{19}F NMR (376 MHz, $CDCl_3$) δ: -72.2 (s, CF_3).

^{15}N NMR (40 MHz, $CDCl_3$) δ: -314.4 (aziridine N).

HRMS (ESI), *m/z*: calcd. for $C_{15}H_{17}ClF_3NO_2Na^+$: 358.0792 $[M+H]^+$; found: 358.0789.

2-(Chloromethyl)-1-(3-iodophenyl)-2-(trifluoromethyl)aziridine (72)

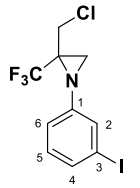

By following the General Procedure **3**, starting from **2,2,2-trifluoro-*N*-(3-iodophenyl) ethanimidoyl chloride** (500 mg, 1.5 mmol, 1.0 equiv), ICH_2Cl (794 mg, 0.3 mL, 4.5 mmol, 3.0 equiv), MeLi-LiBr complex (1.5 M, 2.8 mL, 4.2 mmol, 2.8 equiv) and THF (10 mL), the desired product **72** was obtained in 89% yield (483 mg) as a yellow oil after chromatography on neutral alumina BG2 (98:02 *v/v*, *n*-hexane/diethyl ether).

^{1}H NMR (400 MHz, $CDCl_3$) δ: 7.42 (m, 1H, Ph H-4), 7.30 (t, *J* = 1.9 Hz, 1H, Ph H-2), 7.02 (m, 1H, Ph H-5), 6.94 (m, 1H, Ph H-6), 3.75 (A-part of an AB-system, $^2J_{AB}$ = 13.0 Hz, 1H,

CH_2Cl), 3.42 (B-part of an AB-system, $^2J_{AB}$ = 13.0 Hz, 1H, CH_2Cl), 2.82 (s, 1H, NCH_2), 2.42 (q, *J* = 1.4 Hz, 1H, NCH_2).

^{13}C NMR (100 MHz, $CDCl_3$) δ: 147.2 (Ph C-1), 133.1 (Ph C-4), 130.8 (Ph C-5), 129.3 (Ph C-2), 123.5 (q, *J* = 277.5 Hz, CF_3), 120.1 (Ph C-6), 94.5 (Ph C-3), 44.7 (q, *J* = 34.9 Hz, $\underline{C}CF_3$), 39.6 (CH_2Cl), 33.9 (q, *J* = 1.9 Hz, NCH_2).

^{19}F NMR (376 MHz, $CDCl_3$) δ: -72.3 (s, CF_3).

^{15}N NMR (40 MHz, $CDCl_3$) δ: -316.4 (aziridine N).

HRMS (ESI), *m/z*: calcd. for $C_{10}H_9ClF_3IN^+$: 361.9415 $[M+H]^+$; found: 361.9412.

2-(Chloromethyl)-2-(trifluoromethyl)-1-[2-(trifluoromethyl)phenyl]aziridine (73)

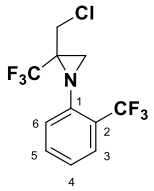

By following the General Procedure **3**, starting from **2,2,2-trifluoro-*N*-[2-(trifluoromethyl)phenyl]ethanimidoyl chloride** (270 mg, 1.0 mmol, 1.0 equiv), ICH_2Cl (529 mg, 0.2 mL, 3.0 mmol, 3.0 equiv), MeLi-LiBr complex (1.5 M, 1.9 mL, 2.8 mmol, 2.8 equiv) and THF (5 mL), the desired product **73** was obtained in 91% yield (276 mg) as a yellow oil after chromatography on neutral alumina BG2 (60:40 *v/v*, *n*-hexane/diethyl ether).

^{1}H NMR (400 MHz, $CDCl_3$) δ: 7.64 (m, 1H, Ph H-3), 7.49 (m, 1H, Ph H-5), 7.19 (m, 1H, Ph H-4), 7.00 (m, 1H, Ph H-6), 4.05 (d, *J* = 13.0 Hz, 1H, CH_2Cl), 3.22 (qd, d *J* = 13.0 Hz, q *J* = 0.9 Hz, 1H, CH_2Cl), 2.89 (s, 1H, NCH_2), 2.71 (s, 1H, NCH_2).

^{13}C NMR (100 MHz, $CDCl_3$) δ: 143.2 (q, *J* = 1.2 Hz, Ph C-1), 132.9 (Ph C-5), 127.6 (q, *J* = 5.6 Hz, Ph C-3), 123.7 (q, *J* = 272.7 Hz, $Ph\underline{C}F_3$), 123.5 (q, *J* = 278.3 Hz, aziridine-CF_3), 123.0 (q, *J* = 1.0 Hz, Ph C-4), 122.7 (q, *J* = 31.1 Hz, Ph C-2), 121.6 (Ph C-6), 46.4 (q, *J* = 35.0 Hz, $\underline{C}CF_3$), 39.6 (CH_2Cl), 33.1 (NCH_2).

^{19}F NMR (376 MHz, $CDCl_3$) δ: -71.7 (q, *J* = 4.7 Hz, aziridine-CF_3), -60.2 (q, *J* = 4.7 Hz, $PhCF_3$).

^{15}N NMR (40 MHz, $CDCl_3$) δ: -315.2 (aziridine N).

HRMS (ESI), *m/z*: calcd. for $C_{11}H_9ClF_6N^+$: 304.0322 $[M+H]^+$; found: 304. 0320.

2-(Chloromethyl)-2-(trifluoromethyl)-1-[4-(trifluoromethyl)phenyl]aziridine (74)

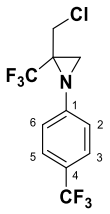

By following the General Procedure **3**, starting from **2,2,2-trifluoro-*N*-[4-(trifluoromethyl)phenyl]ethanimidoyl chloride** (170 mg, 0.6 mmol, 1.0 equiv), ICH_2Cl (318 mg, 0.1 mL, 1.8 mmol, 3.0 equiv), MeLi-LiBr complex (1.5 M, 1.1 mL, 1.7 mmol, 2.8 equiv) and THF (4 mL), the desired product **74** was obtained in 88% yield (160 mg) as a colorless oil after chromatography on neutral alumina BG2 (98:02 *v/v*, *n*-hexane/diethyl ether).

^{1}H NMR (400 MHz, $CDCl_3$) δ: 7.56 (m, 2H, Ph H-3,5), 7.05 (m, 2H, Ph H-2,6), 3.75 (A-part of an AB-system, $^{2}J_{AB}$ = 13.0 Hz, 1H, CH_2Cl), 3.48 (B-part of an AB system, $^{2}J_{AB}$ = 13.0 Hz, 1H, CH_2Cl), 2.88 (s, 1H, NCH_2), 2.49 (q, *J* = 1.4 Hz, 1H, NCH_2).

^{13}C NMR (100 MHz, $CDCl_3$) δ: 149.1 (Ph C-1), 126.7 (q, *J* = 3.8 Hz, Ph C-3,5), 126.1 (q, *J* = 32.8 Hz, Ph C-4), 124.1 (q, *J* = 271.6 Hz, Ph$\underline{C}F_3$), 123.4 (q, *J* = 277.7 Hz, CF_3), 120.6 (Ph C-2,6), 44.8 (q, *J* = 34.8 Hz, $\underline{C}CF_3$), 39.6 (CH_2Cl), 34.0 (q, *J* = 1.8 Hz, NCH_2).

^{19}F NMR (376 MHz, $CDCl_3$) δ: -72.1 (s, CF_3), -62.0 (s, $PhCF_3$).

^{15}N NMR (40 MHz, $CDCl_3$) δ: -315.4 (aziridine N).

HRMS (ESI), *m/z*: calcd. for $C_{11}H_9ClF_6N^+$: 304.0322 $[M+H]^+$; found: 304.0324.

1-(2-Biphenylyl)-2-(chloromethyl)-2-(trifluoromethyl)aziridine (75)

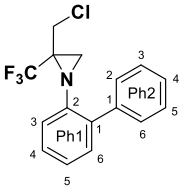

By following the General Procedure **3**, starting from ***N*-(2-biphenylyl)-2,2,2-trifluoroethanimidoyl chloride** (500 mg, 1.8 mmol, 1.0 equiv), ICH_2Cl (953 mg, 0.4 mL, 5.4 mmol, 3.0 equiv), MeLi-LiBr complex (1.5 M, 3.4 mL, 5.0 mmol, 2.8 equiv) and THF (10 mL), the desired product **75** was obtained in 92% yield (516 mg) as a yellow oil after chromatography on neutral alumina BG2 (*n*-hexane).

^{1}H NMR (400 MHz, $CDCl_3$) δ: 7.49 (m, 2H, Ph2 H-2,6), 7.43 (m, 2H, Ph2 H-3,5), 7.36 (m, 1H, Ph2 H-4), 7.30 (m, 1H, Ph1 H-4), 7.28 (m, 1H, Ph1 H-6), 7.15 (m, 1H, Ph1 H-5), 6.96

(m, 1H, Ph1 H-3), 3.62 (dd, *J* = 12.9, 1.1 Hz, 1H, CH_2Cl), 3.03 (d, *J* = 12.9 Hz, 1H, CH_2Cl), 2.60 (d, *J* = 1.1 Hz, 1H, NCH_2), 2.15 (s, 1H, NCH_2).

^{13}C NMR (100 MHz, $CDCl_3$) δ: 143.3 (Ph1 C-2), 138.7 (Ph2 C-1), 134.5 (Ph1 C-1), 131.5 (Ph1 C-6), 129.4 (Ph2 C-2,6), 128.4 (Ph2 C-3,5), 128.3 (Ph1 C-4), 127.4 (Ph2 C-4), 124.0 (Ph1 C-5), 123.5 (q, *J* = 278.0 Hz, CF_3), 120.8 (Ph1 C-3), 45.7 (q, *J* = 34.8 Hz, $\underline{C}CF_3$), 39.4 (CH_2Cl), 34.6 (NCH_2).

^{19}F NMR (376 MHz, $CDCl_3$) δ: -71.9 (s, CF_3).

^{15}N NMR (40 MHz, $CDCl_3$) δ: -314.5 (aziridine N).

HRMS (ESI), *m/z*: calcd. for $C_{16}H_{14}ClF_3N^+$: 312.0761 $[M+H]^+$; found: 312.0759.

1-(3-Biphenylyl)-2-(chloromethyl)-2-(trifluoromethyl)azidirine (76)

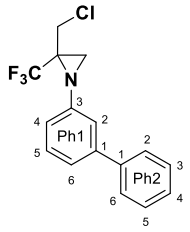

By following the General Procedure **3**, starting from ***N*-(3-biphenylyl)-2,2,2-trifluoroethanimidoyl chloride** (500 mg, 1.8 mmol, 1.0 equiv), ICH_2Cl (953 mg, 0.4 mL, 5.4 mmol, 3.0 equiv), MeLi-LiBr complex (1.5 M, 3.4 mL, 5.0 mmol, 2.8 equiv) and THF (10 mL), the desired product **76** was obtained in 85% yield (477 mg) as a colorless oil after chromatography on neutral alumina BG2 (90:10 *v/v*, *n*-hexane/chloroform).

^{1}H NMR (400 MHz, $CDCl_3$) δ: 7.59 (m, 2H, Ph2 H-2,6), 7.46 (m, 2H, Ph2 H-3,5), 7.38 (m, 2H, Ph1 H-5, Ph2 H-4), 7.33 (m, 1H, Ph1 H-6), 7.19 (m, 1H, Ph1 H-2), 6.95 (m, 1H, Ph1 H-4), 3.79 (dd, *J* = 13.0, 0.8 Hz, 1H, CH_2Cl), 3.45 (d, *J* = 13.0 Hz, 1H, CH_2Cl), 2.88 (s, 1H, NCH_2), 2.49 (q, *J* = 1.4 Hz, 1H, NCH_2).

^{13}C NMR (100 MHz, $CDCl_3$) δ: 146.2 (Ph1 C-3), 142.6 (Ph1 C-1), 140.4 (Ph2 C-1), 129.8 (Ph1 C-5), 128.8 (Ph2 C-3,5), 127.7 (Ph2 C-4), 127.1 (Ph2 C-2,6), 123.7 (q, *J* = 277.2 Hz, CF_3), 123.0 (Ph1 C-6), 119.4 (Ph1 C-2,4), 44.6 (q, *J* = 34.9 Hz, $\underline{C}CF_3$), 39.8 (CH_2Cl), 34.0 (q, *J* = 1.9 Hz, NCH_2).

^{19}F NMR (376 MHz, $CDCl_3$) δ: -72.3 (s, CF_3).

^{15}N NMR (40 MHz, $CDCl_3$) δ: -315.7 (aziridine N).

HRMS (ESI), *m/z*: calcd. for $C_{16}H_{13}ClF_3N^+$: 312.0761 $[M+H]^+$; found: 312.0759.

1-(2-Anthryl)-2-(chloromethyl)-2-(trifluoromethyl)aziridine (77)

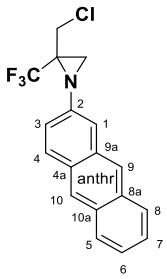

By following the General Procedure **3**, starting from ***N*-(2-anthryl)-2,2,2-trifluoroethanimidoyl chloride** (260 mg, 0.8 mmol, 1.0 equiv), ICH_2Cl (423 mg, 0.2 mL, 2.4 mmol, 3.0 equiv), MeLi-LiBr complex (1.5 M, 1.5 mL, 2.2 mmol, 2.8 equiv) and THF (5 mL), the desired product **77** was obtained in 85% yield (228 mg) as a brown solid (m.p.: 144-145 °C) after chromatography on neutral alumina BG2 (98:02 *v/v*, *n*-hexane/diethyl ether).

^{1}H NMR (400 MHz, $CDCl_3$) δ: 8.38 (s, 1H, anthr H-10), 8.30 (s, 1H, anthr H-9), 7.98 (m, 1H, anthr H-5), 7.97 (m, 1H, anthr H-8), 7.95 (d, *J* = 9.0 Hz, 1H, anthr H-4), 7.48 (m, 1H, anthr H-7), 7.44 (m, 1H, anthr H-6), 7.37 (d, *J* = 2.2 Hz, 1H, anthr H-1), 7.20 (dd, *J* = 9.0, 2.2 Hz, 1H, anthr H-3), 3.83 (dd, *J* = 13.0, 0.9 Hz, 1H, CH_2Cl), 3.40 (d, *J* = 13.0 Hz, 1H, CH_2Cl), 2.97 (d, *J* = 0.9 Hz, 1H, NCH_2), 2.62 (q, *J* = 1.4 Hz, 1H, NCH_2).

^{13}C NMR (100 MHz, $CDCl_3$) δ: 143.1 (anthr C-2), 132.3 (anthr C-8a), 131.8 (anthr C-9a), 131.2 (anthr C-10a), 130.0 (anthr C-4), 129.3 (anthr C-4a) 128.2 (anthr C-5), 127.8 (anthr C-8), 126.5 (anthr C-10), 125.9 (anthr C-7), 125.2 (anthr C-6), 124.8 (anthr C-9), 123.8 (q, *J* = 277.0 Hz, CF_3), 122.1 (anthr C-3), 115.1 (anthr C-1), 44.9 (q, *J* = 35.0 Hz, $\underline{C}CF_3$), 39.7 (CH_2Cl), 34.3 (NCH_2).

^{19}F NMR (376 MHz, $CDCl_3$) δ: -72.4 (s, CF_3).

^{15}N NMR (40 MHz, $CDCl_3$) δ: -314.1 (aziridine N).

HRMS (ESI), *m/z*: calcd. for $C_{18}H_{14}ClF_3N^+$: 336.0761 $[M+H]^+$; found: 336.0757.

2-(Chloromethyl)-1-(1-naphthalenyl)-2-(trifluoromethyl)aziridine (78)

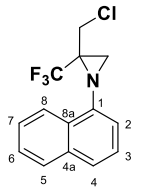

By following the General Procedure **3**, starting from **2,2,2,-trifluoro-*N*-(1-naphthalenyl) ethanimidoyl chloride** (500 mg, 1.9 mmol, 1.0 equiv), ICH_2Cl (1005 mg, 0.4 mL, 5.7 mmol, 3.0 equiv), MeLi-LiBr complex (1.5 M, 3.5 mL, 5.3 mmol, 2.8 equiv) and THF (10

mL), the desired product **78** was obtained in 84% yield (456 mg) as a colorless oil after chromatography on neutral alumina BG2 (98:02 *v/v*, *n*-hexane/diethyl ether).

^{1}H NMR (400 MHz, $CDCl_3$) δ: 8.16 (m, 1H, naphth H-8), 7.86 (m, 1H, naphth H-5), 7.63 (m, 1H, naphth H-4), 7.55 (m, 1H, naphth H-7), 7.54 (m, naphth H-6), 7.39 (m, 1H, naphth H-3), 6.94 (m, 1H, naphth H-2), 3.81 (dd, *J* = 13.1, 1.2 Hz, 1H, CH_2Cl), 2.98 (d, *J* = 1.2 Hz, 1H, NCH_2), 2.90 (d, *J* = 13.1 Hz, 1H, CH_2Cl), 2.70 (s, 1H, NCH_2).

^{13}C NMR (100 MHz, $CDCl_3$) δ: 141.7 (naphth C-1), 134.2 (naphth C-4a), 128.4 (naphth C-5), 128.2 (naphth C-8a), 126.7 (naphth C-6), 126.5 (naphth C-7), 125.5 (naphth C-3), 125.0 (naphth C-4), 124.2 (q, *J* = 277.6 Hz, CF_3), 121.9 (q, *J* = 2.2 Hz, Ph C-8), 115.8 (naphth C-2), 45.9 (q, *J* = 34.7 Hz, $\underline{C}CF_3$), 38.8 (CH_2Cl), 33.2 (q, *J* = 1.6 Hz, NCH_2).

^{19}F NMR (376 MHz, $CDCl_3$) δ: -71.6 (s, CF_3).

^{15}N NMR (40 MHz, $CDCl_3$) δ: -315.9 (aziridine N).

HRMS (ESI), *m/z*: calcd. for $C_{14}H_{12}ClF_3N^+$: 286.0605 $[M+H]^+$; found: 286.0607.

2-(Chloromethyl)-1-(4-ethoxyphenyl)-2-(trifluoromethyl)aziridine (79)

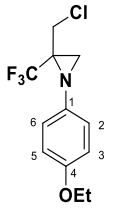

By following the General Procedure **3**, starting from ***N*-(4-ethoxyphenyl)-2,2,2-trifluoroethanimidoyl chloride** (250 mg, 1.0 mmol, 1.0 equiv), ICH_2Cl (526 mg, 0.3 mL, 2.9 mmol, 3.0 equiv), MeLi-LiBr complex (1.5 M, 1.7 mL, 2.8 mmol, 2.8 equiv) and THF (5 mL), the desired product **79** was obtained in 85% yield (238 mg) as an orange oil after chromatography on neutral alumina BG2 (98:02 *v/v*, *n*-hexane/diethyl ether).

^{1}H NMR (400 MHz, $CDCl_3$) δ: 6.87 (m, 2H, Ph H-2,6), 6.83 (m, 2H, Ph H-3,5), 3.99 (q, *J* = 7.0 Hz, 2H, $OC\underline{H}_2CH_3$), 3.70 (dd, *J* = 13.0, 0.9 Hz, 1H, CH_2Cl), 3.34 (d, *J* = 13.0 Hz, 1H, CH_2Cl), 2.78 (d, *J* = 0.6 Hz, 1H, NCH_2), 2.39 (q, *J* = 1.4 Hz, 1H, NCH_2), 1.40 (t, *J* = 7.0 Hz, 3H, $OCH_2C\underline{H}_3$).

^{13}C NMR (100 MHz, $CDCl_3$) δ: 155.7 (Ph C-4), 138.5 (Ph C-1), 123.8 (q, *J* = 276.8 Hz, CF_3), 121.6 (Ph C-2,6), 115.2 (Ph C-3,5), 63.7 ($O\underline{C}H_2CH_3$), 44.6 (q, *J* = 34.7 Hz, $\underline{C}CF_3$), 39.7 (CH_2Cl), 34.0 (NCH_2), 14.8 ($OCH_2\underline{C}H_3$).

^{19}F NMR (376 MHz, $CDCl_3$) δ: -72.5 (s, CF_3).

^{15}N NMR (40 MHz, $CDCl_3$) δ: -318.6 (aziridine N).

HRMS (ESI), *m/z*: calcd. for $C_{12}H_{14}ClF_3NO^+$: 280.0711 $[M+H]^+$; found: 280.0713.

2-(Chloromethyl)-1-(3,5-dimethoxyphenyl)-2-(trifluoromethyl)aziridine (80)

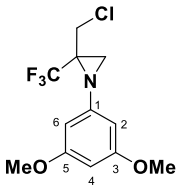

By following the General Procedure **3**, starting from ***N*-(3,5-dimethoxyphenyl)-2,2,2-trifluoroethanimidoyl chloride** (500 mg, 1.9 mmol, 1.0 equiv), ICH_2Cl (988 mg, 0.4 mL, 5.6 mmol, 3.0 equiv), MeLi-LiBr complex (1.5 M, 3.5 mL, 5.3 mmol, 2.8 equiv) and THF (10 mL), the desired product **80** was obtained in 89% yield (500 mg) as a yellow oil after chromatography on neutral alumina BG2 (98:02 *v/v*, *n*-hexane/diethyl ether).

^{1}H NMR (400 MHz, $CDCl_3$) δ: 6.19 (t, *J* = 2.2 Hz, 1H, Ph H-4), 6.11 (d, *J* = 2.2 Hz, 2H, Ph H-2,6), 3.77 (s, 6H, OCH_3), 3.76 (dd, *J* = 13.0, 0.9 Hz, 1H, CH_2Cl), 3.37 (qd, d *J* = 13.0 Hz, q *J* = 0.6 Hz, 1H, CH_2Cl), 2.78 (d, *J* = 0.9 Hz, 1H, NCH_2), 2.39 (q, *J* = 1.4 Hz, 1H, NCH_2).

^{13}C NMR (100 MHz, $CDCl_3$) δ: 161.4 (Ph C-3,5), 147.8 (Ph C-1), 123.7 (q, *J* = 277.2 Hz, CF_3), 99.2 (Ph C-2,6), 96.0 (Ph C-4), 55.4 (OCH_3), 44.6 (q, *J* = 35.0 Hz, $\underline{C}CF_3$), 39.8 (CH_2Cl), 34.0 (NCH_2).

^{19}F NMR (376 MHz, $CDCl_3$) δ: -72.6 (s, CF_3).

^{15}N NMR (40 MHz, $CDCl_3$) δ: -314.8 (NCH_2).

HRMS (ESI), *m/z*: calcd. for $C_{12}H_{14}ClF_3NO_2^+$: 296.0660 $[M+H]^+$; found: 296.0661.

2-(Chloromethyl)-2-(trifluoromethyl)-1-(4-vinylphenyl)aziridine (81)

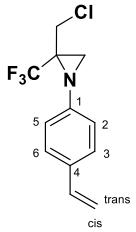

By following the General Procedure **3**, starting from ***N*-(4-ethanylphenyl)-2,2,2-trifluoroethanimidoyl chloride** (450 mg, 1.9 mmol, 1.0 equiv), ICH_2Cl (1005 mg, 0.4 mL, 5.7 mmol, 3.0 equiv), MeLi-LiBr complex (1.5 M, 3.5 mL, 5.3 mmol, 2.8 equiv) and THF (9 mL), the desired product **81** was obtained in 87% yield (432 mg) as a yellow oil after chromatography on neutral alumina BG2 (98:02 *v/v*, *n*-hexane/diethyl ether).

^{1}H NMR (400 MHz, $CDCl_3$) δ: 7.35 (m, 2H, Ph H-3,5), 6.92 (m, 2H, Ph H-2,6), 6.67 (dd, *J* = 17.6, 10.9 Hz, 1H, C<u>H</u>=CH_2), 5.68 (dd, *J* = 17.6, 0.8 Hz, 1H, CH=C<u>H</u>$_2$ trans), 5.20 (dd, *J* = 10.9, 0.8 Hz, 1H, CH=C<u>H</u>$_2$ cis), 3.75 (dd, *J* = 13.0, 0.9 Hz, 1H, CH_2Cl), 3.37 (d, *J* = 13.0 Hz, 1H, CH_2Cl), 2.83 (d, *J* = 0.9 Hz, 1H, NCH_2), 2.43 (q, *J* = 1.4 Hz, 1H, NCH_2).

^{13}C NMR (100 MHz, $CDCl_3$) δ: 145.3 (Ph C-1), 135.9 (<u>C</u>H=CH_2), 133.6 (Ph C-4), 127.2 (Ph C-3,5), 123.7 (q, *J* = 277.2 Hz, CF_3), 120.7 (Ph C-2,6), 113.1 (CH=<u>C</u>H_2), 44.6 (q, *J* = 34.9 Hz, <u>C</u>CF_3), 39.7 (CH_2Cl), 34.0 (q, *J* = 2.0 Hz, NCH_2).

^{19}F NMR (376 MHz, $CDCl_3$) δ: -72.4 (s, CF_3).

^{15}N NMR (40 MHz, $CDCl_3$) δ: -315.7 (aziridine N).

HRMS (ESI), *m/z*: calcd. for $C_{12}H_{12}ClF_3N^+$: 262.0605 $[M+H]^+$; found: 262.0606.

2-(Chloromethyl)-1-[4-(methylsulfanyl)phenyl]-2-(trifluoromethyl)aziridine (82)

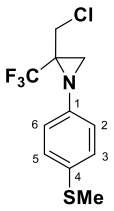

By following the General Procedure **3**, starting from **2,2,2-trifluoro-*N*-[4-(methylsulfanyl)phenyl]ethanimidoyl chloride** (415 mg, 1.6 mmol, 1.0 equiv), ICH_2Cl (847 mg, 0.4 mL, 4.8 mmol, 3.0 equiv), MeLi-LiBr complex (1.5 M, 3.0 mL, 4.5 mmol, 2.8 equiv) and THF (8 mL), the desired product **82** was obtained in 81% yield (365 mg) as a yellow oil after chromatography on neutral alumina BG2 (90:10 *v/v*, *n*-hexane/diethyl ether).

^{1}H NMR (400 MHz, $CDCl_3$) δ: 7.22 (m, 2H, Ph H-3,5), 6.89 (m, 2H, Ph H-2,6), 3.72 (dd, *J* = 13.0, 0.9 Hz, 1H, CH_2Cl), 3.37 (dd, *J* = 13.0, 0.5 Hz, 1H, CH_2Cl), 2.81 (d, *J* = 0.9 Hz, 1H, NCH_2), 2.46 (s, 3H, SCH_3), 2.40 (q, *J* = 1.4 Hz, 1H, NCH_2).

^{13}C NMR (100 MHz, $CDCl_3$) δ: 143.4 (Ph C-1), 133.4 (Ph C-4), 128.5 (Ph C-3,5), 123.7 (q, *J* = 277.2 Hz, CF_3), 121.2 (Ph C-2,6), 44.7 (q, *J* = 34.8 Hz, <u>C</u>CF_3), 39.6 (CH_2Cl), 34.0 (q, *J* = 1.9 Hz, NCH_2), 16.7 (SCH_3).

^{19}F NMR (376 MHz, $CDCl_3$) δ: -72.3 (s, CF_3).

^{15}N NMR (40 MHz, $CDCl_3$) δ: -316.9 (aziridine N).

HRMS (ESI), *m/z*: calcd. for $C_{11}H_{12}ClF_3NS^+$: 282.0326 $[M+H]^+$; found: 282.0328.

1-(1,3-Benzodioxol-5-yl)-2-(chloromethyl)-2-(trifluoromethyl)aziridine (83)

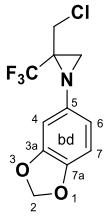

By following the General Procedure **3**, starting from ***N*-(1,3-benzodioxol-5-yl)-2,2,2-trifluoroethanimidoyl chloride** (500 mg, 2.0 mmol, 1.0 equiv), ICH_2Cl (1058 mg, 0.4 mL, 6.0 mmol, 3.0 equiv), MeLi-LiBr complex (1.5 M, 3.7 mL, 5.6 mmol, 2.8 equiv) and THF (10 mL), the desired product **83** was obtained in 86% yield (480 mg) as an orange oil after chromatography on neutral alumina BG2 (95:05 *v/v*, *n*-hexane/diethyl ether).

^{1}H NMR (400 MHz, $CDCl_3$) δ: 6.72 (d, *J* = 8.2 Hz, 1H, bd H-7), 6.51 (d, *J* = 2.2 Hz, 1H, bd H-4), 6.37 (dd, *J* = 8.2, 2.2 Hz, 1H, bd H-6), 5.952 (A-part of an AB-system, $^2J_{AB}$ = 1.4 Hz, 1H, bd H-2), 5.946 (B-part of an AB-system, $^2J_{AB}$ = 1.4 Hz, 1H, bd H-2), 3.74 (dd, *J* = 13.0, 0.9 Hz, 1H, CH_2Cl), 3.37 (d, *J* = 13.0 Hz, 1H, CH_2Cl), 2.78 (d, *J* = 0.9 Hz, 1H, NCH_2), 2.38 (q, *J* = 1.4 Hz, 1H, NCH_2).

^{13}C NMR (100 MHz, $CDCl_3$) δ: 148.4 (bd C-3a), 144.4 (bd C-7a), 140.2 (bd C-5), 123.7 (q, *J* = 277.0 Hz, CF_3), 112.6 (bd C-6), 108.4 (bd C-7), 102.6 (bd C-4), 101.4 (bd C-2), 44.8 (q, *J* = 34.8 Hz, $\underline{C}CF_3$), 39.6 (CH_2Cl), 34.3 (q, *J* = 1.8 Hz, NCH_2).

^{19}F NMR (376 MHz, $CDCl_3$) δ: -72.5 (s, CF_3).

^{15}N NMR (40 MHz, $CDCl_3$) δ: -317.1 (aziridine N).

HRMS (ESI), *m/z*: calcd. for $C_{11}H_{10}ClF_3NO_2^+$: 280.0346 $[M+H]^+$; found: 280.0344.

2-(Chloromethyl)-1-phenyl-2-(trifluoromethyl)aziridine (84)

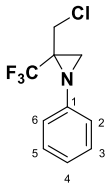

By following the General Procedure **3**, starting from ***N*-phenyl-2,2,2-trifluoroethanimidoyl chloride** (250 mg, 1.2 mmol, 1.0 equiv), ICH_2Cl (635 mg, 0.3 mL, 3.6 mmol, 3.0 equiv), MeLi-LiBr complex (1.5 M, 2.1 mL, 3.4 mmol, 2.8 equiv) and THF (5 mL), the desired product **84** was obtained in 93% yield (263 mg) as a colorless oil after chromatography on neutral alumina BG2 (98:02 *v/v*, *n*-hexane/diethyl ether).

^{1}H NMR (400 MHz, $CDCl_3$) δ: 7.31 (m, 2H, Ph H-3,5), 7.09 (m, 1H, Ph H-4), 6.96 (m, 2H, Ph H-2,6), 3.76 (dd, *J* = 13.0, 0.9 Hz ,1H, CH_2Cl), 3.34 (dq, d *J* = 13.0 Hz, q *J* = 0.5 Hz, 1H, CH_2Cl), 2.83 (d, *J* = 0.9 Hz, 1H, NCH_2), 2.44 (q, *J* = 1.4 Hz, 1H, NCH_2).

^{13}C NMR (100 MHz, $CDCl_3$) δ: 145.7 (Ph C-1), 129.4 (Ph C-3,5), 124.0 (Ph C-4), 123.7 (q, *J* = 277.2 Hz, CF_3), 120.6 (Ph C-2,6), 44.5 (q, *J* = 34.8 Hz, $\underline{C}CF_3$), 39.7 (CH_2Cl), 33.9 (NCH_2).

^{19}F NMR (376 MHz, $CDCl_3$) δ: -72.5 (s, CF_3).

^{15}N NMR (40 MHz, $CDCl_3$) δ: -315.7 (aziridine N).

HRMS (ESI), *m/z*: calcd. for $C_{10}H_{10}ClF_3N^+$: 236.0448 $[M+H]^+$; found: 236.0447.

3.1.4 General Procedure 4 and spectral data of Fluoromethylaziridines 85-91

Scheme 29- To a cooled (-78 °C) solution of trifluoromethylchloroimidate (1.5 equiv) in dry THF chloroiodomethane (1.0 equiv) was added. After 2 min, an ethereal solution of MeLi-LiBr (2.0 equiv, 1.5 M) was added dropwise, using a syringe pump (flow: 0.200 mL/min). The resulting solution was stirred for 1 h. Afterwards, fluoroiodomethane (1.5 equiv) in dry THF: Et_2O (1:1) was added to the reaction mixture. After 2 min, an ethereal solution of MeLi-LiBr (2.0 equiv, 1.5 M) was added dropwise, using a syringe pump (flow: 0.200 mL/min). The resulting solution was stirred for 5 minutes. Then 10% aq solution $NaHCO_3$ (2 mL/mmol substrate) was added and the reaction mixture was extracted with Et_2O (2 x 5 mL) and washed with water (5 mL) and brine (10 mL). The organic phase was dried over anhydrous Na_2SO_4, filtered and, after removal of the solvent under reduced pressure, the so-obtained crude mixture was subjected to chromatography to afford pure compounds.

1-(3-Bromophenyl)-2-(fluoromethyl)-2-(trifluoromethyl)aziridine (85)

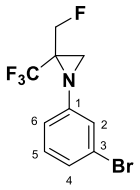

By following the General Procedure **4**, starting from ***N*-(3-bromophenyl)-2,2,2-trifluoroethanimidoyl chloride** (250 mg, 0.8 mmol, 1.5 equiv), ICH_2Cl (88 mg, 0.04 mL, 0.5 mmol, 1.0 equiv), MeLi-LiBr complex (1.5 M, 0.6 mL, 1.0 mmol, 2.0 equiv) and THF (3 mL), ICH_2F (128 mg, 0.05 mL, 0.8 mmol, 1.5 equiv), MeLi-LiBr complex (1.5 M, 0.6 mL, 1.0 mmol, 2.0 equiv) and THF:Et_2O (1:1 mL), the desired product **85** was obtained in 90% yield (215 mg) as a green oil after chromatography on neutral alumina BG2 (90:10 *v/v*, *n*-hexane/diethylether).

^{1}H NMR (400 MHz, $CDCl_3$) δ: 7.21 (m, 1H, Ph H-4), 7.16 (m, 1H, Ph H-5), 7.14 (m, 1H, Ph H-2), 6.96 (m, 1H, Ph H-6), 4.73 (dd, *J* = 48.3, 11.4 Hz, 1H, CH_2F), 4.40 (ddq, d *J* = 46.0, 11.4 Hz, q *J* = 1.0 Hz, 1H, CH_2F), 2.76 (d, *J* = 5.1 Hz, 1H, NCH_2), 2.32 (s, 1H, NCH_2).

^{13}C NMR (100 MHz, $CDCl_3$) δ: 147.7 (Ph C-1), 130.6 (Ph C-5), 127.0 (Ph C-4), 123.6 (d, *J* = 1.4 Hz, Ph C-2), 122.8 (Ph C-3) 119.5 (d, *J* = 1.8 Hz, Ph C-6), 78.6 (d, *J* = 178.0 Hz, CH_2F), 43.7 (dq, q *J* = 35.5 Hz, d *J* = 21.8 Hz, $\underline{C}CF_3$), 31.1 (m, NCH_2).

^{19}F NMR (376 MHz, $CDCl_3$) δ: -226.1 (m, CH_2F), -72.4 (d, *J* = 5.5 Hz, CF_3).

^{15}N NMR (40 MHz, $CDCl_3$) δ: -322.6 (aziridine N).

HRMS (ESI), *m/z*: calcd. for $C_{10}H_9BrF_4N^+$: 297.9850 $[M+H]^+$; found: 297.9851.

1-(4-Chlorophenyl)-2-(fluoromethyl)-2-(trifluoromethyl)azidirine (86)

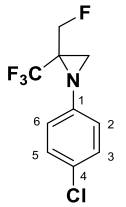

By following the General Procedure **4**, starting from ***N*-(4-chlorophenyl)-2,2,2-trifluoroethanimidoyl chloride** (150 mg, 0.6 mmol, 1.5 equiv), ICH_2Cl (71 mg, 0.03 mL, 0.4 mmol, 1.0 equiv), MeLi-LiBr complex (1.5 M, 0.5 mL, 0.8 mmol, 2.0 equiv) and THF (2 mL), ICH_2F (96 mg, 0.04 mL, 0.6 mmol, 1.5 equiv), MeLi-LiBr complex (1.5 M, 0.5 mL, 0.8 mmol, 2.0 equiv) and THF:Et_2O (0.5:0.5 mL), the desired product **86** was obtained in 82% yield (125 mg) as a colorless oil after chromatography on neutral alumina BG2 (90:10 *v/v*, *n*-hexane/diethyl ether).

^{1}H NMR (400 MHz, $CDCl_3$) δ: 7.26 (m, 2H, Ph H-3,5), 6.94 (m, 2H, Ph H-2,6), 4.73 (dd, *J* = 48.3, 11.3 Hz, 1H, CH_2F), 4.37 (ddq, d *J* = 45.9, 11.3 Hz, q *J* = 1.1 Hz, 1H, CH_2F), 2.76 (d, *J* = 5.2 Hz, 1H, NCH_2), 2.30 (m, 1H, NCH_2).

^{13}C NMR (100 MHz, $CDCl_3$) δ: 144.9 (Ph C-1), 129.4 (Ph C-3,5), 129.2 (Ph C-4), 123.3 (q, *J* = 280.0 Hz, CF_3) 122.0 (d, *J* = 1.7 Hz, Ph C-2,6), 78.6 (d, *J* = 177.9 Hz, CH_2F), 43.7 (dq, d *J* = 22.0 Hz, q *J* = 35.3 Hz, $\underline{C}CF_3$), 31.2 (m, NCH_2).

^{19}F NMR (376 MHz, $CDCl_3$) δ: -226.0 (m, CH_2F), -72.4 (d, *J* = 5.0 Hz, CF_3).

^{15}N NMR (40 MHz, $CDCl_3$) δ: -323.7 (aziridine N).

HRMS (ESI), *m/z*: calcd. for $C_{10}H_9ClF_4N^+$: 254. 0354 $[M+H]^+$; found: 254.0356.

4-[2-(Fluoromethyl)-2-(trifluoromethyl)-1-azidirinyl]benzonitrile (87)

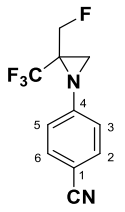

By following the General Procedure **4**, starting from ***N*-(4-cyanophenyl)-2,2,2-trifluoroethenimidoyl chloride** (1000 mg, 4.3 mmol, 1.5 equiv), ICH_2Cl (511 mg, 0.2 mL, 2.9 mmol, 1.0 equiv), MeLi-LiBr complex (1.5 M, 3.8 mL, 5.7 mmol, 2.0 equiv) and THF (10 mL), ICH_2F (688 mg, 0.3 mL, 4.3 mmol, 1.5 equiv), MeLi-LiBr complex (1.5 M, 3.8 mL, 5.7 mmol, 2.0 equiv) and THF:Et_2O (5:5 mL), the desired product **87** was obtained in 79% yield (830 mg) as a brown oil after chromatography on neutral alumina BG2 (95:05 *v/v*, *n*-hexane/ethylacetate).

^{1}H NMR (400 MHz, $CDCl_3$) δ: 7.60 (m, 2H, Ph H-2,6), 7.08 (m, 2H, Ph H-3,5), 4.82 (dd, *J* = 48.3, 11.4 Hz, 1H, CH_2F), 4.39 (dd, *J* = 45.7, 11.4 Hz, CH_2F), 2.84 (d, *J* = 5.1 Hz, 1H, NCH_2), 2.38 (m, 1H, NCH_2).

^{13}C NMR (100 MHz, $CDCl_3$) δ: 150.6 (Ph C-4), 133.5 (Ph C-2,6), 123.0 (dq, q *J* = 277.2 Hz, d *J* = 2.2 Hz, CF_3), 121.2 (d, *J* = 1.8 Hz, Ph C-3,5), 118.7 (C≡N), 107.3 (Ph C-1), 78.4 (d, *J* = 178.6 Hz, CH_2F), 44.0 (dq, q *J* = 35.6 Hz, d *J* = 21.6 Hz, $\underline{C}CF_3$), 31.1 (m, NCH_2).

^{19}F NMR (376 MHz, $CDCl_3$) δ: -226.6 (m, CH_2F), -72.3 (d, *J* = 5.5 Hz, CF_3).

^{15}N NMR (40 MHz, $CDCl_3$) δ: -319.5 (aziridine N).

HRMS (ESI), *m/z*: calcd. for $C_{11}H_9F_4N_2^+$: 245.0696 $[M+H]^+$; found: 245.0694.

4-{4-[2-(Fluoromethyl)-2-(trifluoromethyl)-1-azidirinyl]phenyl}morpholine (88)

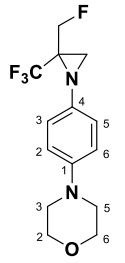

By following the General Procedure **4**, starting from **2,2,2-trifluoro-*N*-[4-(4-morpholinyl)phenyl]ethanimidoyl chloride** (250 mg, 0.8 mmol, 1.5 equiv), ICH_2Cl (88 mg, 0.04 mL, 0.5 mmol, 1.0 equiv), MeLi-LiBr complex (1.5 M, 0.6 mL, 1.0 mmol, 2.0 equiv) and THF (3 mL), ICH_2F (128 mg, 0.05 mL, 0.8 mmol, 1.5 equiv), MeLi-LiBr complex (1.5 M, 0.6 mL, 1.0 mmol, 2.0 equiv) and THF:Et_2O (1:1 mL), the desired

product **88** was obtained in 84% yield (204 mg) as a colorless oil after chromatography on neutral alumina BG2 (80:20 *v/v*, *n*-hexane/chloroform).

^{1}H NMR (400 MHz, $CDCl_3$) δ: 6.92 (m, 2H, Ph H-3,5), 6.85 (m, 2H, Ph H-2,6), 4.65 (dd, *J* = 48.4, 11.2 Hz, 1H, CH_2F), 4.37 (dd, *J* = 46.3, 11.2 Hz, 1H, CH_2F), 3.85 (m, 4H, morph H-2,6), 3.10 (m, 4H, morph H-3,5) 2.71 (d, *J* = 5.2 Hz, 1H, NCH_2), 2.28 (m, 1H, NCH_2).

^{13}C NMR (100 MHz, $CDCl_3$) δ: 147.9 (Ph C-1), 138.9 (Ph C-4), 121.5 (Ph C-3,5), 116.8 (Ph C-2,6), 79.0 (CH_2F), 66.9 (morph C-2,6$_2$), 49.9 (morph C-3,5), 31.2 (m, NCH_2).

^{19}F NMR (376 MHz, $CDCl_3$) δ: -225.5 (t, *J* = 48.4 Hz, CH_2F), -72.4 (s, CF_3).

HRMS (ESI), *m/z*: calcd. for $C_{14}H_{17}F_4N_2O^+$: 305.1272 $[M+H]^+$; found: 305.1273.

2-Methyl-2-propanyl-4-[2-(fluoromethyl)-2-(trifluoromethyl)-1-azidirinyl]benzoate (89)

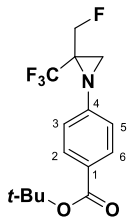

By following the General Procedure **4**, starting from **2-methyl-2-propanyl 4-[(1-chloro-2,2,2-trifluoroethylidene)amino]benzoate** (350 mg, 1.1 mmol, 1.5 equiv), ICH_2Cl (123 mg, 0.05 mL, 0.7 mmol, 1.0 equiv), MeLi-LiBr complex (1.5 M, 1.5 mL, 2.2 mmol, 2.0 equiv) and THF (3.5 mL), ICH_2F (112 mg, 0.05 mL, 0.7 mmol, 1.5 equiv), MeLi-LiBr complex (1.5 M, 1.5 mL, 2.2 mmol, 2.0 equiv) and THF:Et_2O (1.5:1.5 mL), the desired product **89** was obtained in 88% yield (309 mg) as a colorless oil after chromatography on neutral alumina BG2 (80:20 *v/v*, *n*-hexane/chloroform).

^{1}H NMR (400 MHz, $CDCl_3$) δ: 7.94 (m, 2H, Ph H-2,6), 7.01 (m, 2H, Ph H-3,5), 4.72 (dd, *J* = 48.2, 11.3 Hz, 1H, CH_2F), 4.40 (ddq, d *J* = 46.0, 11.3 Hz, q *J* = 0.9 Hz, 1H, CH_2F), 2.81 (d, *J* = 5.0 Hz, 1H, NCH_2), 2.37 (m, 1H, NCH_2), 1.58 (s, 9H, CCH_3).

^{13}C NMR (100 MHz, $CDCl_3$) δ: 165.2 (C=O), 150.2 (Ph C-4), 130.9 (Ph C-2,6), 127.7 (Ph C-1), 123.2 (q, *J* = 277.0 Hz, CF_3) 120.2 (Ph C-3,5), 80.9 ($\underline{C}CH_3$), 78.6 (d, *J* = 177.7 Hz, CH_2F), 43.8 (dq, q *J* = 35.6 Hz, d *J* = 22.0 Hz, $\underline{C}CF_3$), 31.2 (m, NCH_2), 28.2 ($C\underline{C}H_3$).

^{19}F NMR (376 MHz, $CDCl_3$) δ: -226.2 (m, CH_2F), -72.4 (d, *J* = 5.7 Hz, CF_3).

^{15}N NMR (40 MHz, $CDCl_3$) δ: -320.7 (aziridine N).

HRMS (ESI), *m/z*: calcd. for $C_{15}H_{18}F_4NO_2^+$: 320.1268 $[M+H]^+$; found: 320.1270.

1-(3-Biphenylyl)-2-(fluoromethyl)-2-(trifluoromethyl)aziridine (90)

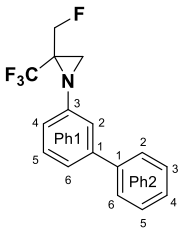

By following the General Procedure **4**, starting from ***N*-(2-biphenylyl)-2,2,2-trifluoroethanimidoyl chloride** (100 mg, 0.4 mmol, 1.5 equiv), ICH_2Cl (53 mg, 0.02 mL, 0.3 mmol, 1.0 equiv), MeLi-LiBr complex (1.5 M, 0.5 mL, 0.8 mmol, 2.0 equiv) and THF (1.5 mL), ICH_2F (64 mg, 0.03 mL, 0.4 mmol, 1.5 equiv), MeLi-LiBr complex (1.5 M, 0.5 mL, 0.8 mmol, 2.0 equiv) and THF:Et_2O (0.5:0.5 mL), the desired product **90** was obtained in 89% yield (105 mg) as a yellow oil after chromatography on neutral alumina BG2 (90:10 *v/v*, *n*-hexane/ethylacetate).

^{1}H NMR (400 MHz, $CDCl_3$) δ: 7.57 (m, 2H, Ph2 H-2,6), 7.45 (m, 2H, Ph2 H-3,5), 7.36 (m, 2H, Ph1 H-5, Ph2 H-4), 7.31 (m, 1H, Ph1 H-6), 7.21 (m, 1H, Ph1 H-2), 6.98 (m, 1H, Ph1 H-4), 4.73 (dd, *J* = 48.3, 11.3 Hz, 1H, CH_2F), 4.46 (dd, d *J* = 46.3, 11.3 Hz, 1H, CH_2F), 2.80 (d, *J* = 5.1 Hz, 1H, NCH_2), 2.37 (s, 1H, NCH_2).

^{13}C NMR (100 MHz, $CDCl_3$) δ: 146.7 (Ph1 C-3), 142.5 (Ph1 C-1), 140.5 (Ph2 C-1), 129.7 (Ph1 C-5), 128.8 (Ph2 C-3,5), 127.6 (Ph2 C-4), 127.1 (Ph2 C-2,6), 123.5 (q, *J* = 276.8 Hz, CF_3) 122.8 (Ph1 C-6), 119.5 (Ph1 C-4), 119.4 (Ph1 C-2), 78.9 (d, *J* = 176.9 Hz, CH_2F), 43.6 (m, $\underline{C}CF_3$), 31.2 (m, NCH_2).

^{19}F NMR (376 MHz, $CDCl_3$) δ: -225.5 (m, CH_2F), -72.4 (s, CF_3).

^{15}N NMR (40 MHz, $CDCl_3$) δ: -322.5 (aziridine N).

HRMS (ESI), *m/z*: calcd. for $C_{16}H_{14}F_4N^+$: 296.1057 $[M+H]^+$; found: 296.1059.

2-(Fluoromethyl)-1-phenyl-2-(trifluoromethyl)aziridine (91)

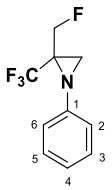

By following the General Procedure **4**, starting from ***N*-phenyl-2,2,2-trifluoroethanimidoyl chloride** (628 mg, 3.1 mmol, 1.5 equiv), ICH_2Cl (370 mg, 0.2 mL, 2.1 mmol, 1.0 equiv), MeLi-LiBr complex (1.5 M, 4.1 mL, 6.2 mmol, 2.0 equiv) and THF (3 mL), ICH_2F (496 mg, 0.2 mL, 3.1 mmol, 1.5 equiv), MeLi-LiBr complex (1.5 M, 4.1 mL, 6.2 mmol, 2.0 equiv) and THF:Et_2O (3:3 mL), the desired product **91** was obtained in

87% yield (591 mg) as a yellow oil after chromatography on neutral alumina BG2 (90:10 *v/v*, *n*-hexane/chloroform).

^{1}H NMR (400 MHz, $CDCl_3$) δ: 7.30 (m, 2H, Ph H-3,5), 7.08 (m, 1H, Ph H-4), 7.00 (m, 2H, Ph H-2,6), 4.66 (dd, *J* = 48.3, 11.4 Hz, 1H, CH_2F), 4.42 (dd, *J* = 46.2, 11.4 Hz, 1H, CH_2F), 2.76 (d, *J* = 5.1 Hz, 1H, NCH_2), 2.33 (s, 1H, NCH_2).

^{13}C NMR (100 MHz, $CDCl_3$) δ: 146.2 (Ph C-1), 129.3 (Ph C-3,5), 123.9 (Ph C-4), 120.6 (Ph C-2,6), 78.8 (d, *J* = 177.0 Hz, CH_2F), 43.3 (m, $\underline{C}CF_3$), 31.1 (m, NCH_2), $\underline{C}F_3$ not found.

^{19}F NMR (376 MHz, $CDCl_3$) δ: -225.7 (m, CH_2F), -72.5 (s, CF_3).

^{15}N NMR (40 MHz, $CDCl_3$) δ: -322.8 (aziridine N).

HRMS (ESI), *m/z*: calcd. for $C_{10}H_{10}F_4N^+$: 220.0744 $[M+H]^+$; found: 220.0746.

3.1.5 General procedure and spectral data of 2-(chloromethyl)-1-[4-(methylsulfinyl) phenyl]-2-(trifluoromethyl)aziridine (92)

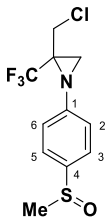

Scheme 30a- By following the procedure reported by Kaiser and co-workers,[323] to a solution of **2-(chloromethyl)-1-[4-(methylsulfanyl)phenyl]-2-(trifluoromethyl) aziridine** (20 mg, 0.07 mmol, 1.0 equiv) and iron(III) chloride (0.4 mg, 0.002 mmol, 0.03 equiv) in acetonitrile (0.5 mL, 1M), periodic acid (18 mg, 0.08 mmol, 1.1 equiv) was added at 0 °C. The resulting mixture was cooled to room temperature and stirred for 3 hours. Saturated aq solution of $Na_2S_2O_3$ was added and extracted with CH_2Cl_2 (3x5 mL). The organic phase was dried over anhydrous Na_2SO_4, filtered and, after removal of the solvent under reduced pressure, the so-obtained crude mixture was subjected to chromatography on neutral alumina BG2 (90:10 v/v, n-hexane/diethyl ether) to afford pure compound **92** in 89% yield (18 mg) as a colorless oil (mixture of diastereomers).

^{1}H NMR (400 MHz, $CDCl_3$) δ: 7.60 (m, 2H, Ph H-3,5), 7.11 (m, 2H, Ph H-2,6), 3.75 (d, *J* = 13.0 Hz, 1H, CH_2Cl), 3.50/3.49 (d, *J* = 13.0 Hz, 1H, CH_2Cl), 3.49 (d, *J* = 13.0 Hz, 1H, CH_2Cl), 2.88 (s, 1H, NCH_2), 2.72 (s, 3H, SCH_3), 2.50 (s, 1H, NCH_2).

^{13}C NMR (100 MHz, $CDCl_3$) δ: 148.75/148.73 (Ph C-1), 140.62/140.59 (Ph C-4), 125.13/125.10 (Ph C-3,5), 123.4 (q, *J* = 277.8 Hz, CF_3), 121.4 (Ph C-2,6), 44.8 (q, *J* = 34.8 Hz, $\underline{C}CF_3$), 43.9 (SCH_3), 39.58/39.55 (CH_2Cl), 34.0 (s, NCH_2).

^{19}F NMR (376 MHz, $CDCl_3$) δ: -72.04 (s, CF_3), -71.98 (s, CF_3).

^{15}N NMR (40 MHz, $CDCl_3$) δ: -315.5 (aziridine N).

HRMS (ESI), *m/z*: calcd. for $C_{11}H_{11}ClF_3NOSNa^+$: 320.0094 $[M+Na]^+$; found: 320.0097.

3.1.6 General procedur and spectral data of 1-{3-[2-(chloromethyl)-2-(trifluoromethyl) -1-azidirinyl]phenyl}ethanone (93)

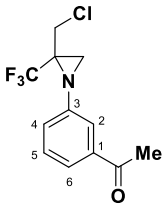

Scheme 30b- By following the procedure reported by Das and coworkers,[324] AuCl (3.0 mg, 0.01 mmol, 0.05 equiv, 5 mol%) was added to MeOH (0.5 mL) under argon atmosphere. The reaction mixture was stirred for 5 minutes and then 2-(chloromethyl)-1-(3-ethynylphenyl)-2-(trifluoromethyl)aziridine (50 mg, 0.2 mmol, 1.0 equiv) was added followed by defined amount of distilled H_2O (4.0 equiv). The resulting mixture was heated overnight at 65 °C and then quenched with water and extracted with CH_2Cl_2 (3 x 5 mL). The organic phase was dried over anhydrous Na_2SO_4, filtered and, after removal of the solvent under reduced pressure, the so-obtained crude mixture was subjected to chromatography on neutral alumina BG2 (50:50 *v/v*, *n*-hexane/chloroform) to afford pure compound **93** in 90% yield (50 mg) as a colorless oil.

^{1}H NMR (400 MHz, $CDCl_3$) δ: 7.67 (m, 1H, Ph H-6), 7.53 (m, 1H, Ph H-2), 7.41 (m, 1H, Ph H-5), 7.21 (m, 1H, Ph H-4), 3.70 (A-part of an AB-system, $^2J_{AB}$ = 13.0 Hz, 1H, CH_2Cl), 3.49 (B-part of an AB-system, $^2J_{AB}$ = 11.6 Hz, 1H, CH_2Cl), 2.87 (s, 1H, NCH_2), 2.60 (s, 3H, $COCH_3$), 2.50 (s, 1H, NCH_2).

^{13}C NMR (100 MHz, $CDCl_3$) δ: 197.5 (C=O), 146.3 (Ph C-3), 138.3 (Ph C-1), 129.6 (Ph C-5), 125.6 (Ph C-4), 124.3 (Ph C-6), 123.5 (q, *J* = 277.5 Hz, CF_3), 119.5 (Ph C-2), 44.7 (q, *J* = 34.7 Hz, $\underline{C}CF_3$), 39.7 (CH_2Cl), 34.0 (NCH_2), 26.7 (CH_3).

^{19}F NMR (376 MHz, $CDCl_3$) δ: -72.0 (s, CF_3).

^{15}N NMR (40 MHz, $CDCl_3$) δ: -316.8 (aziridine N).

HRMS (ESI), *m/z*: calcd. for $C_{12}H_{12}ClF_3NO^+$: 278.0554 $[M+H]^+$; found: 278.0552.

3.1.7 General procedur and spectral data of N^2-allyl-N^1-butyl-2-(chloromethyl)-3,3,3-trifluoro-N^2-{4-[(*E*)-phenyldiazenyl]phenyl}-1,2-propanediamine (94)

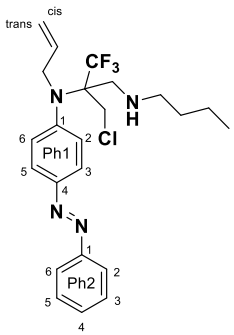

Scheme 30c- By following the procedure reported by Katagiri and coworkers,[326] a solution of allyl iodide (141 mg, 0.8 mmol, 3.5 equiv) in CH_2Cl_2 (0.5 mL) was added to a mixture of **2-(chloromethyl)-1-{4-[(*E*) phenyldiazenyl] phenyl}-2-(trifluoromethyl) aziridine** (80 mg, 0.2 mmol, 1.0 equiv) and $AgBF_4$ (140 mg, 0.7 mmol, 3.0 equiv) in CH_2Cl_2 (0.5 mL) under argon atmosphere at 0 °C. After the reaction mixture was stirred for 15 minutes at 0 °C, *n*-$BuNH_2$ (296 mg, 4.0 mmol, 0.4 mL, 16.6 equiv) was added in one portion. After 10 minutes, the mixture was poured into water and extracted with Et_2O (3 x 5 mL). The organic phase was dried over anhydrous Na_2SO_4, filtered and, after removal of the solvent under reduced pressure, the so-obtained crude mixture was subjected to chromatography on neutral alumina BG2 (50:50 *v/v*, *n*-hexane/chloroform) to afford pure compound **94** in 78% yield (71 mg) as an orange oil.

^{1}H NMR (400 MHz, $CDCl_3$) δ: 7.90 (m, 2H, Ph2 H-2,6), 7.84 (m, 2H, Ph1 H-3,5), 7.52 (m, 2H, Ph2 H-3,5), 7.47 (m, 1H, Ph2, H-4), 7.39 (m, 2H, Ph1 H-2,6), 5.67 (m, 1H, C$\underline{H}$$CH_2$), 4.95 (d, *J* =17.2 Hz, 1H, CHC$\underline{H}_2$), 4.88 (d, *J* = 10.1 Hz, 1H, CHC$\underline{H}_2$), 4.08 (A-part of an AB-system, $^2J_{AB}$ = 11.6 Hz, 1H, CH_2Cl), 4.01 (m, 2H, NCH_2), 3.94 (B-part of an AB-system, $^2J_{AB}$ = 11.6 Hz, 1H, CH_2Cl), 2.98 (A-part of an AB-system, $^2J_{AB}$ = 13.3 Hz, 1H, NHC$\underline{H}_2$), 2.84 (B-part of an AB-system, $^2J_{AB}$ = 13.3 Hz, 1H, $NHCH_2$), 2.55 (m, 2H, NHC$\underline{H}_2CH_2CH_2$), 1.38 (m, 2H, $NHCH_2C\underline{H}_2CH_2$), 1.29 (m, 2H, $NHCH_2CH_2C\underline{H}_2$), 0.88 (t, *J* = 7.2 Hz, 3H, CH_3).

^{13}C NMR (100 MHz, $CDCl_3$) δ: 152.7 (Ph2 C-1), 150.4 (Ph1 C-4), 147.7 (Ph1 C-1), 135.9 (C$\underline{H}$=CH_2), 131.8 (Ph1 C-2,6), 130.9 (Ph2 C-4), 129.1 (Ph2 C-3,5), 127.3 (q, *J* = 293.7 Hz, CF_3), 122.9 (Ph1 C-3,5), 122.8 (Ph2 C-2,6), 116.9 (CH=C$\underline{H}_2$), 67.2 (q, *J* = 22.4 Hz, C$\underline{C}F_3$), 53.2 (CH_2=CH$\underline{C}H_2$), 50.1 (NH$\underline{C}H_2CH_2CH_2$), 49.2 ($NHCH_2$), 43.1 (CH_2Cl), 32.2 ($NHCH_2\underline{C}H_2CH_2$), 20.2 ($NHCH_2CH_2\underline{C}H_2$), 13.9 ($CH_3$).

^{19}F NMR (376 MHz, $CDCl_3$) δ: -69.8 (s, CF_3).

^{15}N NMR (40 MHz, $CDCl_3$) δ: -336.0 (NH), -331.7 (NCH_2), 125.6 (Ph2-$\underline{N}$=N), 124.9 (N=$\underline{N}$-Ph1).

HRMS (ESI), *m/z*: calcd. for $C_{23}H_{29}ClF_3N_4^+$: 453.2027 $[M+H]^+$; found: 453.2025.

BIBLIOGRAPHY

[1] M. Kanteev, M. Goldfeder, A. Fishman, Structure-function correlations in tyrosinases, Protein science : a publication of the Protein Society, 24 (2015) 1360-1369.
[2] V.S. *The PyMol Molecular Graphics System,* LLC: Cambridge, MA, 2017.
[3] F. Solano, On the Metal Cofactor in the Tyrosinase Family, International journal of molecular sciences, 19 (2018).
[4] K. Lerch, Protein and active-site structure of tyrosinase, Progress in clinical and biological research, 256 (1988) 85-98.
[5] C.M. Marusek, N.M. Trobaugh, W.H. Flurkey, J.K. Inlow, Comparative analysis of polyphenol oxidase from plant and fungal species, Journal of inorganic biochemistry, 100 (2006) 108-123.
[6] K. Schaerlaekens, M. Schierova, E. Lammertyn, N. Geukens, J. Anne, L. Van Mellaert, Twin-arginine translocation pathway in Streptomyces lividans, Journal of bacteriology, 183 (2001) 6727-6732.
[7] K. Lerch, Primary structure of tyrosinase from Neurospora crassa. II. Complete amino acid sequence and chemical structure of a tripeptide containing an unusual thioether, The Journal of biological chemistry, 257 (1982) 6414-6419.
[8] C.W. van Gelder, W.H. Flurkey, H.J. Wichers, Sequence and structural features of plant and fungal tyrosinases, Phytochemistry, 45 (1997) 1309-1323.
[9] S.M. Newman, N.T. Eannetta, H. Yu, J.P. Prince, M.C. de Vicente, S.D. Tanksley, J.C. Steffens, Organisation of the tomato polyphenol oxidase gene family, Plant molecular biology, 21 (1993) 1035-1051.
[10] G. Hind, D.R. Marshak, S.J. Coughlan, Spinach thylakoid polyphenol oxidase: cloning, characterization, and relation to a putative protein kinase, Biochemistry, 34 (1995) 8157-8164.
[11] C. Jimenez-Cervantes, J.C. Garcia-Borron, J.A. Lozano, F. Solano, Effect of detergents and endogenous lipids on the activity and properties of tyrosinase and its related proteins, Biochimica et biophysica acta, 1243 (1995) 421-430.
[12] M. Fairhead, L. Thony-Meyer, Role of the C-terminal extension in a bacterial tyrosinase, The FEBS journal, 277 (2010) 2083-2095.
[13] C. Kaintz, S.G. Mauracher, A. Rompel, Type-3 copper proteins: recent advances on polyphenol oxidases, Advances in protein chemistry and structural biology, 97 (2014) 1-35.
[14] T.S. Chang, An updated review of tyrosinase inhibitors, International journal of molecular sciences, 10 (2009) 2440-2475.
[15] J.C. Garcia-Borron, F. Solano, Molecular anatomy of tyrosinase and its related proteins: beyond the histidine-bound metal catalytic center, Pigment cell research, 15 (2002) 162-173.
[16] C.A. Ramsden, P.A. Riley, Tyrosinase: the four oxidation states of the active site and their relevance to enzymatic activation, oxidation and inactivation, Bioorganic & medicinal chemistry, 22 (2014) 2388-2395.
[17] E.J. Land, C.A. Ramsden, P.A. Riley, The mechanism of suicide-inactivation of tyrosinase: a substrate structure investigation, The Tohoku journal of experimental medicine, 212 (2007) 341-348.
[18] C. Dietler, Lerch, K., Oxidases and Related Redox Systems, Pergamon Press, New York, 1982.
[19] K.G. Strothkamp, R.L. Jolley, H.S. Mason, Quaternary structure of mushroom tyrosinase, Biochemical and biophysical research communications, 70 (1976) 519-524.
[20] K. Lerch, Neurospora tyrosinase: structural, spectroscopic and catalytic properties, Molecular and cellular biochemistry, 52 (1983) 125-138.
[21] L.A. Muller, Hinz, U., and Zryd J. P. , Characterization of a tyrosinase from Amanita muscaria involved in betalain biosynthesis, Phytochemistry, 42 (1996) 1511-1515.
[22] K. Kanda, T. Sato, S. Ishii, H. Enei, S. Ejiri, Purification and properties of tyrosinase isozymes from the gill of Lentinus edodes fruiting body, Bioscience, biotechnology, and biochemistry, 60 (1996) 1273-1278.

[23] M. Nakamura, T. Nakajima, Y. Ohba, S. Yamauchi, B.R. Lee, E. Ichishima, Identification of copper ligands in Aspergillus oryzae tyrosinase by site-directed mutagenesis, The Biochemical journal, 350 Pt 2 (2000) 537-545.
[24] S. Halaouli, M. Asther, K. Kruus, L. Guo, M. Hamdi, J.C. Sigoillot, A. Lomascolo, Characterization of a new tyrosinase from Pycnoporus species with high potential for food technological applications, Journal of applied microbiology, 98 (2005) 332-343.
[25] R.O. De Faria, Moure V. R., Balmant, W., Amazonas, M. A. L. D. A., Krieger, N., and Mitchell, D. A., The tyrosinase produced by *Lentinula boryana* (Berk. & Mont.) pegler suffers substrate inhibition by L-DOPA, Food Technology and Biotechnology, 45 (2007) 334-340.
[26] K.U. Zaidi, A.S. Ali, S.A. Ali, I. Naaz, Microbial tyrosinases: promising enzymes for pharmaceutical, food bioprocessing, and environmental industry, Biochemistry research international, 2014 (2014) 854687.
[27] W.T. Ismaya, H.J. Rozeboom, A. Weijn, J.J. Mes, F. Fusetti, H.J. Wichers, B.W. Dijkstra, Crystal structure of Agaricus bisporus mushroom tyrosinase: identity of the tetramer subunits and interaction with tropolone, Biochemistry, 50 (2011) 5477-5486.
[28] W.H. Flurkey, J.K. Inlow, Proteolytic processing of polyphenol oxidase from plants and fungi, Journal of inorganic biochemistry, 102 (2008) 2160-2170.
[29] B. Hazes, K.A. Magnus, C. Bonaventura, J. Bonaventura, Z. Dauter, K.H. Kalk, W.G. Hol, Crystal structure of deoxygenated Limulus polyphemus subunit II hemocyanin at 2.18 A resolution: clues for a mechanism for allosteric regulation, Protein science : a publication of the Protein Society, 2 (1993) 597-619.
[30] G. Della Cioppa, Garger, S. J., Sverlow, G. G., Turpen, T. II, Grill L. K., and Chedekal, M. R., Melanin production by *Streptomyces*, in, 1998.
[31] A.M. McMahon, E.M. Doyle, S. Brooks, K.E. O'Connor, Biochemical characterisation of the coexisting tyrosinase and laccase in the soil bacterium Pseudomonas putida F6, Enzyme Microb Tech, 40 (2007) 1435-1441.
[32] Y. Matoba, T. Kumagai, A. Yamamoto, H. Yoshitsu, M. Sugiyama, Crystallographic evidence that the dinuclear copper center of tyrosinase is flexible during catalysis, The Journal of biological chemistry, 281 (2006) 8981-8990.
[33] M. Sendovski, M. Kanteev, V.S. Ben-Yosef, N. Adir, A. Fishman, First structures of an active bacterial tyrosinase reveal copper plasticity, Journal of molecular biology, 405 (2011) 227-237.
[34] A. Janovitz-Klapp, Richard, F., and Nicolas, J., Polyphenoloxidase from apple, partial purification and some properties, Phytochemistry, 28 (1989) 2903-2907.
[35] J. Raymond, N. Rakariyatham, J.L. Azanza, Purification and Some Properties of Polyphenoloxidase from Sunflower Seeds, Phytochemistry, 34 (1993) 927-931.
[36] J.L. Lee, K.H. Kong, S.H. Cho, Purification and characterization of tyrosinase from Solanum melongena, J Biochem Mol Biol, 30 (1997) 150-156.
[37] N. Rani, B. Joy, T.E. Abraham, Cell suspension cultures of Portulaca grandiflora as potent catalysts for biotransformation of L-tyrosine into L-DOPA, an anti-Parkinson's drug, Pharm Biol, 45 (2007) 48-53.
[38] X. Lai, H.J. Wichers, M. Soler-Lopez, B.W. Dijkstra, Structure and Function of Human Tyrosinase and Tyrosinase-Related Proteins, Chemistry, 24 (2018) 47-55.
[39] X. Lai, M. Soler-Lopez, H.J. Wichers, B.W. Dijkstra, Large-Scale Recombinant Expression and Purification of Human Tyrosinase Suitable for Structural Studies, PloS one, 11 (2016) e0161697.
[40] X. Lai, H.J. Wichers, M. Soler-Lopez, B.W. Dijkstra, Structure of Human Tyrosinase Related Protein 1 Reveals a Binuclear Zinc Active Site Important for Melanogenesis, Angew Chem Int Ed Engl, 56 (2017) 9812-9815.
[41] C. Jimenez-Cervantes, F. Solano, T. Kobayashi, K. Urabe, V.J. Hearing, J.A. Lozano, J.C. Garcia-Borron, A new enzymatic function in the melanogenic pathway. The 5,6-dihydroxyindole-2-carboxylic acid oxidase activity of tyrosinase-related protein-1 (TRP1), The Journal of biological chemistry, 269 (1994) 17993-18000.

[42] P. Aroca, J.C. Garcia-Borron, F. Solano, J.A. Lozano, Regulation of mammalian melanogenesis. I: Partial purification and characterization of a dopachrome converting factor: dopachrome tautomerase, Biochimica et biophysica acta, 1035 (1990) 266-275.
[43] K. Tsukamoto, I.J. Jackson, K. Urabe, P.M. Montague, V.J. Hearing, A second tyrosinase-related protein, TRP-2, is a melanogenic enzyme termed DOPAchrome tautomerase, The EMBO journal, 11 (1992) 519-526.
[44] P. Aroca, F. Solano, J.C. Garcia-Borron, J.A. Lozano, Specificity of dopachrome tautomerase and inhibition by carboxylated indoles. Considerations on the enzyme active site, The Biochemical journal, 277 (Pt 2) (1991) 393-397.
[45] C. Olivares, F. Solano, New insights into the active site structure and catalytic mechanism of tyrosinase and its related proteins, Pigment cell & melanoma research, 22 (2009) 750-760.
[46] K. Urabe, P. Aroca, K. Tsukamoto, D. Mascagna, A. Palumbo, G. Prota, V.J. Hearing, The inherent cytotoxicity of melanin precursors: a revision, Biochimica et biophysica acta, 1221 (1994) 272-278.
[47] Q. Michard, S. Commo, J. Rocchetti, F. El Houari, A.M. Alleaume, K. Wakamatsu, S. Ito, B.A. Bernard, TRP-2 expression protects HEK cells from dopamine- and hydroquinone-induced toxicity, Free radical biology & medicine, 45 (2008) 1002-1010.
[48] V. del Marmol, F. Beermann, Tyrosinase and related proteins in mammalian pigmentation, FEBS letters, 381 (1996) 165-168.
[49] T. Pillaiyar, V. Namasivayam, M. Manickam, S.H. Jung, Inhibitors of Melanogenesis: An Updated Review, Journal of medicinal chemistry, (2018).
[50] R. Halaban, R.S. Patton, E. Cheng, S. Svedine, E.S. Trombetta, M.L. Wahl, S. Ariyan, D.N. Hebert, Abnormal acidification of melanoma cells induces tyrosinase retention in the early secretory pathway, The Journal of biological chemistry, 277 (2002) 14821-14828.
[51] K. Ray, M. Chaki, M. Sengupta, Tyrosinase and ocular diseases: some novel thoughts on the molecular basis of oculocutaneous albinism type 1, Progress in retinal and eye research, 26 (2007) 323-358.
[52] G.M. Halliday, A. Ophof, M. Broe, P.H. Jensen, E. Kettle, H. Fedorow, M.I. Cartwright, F.M. Griffiths, C.E. Shepherd, K.L. Double, Alpha-synuclein redistributes to neuromelanin lipid in the substantia nigra early in Parkinson's disease, Brain : a journal of neurology, 128 (2005) 2654-2664.
[53] W. Pan, S. Kwak, Y. Liu, Y. Sun, Z. Fang, B. Qin, Y. Yamamoto, Traditional chinese medicine improves activities of daily living in Parkinson's disease, Parkinson's disease, 2011 (2011) 789506.
[54] S.J. Lubbe, V. Escott-Price, A. Brice, T. Gasser, A.M. Pittman, J. Bras, J. Hardy, P. Heutink, N.M. Wood, A.B. Singleton, D.G. Grosset, C.B. Carroll, M.H. Law, F. Demenais, M.M. Iles, D.T. Bishop, J. Newton-Bishop, N.M. Williams, H.R. Morris, Rare variants analysis of cutaneous malignant melanoma genes in Parkinson's disease, Neurobiology of aging, 48 (2016) 222 e221-222 e227.
[55] T. Pillaiyar, M. Manickam, V. Namasivayam, Skin whitening agents: medicinal chemistry perspective of tyrosinase inhibitors, Journal of enzyme inhibition and medicinal chemistry, 32 (2017) 403-425.
[56] H. Ando, H. Kondoh, M. Ichihashi, V.J. Hearing, Approaches to identify inhibitors of melanin biosynthesis via the quality control of tyrosinase, The Journal of investigative dermatology, 127 (2007) 751-761.
[57] S.H. Kidson, J.B. De Haan, Effect of thymidine analogs on tyrosinase activity and mRNA accumulation in mouse melanoma cells, Experimental cell research, 188 (1990) 36-41.
[58] B.B. Fuller, I. Niekrasz, G.E. Hoganson, Down-regulation of tyrosinase mRNA levels in melanoma cells by tumor promoters and by insulin, Molecular and cellular endocrinology, 72 (1990) 81-87.

[59] T. Kuzumaki, A. Matsuda, K. Wakamatsu, S. Ito, K. Ishikawa, Eumelanin biosynthesis is regulated by coordinate expression of tyrosinase and tyrosinase-related protein-1 genes, Experimental cell research, 207 (1993) 33-40.
[60] H. Ando, A. Itoh, Y. Mishima, M. Ichihashi, Correlation between the number of melanosomes, tyrosinase mRNA levels, and tyrosinase activity in cultured murine melanoma cells in response to various melanogenesis regulatory agents, Journal of cellular physiology, 163 (1995) 608-614.
[61] M. Martinez-Esparza, C. Jimenez-Cervantes, F. Beermann, P. Aparicio, J.A. Lozano, J.C. Garcia-Borron, Transforming growth factor-beta1 inhibits basal melanogenesis in B16/F10 mouse melanoma cells by increasing the rate of degradation of tyrosinase and tyrosinase-related protein-1, The Journal of biological chemistry, 272 (1997) 3967-3972.
[62] M. Martinez-Esparza, C. Jimenez-Cervantes, F. Solano, J.A. Lozano, J.C. Garcia-Borron, Mechanisms of melanogenesis inhibition by tumor necrosis factor-alpha in B16/F10 mouse melanoma cells, European journal of biochemistry, 255 (1998) 139-146.
[63] M. Tachibana, K. Takeda, Y. Nobukuni, K. Urabe, J.E. Long, K.A. Meyers, S.A. Aaronson, T. Miki, Ectopic expression of MITF, a gene for Waardenburg syndrome type 2, converts fibroblasts to cells with melanocyte characteristics, Nature genetics, 14 (1996) 50-54.
[64] C. Jimenez-Cervantes, M. Martinez-Esparza, C. Perez, N. Daum, F. Solano, J.C. Garcia-Borron, Inhibition of melanogenesis in response to oxidative stress: transient downregulation of melanocyte differentiation markers and possible involvement of microphthalmia transcription factor, Journal of cell science, 114 (2001) 2335-2344.
[65] D.S. Kim, S.Y. Kim, J.H. Chung, K.H. Kim, H.C. Eun, K.C. Park, Delayed ERK activation by ceramide reduces melanin synthesis in human melanocytes, Cellular signalling, 14 (2002) 779-785.
[66] D.S. Kim, S.H. Park, S.B. Kwon, S.W. Youn, K.C. Park, Effects of lysophosphatidic acid on melanogenesis, Chemistry and physics of lipids, 127 (2004) 199-206.
[67] G. Imokawa, Y. Mishima, Loss of melanogenic properties in tyrosinases induced by glucosylation inhibitors within malignant melanoma cells, Cancer research, 42 (1982) 1994-2002.
[68] G. Imokawa, Analysis of initial melanogenesis including tyrosinase transfer and melanosome differentiation through interrupted melanization by glutathione, The Journal of investigative dermatology, 93 (1989) 100-107.
[69] M. Terao, K. Tomita, T. Oki, L. Tabe, M. Gianni, E. Garattini, Inhibition of melanogenesis by BMY-28565, a novel compound depressing tyrosinase activity in B16 melanoma cells, Biochemical pharmacology, 43 (1992) 183-189.
[70] J. Franchi, M.C. Coutadeur, C. Marteau, M. Mersel, A. Kupferberg, Depigmenting effects of calcium D-pantetheine-S-sulfonate on human melanocytes, Pigment cell research, 13 (2000) 165-171.
[71] S.M. Petrescu, N. Branza-Nichita, G. Negroiu, A.J. Petrescu, R.A. Dwek, Tyrosinase and glycoprotein folding: roles of chaperones that recognize glycans, Biochemistry, 39 (2000) 5229-5237.
[72] S.M. Petrescu, A.J. Petrescu, H.N. Titu, R.A. Dwek, F.M. Platt, Inhibition of N-glycan processing in B16 melanoma cells results in inactivation of tyrosinase but does not prevent its transport to the melanosome, The Journal of biological chemistry, 272 (1997) 15796-15803.
[73] N. Branza-Nichita, A.J. Petrescu, R.A. Dwek, M.R. Wormald, F.M. Platt, S.M. Petrescu, Tyrosinase folding and copper loading in vivo: a crucial role for calnexin and alpha-glucosidase II, Biochemical and biophysical research communications, 261 (1999) 720-725.
[74] H. Saeki, A. Oikawa, Synthesis and degradation of tyrosinase in cultured melanoma cells, Journal of cellular physiology, 104 (1980) 171-175.
[75] J.L. Wilmer, F.G. Burleson, F. Kayama, J. Kanno, M.I. Luster, Cytokine induction in human epidermal keratinocytes exposed to contact irritants and its relation to chemical-induced inflammation in mouse skin, The Journal of investigative dermatology, 102 (1994) 915-922.

[76] K.F. Sachsenmeier, N. Sheibani, S.J. Schlosser, B.L. Allen-Hoffmann, Transforming growth factor-beta 1 inhibits nucleosomal fragmentation in human keratinocytes following loss of adhesion, The Journal of biological chemistry, 271 (1996) 5-8.
[77] K. Nakamura, M. Yoshida, H. Uchiwa, Y. Kawa, M. Mizoguchi, Down-regulation of melanin synthesis by a biphenyl derivative and its mechanism, Pigment cell research, 16 (2003) 494-500.
[78] A. Kageyama, M. Oka, T. Okada, S. Nakamura, T. Ueyama, N. Saito, V.J. Hearing, M. Ichihashi, C. Nishigori, Down-regulation of melanogenesis by phospholipase D2 through ubiquitin proteasome-mediated degradation of tyrosinase, The Journal of biological chemistry, 279 (2004) 27774-27780.
[79] A.M. Hall, L. Krishnamoorthy, S.J. Orlow, 25-hydroxycholesterol acts in the Golgi compartment to induce degradation of tyrosinase, Pigment cell research, 17 (2004) 396-406.
[80] H. Ando, Y. Funasaka, M. Oka, A. Ohashi, M. Furumura, J. Matsunaga, N. Matsunaga, V.J. Hearing, M. Ichihashi, Possible involvement of proteolytic degradation of tyrosinase in the regulatory effect of fatty acids on melanogenesis, Journal of lipid research, 40 (1999) 1312-1316.
[81] G. Imokawa, T. Kobayashi, M. Miyagishi, K. Higashi, Y. Yada, The role of endothelin-1 in epidermal hyperpigmentation and signaling mechanisms of mitogenesis and melanogenesis, Pigment cell research, 10 (1997) 218-228.
[82] T. Yokota, H. Nishio, Y. Kubota, M. Mizoguchi, The inhibitory effect of glabridin from licorice extracts on melanogenesis and inflammation, Pigment cell research, 11 (1998) 355-361.
[83] K. Maeda, M. Naganuma, Topical trans-4-aminomethylcyclohexanecarboxylic acid prevents ultraviolet radiation-induced pigmentation, Journal of photochemistry and photobiology. B, Biology, 47 (1998) 136-141.
[84] S. Ferro, G. Certo, L. De Luca, M.P. Germano, A. Rapisarda, R. Gitto, Searching for indole derivatives as potential mushroom tyrosinase inhibitors, Journal of enzyme inhibition and medicinal chemistry, 31 (2016) 398-403.
[85] F.W. Parrish, B.J. Wiley, E.G. Simmons, L. Long, Jr., Production of aflatoxins and kojic acid by species of Aspergillus and Penicillium, Applied microbiology, 14 (1966) 139.
[86] S.Y. Lee, N. Baek, T.G. Nam, Natural, semisynthetic and synthetic tyrosinase inhibitors, Journal of enzyme inhibition and medicinal chemistry, 31 (2016) 1-13.
[87] S.G. Waley, Kinetics of suicide substrates. Practical procedures for determining parameters, The Biochemical journal, 227 (1985) 843-849.
[88] F. Garcia-Canovas, J. Tudela, R. Varon, A.M. Vazquez, Experimental methods for kinetic study of suicide substrates, Journal of enzyme inhibition, 3 (1989) 81-90.
[89] I. Kubo, I. Kinst-Hori, S.K. Chaudhuri, Y. Kubo, Y. Sanchez, T. Ogura, Flavonols from Heterotheca inuloides: tyrosinase inhibitory activity and structural criteria, Bioorganic & medicinal chemistry, 8 (2000) 1749-1755.
[90] I. Kubo, I. Kinsthori, K. Ishiguro, S.K. Chaudhuri, Y. Sanchez, T. Ogura, Tyrosinase Inhibitory Flavonoids from Heterotheca Inuloides and Their Structural Functions, Bioorg Med Chem Lett, 4 (1994) 1443-1446.
[91] L.P. Xie, Q.X. Chen, H. Huang, H.Z. Wang, R.Q. Zhang, Inhibitory effects of some flavonoids on the activity of mushroom tyrosinase, Biochemistry. Biokhimiia, 68 (2003) 487-491.
[92] J.K. No, D.Y. Soung, Y.J. Kim, K.H. Shim, Y.S. Jun, S.H. Rhee, T. Yokozawa, H.Y. Chung, Inhibition of tyrosinase by green tea components, Life sciences, 65 (1999) PL241-246.
[93] Y.J. Kim, Rhamnetin attenuates melanogenesis by suppressing oxidative stress and pro-inflammatory mediators, Biological & pharmaceutical bulletin, 36 (2013) 1341-1347.
[94] I. Kubo, I. Kinst-Hori, Flavonols from saffron flower: tyrosinase inhibitory activity and inhibition mechanism, Journal of agricultural and food chemistry, 47 (1999) 4121-4125.
[95] H. Matsuda, K. Tokuoka, J. Wu, T. Tanaka, M. Kubo, Inhibitory effects of methanolic extract from corydalis tuber against types I-IV allergic models, Biological & pharmaceutical bulletin, 18 (1995) 963-967.

[96] H. Gao, J. Nishida, S. Saito, J. Kawabata, Inhibitory effects of 5,6,7-trihydroxyflavones on tyrosinase, Molecules, 12 (2007) 86-97.
[97] C. Zhang, Y. Lu, L. Tao, X. Tao, X. Su, D. Wei, Tyrosinase inhibitory effects and inhibition mechanisms of nobiletin and hesperidin from citrus peel crude extracts, Journal of enzyme inhibition and medicinal chemistry, 22 (2007) 91-98.
[98] K. Itoh, N. Hirata, M. Masuda, S. Naruto, K. Murata, K. Wakabayashi, H. Matsuda, Inhibitory effects of Citrus hassaku extract and its flavanone glycosides on melanogenesis, Biological & pharmaceutical bulletin, 32 (2009) 410-415.
[99] Y.B. Ryu, T.J. Ha, M.J. Curtis-Long, H.W. Ryu, S.W. Gal, K.H. Park, Inhibitory effects on mushroom tyrosinase by flavones from the stem barks of Morus lhou (S.) Koidz, Journal of enzyme inhibition and medicinal chemistry, 23 (2008) 922-930.
[100] S.H. Jeong, Y.B. Ryu, M.J. Curtis-Long, H.W. Ryu, Y.S. Baek, J.E. Kang, W.S. Lee, K.H. Park, Tyrosinase inhibitory polyphenols from roots of Morus lhou, Journal of agricultural and food chemistry, 57 (2009) 1195-1203.
[101] E.T. Arung, K. Shimizu, R. Kondo, Inhibitory effect of artocarpanone from Artocarpus heterophyllus on melanin biosynthesis, Biological & pharmaceutical bulletin, 29 (2006) 1966-1969.
[102] Z.P. Zheng, K.W. Cheng, J.T. To, H. Li, M. Wang, Isolation of tyrosinase inhibitors from Artocarpus heterophyllus and use of its extract as antibrowning agent, Molecular nutrition & food research, 52 (2008) 1530-1538.
[103] M. Miyazawa, N. Tamura, Inhibitory compound of tyrosinase activity from the sprout of Polygonum hydropiper L. (Benitade), Biological & pharmaceutical bulletin, 30 (2007) 595-597.
[104] T. Masuda, D. Yamashita, Y. Takeda, S. Yonemori, Screening for tyrosinase inhibitors among extracts of seashore plants and identification of potent inhibitors from Garcinia subelliptica, Bioscience, biotechnology, and biochemistry, 69 (2005) 197-201.
[105] H.J. Kim, S.H. Seo, B.G. Lee, Y.S. Lee, Identification of tyrosinase inhibitors from Glycyrrhiza uralensis, Planta medica, 71 (2005) 785-787.
[106] S. Baek, J. Kim, D. Kim, C. Lee, D.K. Chung, Inhibitory effect of dalbergioidin isolated from the trunk of Lespedeza cyrtobotrya on melanin biosynthesis, Journal of microbiology and biotechnology, 18 (2008) 874-879.
[107] J.H. Kim, M.R. Kim, E.S. Lee, C.H. Lee, Inhibitory effects of calycosin isolated from the root of Astragalus membranaceus on melanin biosynthesis, Biological & pharmaceutical bulletin, 32 (2009) 264-268.
[108] B. Fu, H. Li, X. Wang, F.S. Lee, S. Cui, Isolation and identification of flavonoids in licorice and a study of their inhibitory effects on tyrosinase, Journal of agricultural and food chemistry, 53 (2005) 7408-7414.
[109] X. Zhang, X. Hu, A. Hou, H. Wang, Inhibitory effect of 2,4,2',4'-tetrahydroxy-3-(3-methyl-2-butenyl)-chalcone on tyrosinase activity and melanin biosynthesis, Biological & pharmaceutical bulletin, 32 (2009) 86-90.
[110] K. Shimizu, R. Kondo, K. Sakai, Inhibition of tyrosinase by flavonoids, stilbenes and related 4-substituted resorcinols: structure-activity investigations, Planta medica, 66 (2000) 11-15.
[111] Q.X. Chen, L.N. Ke, K.K. Song, H. Huang, X.D. Liu, Inhibitory effects of hexylresorcinol and dodecylresorcinol on mushroom (Agaricus bisporus) tyrosinase, Protein J, 23 (2004) 135-141.
[112] M. Takahashi, K. Takara, T. Toyozato, K. Wada, A novel bioactive chalcone of Morus australis inhibits tyrosinase activity and melanin biosynthesis in B16 melanoma cells, Journal of oleo science, 61 (2012) 585-592.
[113] S.K. Radhakrishnan, R.G. Shimmon, C. Conn, A.T. Baker, Azachalcones: a new class of potent polyphenol oxidase inhibitors, Bioorg Med Chem Lett, 25 (2015) 1753-1756.
[114] S.K. Radhakrishnan, R.G. Shimmon, C. Conn, A.T. Baker, Evaluation of Novel Chalcone Oximes as Inhibitors of Tyrosinase and Melanin Formation in B16 Cells, Arch Pharm, 349 (2016) 20-29.

[115] B.D. Gehm, J.M. McAndrews, P.Y. Chien, J.L. Jameson, Resveratrol, a polyphenolic compound found in grapes and wine, is an agonist for the estrogen receptor, Proceedings of the National Academy of Sciences of the United States of America, 94 (1997) 14138-14143.
[116] E. Chaita, G. Lambrinidis, C. Cheimonidi, A. Agalou, D. Beis, I. Trougakos, E. Mikros, A.L. Skaltsounis, N. Aligiannis, Anti-Melanogenic Properties of Greek Plants. A Novel Depigmenting Agent from Morus alba Wood, Molecules, 22 (2017).
[117] D.C. Franco, G.S. de Carvalho, P.R. Rocha, R. da Silva Teixeira, A.D. da Silva, N.R. Raposo, Inhibitory effects of resveratrol analogs on mushroom tyrosinase activity, Molecules, 17 (2012) 11816-11825.
[118] S.J. Bae, Y.M. Ha, J.A. Kim, J.Y. Park, T.K. Ha, D. Park, P. Chun, N.H. Park, H.R. Moon, H.Y. Chung, A novel synthesized tyrosinase inhibitor: (E)-2-((2,4-dihydroxyphenyl)diazenyl)phenyl 4-methylbenzenesulfonate as an azo-resveratrol analog, Bioscience, biotechnology, and biochemistry, 77 (2013) 65-72.
[119] S.S. Kuniyoshi, Y.; Ryuichiro, K., A new stilbene with tyrosinase inhibitory activity from *Chlorophora excelsa*, Chem Pharm Bull, 51 (2003) 318-319.
[120] K. Ohguchi, T. Tanaka, I. Iliya, T. Ito, M. Iinuma, K. Matsumoto, Y. Akao, Y. Nozawa, Gnetol as a potent tyrosinase inhibitor from genus Gnetum, Biosci Biotech Bioch, 67 (2003) 663-665.
[121] T. Yokozawa, Y.J. Kim, Piceatannol inhibits melanogenesis by its antioxidative actions, Biological & pharmaceutical bulletin, 30 (2007) 2007-2011.
[122] S. Song, H. Lee, Y. Jin, Y.M. Ha, S. Bae, H.Y. Chung, H. Suh, Syntheses of hydroxy substituted 2-phenyl-naphthalenes as inhibitors of tyrosinase, Bioorg Med Chem Lett, 17 (2007) 461-464.
[123] K. Jones, J. Hughes, M. Hong, Q. Jia, S. Orndorff, Modulation of melanogenesis by aloesin: a competitive inhibitor of tyrosinase, Pigment cell research, 15 (2002) 335-340.
[124] S. Choi, S.K. Lee, J.E. Kim, M.H. Chung, Y.I. Park, Aloesin inhibits hyperpigmentation induced by UV radiation, Clinical and experimental dermatology, 27 (2002) 513-515.
[125] Y. Masamoto, H. Ando, Y. Murata, Y. Shimoishi, M. Tada, K. Takahata, Mushroom tyrosinase inhibitory activity of esculetin isolated from seeds of Euphorbia lathyris L, Bioscience, biotechnology, and biochemistry, 67 (2003) 631-634.
[126] X.L. Piao, S.H. Baek, M.K. Park, J.H. Park, Tyrosinase-inhibitory furanocoumarin from Angelica dahurica, Biological & pharmaceutical bulletin, 27 (2004) 1144-1146.
[127] V.U. Ahmad, F. Ullah, J. Hussain, U. Farooq, M. Zubair, M.T. Khan, M.I. Choudhary, Tyrosinase inhibitors from Rhododendron collettianum and their structure-activity relationship (SAR) studies, Chemical & pharmaceutical bulletin, 52 (2004) 1458-1461.
[128] A.M. Girelli, E. Mattei, A. Messina, A.M. Tarola, Inhibition of polyphenol oxidases activity by various dipeptides, Journal of agricultural and food chemistry, 52 (2004) 2741-2745.
[129] H. Morita, T. Kayashita, H. Kobata, A. Gonda, K. Takeya, H. Itokawa, Pseudostellarins D-F, New Tyrosinase Inhibitory Cyclic-Peptides from Pseudostellaria-Heterophylla, Tetrahedron, 50 (1994) 9975-9982.
[130] A. Abu Ubeid, L. Zhao, Y. Wang, B.M. Hantash, Short-sequence oligopeptides with inhibitory activity against mushroom and human tyrosinase, The Journal of investigative dermatology, 129 (2009) 2242-2249.
[131] H. Kim, J. Choi, J.K. Cho, S.Y. Kim, Y.S. Lee, Solid-phase synthesis of kojic acid-tripeptides and their tyrosinase inhibitory activity, storage stability, and toxicity, Bioorg Med Chem Lett, 14 (2004) 2843-2846.
[132] B. Reddy, T. Jow, B.M. Hantash, Bioactive oligopeptides in dermatology: Part I, Experimental dermatology, 21 (2012) 563-568.
[133] D.F. Li, P.P. Hu, M.S. Liu, X.L. Kong, J.C. Zhang, R.C. Hider, T. Zhou, Design and synthesis of hydroxypyridinone-L-phenylalanine conjugates as potential tyrosinase inhibitors, Journal of agricultural and food chemistry, 61 (2013) 6597-6603.

[134] D.Y. Zhao, M.X. Zhang, X.W. Dong, Y.Z. Hu, X.Y. Dai, X. Wei, R.C. Hider, J.C. Zhang, T. Zhou, Design and synthesis of novel hydroxypyridinone derivatives as potential tyrosinase inhibitors, Bioorg Med Chem Lett, 26 (2016) 3103-3108.
[135] Y.J. Kim, J.K. No, J.H. Lee, H.Y. Chung, 4,4'-Dihydroxybiphenyl as a new potent tyrosinase inhibitor, Biological & pharmaceutical bulletin, 28 (2005) 323-327.
[136] K. Bao, Y. Dai, Z.B. Zhu, F.J. Tu, W.G. Zhang, X.S. Yao, Design and synthesis of biphenyl derivatives as mushroom tyrosinase inhibitors, Bioorganic & medicinal chemistry, 18 (2010) 6708-6714.
[137] H.C. Kwong, C.S. Chidan Kumar, S.H. Mah, T.S. Chia, C.K. Quah, Z.H. Loh, S. Chandraju, G.K. Lim, Novel biphenyl ester derivatives as tyrosinase inhibitors: Synthesis, crystallographic, spectral analysis and molecular docking studies, PloS one, 12 (2017) e0170117.
[138] S. Mutahir, M.A. Khan, I.U. Khan, M. Yar, M. Ashraf, S. Tariq, R.L. Ye, B.J. Zhou, Organocatalyzed and mechanochemical solvent-free synthesis of novel and functionalized bis-biphenyl substituted thiazolidinones as potent tyrosinase inhibitors: SAR and molecular modeling studies, European journal of medicinal chemistry, 134 (2017) 406-414.
[139] T. Oyama, S. Takahashi, A. Yoshimori, T. Yamamoto, A. Sato, T. Kamiya, H. Abe, T. Abe, S.I. Tanuma, Discovery of a new type of scaffold for the creation of novel tyrosinase inhibitors, Bioorganic & medicinal chemistry, 24 (2016) 4509-4515.
[140] T. Oyama, A. Yoshimori, S. Takahashi, T. Yamamoto, A. Sato, T. Kamiya, H. Abe, T. Abe, S.I. Tanuma, Structural insight into the active site of mushroom tyrosinase using phenylbenzoic acid derivatives, Bioorg Med Chem Lett, 27 (2017) 2868-2872.
[141] S. Ferro, L. De Luca, M.P. Germano, M.R. Buemi, L. Ielo, G. Certo, M. Kanteev, A. Fishman, A. Rapisarda, R. Gitto, Chemical exploration of 4-(4-fluorobenzyl)piperidine fragment for the development of new tyrosinase inhibitors, European journal of medicinal chemistry, 125 (2017) 992-1001.
a) De Luca, L.; **Ielo, L.**; Ferro, S.; Buemi, M.R.; Certo G.; Germanò M. P.; Rapisarda A.; Gitto, R.; *"Synthesis, biological evaluation and docking studies of new indole-compounds as tyrosinase inhibitors"*. Società Chimica Italiana Convegno Congiunto delle Sezioni Calabria e Sicilia, Catanzaro (Italy). 3-4 December 2015, Pag. 53.
[142] P. Thanigaimalai, K.C. Lee, V.K. Sharma, C. Joo, W.J. Cho, E. Roh, Y. Kim, S.H. Jung, Structural requirement of phenylthiourea analogs for their inhibitory activity of melanogenesis and tyrosinase, Bioorg Med Chem Lett, 21 (2011) 6824-6828.
[143] P. Thanigaimalai, T.A. Hoang, K.C. Lee, S.C. Bang, V.K. Sharma, C.Y. Yun, E. Roh, B.Y. Hwang, Y. Kim, S.H. Jung, Structural requirement(s) of N-phenylthioureas and benzaldehyde thiosemicarbazones as inhibitors of melanogenesis in melanoma B 16 cells, Bioorg Med Chem Lett, 20 (2010) 2991-2993.
[144] J. Choi, S.J. Park, J.G. Jee, Analogues of ethionamide, a drug used for multidrug-resistant tuberculosis, exhibit potent inhibition of tyrosinase, European journal of medicinal chemistry, 106 (2015) 157-166.
[145] D.S. Cooper, Antithyroid drugs, The New England journal of medicine, 311 (1984) 1353-1362.
[146] A. You, J. Zhou, S. Song, G. Zhu, H. Song, W. Yi, Structure-based modification of 3-/4-aminoacetophenones giving a profound change of activity on tyrosinase: from potent activators to highly efficient inhibitors, European journal of medicinal chemistry, 93 (2015) 255-262.
[147] A. You, J. Zhou, S. Song, G. Zhu, H. Song, W. Yi, Rational design, synthesis and structure-activity relationships of 4-alkoxy- and 4-acyloxy-phenylethylenethiosemicarbazone analogues as novel tyrosinase inhibitors, Bioorganic & medicinal chemistry, 23 (2015) 924-931.
[148] S.Y. Kwak, J.K. Yang, H.R. Choi, K.C. Park, Y.B. Kim, Y.S. Lee, Synthesis and dual biological effects of hydroxycinnamoyl phenylalanyl/prolyl hydroxamic acid derivatives as tyrosinase inhibitor and antioxidant, Bioorg Med Chem Lett, 23 (2013) 1136-1142.

[149] H.R. Li, M. Habasi, L.Z. Xie, H.A. Aisa, Effect of chlorogenic acid on melanogenesis of B16 melanoma cells, Molecules, 19 (2014) 12940-12948.
[150] L. Saghaie, M. Pourfarzam, A. Fassihi, B. Sartippour, Synthesis and tyrosinase inhibitory properties of some novel derivatives of kojic acid, Research in pharmaceutical sciences, 8 (2013) 233-242.
[151] H.B.H.A.S.e.a. Rho, Synthesis of new antimelanogenic compounds containing two molecules of kojic acid, Bull Kor Chem Soc, 29 (2008) 1569-1571.
[152] J.M. Noh, S.Y. Kwak, H.S. Seo, J.H. Seo, B.G. Kim, Y.S. Lee, Kojic acid-amino acid conjugates as tyrosinase inhibitors, Bioorg Med Chem Lett, 19 (2009) 5586-5589.
[153] A. Yoshimori, T. Oyama, S. Takahashi, H. Abe, T. Kamiya, T. Abe, S. Tanuma, Structure-activity relationships of the thujaplicins for inhibition of human tyrosinase, Bioorganic & medicinal chemistry, 22 (2014) 6193-6200.
[154] T.O. Katagiri, T.; Oyobikawa, M.; Futaki, K.; Shaku, M.; Kawai, M.; Takenouchi, M., Inhibitory action of 4-nbutylresorcinol on melanogenesis and its skin whitening effects, J. Soc. Cosmet. Chem, 35 (2001) 42-49.
[155] S.Y. Huh, J.W. Shin, J.I. Na, C.H. Huh, S.W. Youn, K.C. Park, The Efficacy and Safety of 4-n-butylresorcinol 0.1% Cream for the Treatment of Melasma: A Randomized Controlled Split-face Trial, Ann Dermatol, 22 (2010) 21-25.
[156] S.Y. Huh, J.W. Shin, J.I. Na, C.H. Huh, S.W. Youn, K.C. Park, Efficacy and safety of liposome-encapsulated 4-n-butylresorcinol 0.1% cream for the treatment of melasma: A randomized controlled split-face trial, J Dermatol, 37 (2010) 311-315.
[157] N.T.M. Mohan, A. Gowda, A.K. Jaiswal, B.C.S. Kumar, P. Shilpashree, B. Gangaboraiah, M. Shamanna, Assessment of efficacy, safety, and tolerability of 4-n-butylresorcinol 0.3% cream: an Indian multicentric study on melasma, Clin Cosmet Investi, 9 (2016) 21-27.
[158] H.M. Wang, C.Y. Chen, Z.H. Wen, Identifying melanogenesis inhibitors from Cinnamomum subavenium with in vitro and in vivo screening systems by targeting the human tyrosinase, Experimental dermatology, 20 (2011) 242-248.
[159] Z.C. Li, L.H. Chen, X.J. Yu, Y.H. Hu, K.K. Song, X.W. Zhou, Q.X. Chen, Inhibition Kinetics of Chlorobenzaldehyde Thiosemicarbazones on Mushroom Tyrosinase, Journal of agricultural and food chemistry, 58 (2010) 12537-12540.
[160] R. Haudecoeur, M. Carotti, A. Gouron, M. Maresca, E. Buitrago, R. Hardre, E. Bergantino, H. Jamet, C. Belle, M. Reglier, L. Bubacco, A. Boumendjel, 2-Hydroxypyridine-N-oxide-Embedded Aurones as Potent Human Tyrosinase Inhibitors, ACS medicinal chemistry letters, 8 (2017) 55-60.
[161] S.M. An, S.I. Lee, S.W. Choi, S.W. Moon, Y.C. Boo, p-Coumaric acid, a constituent of Sasa quelpaertensis Nakai, inhibits cellular melanogenesis stimulated by alpha-melanocyte stimulating hormone, The British journal of dermatology, 159 (2008) 292-299.
[162] K. Song, S.M. An, M. Kim, J.S. Koh, Y.C. Boo, Comparison of the antimelanogenic effects of p-coumaric acid and its methyl ester and their skin permeabilities, Journal of dermatological science, 63 (2011) 17-22.
[163] Y.K. Seo, S.J. Kim, Y.C. Boo, J.H. Baek, S.H. Lee, J.S. Koh, Effects of p-coumaric acid on erythema and pigmentation of human skin exposed to ultraviolet radiation, Clinical and experimental dermatology, 36 (2011) 260-266.
[164] K. Ezzedine, V. Eleftheriadou, M. Whitton, N. van Geel, Vitiligo, Lancet, 386 (2015) 74-84.
[165] L.R. A., Oculocutaneous Albinism Type 1, GeneReviews, (2000).
[166] M. Nomakhosi, A. Heidi, Natural options for management of melasma, a review, Journal of cosmetic and laser therapy : official publication of the European Society for Laser Dermatology, (2018) 1-12.
[167] AIRC, [https://www.airc.it/cancro/tumori/melanoma-cutaneo/], (2013).
[168] S. Parvez, M. Kang, H.S. Chung, H. Bae, Naturally occurring tyrosinase inhibitors: mechanism and applications in skin health, cosmetics and agriculture industries, Phytotherapy research : PTR, 21 (2007) 805-816.

[169] P.G. Engasser, Ochronosis caused by bleaching creams, Journal of the American Academy of Dermatology, 10 (1984) 1072-1073.
[170] A.A. Fisher, Current contact news. Hydroquinone uses and abnormal reactions, Cutis, 31 (1983) 240-244, 250.
[171] C. Romaguera, F. Grimalt, Leukoderma from hydroquinone, Contact dermatitis, 12 (1985) 183.
[172] E.V. Curto, C. Kwong, H. Hermersdorfer, H. Glatt, C. Santis, V. Virador, V.J. Hearing, Jr., T.P. Dooley, Inhibitors of mammalian melanocyte tyrosinase: in vitro comparisons of alkyl esters of gentisic acid with other putative inhibitors, Biochemical pharmacology, 57 (1999) 663-672.
[173] H. Zhou, J.K. Kepa, D. Siegel, S. Miura, Y. Hiraki, D. Ross, Benzene metabolite hydroquinone up-regulates chondromodulin-I and inhibits tube formation in human bone marrow endothelial cells, Molecular pharmacology, 76 (2009) 579-587.
[174] N. Fujimoto, H. Onodera, K. Mitsumori, T. Tamura, S. Maruyama, A. Ito, Changes in thyroid function during development of thyroid hyperplasia induced by kojic acid in F344 rats, Carcinogenesis, 20 (1999) 1567-1571.
[175] V. Spinola, B. Mendes, J.S. Camara, P.C. Castilho, Effect of time and temperature on vitamin C stability in horticultural extracts. UHPLC-PDA vs iodometric titration as analytical methods, Lwt-Food Sci Technol, 50 (2013) 489-495.
[176] V. Arulmozhi, K. Pandian, S. Mirunalini, Ellagic acid encapsulated chitosan nanoparticles for drug delivery system in human oral cancer cell line (KB), Colloids and surfaces. B, Biointerfaces, 110 (2013) 313-320.
[177] N. Khan, H. Mukhtar, Tea polyphenols for health promotion, Life sciences, 81 (2007) 519-533.
[178] H. Shimogaki, Y. Tanaka, H. Tamai, M. Masuda, In vitro and in vivo evaluation of ellagic acid on melanogenesis inhibition, International journal of cosmetic science, 22 (2000) 291-303.
[179] C. Saliou, M. Kitazawa, L. McLaughlin, J.P. Yang, J.K. Lodge, T. Tetsuka, K. Iwasaki, J. Cillard, T. Okamoto, L. Packer, Antioxidants modulate acute solar ultraviolet radiation-induced NF-kappa-B activation in a human keratinocyte cell line, Free radical biology & medicine, 26 (1999) 174-183.
[180] L. Packer, E.H. Witt, H.J. Tritschler, alpha-Lipoic acid as a biological antioxidant, Free radical biology & medicine, 19 (1995) 227-250.
[181] Y. Funasaka, A.K. Chakraborty, M. Komoto, A. Ohashi, M. Ichihashi, The depigmenting effect of alpha-tocopheryl ferulate on human melanoma cells, The British journal of dermatology, 141 (1999) 20-29.
[182] S.P. Leelananda, S. Lindert, Computational methods in drug discovery, Beilstein journal of organic chemistry, 12 (2016) 2694-2718.
[183] P. Aparoy, K.K. Reddy, P. Reddanna, Structure and ligand based drug design strategies in the development of novel 5- LOX inhibitors, Current medicinal chemistry, 19 (2012) 3763-3778.
[184] I.D. Kuntz, J.M. Blaney, S.J. Oatley, R. Langridge, T.E. Ferrin, A geometric approach to macromolecule-ligand interactions, Journal of molecular biology, 161 (1982) 269-288.
[185] D.B. Kitchen, H. Decornez, J.R. Furr, J. Bajorath, Docking and scoring in virtual screening for drug discovery: methods and applications, Nature reviews. Drug discovery, 3 (2004) 935-949.
[186] N. Brooijmans, I.D. Kuntz, Molecular recognition and docking algorithms, Annual review of biophysics and biomolecular structure, 32 (2003) 335-373.
[187] P. Kolb, R.S. Ferreira, J.J. Irwin, B.K. Shoichet, Docking and chemoinformatic screens for new ligands and targets, Current opinion in biotechnology, 20 (2009) 429-436.
[188] G. Jones, P. Willett, Docking small-molecule ligands into active sites, Current opinion in biotechnology, 6 (1995) 652-656.
[189] D.A. Gschwend, A.C. Good, I.D. Kuntz, Molecular docking towards drug discovery, Journal of molecular recognition : JMR, 9 (1996) 175-186.

[190] G.M. Verkhivker, D. Bouzida, D.K. Gehlhaar, P.A. Rejto, S. Arthurs, A.B. Colson, S.T. Freer, V. Larson, B.A. Luty, T. Marrone, P.W. Rose, Deciphering common failures in molecular docking of ligand-protein complexes, Journal of computer-aided molecular design, 14 (2000) 731-751.
[191] G. Jones, P. Willett, R.C. Glen, A.R. Leach, R. Taylor, Development and validation of a genetic algorithm for flexible docking, Journal of molecular biology, 267 (1997) 727-748.
[192] M.L. Verdonk, J.C. Cole, M.J. Hartshorn, C.W. Murray, R.D. Taylor, Improved protein-ligand docking using GOLD, Proteins, 52 (2003) 609-623.
[193] D. Fischer, R. Norel, H. Wolfson, R. Nussinov, Surface motifs by a computer vision technique: searches, detection, and implications for protein-ligand recognition, Proteins, 16 (1993) 278-292.
[194] A. Miranker, M. Karplus, Functionality maps of binding sites: a multiple copy simultaneous search method, Proteins, 11 (1991) 29-34.
[195] M.B. Eisen, D.C. Wiley, M. Karplus, R.E. Hubbard, HOOK: a program for finding novel molecular architectures that satisfy the chemical and steric requirements of a macromolecule binding site, Proteins, 19 (1994) 199-221.
[196] D.S. Goodsell, H. Lauble, C.D. Stout, A.J. Olson, Automated docking in crystallography: analysis of the substrates of aconitase, Proteins, 17 (1993) 1-10.
[197] G. Jones, P. Willett, R.C. Glen, Molecular recognition of receptor sites using a genetic algorithm with a description of desolvation, Journal of molecular biology, 245 (1995) 43-53.
[198] D.R. Westhead, D.E. Clark, C.W. Murray, A comparison of heuristic search algorithms for molecular docking, Journal of computer-aided molecular design, 11 (1997) 209-228.
[199] C.A. Baxter, C.W. Murray, D.E. Clark, D.R. Westhead, M.D. Eldridge, Flexible docking using Tabu search and an empirical estimate of binding affinity, Proteins, 33 (1998) 367-382.
[200] W.D. Cornell, P. Cieplak, C.I. Bayly, I.R. Gould, K.M. Merz, D.M. Ferguson, D.C. Spellmeyer, T. Fox, J.W. Caldwell, P.A. Kollman, A 2nd Generation Force-Field for the Simulation of Proteins, Nucleic-Acids, and Organic-Molecules, J Am Chem Soc, 117 (1995) 5179-5197.
[201] K.P. Weiner SJ., Case DA., Singh UC., Ghio C., Alagona G., Profeta S Jr. Weiner P., New Force Field for Molecular Mechanical Simulation of Nucleic Acids and Proteins, J. Am. Chem. Soc., 106 (1984) 765-784.
[202] B.R. Brooks BR, Olafson BD, States DJ, Swaminathan S, Karplus M., CHARMM: A program for macromolecular energy, minimization, and dynamics calculations, J. Comput. Chem., 4 (1983) 187-217.
[203] T. Schulz-Gasch, M. Stahl, Scoring functions for protein-ligand interactions: a critical perspective, Drug discovery today. Technologies, 1 (2004) 231-239.
[204] R.A. Friesner, J.L. Banks, R.B. Murphy, T.A. Halgren, J.J. Klicic, D.T. Mainz, M.P. Repasky, E.H. Knoll, M. Shelley, J.K. Perry, D.E. Shaw, P. Francis, P.S. Shenkin, Glide: a new approach for rapid, accurate docking and scoring. 1. Method and assessment of docking accuracy, Journal of medicinal chemistry, 47 (2004) 1739-1749.
[205] M. Rarey, B. Kramer, T. Lengauer, G. Klebe, A fast flexible docking method using an incremental construction algorithm, Journal of molecular biology, 261 (1996) 470-489.
[206] A. Krammer, P.D. Kirchhoff, X. Jiang, C.M. Venkatachalam, M. Waldman, LigScore: a novel scoring function for predicting binding affinities, Journal of molecular graphics & modelling, 23 (2005) 395-407.
[207] H.J. Bohm, LUDI: rule-based automatic design of new substituents for enzyme inhibitor leads, Journal of computer-aided molecular design, 6 (1992) 593-606.
[208] M.D. Eldridge, C.W. Murray, T.R. Auton, G.V. Paolini, R.P. Mee, Empirical scoring functions: I. The development of a fast empirical scoring function to estimate the binding affinity of ligands in receptor complexes, Journal of computer-aided molecular design, 11 (1997) 425-445.
[209] S.-Y.a.X.Z. Huang, Mean-force scoring functions for protein-ligand binding, Annu. Rep. Comput. Chem, 6 (2010) 281-296.

[210] P.D. Thomas, K.A. Dill, An iterative method for extracting energy-like quantities from protein structures, Proceedings of the National Academy of Sciences of the United States of America, 93 (1996) 11628-11633.
[211] P.D. Thomas, K.A. Dill, Statistical potentials extracted from protein structures: How accurate are they?, Journal of molecular biology, 257 (1996) 457-469.
[212] H. Gohlke, M. Hendlich, G. Klebe, Knowledge-based scoring function to predict protein-ligand interactions, Journal of molecular biology, 295 (2000) 337-356.
[213] W.T.M. Mooij, M.L. Verdonk, General and targeted statistical potentials for protein-ligand interactions, Proteins-Structure Function and Bioinformatics, 61 (2005) 272-287.
[214] I. Muegge, Y.C. Martin, A general and fast scoring function for protein-ligand interactions: a simplified potential approach, Journal of medicinal chemistry, 42 (1999) 791-804.
[215] P.a.P.K. Weiner, AMBER - assisted model building with energy refinementla general program for modeling molecules and their interactions, J Comput Chem, 2 (1981) 287-303.
[216] L. Nilsson, M. Karplus, Empirical Energy Functions for Energy Minimization and Dynamics of Nucleic-Acids, Journal of Computational Chemistry, 7 (1986) 591-616.
[217] W. Wang, O. Donini, C.M. Reyes, P.A. Kollman, Biomolecular simulations: recent developments in force fields, simulations of enzyme catalysis, protein-ligand, protein-protein, and protein-nucleic acid noncovalent interactions, Annual review of biophysics and biomolecular structure, 30 (2001) 211-243.
[218] D. Huang, A. Caflisch, Efficient evaluation of binding free energy using continuum electrostatics solvation, Journal of medicinal chemistry, 47 (2004) 5791-5797.
[219] H.Y. Liu, I.D. Kuntz, X.Q. Zou, Pairwise GB/SA scoring function for structure-based drug design, J Phys Chem B, 108 (2004) 5453-5462.
[220] N. Huang, C. Kalyanaraman, K. Bernacki, M.P. Jacobson, Molecular mechanics methods for predicting protein-ligand binding, Physical chemistry chemical physics : PCCP, 8 (2006) 5166-5177.
[221] G.M. Morris, D.S. Goodsell, R.S. Halliday, R. Huey, W.E. Hart, R.K. Belew, A.J. Olson, Automated docking using a Lamarckian genetic algorithm and an empirical binding free energy function, Journal of Computational Chemistry, 19 (1998) 1639-1662.
[222] C.M. Oshiro, I.D. Kuntz, J.S. Dixon, Flexible Ligand Docking Using a Genetic Algorithm, Journal of computer-aided molecular design, 9 (1995) 113-130.
[223] G. Jones, P. Willett, R.C. Glen, Molecular Recognition of Receptor-Sites Using a Genetic Algorithm with a Description of Desolvation, Journal of molecular biology, 245 (1995) 43-53.
[224] G. Wolber, T. Langer, LigandScout: 3-D pharmacophores derived from protein-bound ligands and their use as virtual screening filters, Journal of chemical information and modeling, 45 (2005) 160-169.
[225] L. Pauling, The Nature of the Chemical Bond, 2nd ed ed., Cornell University New York, 1948.
[226] E. Lionta, G. Spyrou, D.K. Vassilatis, Z. Cournia, Structure-based virtual screening for drug discovery: principles, applications and recent advances, Current topics in medicinal chemistry, 14 (2014) 1923-1938.
[227] C.A. Lipinski, F. Lombardo, B.W. Dominy, P.J. Feeney, Experimental and computational approaches to estimate solubility and permeability in drug discovery and development settings, Advanced drug delivery reviews, 46 (2001) 3-26.
[228] K. Lida, Hase, K., Shimomura, K., Sudo, S., Kadota, S., Namba, T., Potent inhibitors of tyrosinase activity and melanin biosynthesis from rheum officinale, Planta medica, 61 (1995) 425-428.
[229] W. Kahn, Andrawis, A., Inhibition of mushroom tyrosinase by tropolone, Phytochemistry, 24 (1985) 905-908.
[230] J.L. Herndon, A. Ismaiel, S.P. Ingher, M. Teitler, R.A. Glennon, Ketanserin analogues: structure-affinity relationships for 5-HT2 and 5-HT1C serotonin receptor binding, Journal of medicinal chemistry, 35 (1992) 4903-4910.

[231] S. Ferro, B. Deri, M.P. Germano, R. Gitto, L. Ielo, M.R. Buemi, G. Certo, S. Vittorio, A. Rapisarda, Y. Pazy, A. Fishman, L. De Luca, Targeting Tyrosinase: Development and Structural Insights of Novel Inhibitors Bearing Arylpiperidine and Arylpiperazine Fragments, Journal of medicinal chemistry, 61 (2018) 3908-3917.

a) **Ielo L.**; Ferro S.; De Luca L.; Germanò M.P.;Buemi M.R.; Certo G.; Kanteev M.;Fishman A.;Rapisarda A; and Gitto R.; *"4-benzylpiperidine and 1-benzylpiperazine derivatives: a new class of compounds as tyrosinase inhibitors"*. XXIV NMMC&10th NPCF, Perugia (Italy), 11-14 September 2016, Pag. PC-95.

b) **Ielo L.**; Ferro S.;De Luca L.; Germanò M. P.; Buemi M.R.; Certo G.; Kanteev M.; Fishman A.;Rapisarda, A; and Gitto, R.; *"Tyrosinase inhibitors: synthesis, biological essays and docking studies of a new class of compounds"*. MuTaLig COST ACTION CA15135 WG meeting, Budapest (Hungary), 17-20 November, 2016, Pag 52.

c) **Ielo L**.; Gitto R.; Ferro S.; Germanò M.P.; Buemi M.R.; Fishman A.; Rapisarda A.; De Luca L.; *"Discover of New Potent Tyrosinase Inhibitors: Computational and Experimental studies"*. 7th Paul Ehrlich MedChem EuroPhD Network Symposium, 25-27 August, 2017, Vienna (Austria), Pag. 46.

d) **Ielo L**.; De Luca L.; Ferro S.; Germanò M.P.; Buemi M.R.; Fishman A.; Rapisarda A.; Gitto R.; *"Computational and Experimental Structural Studies Leading to New Potent Tyrosinase Inhibitors Bearing 4-Fluorobenzyl moiety"*. XXVI Congresso Nazionale della Società Chimica Italiana, 10-14 September, 2017, Paestum (Italy), Pag 45.

e) **Ielo L**.; Ferro S.; Gitto R.; Vittorio S.; Germanò M.P.; Rapisarda A.; De Luca L.; *"Discovery of a new class of potent tyrosinase inhibitors bearing 4'fluorobenzyl moiety"*. Società Chimica Italiana Congresso Congiunto delle Sezioni Sicilia e Calabria, 9-10 February, 2018, Catania (Italy).

f) **Ielo L**. *"Rational design, synthesis and biological evaluation of a new class of tyrosinase inhibitors"*. European School of Medicinal Chemistry ESMEC XXXVIII Advanced Course of Medicinal Chemistry and Seminar for PhD students, 1-5 July, 2018, Urbino (Italy), Pag 63.

g) **Ielo L.**; Ferro S.; Deri B.; Germanò M.P.; Gitto R.; Buemi M.R.; Certo G.; Vittorio S.; Rapisarda A.; Pazy Y.; Fishman A.; De Luca L. *"Design, synthesis and biological investigation of novel arylpiperidine/arylpiperazine derivatives as Tyrosinase inhibitors"*. Italian-Spanish-Portuguese Joint Meeting in Medicinal Chemistry MedChemSicily2018, 17-20 July, 2018, Palermo (Italy).

[232] M. Goldfeder, M. Kanteev, S. Isaschar-Ovdat, N. Adir, A. Fishman, Determination of tyrosinase substrate-binding modes reveals mechanistic differences between type-3 copper proteins, Nature communications, 5 (2014) 4505.

[233] B. Deri, M. Kanteev, M. Goldfeder, D. Lecina, V. Guallar, N. Adir, A. Fishman, The unravelling of the complex pattern of tyrosinase inhibition, Scientific reports, 6 (2016) 34993.

[234] M. Goldfeder, M. Egozy, V. Shuster Ben-Yosef, N. Adir, A. Fishman, Changes in tyrosinase specificity by ionic liquids and sodium dodecyl sulfate, Applied microbiology and biotechnology, 97 (2013) 1953-1961.

[235] R.A. Laskowski, M.B. Swindells, LigPlot+: multiple ligand-protein interaction diagrams for drug discovery, J Chem Inf Model, 51 (2011) 2778-2786.

[236] S. Hassani, K. Haghbeen, M. Fazli, Non-specific binding sites help to explain mixed inhibition in mushroom tyrosinase activities, European journal of medicinal chemistry, 122 (2016) 138-148.

[237] A. Gaulton, L.J. Bellis, A.P. Bento, J. Chambers, M. Davies, A. Hersey, Y. Light, S. McGlinchey, D. Michalovich, B. Al-Lazikani, J.P. Overington, ChEMBL: a large-scale bioactivity database for drug discovery, Nucleic acids research, 40 (2012) D1100-1107.

[238] S. Pignatti, Flora d'Italia, 1982.

[239] F.A. Ramos, Y. Takaishi, M. Shirotori, Y. Kawaguchi, K. Tsuchiya, H. Shibata, T. Higuti, T. Tadokoro, M. Takeuchi, Antibacterial and antioxidant activities of quercetin oxidation products from yellow onion (Allium cepa) skin, Journal of agricultural and food chemistry, 54 (2006) 3551-3557.

[240] K. Tamao, Sumitani, K., Kumada, M-, Selective carbon-carbon bond formation by cross-coupling of Grignard reagents with organic halides. Catalysis by nickel-phosphine complexes, J. Am. Chem. Soc., 94 (1972) 4374–4376.
[241] V. Pace, A. Pelosi, D. Antermite, O. Rosati, M. Curini, W. Holzer, Bromomethyllithium-mediated chemoselective homologation of disulfides to dithioacetals, Chem Commun, 52 (2016) 2639-2642.
[242] H. Decker, F. Tuczek, The Recent Crystal Structure of Human Tyrosinase Related Protein 1 (HsTYRP1) Solves an Old Problem and Poses a New One, Angew Chem Int Ed Engl, 56 (2017) 14352-14354.
[243] E. Favre, A. Daina, P.A. Carrupt, A. Nurisso, Modeling the met form of human tyrosinase: a refined and hydrated pocket for antagonist design, Chemical biology & drug design, 84 (2014) 206-215.
[244] T. Mann, W. Gerwat, J. Batzer, K. Eggers, C. Scherner, H. Wenck, F. Stab, V.J. Hearing, K.H. Rohm, L. Kolbe, Inhibition of Human Tyrosinase Requires Molecular Motifs Distinctively Different from Mushroom Tyrosinase, The Journal of investigative dermatology, 138 (2018) 1601-1608.
[245] W.C. Chen, T.S. Tseng, N.W. Hsiao, Y.L. Lin, Z.H. Wen, C.C. Tsai, Y.C. Lee, H.H. Lin, K.C. Tsai, Discovery of highly potent tyrosinase inhibitor, T1, with significant anti-melanogenesis ability by zebrafish in vivo assay and computational molecular modeling, Scientific reports, 5 (2015) 7995.
[246] E. Bruno, M.R. Buemi, A. Di Fiore, L. De Luca, S. Ferro, A. Angeli, R. Cirilli, D. Sadutto, V. Alterio, S.M. Monti, C.T. Supuran, G. De Simone, R. Gitto, Probing Molecular Interactions between Human Carbonic Anhydrases (hCAs) and a Novel Class of Benzenesulfonamides, Journal of medicinal chemistry, 60 (2017) 4316-4326.
[247] R. Gitto, L. De Luca, S. Ferro, M.R. Buemi, E. Russo, G. De Sarro, L. Costa, L. Ciranna, O. Prezzavento, E. Arena, S. Ronsisvalle, G. Bruno, A. Chimirri, Synthesis and biological characterization of 3-substituted-1H-indoles as ligands of GluN2B-containing N-methyl-D-aspartate receptors, Journal of medicinal chemistry, 54 (2011) 8702-8706.
[248] S. Ferro, M.R. Buemi, L. De Luca, F.E. Agharbaoui, C. Pannecouque, A.M. Monforte, Searching for novel N-1-substituted benzimidazol-2-ones as non-nucleoside HIV-1 RT inhibitors, Bioorganic & medicinal chemistry, 25 (2017) 3861-3870.
[249] A. Kamal, A.V. Subba Rao, M.V. Vishnuvardhan, T. Srinivas Reddy, K. Swapna, C. Bagul, N.V. Subba Reddy, V. Srinivasulu, Synthesis of 2-anilinopyridyl-triazole conjugates as antimitotic agents, Organic & biomolecular chemistry, 13 (2015) 4879-4895.
[250] *Discovery Studio*, 2.5.5; Accelrys: San Diego, CA, 2009. Available at http://www.accelrys.com.
[251] Y. Masamoto, H. Ando, Y. Murata, Y. Shimoishi, M. Tada, K. Takahata, Mushroom tyrosinase inhibitory activity of esculetin isolated from seeds of Euphorbia lathyris L, Bioscience, biotechnology, and biochemistry, 67 (2003) 631-634.
[252] M.P. Germano, F. Cacciola, P. Donato, P. Dugo, G. Certo, V. D'Angelo, L. Mondello, A. Rapisarda, Betula pendula leaves: polyphenolic characterization and potential innovative use in skin whitening products, Fitoterapia, 83 (2012) 877-882.
[253] V. Pace, L. Castoldi, S. Monticelli, M. Rui, S. Collina, New Perspectives in Lithium Carbenoid Mediated Homologations, Synlett, 28 (2017) 879-888.
[254] V. Pace, G. Verniest, J.V. Sinisterra, A.R. Alcantara, N. De Kimpe, Improved Arndt-Eistert synthesis of alpha-diazoketones requiring minimal diazomethane in the presence of calcium oxide as acid scavenger, The Journal of organic chemistry, 75 (2010) 5760-5763.
[255] G. Maas, New syntheses of diazo compounds, Angew Chem Int Ed Engl, 48 (2009) 8186-8195.
[256] A. Ford, H. Miel, A. Ring, C.N. Slattery, A.R. Maguire, M.A. McKervey, Modern Organic Synthesis with alpha-Diazocarbonyl Compounds, Chemical reviews, 115 (2015) 9981-10080.

[257] J. Barluenga, J.L. Fernandezsimon, J.M. Concellon, M. Yus, Methylenation of Carbonyl-Compounds Using Chloromethyl-Lithium - a New Method for Terminal and Exocyclic Olefins, J Chem Soc Chem Comm, (1986) 1665-1665.
[258] C.M. Corey E. J., Dimethylsulfoxonium Methylide, J. Am. Chem. Soc, 84 (1962) 867–868.
[259] D. Basavaiah, A.J. Rao, T. Satyanarayana, Recent advances in the Baylis-Hillman reaction and applications, Chemical reviews, 103 (2003) 811-892.
[260] G. Köbrich, The chemistry of Carbenoids and Other Thermolabile Organolithium Compounds. , Angew Chem Internat Edit, 11 (1972) 473-485.
[261] V. Pace, W. Holzer, N. De Kimpe, Lithium Halomethylcarbenoids: Preparation and Use in the Homologation of Carbon Electrophiles, Chem Rec, 16 (2016) 2061-2076.
[262] C.L.E. Closs G. L., Stereospecific Formation of Cyclopropanes by Reaction of Diphenyldibromomethane with Methyllithium and Olefins, Angew Chem Int Ed, 1 (1962) 334-335.
[263] M.R.A. Closs G. L., Formation of Arylcyclopropanes from Olefins, Benzal Bromides, and Organolithium Compounds and from Photolysis of Aryldiazomethanes, J Am Chem Soc, 86 (1964) 4042-4053.
[264] L. Castoldi, S. Monticelli, R. Senatore, L. Ielo, V. Pace, Homologation chemistry with nucleophilic alpha-substituted organometallic reagents: chemocontrol, new concepts and (solved) challenges, Chem Commun (Camb), 54 (2018) 6692-6704.
[265] S.R.D. Simmons H. E., A new synthesis of cyclopropanes from olefins, J. Am. Chem. Soc, 80 (1958) 5323–5324.
[266] G.A. Köbrich, A.; Ansari, F.; Breckoff, W. E.; Büttner, H.; Drischel, W.; Fischer, R. H.; Flory, K.; Fröhlich, H.; Goyert, W.; Heinemann, H.; Hornke, I.; Merkle, H. R.; Trapp, H.; Zündorf, W., Chemistry of Stable α-Halogenoorganolithium Compounds and the Mechanism of Carbenoid Reactions, Angew. Chem. Internat. Edit, 6 (1967) 41-52.
[267] R.K. Tarhouni, B.; Rambaud, M.; Villieras, J. , Monohalomethyllithium XCH2Li: stabilization of a potential synthetic reagent, Tetrahedron Letters, 25 (1984) 835-838.
[268] J.L. Barluenga, L.; Yus, M.; Concellòn, J. M., Reactivity of in situ Generated Dihalomethyllithium towards Dicarboxylic Acid Diesters and Lactones: Synthetic Applications, Tetrahedron, 47 (1991) 7875-7886.
[269] J.B. Barluenga, B.; Alonso, A.; Concellon, J. M. , The First Preparation of Chiral Functionalised Ketones and their Synthetic Uses, J. Soc. Chem. Commun. , (1994) 696-670.
[270] J.B. Barluenga, B.; Concellòn, J. M. , Highly Diastereoselective Synthesis of Threo or Erythro Aminoalkyl Epoxides from a-AminoAcids, J. Org. Chem., 60 (1995) 6696-6699.
[271] D.S. Matteson, Sadhu, K. M., (Chloromethyl) Lithium in an efficient conversion of carbonyl compounds to chlorohydrins or oxiranes, Tetrahedron Letters, 27 (1986) 795-798.
[272] M.D.S. Michnick T.J., (Bromomethyl) lithium: Efficient in situ Reactions, Synlett, (1991) 631–632.
[273] T.B. Loupy A., Salt Effects in Organic and Organometallic Chemistry, VCH,Weinheim, 1992, VCH, Weinheim, (1992).
[274] V. Pace, L. Castoldi, W. Holzer, Synthesis of alpha,beta-unsaturated alpha'-haloketones through the chemoselective addition of halomethyllithiums to Weinreb amides, The Journal of organic chemistry, 78 (2013) 7764-7770.
[275] V. Pace, W. Holzer, G. Verniest, A.R. Alcantara, N. De Kimpe, Chemoselective Synthesis of N-Substituted alpha-Amino-alpha '-chloro Ketones via Chloromethylation of Glycine-Derived Weinreb Amides, Adv Synth Catal, 355 (2013) 919-926.
[276] V. Pace, L. Castoldi, W. Holzer, Chemoselective Additions of Chloromethyllithium Carbenoid to Cyclic Enones: A Direct Access to Chloromethyl Allylic Alcohols, Adv Synth Catal, 356 (2014) 1761-1766.
[277] V. Pace, L. Castoldi, P. Hoyos, J.V. Sinisterra, M. Pregnolato, J.M. Sanchez-Montero, Highly regioselective control of 1,2-addition of organolithiums to alpha,beta-unsaturated

compounds promoted by lithium bromide in 2-methyltetrahydrofuran: a facile and eco-friendly access to allylic alcohols and amines, Tetrahedron, 67 (2011) 2670-2675.
[278] C. J., Organolithium: Selectivity for Synthesis Pergamon, Oxford, (2002).
[279] P. Knochel, W. Dohle, N. Gommermann, F.F. Kneisel, F. Kopp, T. Korn, I. Sapountzis, V.A. Vu, Highly functionalized organomagnesium reagents prepared through halogen-metal exchange, Angew Chem Int Ed Engl, 42 (2003) 4302-4320.
[280] Lithium Compounds in Organic Synthesis: From Fundamentals to Applications, Wiley-VCH, Weinheim, 2014.
[281] V. Pace, L. Castoldi, W. Holzer, Addition of lithium carbenoids to isocyanates: a direct access to synthetically useful N-substituted 2-haloacetamides, Chem Commun, 49 (2013) 8383-8385.
[282] Y. Honda, S. Katayama, M. Kojima, T. Suzuki, N. Kishibata, K. Izawa, New approaches to the industrial synthesis of HIV protease inhibitors, Organic & biomolecular chemistry, 2 (2004) 2061-2070.
[283] K. Izawa, T. Onishi, Industrial syntheses of the central core molecules of HIV protease inhibitors, Chemical reviews, 106 (2006) 2811-2827.
[284] V. Pace, Halomethyllithium Carbenoids: Versatile Reagents for the Homologation of Electrophilic Carbon Units, Aust J Chem, 67 (2014) 311-313.
[285] S. Avolio, C. Malan, I. Marek, P. Knochel, Preparation and reactions of functionalized magnesium carbenoids, Synlett, (1999) 1820-1822.
[286] V. Pace, L. Castoldi, A.D. Mamuye, W. Holzer, Homologation of Isocyanates with Lithium Carbenoids: A Straightforward Access to alpha-Halomethyl- and alpha,alpha-Dihalomethylamides, Synthesis-Stuttgart, 46 (2014) 2897-2909.
[287] J.A. Bull, T. Boultwood, T.A. Taylor, Highly cis-selective synthesis of iodo-aziridines using diiodomethyllithium and in situ generated N-Boc-imines, Chem Commun, 48 (2012) 12246-12248.
[288] T. Boultwood, D.P. Affron, A.D. Trowbridge, J.A. Bull, Synthesis of cis-C-Iodo-N-Tosyl-Aziridines using Diiodomethyllithium: Reaction Optimization, Product Scope and Stability, and a Protocol for Selection of Stationary Phase for Chromatography, Journal of Organic Chemistry, 78 (2013) 6632-6647.
[289] R.W. Hoffmann, The quest for chiral Grignard reagents, Chem Soc Rev, 32 (2003) 225-230.
[290] P.R. Blakemore, S.P. Marsden, H.D. Vater, Reagent-controlled asymmetric homologation of boronic esters by enantioenriched main-group chiral carbenoids, Org Lett, 8 (2006) 773-776.
[291] P.R. Blakemore, M.S. Burge, Iterative stereospecific reagent-controlled homologation of pinacol boronates by enantioenriched alpha-chloroalkyllithium reagents, Journal of the American Chemical Society, 129 (2007) 3068-+.
[292] D.A. Cogan, G.C. Liu, K.J. Kim, B.J. Backes, J.A. Ellman, Catalytic asymmetric oxidation of tert-butyl disulfide. Synthesis of tert-butanesulfinamides, tert-butyl sulfoxides, and tert-butanesulfinimines, Journal of the American Chemical Society, 120 (1998) 8011-8019.
[293] C. Bolm, Bienewald, F., Asymmetric Sulfide Oxidation with Vanadium Catalysts and H_2O_2, Angew Chem Int Ed, 34 (1996) 2640-2642.
[294] T. Satoh, T. Oohara, Y. Ueda, K. Yamakawa, Alpha,Beta-Epoxy Sulfoxides as Useful Intermediate in Organic-Synthesis .14. The Practical Procedure for a Preparation of 1-Chloroalkyl Para-Tolyl Sulfoxides in High Optically-Active Form - a Very Short Synthesis of Optically-Active Disparlure, Tetrahedron Letters, 29 (1988) 313-316.
[295] D.C. Kapeller, F. Hammerschmidt, Preparation and configurational stability of chiral chloro-[D1]methyllithiums of 98% enantiomeric excess, J Am Chem Soc, 130 (2008) 2329-2335.
[296] R. Appel, Tertiary Phosphane/Tetrachloromethane, a Versatile Reagent for Chlorination, Dehydration, and P□N Linkage, Angew Chem Int Ed, 14 (1975) 801-811.
[297] L. Castoldi, L. Ielo, P. Hoyos, M.J. Hernaiz, L. De Luca, A.R. Alcantara, W. Holzer, V. Pace, Merging lithium carbenoid homologation and enzymatic reduction: A combinative approach to the HIV-protease inhibitor Nelfinavir, Tetrahedron, 74 (2018) 2211-2217.

[298] D. Castagnolo, L. Degennaro, R. Luisi, J. Clayden, Enantioselective carbolithiation of S-alkenyl-N-aryl thiocarbamates: kinetic and thermodynamic control, Organic & biomolecular chemistry, 13 (2015) 2330-2340.
[299] V. Pace, I. Murgia, S. Westermayer, T. Langer, W. Holzer, Highly efficient synthesis of functionalized alpha-oxyketones via Weinreb amides homologation with alpha-oxygenated organolithiums, Chem Commun, 52 (2016) 7584-7587.
[300] R. Senatore, L. Ielo, E. Urban, W. Holzer, V. Pace, Substituted alpha-Sulfur Methyl Carbanions: Effective Homologating Agents for the Chemoselective Preparation of beta-Oxo Thioethers from Weinreb Amides, Eur J Org Chem, (2018) 2466-2470.
[301] R. Senatore, L. Castoldi, L. Ielo, W. Holzer, V. Pace, Expeditious and Chemoselective Synthesis of alpha-Aryl and alpha-Alkyl Selenomethylketones via Homologation Chemistry, Org Lett, 20 (2018) 2685-2688.
[302] V. Pace, L. Castoldi, E. Mazzeo, M. Rui, T. Langer, W. Holzer, Efficient Access to All-Carbon Quaternary and Tertiary alpha-Functionalized Homoallyl-type Aldehydes from Ketones, Angew Chem Int Ed Engl, 56 (2017) 12677-12682.
[303] D. Savoia, G. Alvaro, R. Di Fabio, A. Gualandi, C. Fiorelli, Asymmetric synthesis of 2-(2-pyridyl)aziridines from 2-pyridineimines bearing stereogenic N-alkyl substituents and regioselective opening of the aziridine ring, Journal of Organic Chemistry, 71 (2006) 9373-9381.
[304] J.M. Concellon, H. Rodriguez-Solla, C. Simal, Addition Reactions of Iodomethyllithium to Imines. A Direct and Efficient Synthesis of Aziridines and Enantiopure Amino Aziridines, Org Lett, 10 (2008) 4457-4460.
[305] J.M. Concellon, H. Rodriguez-Solla, P.L. Bernad, C. Simal, Addition Reactions of Chloro- or Iodomethyllithium to Imines. Synthesis of Enantiopure Aziridines and beta-Chloroamines, Journal of Organic Chemistry, 74 (2009) 2452-2459.
[306] D.C. Kail, P.M. Krizkova, A. Wieczorek, F. Hammerschmidt, On the Configurational Stability of Chiral, Nonracemic Fluoro- and Iodo-[D1]Methyllithiums, Chem-Eur J, 20 (2014) 4086-4091.
[307] S. Monticelli, V. Pace, Fluoroiodomethane: A Versatile CH2F Source, Aust J Chem, 71 (2018) 473-475.
[308] J.Y. Hu, B. Gao, L.C. Li, C.F. Ni, J.B. Hu, Palladium-Catalyzed Monofluoromethylation of Arylboronic Esters with Fluoromethyl Iodide, Org Lett, 17 (2015) 3086-3089.
[309] L. Degennaro, F. Fanelli, A. Giovine, R. Luisi, External Trapping of Halomethyllithium Enabled by Flow Microreactors, Adv Synth Catal, 357 (2015) 21-27.
[310] A. Hafner, V. Mancino, M. Meisenbach, B. Schenkel, J. Sedelmeier, Dichloromethyllithium: Synthesis and Application in Continuous Flow Mode, Organic Letters, 19 (2017) 786-789.
[311] J.B. Sweeney, Aziridines: epoxides' ugly cousins?, Chem Soc Rev, 31 (2002) 247-258.
[312] F.M.D. Ismail, D.O. Levitsky, V.M. Dembitsky, Aziridine alkaloids as potential therapeutic agents, Eur J Med Chem, 44 (2009) 3373-3387.
[313] M. Kasai, M. Kono, Studies on the Chemistry of Mitomycins, Synlett, (1992) 778-790.
[314] P.D.S.C.J. Sentera, Selective activation of anticancer prodrugs by monoclonal antibody–enzyme conjugates, Adv. Drug. Del. Rev, 53 (2001) 247-264.
[315] N.A. Meanwell, Fluorine and Fluorinated Motifs in the Design and Application of Bioisosteres for Drug Design, J. Med. Chem.
[316] S. Kenis, M. D'Hooghe, G. Verniest, V.D. Nguyen, T.A. Thi, T.V. Nguyen, N. De Kimpe, Straightforward synthesis of 1-alkyl-2-(trifluoromethyl)aziridines starting from 1,1,1-trifluoroacetone, Organic & biomolecular chemistry, 9 (2011) 7217-7223.
[317] F. Meyer, Trifluoromethyl nitrogen heterocycles: synthetic aspects and potential biological targets, Chem Commun, 52 (2016) 3077-3094.
[318] Y.Y. Duan, B. Zhou, J.H. Lin, J.C. Xiao, Diastereoselective Johnson-Corey-Chaykovsky trifluoroethylidenation, Chem Commun, 51 (2015) 13127-13130.

[319] A. Meszaros, A. Szekely, A. Stirling, Z. Novak, Design of Trifluoroalkenyl Iodonium Salts for a Hypervalency-Aided Alkenylation-Cyclization Strategy: Metal-Free Construction of Aziridine Rings, Angew Chem Int Ed Engl, 57 (2018) 6643-6647.
[320] K. Uneyama, H. Amii, T. Katagiri, T. Kobayashi, T. Hosokawa, A rich chemistry of fluorinated imidoyl halides, Journal of Fluorine Chemistry, 126 (2005) 165-171.
[321] L. Castoldi, W. Holzer, T. Langer, V. Pace, Evidence and isolation of tetrahedral intermediates formed upon the addition of lithium carbenoids to Weinreb amides and N-acylpyrroles, Chem Commun, 53 (2017) 9498-9501.
[322] G. Parisi, M. Colella, S. Monticelli, G. Romanazzi, W. Holzer, T. Langer, L. Degennaro, V. Pace, R. Luisi, Exploiting a "Beast" in Carbenoid Chemistry: Development of a Straightforward Direct Nucleophilic Fluoromethylation Strategy, J Am Chem Soc, 139 (2017) 13648-13651.
[323] D. Kaiser, L.F. Veiros, N. Maulide, Bronsted Acid-Mediated Hydrative Arylation of Unactivated Alkynes, Chemistry, 22 (2016) 4727-4732.
[324] A.K. Das, S. Park, S. Muthaiah, S.H. Hong, Ligand- and Acid-Free Gold(I) Chloride Catalyzed Hydration of Terminal Alkynes, Synlett, 26 (2015) 2517-2520.
[325] S. Stankovic, M. D'hooghe, S. Catak, H. Eum, M. Waroquier, V. Van Speybroeck, N. De Kimpe, H.J. Ha, Regioselectivity in the ring opening of non-activated aziridines, Chem Soc Rev, 41 (2012) 643-665.
[326] M.T. Toshimasa Katagiri, Yasuyuki Fujiwara, Hideki Ihara, Kenji Uneyama, General Syntheses of Optically Active a-Trifluoromethylated Amines via Ring-Opening Reactions of Benzyl-2-trifluoromethylaziridine, Journal of Organic Chemistry, 64 (1999) 7323-7329.
[327] Z.C. Jiangtao Zhu, Haibo Xie, Shan Li, Yongming Wu, A General and Straightforward Method for the Synthesis of 2-Trifluoromethylbenzothiazoles, Organic Letter, 12 (2010) 2434-2436.
[328] M.A.V. Alexander S. Bunev a, Vladimir E. Statsyuk, Gennady I. Ostapenko, Alexander S. Peregudov, Synthesis of 1-aryl-4-tosyl-5-(trifluoromethyl)-1H-imidazoles, Journal of Fluorine Chemistry, 163 (2014) 34-37.
[329] A.D. Fariba Rahmani, Synthesis of Trifluoromethylated Pyrroles via a One-Pot Three-Component Reaction, Synlett, 28 (2017) A-C.
[330] A.D. Fariba Rahmani, Mahin Ramezani, Alireza Bazmandegan-Shamili, Synthesis and Photophysical Properties of 3-(Trifluoromethyl)-2H-imidazo[5,1-a]isoquinolinium Chloride Derivatives, Synlett, 28 (2017) A-E.
[331] Z.C. Jiangtao Zhu, Haibo Xie, Shan Li, Yongming Wua, An efficient method to access 2-fluoroalkylbenzimidazoles by PIDA oxidation of amidines, Journal of Fluorine Chemistry, 133 (2012) 134-138.
[332] W.F. Mei Zhu, Guanglong Zou, Chen Xu, Zhiqiang Wang, Palladium-catalyzed intramolecular C H bond functionalization of trifluoroacetimidoyl chloride derivatives: Synthesis of 6-trifluoromethyl-phenanthridines, Journal of Fluorine Chemistry, 163 (2014) 23-27.